UNIVERSITY OF OKLAHOMA

GRADUATE COLLEGE

SEISMIC VULNERABILITY OF RESIDENTIAL STRUCTURES IN NICARAGUA

A DISSERTATION

SUBMITTED TO THE GRADUATE FACULTY

in partial fulfillment of the requirements for the

Degree of

DOCTOR OF PHILOSOPHY

By

LISA HOLLIDAY
Norman, Oklahoma
2009

SEISMIC VULNERABILITY OF RESIDENTIAL STRUCTURES IN NICARAGUA

A DISSERTATION APPROVED FOR THE
SCHOOL OF CIVIL ENGINEERING AND ENVIRONMENTAL SCIENCE

BY

Dr. Kyran Mish, Chair

Dr. Patricia Gilman

Dr. Christopher Ramseyer

Dr. Luther White

Dr. Jinsong Pei

Dr. Kanthasamy Muraleetharan

Acknowledgements

First I would like to thank Dr. Kyran Mish for not only leading by example, but also for creating an atmosphere that encourages the unbridled pursuit of knowledge.

Thanks to my committee for generously offering their time.

Special thanks to Dr. Thomas Kang for his limitless patience in helping me create and troubleshoot my computer models.

Thanks to Professor Polat Gülkan for hosting me for a fun filled year at Middle East Technical University in Ankara, Turkey.

Thanks to my colleague Dr. Dominik Lang for his example and encouragement.

Thanks to the Fullbight Foundation and the David L Boren Awards for International studies for appreciating the value of international studies.

And especially thanks to my wonderful husband, Chris, who has always supported my crazy ambitions.

Table of Contents

List of Tables

List of Figures

Abstract

In recent times, many parts of the world have seen a trend of increased construction with reinforced concrete and masonry block systems. These systems can provide excellent seismic resistance when they are designed by an engineer, built by well-trained workers, constructed of quality materials and all in conformance with building codes. Unfortunately, many structures are constructed without one or more of these requirements. Property owners are building multi-story buildings while paying little attention to building codes or seismic resistance. Adding to the problem, reinforced concrete and masonry block systems enable construction with longer spans, larger openings, and irregular shapes; all of which reduce the earthquake resistance of a building. Such buildings are deceptive because they appear safe, perform well under gravity loads and do not sag or lean. Such buildings are also heavy which adds to the illusion of safety. There is often no consideration given to lateral loads - exactly the type of loads experienced during an earthquake. When an earthquake occurs, it creates a fast cyclic lateral load. The weight of the building increases the lateral loads created by an earthquake, which when lacking sufficient design, results in collapse.

Designing structures to withstand the impact of a major catastrophe is a daunting task under the best of circumstances. For developing countries, this task is nearly impossible. This research evaluates the structural systems of existing buildings in Nicaragua, sampling buildings made from both engineered and earthen materials, and makes recommendations for low-cost enhancements that will improve their structural integrity.

1. Introduction

On December 22, 2003, an earthquake of magnitude 6.5 on the Richter scale rocked San Simeon, California, resulting in the deaths of two people. Four days later, a quake of similar magnitude – 6.6 on the Richter scale – struck outside of Bam, Iran, with catastrophically different results. From this earthquake an estimated 27,000 people died, 30,000 were injured, and 85 percent of the nearby buildings were damaged or destroyed. These terrible disasters are not new; the Managua, Nicaragua, earthquake of 1972 was slightly smaller, but yet it still killed more than 10,000 people, left hundreds of thousands homeless, and created a legacy of civil unrest that lasted for decades. The lack of quality seismic-resistant construction in developing countries is in large part the cause for this tragic disparity.

Prevention of major catastrophes is a daunting task, even for first-world governments. For developing countries, this task is nearly impossible. Research focus needs to be placed on inexpensive measures that will save lives, such as improvements that can be made to new and existing structures to increase structural stability during devastating events. The focus of this research will be to evaluate the structural systems of existing buildings, and then to make recommendations for low-cost enhancements that will improve the structural integrity of buildings in developing nations.

In recent times, the trend in many parts of the world has been to build with reinforced concrete and masonry blocks. These systems can provide excellent seismic resistance when they are designed by an engineer, are made of quality materials, and are built by well-trained workers in conformance with building codes. Unfortunately, this is not the way many of these structures are being built. Property owners themselves are building multi-story buildings, paying little attention to building codes or seismic resistance. Adding to the problem, these new materials also allow longer spans, large openings, and irregular shapes, all of which reduce the earthquake resistance of a building. These buildings are deceptive because they seem safe, they perform well under gravity loads and they do not sag or lean. These buildings are also relatively heavy which adds to the illusion of a safe building. However, there often is no consideration given to lateral loads, the kind of loads they will experience during an earthquake. When an earthquake occurs, it applies a fast cyclic lateral load to structures. The weight of a building increases the lateral loads created by the earthquake, which can cause the building to collapse.

In much of Central America, houses were once built of locally grown or gathered materials. This non-engineered vernacular construction was the result of ancient traditions that evolved over time to form regional solutions. Vernacular construction in Central America includes bahareque (hollow bamboo), timber framing, adobe, and even the prehistoric pyramids made of stone. Each of these construction types has developed over time to resist earthquake devastation. Bahareque and timber-framed houses are very light and flexible and when well tied together will resist earthquake damage with their substantial flexibility. Alternatively, adobe structures and the pyramids with their thick walls rely on a high thickness-to-height ratio to survive earthquakes.

2. Motivation

In Nicaragua, the damage to buildings and other structures from the Earthquake in 1972 remain some thirty years later. Yet while talent and large resources are solving problems related to high tech seismic solutions, it seems as low tech solutions are falling by the wayside. For this reason this study focuses on low cost earthquake solutions for the developing world and Nicaragua seems the ideal place to deploy them.

Also, many improvements have been made to construction materials in the last 100 years. At first glance this would seem to improve the quality of earthquake resistant housing in the developing world but the opposite has been seen. Using higher quality materials allows individual homeowners to build structures larger and with greater spans. However, doing this without the guidance from professionals can lead to unsafe practices and homeowners may have a false sense of security from using higher quality materials.

3. Literature Review of Earthquakes in Nicaragua

3.1. Geography and Plate Tectonics in the Region

All parts of Nicaragua are affected in some way by earthquakes and volcanic activity according to Saint-Amand (1973) and Santos (1973). Nicaragua is located on the western edge of the Caribbean Plate as shown in figure 3.1. The Caribbean plate is a piece of the earth's crust that resembles a small continent, although much of it is covered by the Caribbean Sea. The eastern edge is formed by the Lesser Antilles. The western edge borders the Cocos Plate and forms a portion of the Ring of Fire, shown in Figure 3.2, which dominates the tectonics of the Region. Sea floor spreading of the Cocos Plate to the west and the Caribbean plate to the east apply compressive pressure normal to the Pacific coastline. The spreading which occurs in both the Pacific Plate further north and the Cocos Plates is referred to as the Middle America Trench or the Boundary Plate. The Cocos Plate is being forced under the Caribbean Plate (subduction) at a rate of 6-8 cm per year (Saint-Amand, 1973; Santos, 1973).

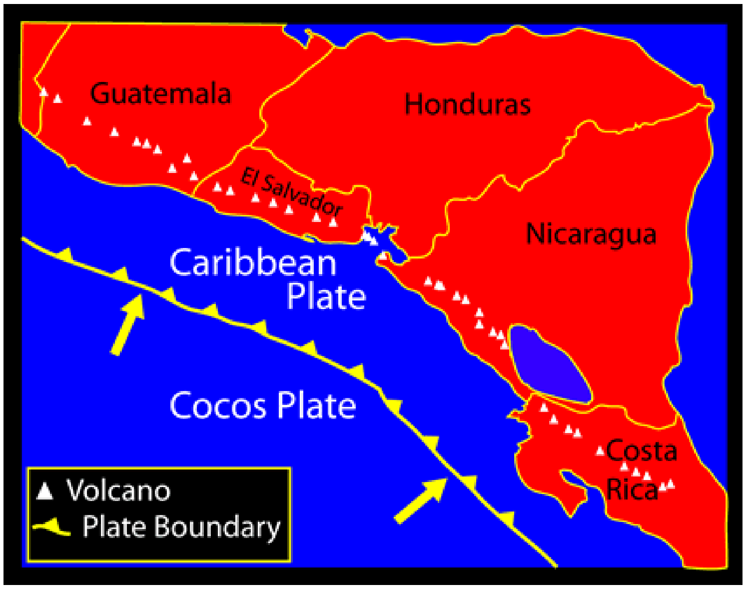

Figure 3.1. Sea floor spreading

http://sio.ucsd.edu/volcano/expedition/cocos.html

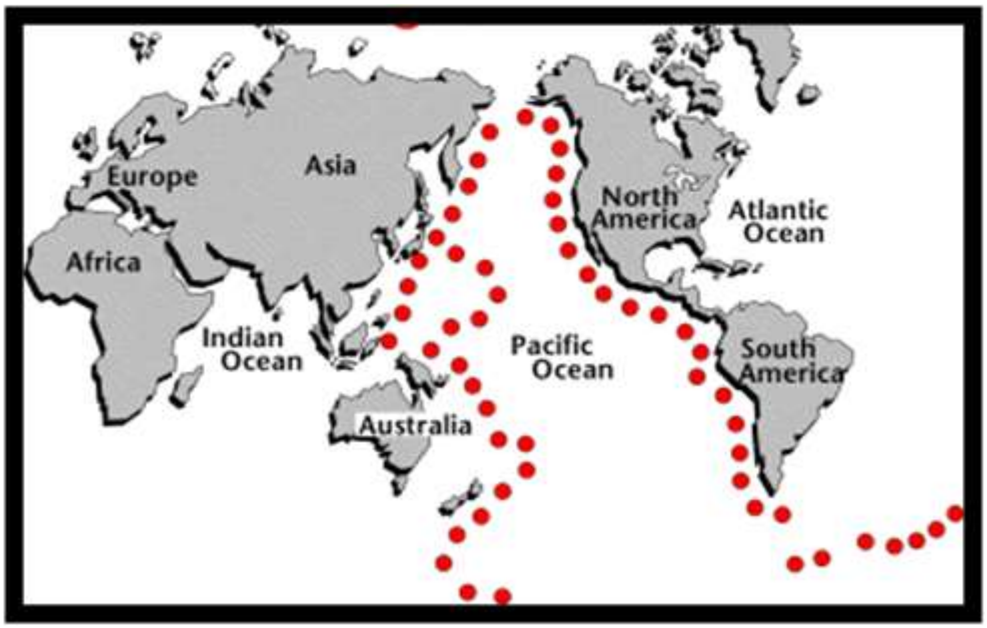

Figure 3.2. Ring of fire

http://www.eia.doe.gov/kids

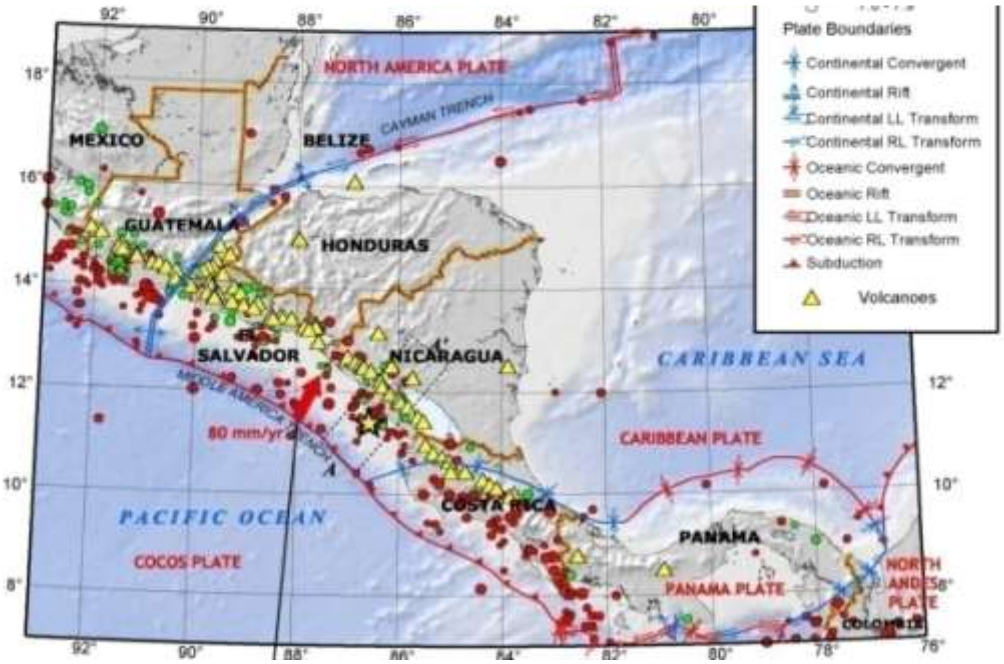

Figure 3.3. Plate tectonics and seismic activity of Central America (USGS, 2007)

Nicaragua can be divided into two distinctive geographies (Saint-Amand, 1973; Santos, 1973). The country's eastern portion is a coastal plain bounded by the Caribbean on the east. The western portion is described by Saint-Amand as an irregular upland composed of tertiary volcanoes and pyroclastics. The average altitude in the highlands is about 500 meters with peaks reaching 1,000 meters and the tallest peaks reaching 1,500-2,000 meters.

The western pacific coast region contains a long central valley called the Nicaraguan Graben (Saint-Amand, 1973; Santos, 1973). "A Graben is a depressed block of land bordered by parallel faults." (Wikipedia, 2009)

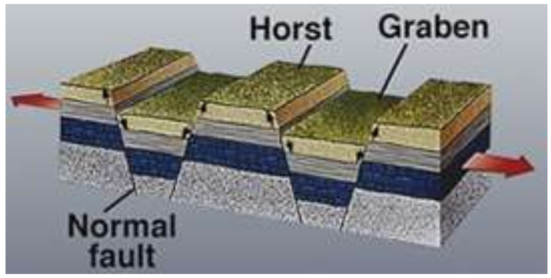

Figure 3.4. Graben

http://en.wikipedia.org/wiki/File:Horst_graben.jpg

The valley is bounded on the northwest by a fault referred to as the boundary fault. The Graben extends from the Pacific Ocean at the Gulf of Fonseca into Costa Rica where it joins with the Costa Rican Coastal Plain.

The great lakes of Nicaragua and Managua lie in the Graben. The Graben is relatively flat except where faulting has caused some relief and within the hills created by the chain of Quaternary volcanoes on the floor of the valley. The Graben is still in the process of formation (Plakfer, 1972).

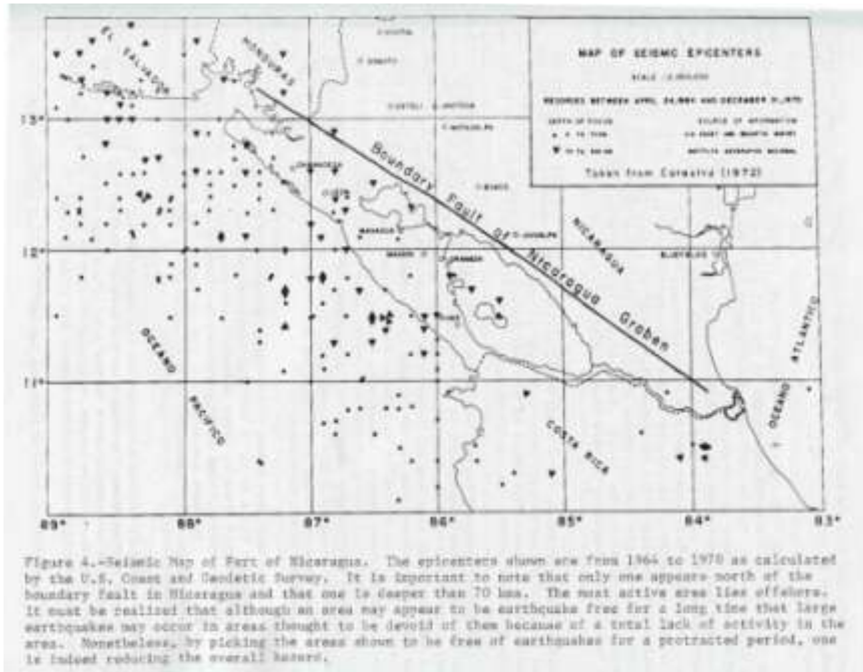

Figure 3.5. Picture of Nicaragua and Graben (Saint-Amand, 1973)

3.1.1. Faults of Nicaragua

The Graben contains a boundary fault nearly parallel with a string of volcanoes called the "Cordillera de Marrabios." From this fault there are many cross faults (Plakfer, 1972; Saint-Amand, 1972)

Figure 3.6. Boundary fault and Cordillera de Los Marrabios (Saint-Amand, 1973)

The faults in the Managua area are well documented and can be seen in the USGS map shown in Figure 3.7. They radiate out of the Cordillera de Marrabios fault.

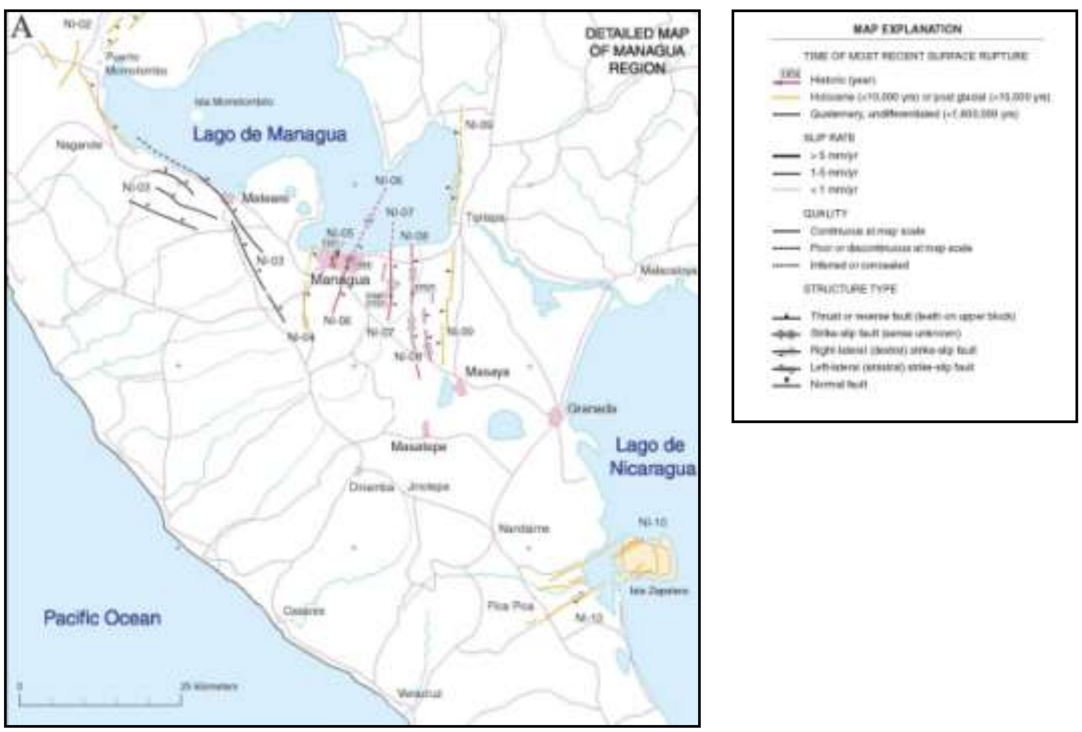

Figure 3.7. USGS map of Nicaraguan faults

These faults are NE-N directed faults which are nearly parallel to one another. This creates very narrow (approx 1 km) blocks of the earth's crust in the E-W direction which are very long in the N-NE direction (Faccioli,1973; Santos, 1973). Santos states that these moving strips of land are the reason Lake Managua is shaped like a number eight.

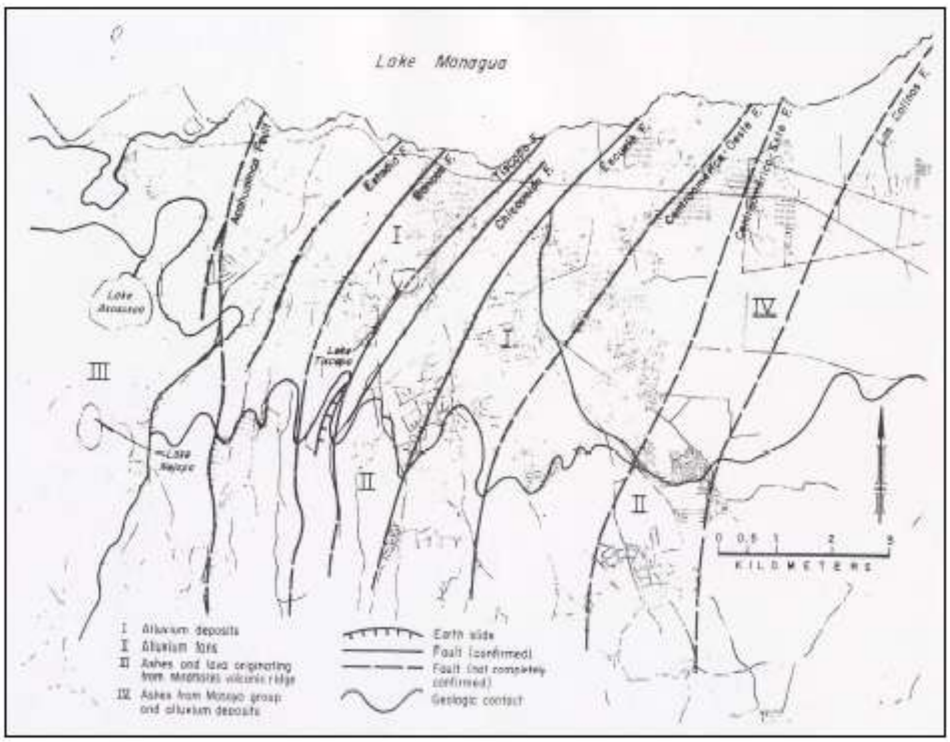

Figure 3.8. Faults of the Managua area as defined by Faccoili, et al (Faccioli, 1973)

3.1.2. Soil Conditions

The city is built on a flat alluvial plain which slopes gently towards the lake (Valera, 1973). The alluvium underlying the city is thought to be several thousand feet thick and consists of thick layers formed by volcanic ash-laden mud flows and thinner beds deposited by streams. Interspersed are also layers of course and fine volcanic rock, as well as cinders and pumice formed during the eruptions of nearby volcanoes.

Foundation investigations performed at various locations around Managua provide valuable information on the subsurface soil conditions (Valera, 1973). Foundation investigations during the years preceding the 1972 earthquake are summarized in table 3.1.

The depth to rock-like material is of interest for the purpose of seismic wave propagation. In the Managua area the rock-like material is called “cantera” or volcanic sandstone, but in fact it is volcanic tuff agglomerate (Valera, 1973). The depth to cantera can be seen in the table and varies between 3 feet and 27 feet.

Since liquefaction can only occur in saturated granular soils it is also of seismic interest to note the location of the water table. It appears that the ground water table is at considerable depth below the ground surface except at the northernmost portion of the city which is adjacent to the lake (Valera, 1973; Plakfer, 1973).

TABLE 2

SUMMARY OF FOUNDATION INVESTIGATIONS

Location No.	Maximum Depth Explored (ft)	Depth to Water Table (ft)	Depth to Cantera(ft)	Type of Foundation	Allowable Soil Pressure kg/cm^2
1	126	61	7	Mat or foot-ings	2.6 to 3
2	38	N.E.[1]	3	Footings	4
3	23	N.E.	6 to 15	Footings	6
4	121	13	71	Footings	1.2 to 2.3[2]
5	40	6	N.E.	Mat or foot-ings	2.0 to 3.5[2]
6	28	N.E.	4 to 9	Footings	4.5
7	24	N.E.	N.E.	Footings	3.5 to 6.5
8	24	N.E.	10	Footings	3.5 to 4
9	67	N.E.	12	Footings	10
10	51	N.E.	42	Footings	4
11	30	N.E.	12	Footings	8
12	26	N.E.	12 to 22	Footings	3 to 5
13	43	N.E.	N.E.	Footings	3 to 4
14	40	N.E.	10 to 27	Footings	2 to 6.5
15	58	17	N.E.	Mat or foot-ings	3 to 3.5
16	75	31	N.E.	Footings	2
17	30	N.E.	N.E.	Mat	1.6[2]

[1] N.E. - Water Table Not Encountered

[2] Effect of Submergence Considered

Table 3.1. Soils in Nicaragua determined from foundation investigations (Valera, 1973)

.

3.2. Past Earthquakes in the Region

3.2.1. Seismic History

According to seismic records recounted by Leeds (1973), seismic activity in

Nicaragua is frequent. From 1520 to 1973 there were some 452 recorded events; of those, 99 are considered destructive based on magnitude (M) > 6.0. The number of earthquakes recorded, both by instruments and by personal accounts, is impressive considering the lack of records and seismic stations for most of that period. The first seismograph was installed in 1961 and no others operated until after the earthquake in 1972 (Leeds, 1973).

The Blume Institute compiled a list of earthquake activity until 1973 (Shah, 1975). The USGS has prepared several maps indicating the seismic events in Nicaragua. Figure 3.9 is a map depicting the earthquake of October 9, 2004. This map also shows all the significant seismic activity for 1900-2002. It appears there has only been one seismic event east of the boundary fault of Nicaragua Graben, which separates the seismically active west side of Nicaragua from the less active eastern half. From the map, the frequency of seismic activity is apparent.

In spite of the lack of instruments and the repeated destruction of records, many earthquakes are mentioned in world literature. Exploring the new world provided many exciting surprises to the Spanish explorers and they documented many of them (Leeds, 1973). The sixteenth century reports are the most complete because this was the Europeans' first exposure to this exciting new world.

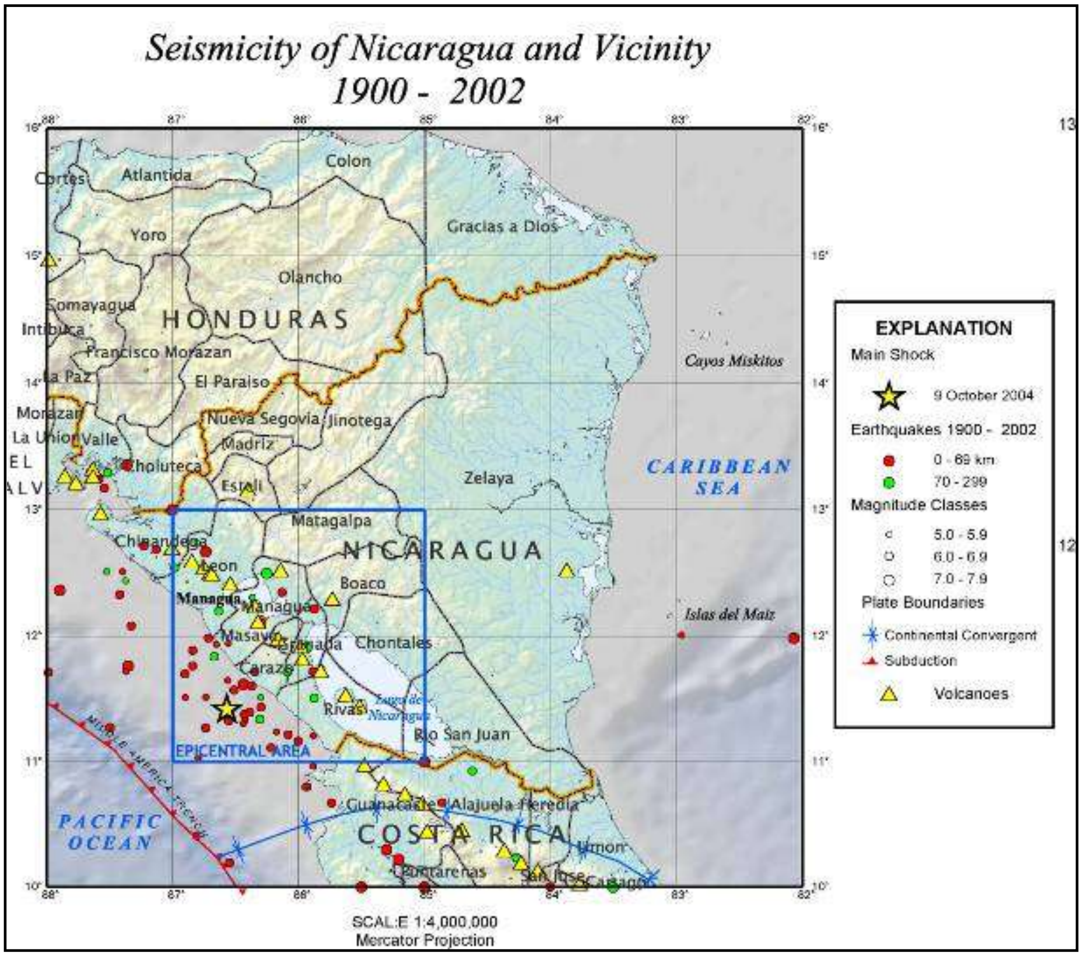

Figure 3.9. USGS seismicity map for the earthquake of October 9, 2004

Interest dwindled during the next two centuries and was rekindled in the 1800's. In 1888 Ferdinand Montessus de Ballore published an exhaustive catalog of earthquakes and volcanic eruptions in Central America. Unfortunately, historical records are a function of 1) the level of perception, and 2) interest of the observer.

Reinoso, et al (2003) compiled a list of the major recorded earthquakes through history. They have been translated and are listed in table 3.2.

Historic Seismic Events	
1528	Earthquake destroys Old Leon, located near Momotombo volcano.
1610	Old Leon again is destroyed by a strong earthquake and is also affected by the eruption of Momotombo volcano. As consequence the city is transferred to its present location.
1648	Strong earthquake causes serious damages in the constructions of Leon; some dead and many wounded.
1663	Destruction of the city of Leon. It was felt with much violence in Granada. It affected the channel of the San Juan's river leaving it unraveled.
1772 (March)	Strong earthquake shakes a great part of Nicaragua, especially Masaya, Granada and Managua.
1844 (May)	Destruction of the city of Rivas; damages in the North of San Juan; alteration of the level of waters of the Tipitapa river and the Lake of Nicaragua; damage in the channel of the San Juan river.
1853	Strong detonation of Santiago volcano; there is telluric movement but no violent agitation of waters of the Lagoon of Masaya, near the wells and Tiscapa.
1865	Strong earthquakes felt in Leon, Masaya and Granada; changes in the topography of the Tipitapa river.
1865 (October)	Earthquakes felt in all Nicaragua. Fracture of the Cathedral of Leon as well as the Government building, the Seminary and other buildings. Damages to the Cathedral of Managua and the Market of San Miguel occur in the city. Damages in almost all of the constructions of Chinandega. Earthquake also felt in San Jose, Costa Rica.

Historic Seismic Events	
1898 (April) 1931 (March) 1938 (April and May) 1950 (July) 1950 (December)	Hard earthquake felt from the Lake of Nicaragua to the Gulf of Fonseca and part of El Salvador. Much damage in the city especially the Cathedral of Leon; in Managua there was considerable damage; destruction of several houses in Chinandega; in Leon destruction of the Church of Guadalupe, damage to the church Santa Ana as well as of schools.
1918 (July)	Strong earthquakes are felt in a large portion of the national territory, especially in Managua, San Francisco of the Butcher, Granada and Masaya.
1919 (March)	Violent seismic activity from the 19 of March to the 12 of December. Major damages produced on the 29th of June: in Leon the bells of the church of Zaragoza fell on one of their towers shattering it, statues fell from their bases; damage of other buildings and houses. In Corinto collapses and cracks in the land and forts took place, roars of the sea, loss of balance of the people in the streets. Felt strongly in Managua, cracking of the buildings and paralyzation of traffic. Other cities where it was felt strongly: Chinandega, Chichigalpa, Granada, Diriomo, Diriá, Masaya, Catarina, Ocotal, Carazo, San Juan Del Sur, Matagalpa, Jinotega and Tecolostote.
1926 (November)	Intense seismic movement affects Managua for nearly a minute. Numerous deaths and injuries; calculation of material damages in 4 million dollars; 50% of its constructions damaged including the National Palace and the Cathedral. The earthquake is felt in a large portion of Nicaragua. Worse damages take place in Leon with 80% of the constructions damaged and others in ruin; collapse of the towers of the old Cathedral and cracking of its walls.
1931 (March)	Destruction of the city of Managua; many injuries and deaths. Ground cracking took place. The earthquake was felt in Granada, Rivas, San Carlos and great area to the West of the country.

Historic Seismic Events	
1938 (April and May)	Series of earthquakes causes great damages in the populations of the West. People evacuated upwards due to the seismic movement. The church of the Laborío in Leon partially collapsed; many damaged houses and others collapsed. In Telica many damaged and collapsed houses; presbiterio of the Church sank. Earthquakes felt in the North zone of the country. In Managua, split of Eastern wall of the second floor of the National Bank of Nicaragua and the elevator stop working; damages in buildings of the Ministry of Interior, Court of the Criminal and National District among others.
1950 (July)	Volcano Telica erupted; tremors were felt in Leon, Chinandega and Managua.
1950 (December)	Strong tremors felt in Chinandega. Black Hill, Telica and Santiago volcanoes erupted. Strong seismic movements felt in the Pacific Coast, from Corinto to Nagarote.
1951 (July)	Earthquake opens crack of considerable size in the cemetery of Granada; destruction of many mausoleos, damages in the chapel of the cemetery, some corpses were unburied by it. Earthquake felt in other parts of the country.
1951 (August)	The Cosiguina and Telica volcanoes erupted. Strong earthquakes felt in Chinandega (August) (with fall of some houses), in Leon, Somotillo, Estelí, Sébaco, Matagalpa, Jinotega, New Segovia, Managua and El Salvador. Eruption of the Conception shakes the Island of Ometepe violently.
1952	Hoyo volcano experienced a violent eruption. Rumblings of the Conception are heard in parts of Granada and Masaya.
1953	Departments of the north affected by violent seismic movements during most all the year; fall of some houses and huída from the inhabitants to other sites.
1954 (February)	Violent tremor felt in almost all the country, except Chontales and the Atlantic Coast. Felt especially in Chinandega and Managua.
1955 (March)	Violent seismic movements felt in Leon, Chinandega, Masaya, Carazo, Granada, Chontales, Boaco, Jinotega, Estelí and Ocotal.

Historic Seismic Events	
1955 (April)	Strong earthquake causes many damages in the West of the country. Damages numerous in Mateare.
1956 (October)	Strong seismic movement is felt in Managua and great part of the coast of the Pacific. Tolled of the bells of the Cathedral. In Diramba the clock of the tower stopped its march.
1958 (November)	Strong tremor felt in Managua, Chinandega, Morazán Port, Corinto, Sandino Port, Rama and Waspán.
1968 (January)	Strong earthquake produced much damage in the Central America colony of Managua. The earthquake in Granada, Masaya, San Marcos, Chontales, Jinotepe, Masatepe and Leon felt.
1972 (December)	Destruction of the city of Managua; more than 10,000 dead and total destruction of the economy of the country that still lingers today.
1984 (August)	Seismic Cluster in Ticuantepe. Visible superficial Fracturing by several kilometers.
1984	Seismic Cluster in Chinandega. Superficial Fracturing.
1985	Earthquake in Rivas with some damages occurred in depopulated zones.
1992 (September)	Tidal wave. More than 100 deaths and strong impact to the national economy.

Table 3.2. Notable seismic events of Nicaragua (Reinoso, 2003)

3.2.2. Earthquake of 1931

Leeds (1973) and Plakfer and Brown (1973) reported that the earthquake of 1972 was not the first earthquake of its type to occur in Managua. There was a strikingly similar earthquake on March 31, 1931, when the population was just 60,000. All earthquake faults related to the 1972 event were roughly parallel to the fault that was mapped after the 1931 earthquake. The instrument records of this earthquake are weak, but re-examination of the local nature of the damage and the surface faulting implies that the epicenter must have been close to the city. The magnitude of this earthquake was low (5.6), but caused considerable damage ($15,000,000) and 1,100 deaths.

In 1931 a number of new buildings had just been constructed and nearly all were severely damaged by the earthquake (Leeds, 1973; Plakfer, 1973). Only the steel frame of the new cathedral was left standing. Fires broke out after the main shock and the main water main leading from the reservoir to the city was pulled apart where it crossed the fault. As a consequence fire fighting capabilities were severely handicapped – a situation comparable to that which occurred in 1972. The national penitentiary collapsed killing everyone except those in the yard. The newly constructed palace of communications was severely damaged and fire gutted the building, destroying all government files except those kept in safes. The new presidential palace was destroyed and parts of it slid into the crater.

Taquezal and stone buildings were generally damaged while wooden and concrete buildings fared well. The aftershocks on April 7, 1931 damaged the few remaining buildings that survived the main event (Leeds, 1973).

3.2.3. Earthquake of 1972

3.2.3.1. General Facts

On December 23, 1972 at 30 minutes after midnight Managua was shaken by an infamous earthquake that was described by Saint-Amand (1973), Plakfer and Brown (1973), Dewey et al (1973, and Leeds (1973). The surface wave magnitude was 6.2 and the body wave magnitude was 5.6. It had a focus depth just 5 km below the surface thus intensifying the damage. The duration of the ground shaking was about 10 seconds. There was an accelerogram at the Esso Refinery west of the city and 4 seismoscopes at various locations around the city that recorded the main shock and some strong aftershocks. The accelerograph recorded maximum horizontal ground accelerations of 0.39 times gravity and several peaks of 0.2 times gravity. The maximum recorded accelerations were 0.39 east-west, 0.34 north-south, and 0.33 vertical. Wright and Kramer (1973) estimate that near the epicenter, accelerations were probably closer to 0.5 times gravity. There were several aftershocks, the largest of which occurred on March 31, 1973 (Dewey et al, 1973; Duke, 1973; Plakfer, 1973; Sint-Amand, 1973; Shah, 1975)

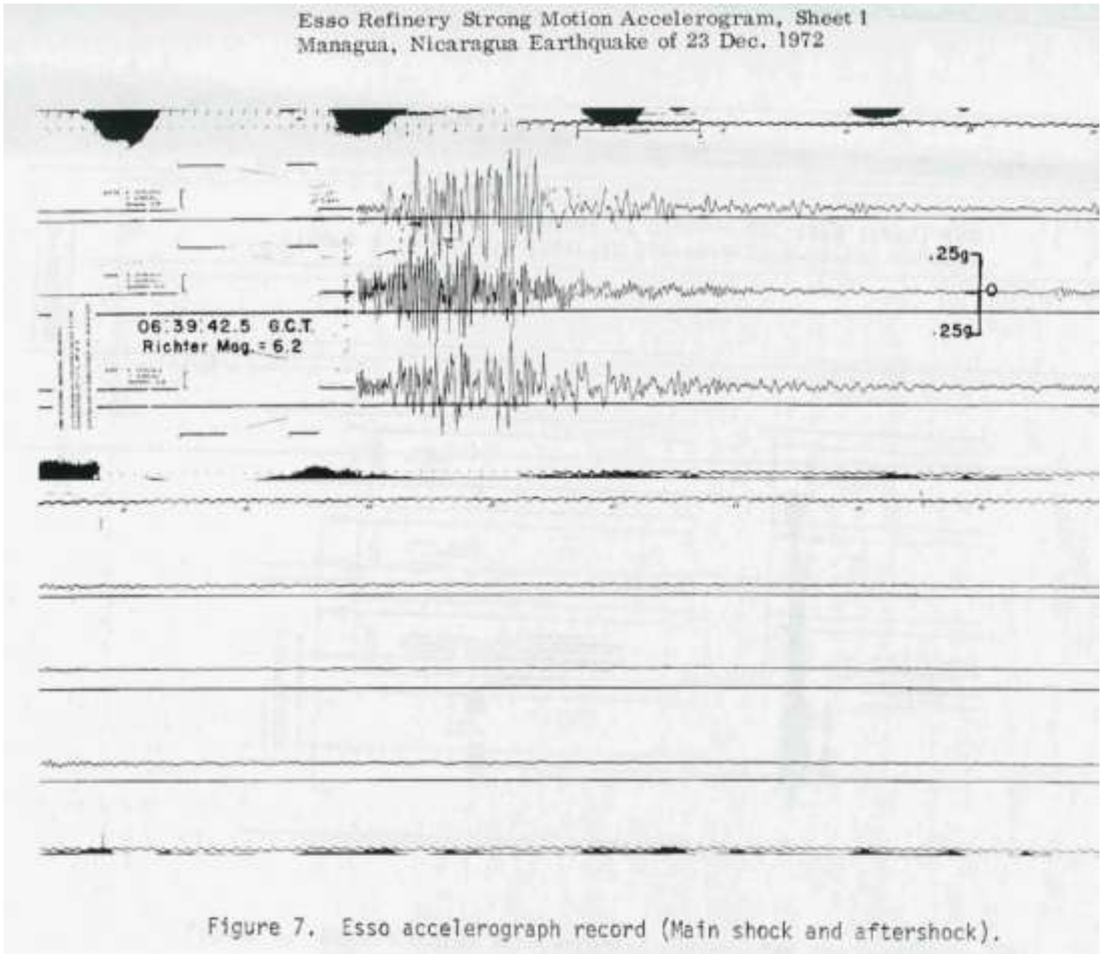

Figure 3.10. Strong ground motion accelerogram from the Esso refinery (Knudson and Hansen, 1973)

Managua, population 450,000, housed 20 to 25% of the population of Nicaragua. Some 8,000 or more people were killed, 20,000 injured and the property damage exceeded one billion dollars (US). This loss was equivalent to 100% of the gross national product. At the time, these statistics were reported by Amrhein et al. (1973), Wright and Kramer (1973), Pereira (1973) and they represented the most severe economic loss that any western hemisphere nation had ever undergone.

Included in the damage was the destruction of the fire department and the rupture of water mains. Several fires broke out days after the earthquake (Amrhein, 1973). Apparently many properties insured for fire were not insured for an earthquake. Between the earthquake and the fires, 600 city blocks of Managua were condemned, cordoned off with barbed wire, and then demolished. This left 7,000,000 m^3 of rubble that had to be removed (Shah, 1975).

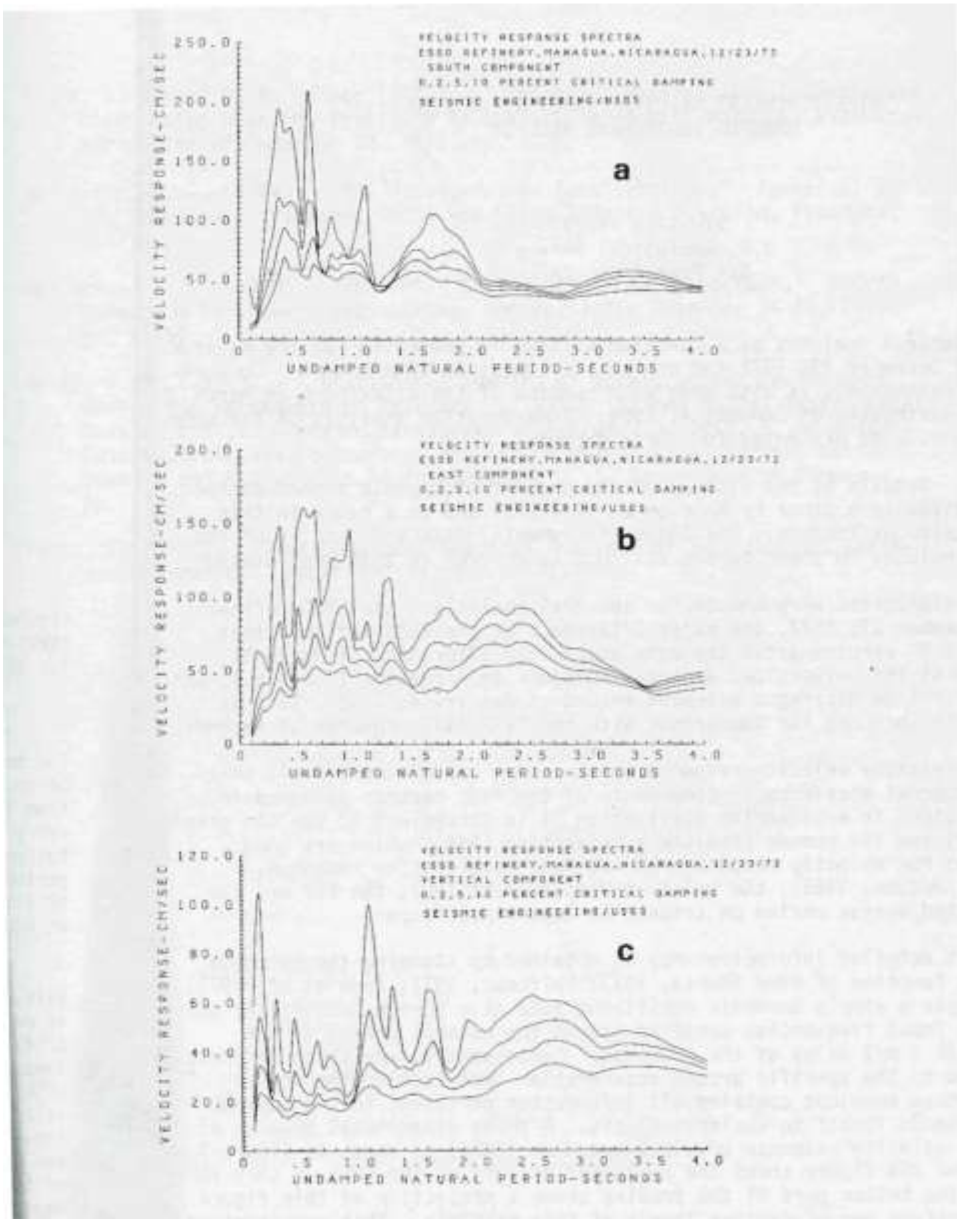

Figure 2. Maximum relative velocity response spectra for the Managua earthquake of December 23, 1972, ESSO Refinery accelerogram.

Figure 3.11. Accelerogram output and response spectra (Shah, 1975)

3.2.3.2. Reports on Shaking

The Managua earthquake created minor ground cracking in a broad area in the center of the city (Meehan, 1973). Several types of cracking were identified including faults, landslides, and local subsidence associated with settlement and compaction.

Surface fault ruptures and offsets occurred along two major and two minor parallel fault traces. The two major faults (A and B) were nearly parallel and about 400 meters apart. They both passes through densely populated areas of the city. The smaller faults (C and D) are nearly parallel to the major faults, but are smaller in length and offset. The faults can be shown in the Figure 3.12.

The two main faults (A and B) varied in width from 3' to 25'and were offset with a left lateral slip with a maximum slip of 12" (Meehan, 1973). Pierre Saint-Amand (1973) reported the main surface fault break was 6 km long and exhibited left lateral displacement up to 38 cm. There were also three other breaks, parallel to the main break, one of which went right through the densest part of the downtown area. In total, there was some movement of 9 different faults in the urban area.

An area of 36 square km including most of the city experienced shaking of degree VII or greater on the Modified Mercalli Scale (1956 version). Within this zone there were three zones of approximately one-half square km which experienced VIII or greater (Duke, 1973; Hansen, 1973).

The shaking was recorded as is shown in figure 3.13.

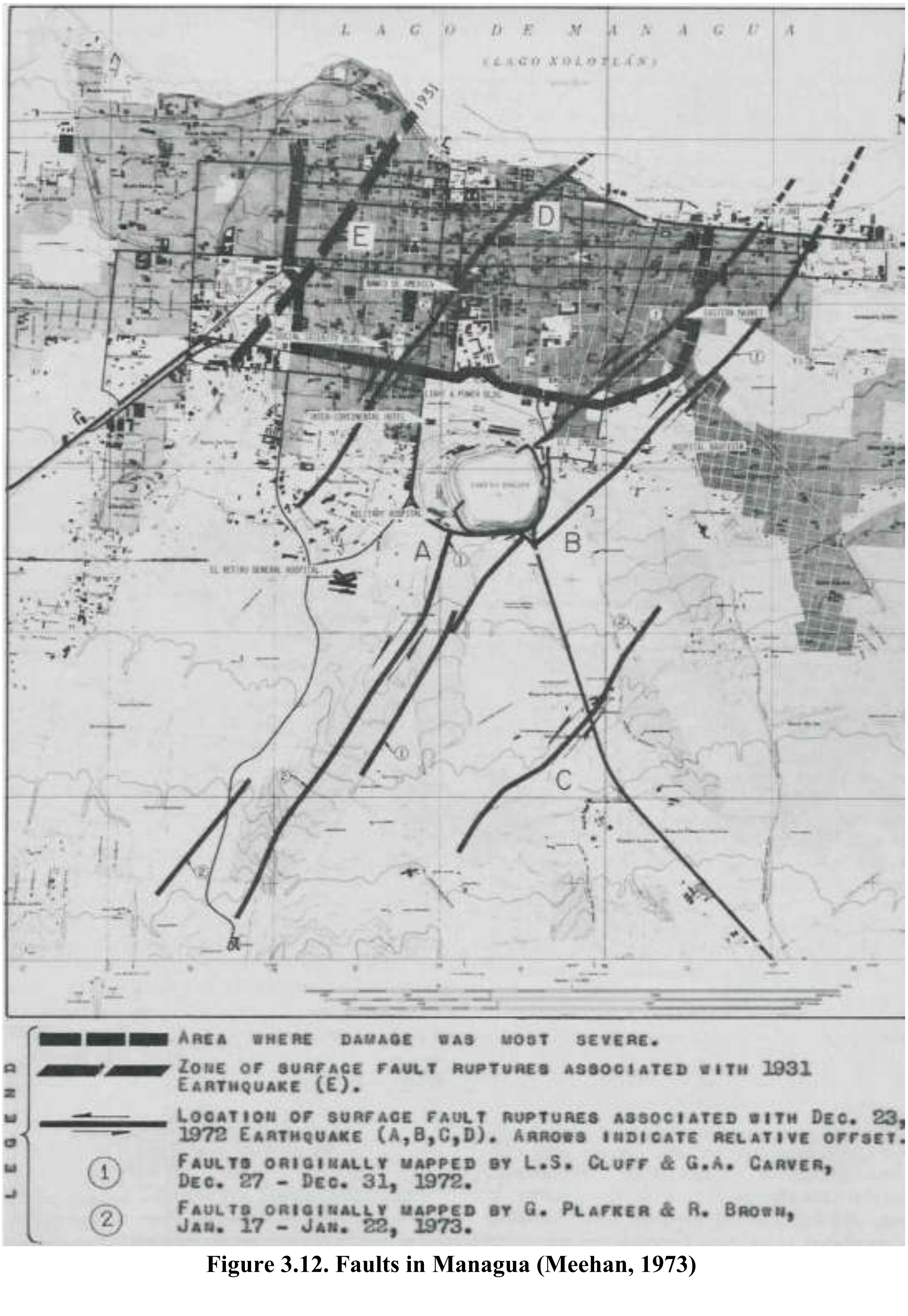

Figure 3.12. Faults in Managua (Meehan, 1973)

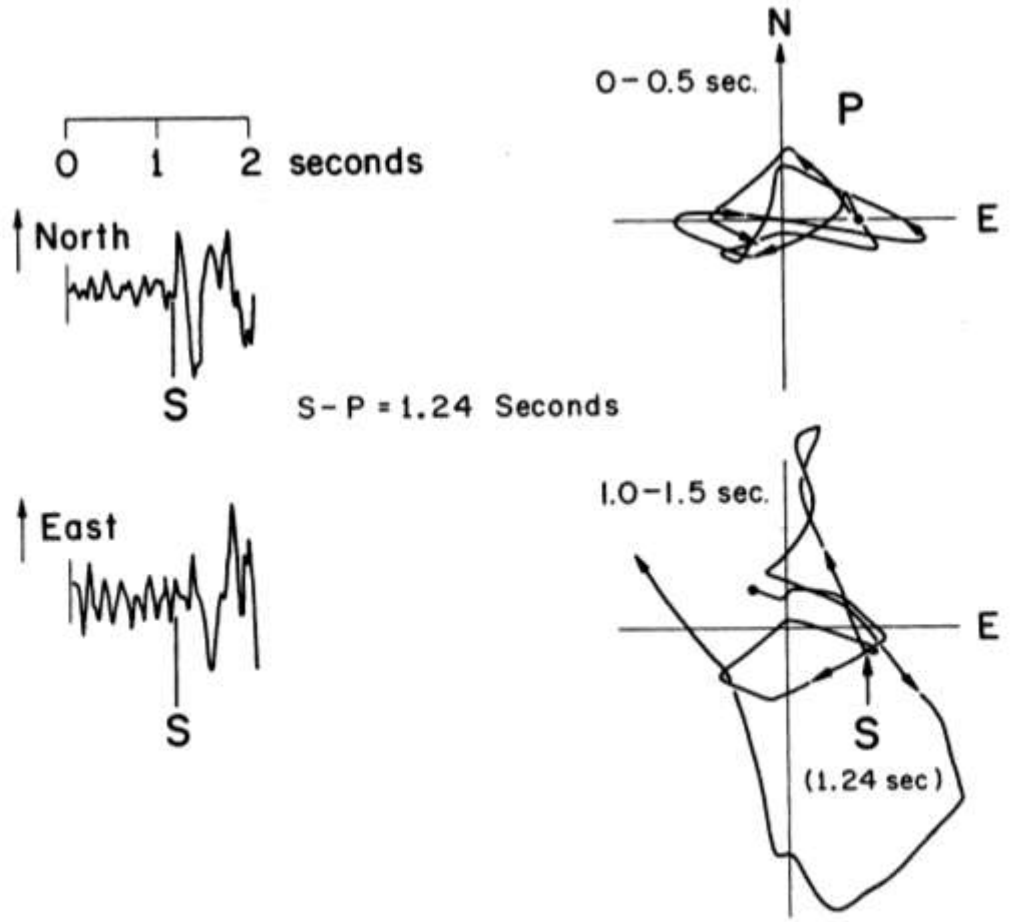

Figure 2. Left: horizontal components of first two seconds of ESSO refinery accelerogram. Right: particle motion from 0. to 0.5 seconds and 1.0 to 1.5 seconds after record beginning.

Figure 3.13. Record of ground motion (Dewey et al, 1973)

There were two areas of increased shaking (Saint-Amand, 1973). In the cementario San Pedro, the movement appeared to be almost vertical and must have been close to 1 g in vertical acceleration. Many heavy gravestones and monuments bounced of their pedestals and then continued to bounce after falling. Another area of intense shaking was found 4 blocks south of the Banco de America. In these two areas shaking reached IX to X on the Modified Mercalli Scale. The zone of intense shaking extended under Lake Managua and it is likely that the center of shaking was on the lake shore. This assessment also agrees with the isosimal map produced by Hensen (1973).

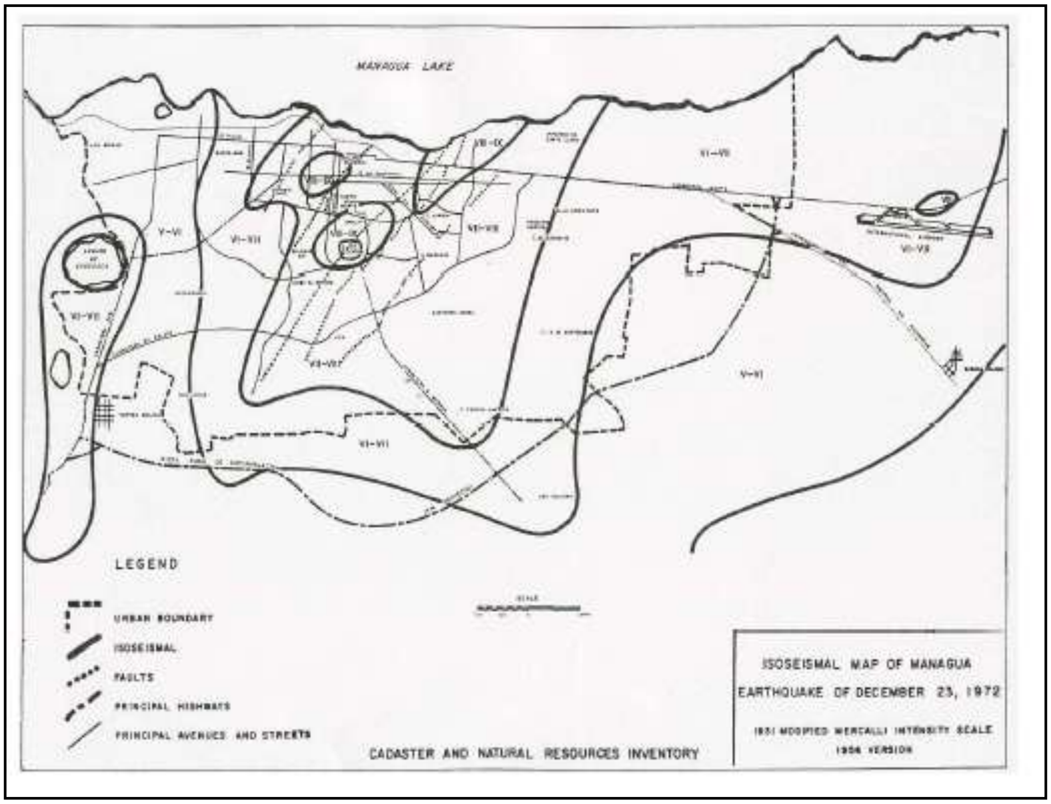

Figure 3.14. Isoseismal map of Managua (Hansen, 1973)

Dewey, et al (1973) shows a slightly different map of the shaking based on observations and aerial photographs.

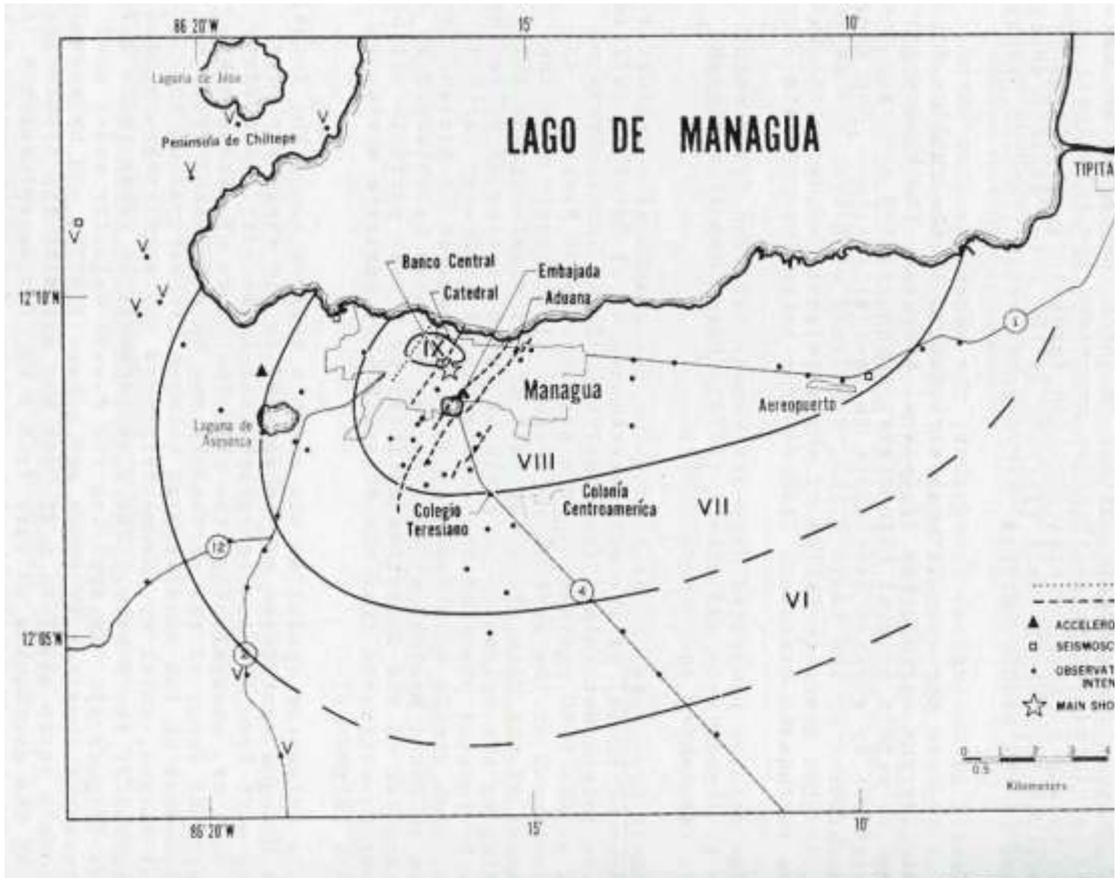

Figure 1. Isoseismal map, Managua earthquakes of 23 December 1972. Dashe are fault traces from Brown and others (1973).

Figure 3.15. Isoseismal map (Dewey et al, 1973)

With the P-Wave and S-Wave arrival times taken at the Esso Refinery accelerograph, the epicenter was determined to be no further than 6 km from the accelerograph (Ward, 1973). The location of the epicenter was found by analyzing aftershocks. This epicenter can be seen in figure 3.16.

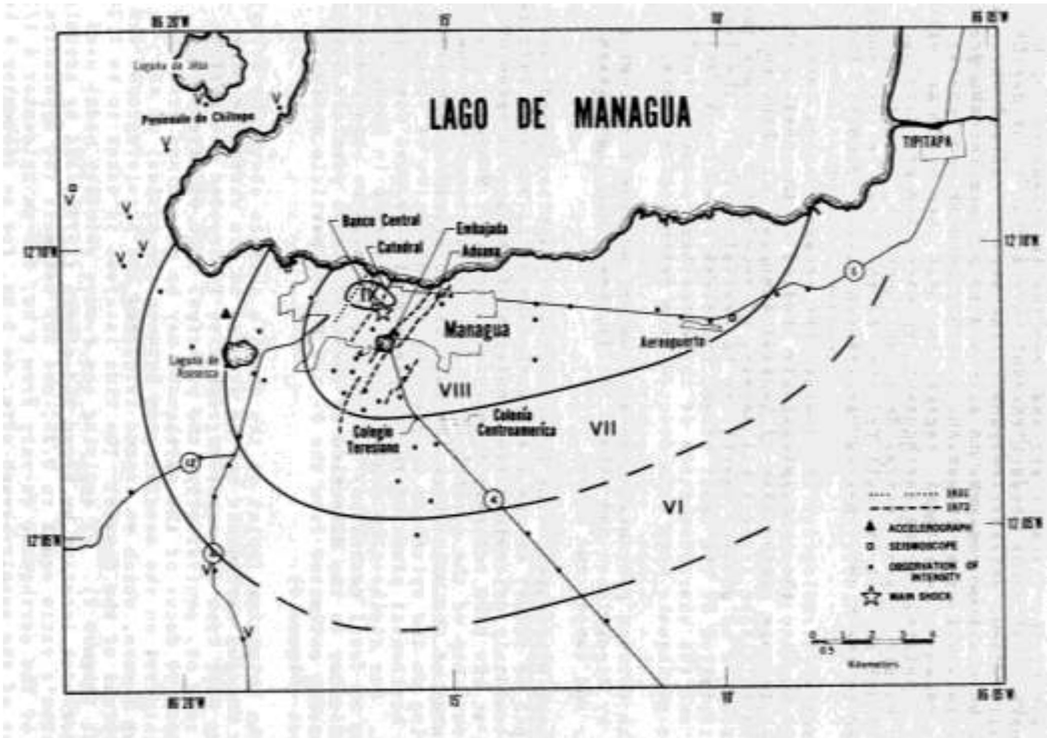

Figure 1. Isoseismal map, Managua earthquakes of 23 December 1972. Dashed lines are fault traces from Brown and others (1973).

Figure 3.16. Epicenter location (Dewey et al, 1973)

People were asked to describe the shaking they felt during the main shock. “They reported: a series of short vertical shakes, followed quickly by horizontal motion of no distinct direction and after a few seconds, and at the end of the severe shaking, a definite downward drop ‘as if the bottom had fallen out’” (Saint-Amand, 1973).

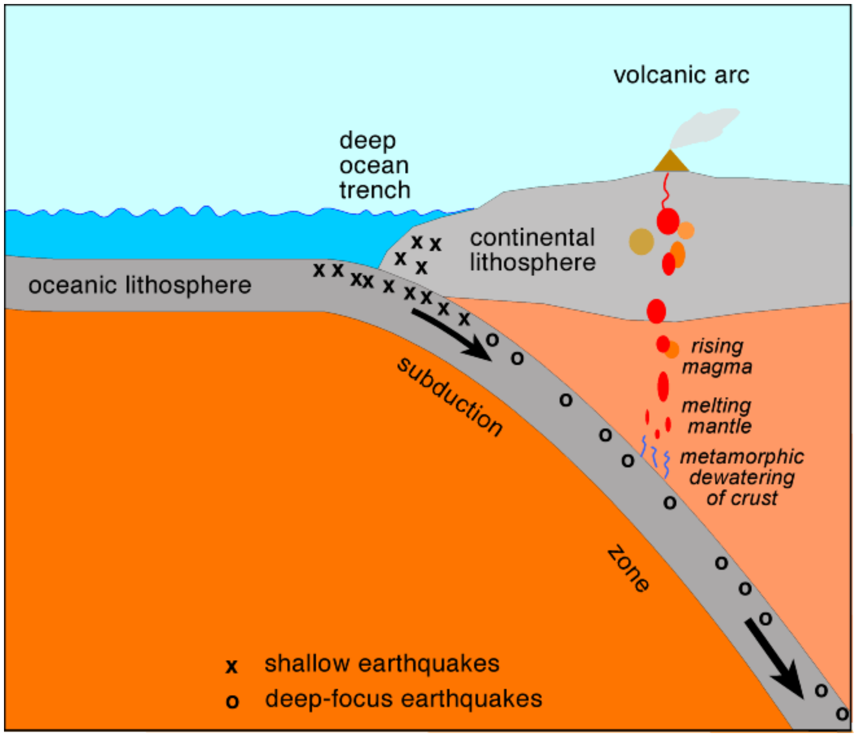

Figure 3.17. Subduction

http://myweb.cwpost.liu.edu/vdivener/notes/subd_zone.htm

J.W. Dewey et al (1973) reports the Managua earthquake of 1972 was a member of a class of Central American earthquakes called "shallow-focus volcanic terrane earthquakes" that occur in or near regions of Quaternary volcanos at shallow depths of focus. They differ from the more numerous "shallow-focus Benioff zone earthquakes" that occur west of the volcanos, and also from the intermediate depth earthquakes that occur beneath the volcanic arc at great depths. These "shallow-focus volcanic-terrane" earthquakes of Central America tend to be small in size and produce intense ground shaking in small areas. Because they occur in densely populated areas, they are the principal seismic hazard for Central American countries even though they account for a small portion of the seismic energy in the area.

It was later determined that this earthquake was a left-lateral strike-slip fault rupture on a fault that strikes northeast (Dewey et al, 1973). The fault surface upon which the significant portion of seismic energy was released was probably about 15 km long and extended from the surface about 7 km in depth. The foreshocks were not large enough to trigger the seismograms for La Palma, El Salvador and therefore the magnitude must have been smaller than 3.5. There were two large aftershocks within an hour of the main shock with Mb of 5.0 and 5.2. The hypocenters, or origin below the surface, of these aftershocks lay near that of the main shock. In addition to the main fault line there were at least three other fault lines. These can be seen on the map in figure 3.18 (Plakfer, 1973).

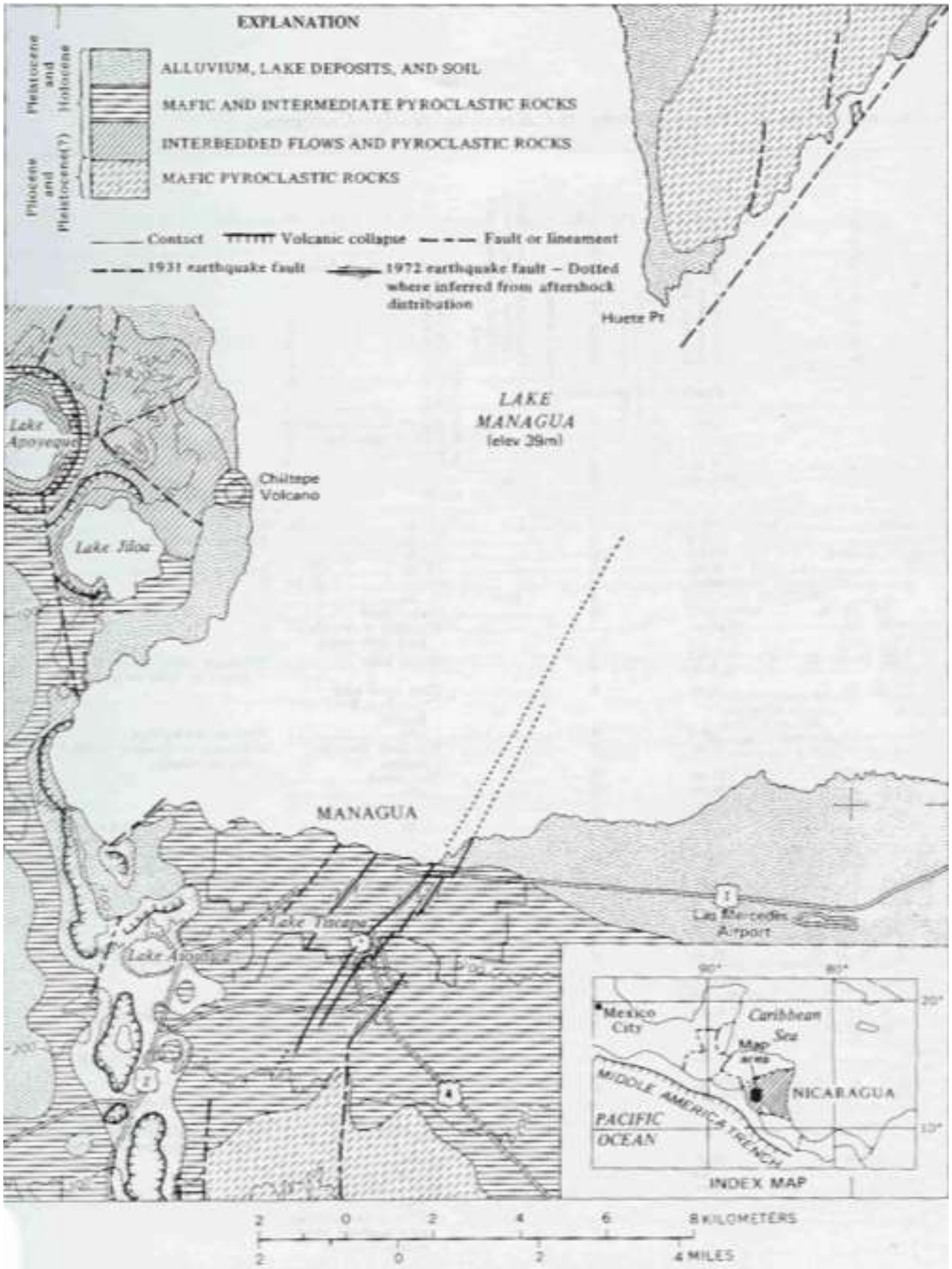

Figure 3.18. Managua faults (Plakfer, 1973)

3.3. Performance of Structures During Past Earthquakes

3.3.1. Construction Practices Following the 1931 Earthquake

Chamorro (1973) describes the earthquake of 1931 as destroying most buildings made of adobe and stone construction, while the taquezal construction fared better. Partly because of this and partly because it was a vernacular solution to the construction problem, taquezal became the primary type of construction for the next 15 years. During that time, some twenty concrete buildings and a few steel buildings were constructed in the city of Managua by foreign engineers (Chamorro, 1973). Figure 3.19 shows an example of taquezal construction.

Figure 3.19. Taquezal construction, Rivas, Nicaragua

3.3.2. General Performance of Buildings Following the 1972 Earthquake

The performance of the buildings of Managua during the earthquake could be recounted in great detail. Instead, some trends in building materials, design, and construction have been summarized. There were all the same structural failures that have been seen throughout the world and these were reported by Wright and Kramer (1973), Sozen and Matthiesen (1975), Meehan et al. (1973), and Amrhein (1973), and can be summarized to include:

- Pounding between adjacent buildings
- Failure of short columns in shear (typically in school buildings)
- Soft story failures
- Lack of quality connections (especially to diaphragms)
- Ties and development to improve ductility
- Poor performance of unreinforced masonry
- Non-structural masonry which changes the behavior of the structure
- Excessively heavy roof systems
- Torsional effects

3.3.3. History of Structural Engineering in Nicaragua

Nicaragua won independence from Spain in 1821. In 1854 Managua -- a small village at the time -- was made capital of Nicaragua (Duke, 1973). Duke (1973) goes on to explain that the professions of architecture and engineering were rarely encountered in Nicaragua until after the 1931 earthquake. The building styles that emerged since the 1940's are of foreign origin. In the 1950's the design professions began to evolve and then in the 1960's high rise buildings began to be constructed. During this time earthquake resistant design was introduced by a number of engineers and architects, but it was not required by local building codes (Duke, 1973).

Chomorro (1973) describes the times at the end of the Second World War there was a…"…great change in the construction industry in the country. At that time a new generation of young architects and engineers were ready to take command of the construction industry, and were substituting the tradional local builders in most important construction projects. Also, around this time, the recently founded engineering school was graduating its first class.

> For the first time Nicaraguan architects and engineers were planning, designing, and constructing, totally on their own, their first generation of buildings…. (they were) handling new materials and types of construction without much experience or tradition to support them. Usually work was started with only general plans, including structural plans, which were completed as work advanced. This type of organization, although very common in some countries, at times of rapid technological changes, does not produce the best overal results, specifically, at times of rapid technology changes, or to complex problems like earthquake design. New styles and methods of construction introduced to the country. Reinforced or partially reinforced masonry replaced taquezal as the main type of construction, and reinforced concrete became of common usage. Although engineers were aware of the earthquake problem, buildings were generally designed, frequently, only for gravity loads. Design was based solely on strength requirements, using ACI or other foreign codes as a reference. Since stiffness was not a design criteria, the trend was toward slender structures (Chomorro, 1973).

Chomorro explained that “Seismic forces were used, probably, for the design of some buildings, but not very frequently.” Also, because most buildings were reinforced concrete frames, engineers did not have much training and experience with the design of braced steel and timber structures (Chomorro, 1973). This meant that engineers did not have frequent exposure to load paths, even in simple structures. Consequently, diaphragm, chord, and connection stresses were often not well detailed. This was not critical while engineers were designing reinforced concrete structures with solid slabs, but later when precast construction was used, these stresses and details became critical and were often overlooked (Chomorro, 1973).

During this time (around 1940) there was little local professional engineering tradition in the country (Chomorro, 1973). Thus there was, no body of knowledge, no training or experience that is normally found in engineering offices, no universities, no regulatory agencies, or even a building code in common use. "To complete the perspective, one should also keep in mind that there exists a time lag of about 10 to 20 years, in the office design practices …in relation to the current knowledge of countries of advanced technology" (Chomorro, 1973).

Chomorro (1973) goes on to explain, during the 1960's engineers became aware that it was inefficient to maintain the old master-builder type organization and it made it more difficult to stay informed of new technologies. A group decision was made to separate engineering design practice from construction work. This was a monumental decision even for a country where a most of its construction is made of one and two story structures. As a result there was a general improvement in building practices. Designs and plans became more detailed and often the Uniform Building Code was used as a design standard; modern and reliable methods of construction were more frequently used; supervision of construction improved; and private laboratories for soil testing and quality control became available for the first time to practicing engineers (Chomorro, 1973).

However, designs were still based mainly on strength requirements and little thought was given to attaining proper stiffness, or to distribution of this stiffness among stories or elements (Chomorro, 1973). Due consideration was not given to: relative or sudden changes in stiffness, torsional requirements, drift control, or pounding between adjacent buildings.

The performance of the buildings of Managua during the earthquake could be recounted in great detail. Instead here is a summary of trends in building materials, design, and construction. There were all the same structural failures seen throughout the world. These failures include (Shah, 1973; Klopfenstien, 1973; Meehan, 1973; Amrhein, 1973; OES, 1973):

- pounding (or contact) between adjacent buildings
- failure of short columns in shear (typically in school buildings)
- soft story failures
- lack of quality connections (especially to diaphragms)
- ties, and development to improve ductility
- unreinforced masonry
- non-structural masonry which changes the behavior of the structure
- excessively heavy roof systems
- torsional effects

3.3.4. Performance of Taquezal Buildings

Duke (1973) described taquezal "the indigenous housing construction, called taquezal, consists of earth infilled between closely spaced wood elements and is usually limited to one or two stories." Teran, (1973), Amrhein et al (1973), and OES (1973) all have similar decriptions of taquezal. The roof is constructed of timber frames covered by heavy Spanish colonial tiles. The walls are framed with vertical timbers approximately 4" x 4" or 6" x 6" approximately 24" on centers and completely covered by horizontal slats of wood (approximately 8" on centers) and filled with mud, stones, clay bricks, or other available material. The word taquezal means pocket in Spanish and construction is so named because the "pockets" are filled with mud. The entire surface is then plastered with mortar made of mud with some lime, finely stuccoed and painted. This type of construction has good insulating properties to combat the tropical heat but is overly heavy and does not have any cross bracing.

Teran (1973) reported that taquezal construction was devastated by the earthquake in 1972. 95% of the total number of deaths occurred in taquezal structures. Several American engineers have stated that taquezal construction should not be used in earthquake areas. Amand stated "Damage to houses make of taquezal was extreme!"

Amrhein et al stated "This mode of construction (taquezal) was the major cause of the high death toll and, as stated previously, should be banned in earthquake-prone areas such as Managua." Still some engineers have a different view. Periera and Creegan (1973) stated "By way of history, taquezal had performed well in the terremoto of 1931 - and because of that record was the popular structural system during that reconstruction. For all that you will hear about it, it is our position that when properly designed, constructed and maintained taquezal is a fine system….and very appropriate for the tropics – especially in the pre "air-conditioned" era." But the operative words in that description are "designed" and "maintained." There were a lot of bad connections in the taquezal homes. But perhaps more importantly, the timber structure hidden under plaster and in intimate contact with earth since its construction was rotten (Periera and Creegan, 1973). Dry rot, insect damage and water damage was the general condition. The implication here is that these structures would not have been killers had the terremoto of 1972 been in 1936. Therefore the lesson to be learned relates to maintenance.

3.3.5. Performance of Concrete and Masonry Buildings

3.3.5.1. Small Concrete Structures

Small concrete structures failed because of a lack of reinforcement, poorly connected reinforcement, and inadequate ties and stirrups, as reported by Saint-Amand (1973). The concrete itself was not as strong as it should have been because it was made with pumice (piedra pomez) used as sand and aggregate. Pumice is soft and easily fractures, doesn't absorb the cement paste and reacts with the reinforcing steel. In 1931 engineers stated that pumice should not be used in the mixing of concrete.

3.3.5.2. Hollow Clay Tile

Hollow clay tile was used extensively in Managua for walls, partitions, frame infills, and below windows as spandrels. Amrhein et al (1973) reported the tile performed poorly. In most cases these walls were considered non-structural but in fact they changed the response of the structure from a flexible frame to a rigid shear wall system. The result was a decrease in the natural period of the building and therefore increased the seismic response of the structure.

3.3.5.3. Concrete Block Masonry

Concrete block masonry was used in Managua for both structural and nonstructural walls, as recounted by Amrhein et al (1973). There were two types: specified block – which meet some strength requirements and unspecified block – which was used in housing and unimportant commercial or industrial projects. Concrete block construction fared better than hollow clay tile, but did sustained considerable damage. The workmanship was generally poor and there often was no mortar in the head joints, joints were not tooled, walls were unreinforced and not tied to frames, etc. There were exceptions for instance larger buildings such as the Esso Refinery, where the headquarters laboratory building showed great workmanship.

3.3.5.4. Brick Masonry

Brick masonry, as reported by Amrehein et al (1973) and Berg and Degenkolb (1973), was generally well detailed and showed good craftsmanship when exposed and didn't when covered with plaster. As one would expect, the exposed brick performed well and the covered brick did not. The workmanship and detailing of confined masonry buildings also generally followed this trend. There was a housing addition, still under construction, where the infilled concrete blocks were not well attached to the frames and the infilled blocks failed.

3.3.5.5. Reinforced Concrete Buildings

Reinforced concrete buildings and their connection details varied in quality from excellent to poor according to Amrhein et al (1973). The Bank of America building is an example of excellent performance and the Estadio General Somoza Stadium was an example of poor performance. The stadium had inadequate steel ratios and anchorage.

3.3.5.6. Pre-cast Concrete

Pre-cast concrete also showed inadequate construction (Amrhein et al, 1973). The pre-cast elements themselves were of good quality but were often not well attached or were supported by weak members. For example there were several housing tracts that were made of pre-cast elements. Many of the roofs slipped off completely. These pre-cast roof elements were held in place primarily with gravity connections. In some instances there was only a 2” long x ¼” weld holding them in place. These housing tracts were generally “a house of cards” (Amrhein, et al, 1973).

There was also a general lack of inspection of construction (Amrhein et al, 1973). Serious discrepancies between design plans and actual construction existed. For example, the Intercontinental Hotel plans called for 6” thick cast concrete exterior walls, instead unreinforced concrete masonry walls were built. Also, often connection details were flagrantly different from the plans and inadequate connections were apparent in most construction. After considering all the faults of the different types of concrete and masonry buildings, it is worth noting that these failures caused few deaths.

3.3.6. Performance of Tall Buildings

The tall buildings in Managua were well studied after the earthquake. Instead of going into the details of each building, some general trends will be restated.

There were several low to moderate rise buildings in Managua that were designed generally in accordance with American design standards of the time. These buildings generally performed well and prevented loss of life. However the structural and non-structural damage varied.

3.3.6.1. Shear Walls vs. Frames

There were several comparable buildings in Managua that differed in the structural systems reported by Sozen and Matthiesen (1975). Some were constructed with shear walls while others were constructed with frames. A good example of this difference in framing and performance is the contrast between the Banco de America building which was constructed with four stiff shear walls at the core and the Banco Central building which relied on frames for lateral resistance. Both buildings sustained some damage, but the Banco de America building (shear walls) remained virtually intact while the Banco Central building (frames) interior was a complete shambles. In fact the Banco Central building deflected so greatly that it jammed most of the doorways, thus blocking exits. If the earthquake had occurred in the middle of the day and been followed by a fire this would have been devastating.

Figure 3.20. Banco Central on left and Banco de America on right (Sozen and Matthiesen, 1975)

This was shown again when comparing the Enaluf building with the La Protectora building and the INSS building. The Enaluf building utilized both shear walls and frames while the other two buildings relied on frames alone. Although there was some damage to the Enaluf building the same performance pattern was repeated (Wright 1973; Sozen and Matthiesen 1975).

Figure 3.21. ENALUF (Light and Power) Building, notice the soft first story (Sozen and Matthiesen, 1975).

3.3.7. Soil Failures

From a soils engineering point of view, the Managua earthquake did not produce any spectacular damage such as liquefaction or large landslides, according to Duke (1973) and Saint-Amand (1973). There were some isolated landslides that took place on the steep slopes of the calderas of Laguna Tiscapa and Laguna Asososca. The crater of Volcan Tiscapa was the site of some substantial buildings including the presidential palace and the US Embassy. The structures and roads in this area suffered considerable damage. This was nearly identical to the damage that occurred during the 1931 earthquake. It was recommended that this area should not be rebuilt.

Plakfer (1973) and Valera (1973) reported that although Managua rests on a thick deposit of unconsolidated materials, there was no obvious damage related to differential compaction, liquefaction, and lateral spreading of foundations. This is probably because of the permeability of the predominantly volcanic deposits, the low water table, an unusually dry rainy season preceding the earthquake and the short duration of shaking. There was some minor settlement of soils and these were mostly limited to man-made fills. These included Theater Ruben Dario, Banco Central, the road around the Asococsca crater and the Esso Refinery, but all failures were minor.

Managua gets all of its water from Laguna Asososca. The intake structure for the water supply system was located at the bottom of a steep slope where some land-sliding occurred. If the landslides had been more severe, the entire water supply could have been destroyed at a very critical time (Valera, 1973).

3.3.8. Emergency Services

Most critical facilities in Managua were destroyed by the earthquake. The following are grim examples (Shah, 1975):

- The fire station collapsed trapping the fire-fighting equipment.
- The Red Cross building collapsed on their ambulances and supplies.
- The INSS Hospital suffered enough damage to render it not only useless but also hazardous to its occupants.
- The General Hospital was severely damaged but fortunately many supplies were stored in a warehouse building behind the hospital. Most of the supplies were on steel shelves which supported the building when the walls fell and columns sheared.
- Radio communications were run through a very weak building but fortunately it was far enough outside of town that collapse was incipient rather than actual.
- Also, the vital switch gear at the power plant was located in a weak masonry building which was close to collapse.

3.4. Seismic Building Codes in Nicaragua

In April 1972, the first lateral force code, a modified version of the SEOAC (Structural Engineers Association of California) Code, became law in the country, but its regulation never took effect. After the earthquake of 1972, there was great enthusiasm for updating the building stock and ensuring the safety of the occupants. Today there is a modern seismic code in Nicaragua and large buildings and government offices may be built to these codes, but it is still possible to build residential and commercial structures without complying with these codes. The seismic code breaks the country into 6 zones. The map is shown in Figure 3.22. Figure 3.23 shows the current USGS seismic hazard map for Central America. The modern map shows some slight differences, but is generally in agreement with the map from 1973.

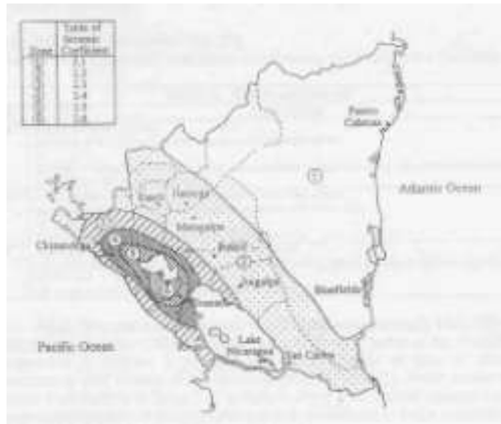

Figure 3.22. Seismic zones of Nicaragua

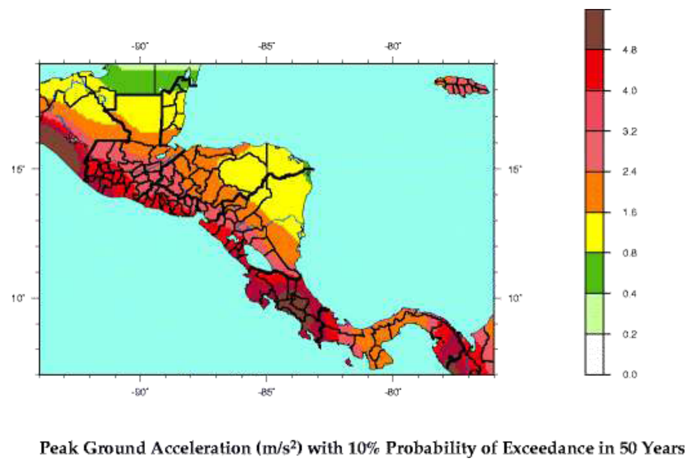

Figure 3.23. Future seismic predictions
http://neic.usgs.gov/neis/world/central_america/gshap.html

Dewey et al (1973) states “On the basis of our present knowledge we must regard the entire western portions of the Nicaraguan depression and associated volcanic terrain as being equally likely to experience a shock similar to that which struck Managua.”

Dewey et al (1973) describes, there are three types of earthquakes that could strike Nicaragua, the shallow-focus volcanic terrain earthquake similar to the earthquake that struck in 1972, large intermediate depth inland earthquakes beneath the Nicaraguan mainland, such as the magnitude 7.2 (PAS) shock of 1926, and larger off-shore earthquakes from the Benioff zone.

The shallow-focus volcanic-terrain earthquake zone associated with the region's Quaternary volcanism is the most significant seismic hazard in Nicaragua. This type of earthquake can be expected to be comparable in magnitude to that of 1972 and 1931 and can reasonably be expected every 50 years. Some of these earthquakes will be accompanied by surface faulting like that which occurred in 1972 and 1931. The maximum hazard from surface faulting is along the trace of know active faults, of which there are 5 or more. In terms of the damage they cause, secondary effects such as slope failure, liquefaction, and compaction will be far less significant than damage from shaking and fault displacement (Plakfer and Brown, 1973).

Larger earthquakes are possible from other fault zones (Leeds,1973; Dewey et al, 1973). These can create earthquakes as large as 8.0 and can be expected every few centuries. These will not occur on the faults under the city of Managua but aftershocks will occur near the city and could be destructive. While more infrequent, large off-shore earthquakes may cause damage to long-period structures.

Managua has a slight possibility of renewed volcanic activity (Saint-Amand, 1973). However, the areas of Leon and Granada have a higher level of hazard from volcanic activity and from large earthquakes than does Managua but damaging earthquakes will be less frequent.

3.5. Seismic Hazard Studies

In 1975, researchers affiliated with John A. Blume Earthquake Engineering Center (Shah et al., 1975) constructed a complete hazard analysis for Nicaragua. There were two main sources considered, the National Earthquake Information Center (NEIC) and National Oceanic and Atmospheric Administration (NOAA) data files covering the period from January 1900 to August 1973, and the Catalog of Nicaraguan Earthquakes, 1520-1973 by Leeds (1973). Between these two sources, seismic activity data was gathered for 73 years for the whole country and 123 years for the earthquakes associated with volcanic activity associated with the Cordillera de los Marrabios. There were 466 earthquakes with complete data and they were plotted as a function of depth. From these plots seismic sources were isolated. The general seismic pattern of Nicaragua was divided into the following regions:

- **The Benioff Zone** – This zone dips northeast toward the Nicaraguan coast and is marked by numerous earthquakes covering the whole range of magnitude (as depth increases) and it extends several hundred kilometers below ground. The general trend is shallower earthquakes near the coast, and deeper earthquakes moving inland.
- **Local Seismic Sources** – Such local zones are identified under Managua. These sources do not produce major earthquakes such as those on the Benioff Zone. However, they are shallow and located near population centers and have caused much destruction in the past.

- **Volcanic Activity** – There is seismic activity from the line of volcanoes from Northwest to Southeast (Cordillera de los Marrabios).
- **Shallow Regions** – There are two shallow regions, one coinciding with the Pacific shore between Lake Managua and the Costa Rica border, the other in the Gulf of Foneca.
- **Atlantic Coast** –This coast is of low seismicity.

In 1987, similar work was done by Larsson and Mattson (1987), primarily dealing with risk from the Benioff Zone. This study used 82 seismic records and a 4-source model using line-sources, area-sources, and point-sources. The iso-acceleration maps created from this study vary slightly. It should be noted that this method constitutes a macro-seismic hazard and local effects are not taken into account. Particular areas of interest should be analyzed by microzonation. Shah et al. (1975) also performed a damage study based on the structures being "constructed similar to those in Southern California." Most structures in Nicaragua bear little resemblance to those in Southern California, with the exception of a few multistory buildings, and this is an area that requires much more study.

3.6. Other Performance Prediction Studies

3.6.1. Seismic Vulnerability Studies

Recently, the structures of Managua have been studied by Reinoso et al. (2004), and the structures of Leon by Solis-Ugarte et al. (2004), but the vulnerability of much of the country remains unstudied. The Managua study is in progress. The Leon study addresses both hazard and vulnerability. The vulnerability is determined according to the scale of vulnerability using the "Benedetti-Petrini" method; the vulnerability index is obtained by means of a weighted sum of the numerical values that express the seismic quality of each one of the structural and nonstructural parameters that play an important role in the seismic behavior of the structures. This method determines vulnerability by survey rather than by analysis. This study could be complemented by a more in depth analysis of the structures, such as a push-over analysis, or even dynamic analysis.

Recently NORSAR (The Norwegian Seismic Array) has taken on the task of determining the seismic risk for the countries of Nicaragua, El Salvador, and Guatemala. To start this research they gathered all the available researchers, including the researchers from the neighboring countries of Honduras, Panama, and Costa Rica, at a conference in Guatemala City during February 2007. NORSAR plans to take surveys of several cities in the three countries and do an extensive hazard analysis of the countries. With the hazard analysis, they will combine vulnerability of the structures to determine the total risk to the population. It was agreed that the vulnerability curves from this research will help accomplish this task.

3.6.2. Microzonation

Following the Managua earthquake of 1972 Robert E. Wallace recommended a zoning map for Managua based only on surface faulting. The purposed map is shown in figure 3.24.

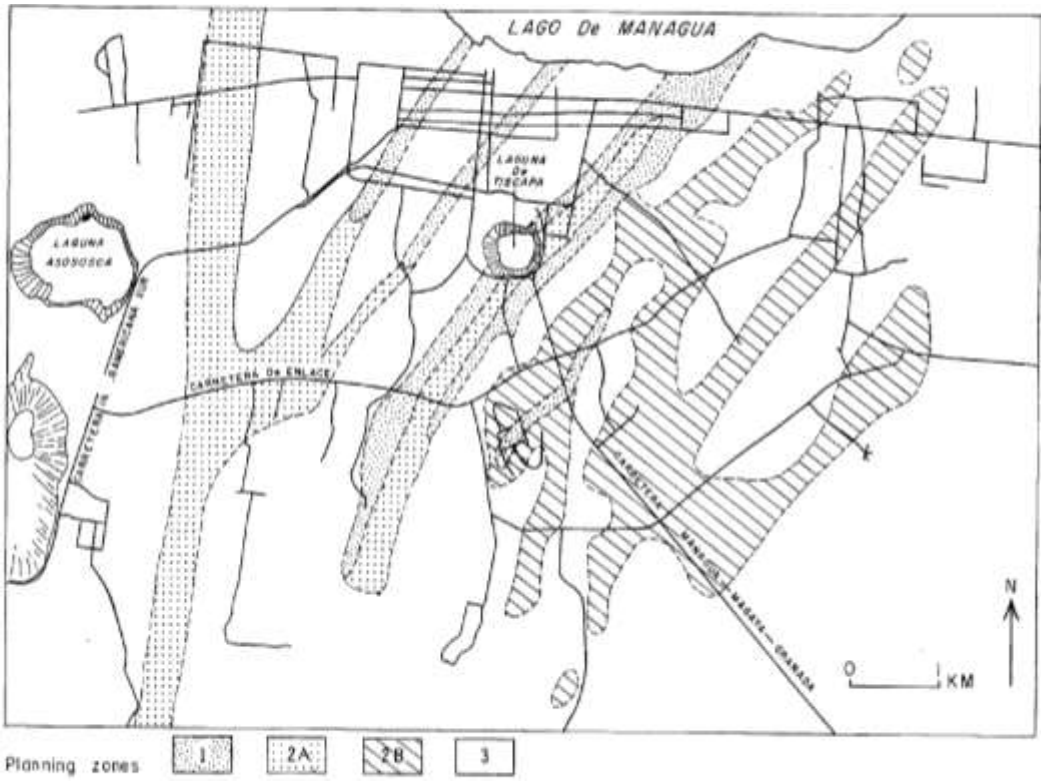

Figure 3.24. Zoning recommended by Wallace, (Wallace, 1973)

Descriptions of zones:

Zone 1 – areas where surface faulting occurred during the 1931 or 1972 earthquakes

Zone 2A – areas of known faults or projections of known faults

Zone 2B – areas where many surface fractures occurred during the 1972 earthquake

Zone 3 – areas of little or no known faulting

Other experts disagreed; Amand stated "During the 1972 earthquake at least nine faults in the urban area moved. The faults are adequately wide and so numerous that avoidance of the faults in reconstruction is well nigh impossible and certainly impractical.”

The sub-soil performed generally well during the 1972 earthquake, but that the possibility of soil amplification should be studied. Faccioli et al (1973) started by studying the soil types and testing the shear wave velocities at 4 typical sites. From these 4 sites they determined that two soil types would be sufficient and that they do not amplify the accelerations recorded at the ESSO Refinery.

Later the government agency Instituto Nicaragüense de Estudios Territoriales (INETER), built on this work and performed tests to determine the horizontal and vertical wave components (H/V Method) and from this calculated soil amplification factors for the city of Managua. This resulted in only one seismic amplification zone for the city of Managua.

Figure 3.25. INETER microzonation map (INETER, 2000)

Reinso et al use a more defined map calculated by Escobar and Corea in 1989. The maps were constructed considering 170 sonar waves and two earthquake models (moderate and severe).

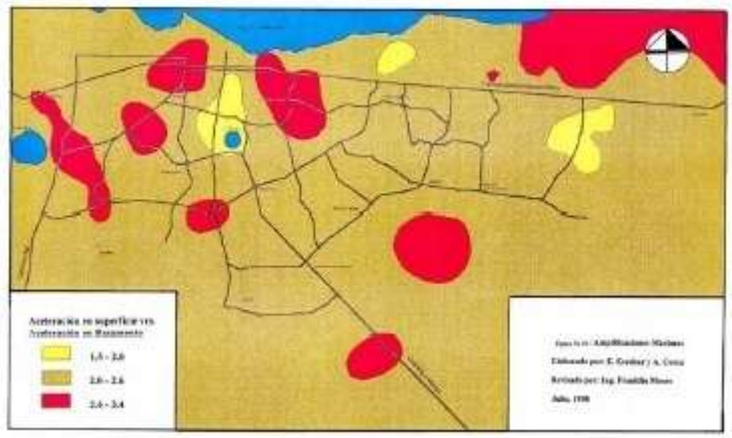

Figure 3.26. Managua soil amplifications for magnitude 5.4 (Escobar and Corea 1989)

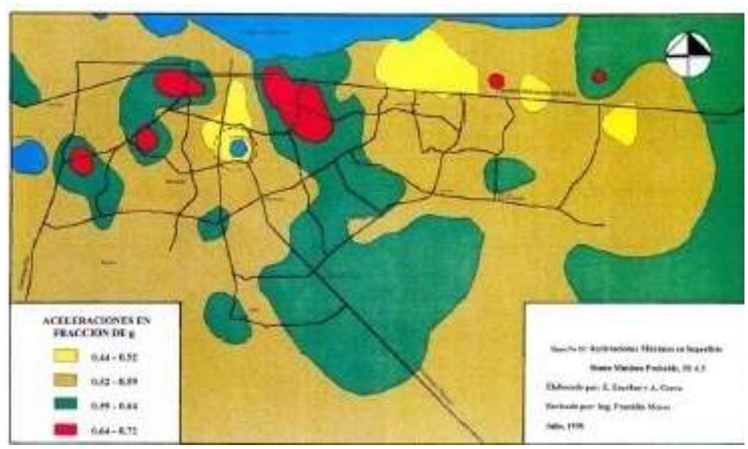

Figure 3.27. Managua soil amplifications for magnitude 6.5 (Escobar and Corea 1989)

4. Review of Earthen Construction Earthquake Resistant Design

Early Civilizations made shelters from the materials they found around them: soil, wood, and stones. McHenry (1984) describes the earliest shelters as seasonal shelters made of brush and small wood members, usually covered with mud for waterproofing. From this grew the earthen structures we know today as: adobe, rammed earth, taquezal , bahareque, and structures of stones. In this section earthen structures will be limited to structures constructed of soil.

4.1. Earthen Construction Types and Practices

Adobe buildings are constructed using bricks of dried soil. Rammed earth buildings (also called tapial in Spanish) are constructed by compacting soil between forms and then removing the forms.

Figure 4.1. Adobe building in Leon, Nicaragua undergoing repairs

Figure 4.2. Rammed earth home in the Southwestern United States
http://www.rammedearth.com/gallery.html

Taquezal buildings are constructed by erecting a framing system of wood (usually cut) and then packing that frame with mud and sometimes stones. The term taquezal seems to be specific to Central America and specifically Nicaragua, but the construction practice occurs in other parts of the world. Bahareque buildings are similar to taquezal except they are framed of bamboo and then packed with mud.

Figure 4.3. Taquezal house in Leon, Nicaragua undergoing repairs

Figure 4.4. Baharaque building in San Ramon, Nicaragua

4.2. Design of Earthen Construction

There are design aids to assist in the design of adobe and rammed earth buildings. One of particular value is *Adobe and Rammed Earth Buildings: design and* *construction* by Paul Graham McHenry, Jr. (Chapter 13 – Structural Engineering for Earth Building was written by Gerald W. May Ph.D.). This book provides great practical design details and recommendations, but this review will limit the summary to engineering properties of design.

Chapter 13 offers some good insights into engineering concerns for earthen buildings. May states that in general adobe construction considerations are similar to those that govern unreinforced masonry design except with larger variations in material and workmanship and therefore high safety factors and conservative design is required. However adobe bricks differ from masonry bricks in one major difference: the bricks and mortar in adobe walls consist of the same material. The wall tends to be more homogeneous and cracks occur across bricks, rather than following the stair-step pattern often seen in burned bricks with cement mortar masonry. Adobe bricks also contain great energy absorbing properties. This becomes apparent when adobe walls are hit with a wrecking ball.

4.2.1. Wall Sizes

May listed common minimum thickness in the United States is 10" for a one-story wall and 14" for two stories and table4.1 shows ther minimum wall slenderness (May, 1984).

Higher aspect ratios can be tolerated if the wall is laterally supported at the top. If a wall is not supported at the top it is conservative practice to design with half of the normal slenderness ratios.

TABLE 13.1

Maximum Wall Heights (in feet)

	Slenderness aspect ratio		
Wall thickness (in.)	8	10	15
10	6.7	8.3	12.5
14	9.3	11.7	17.5
20	13.3	16.7	25.0
28	18.7	23.3	35.0

Table 4.1. Maximum earthen wall heights (May, 1984)

May (1984) recommends the following conservative rules of thumb for proportioning wall openings in adobe buildings:

- The slenderness ratio (h/a) of the outside corner wall pier should be no more than four, and the minimum width should be 4 ft.
- The total length of openings should not exceed one third of the length of the wall between cross walls.
- The bearing length of lintel beams on each side of an opening should not be less than 18 in.

The Building code of Peru recommends the maximum length of the wall between braces must be 12 times the thickness of the wall and the openings must be centered and short and adhere to the following dimensions (Vargas et al, 2006).

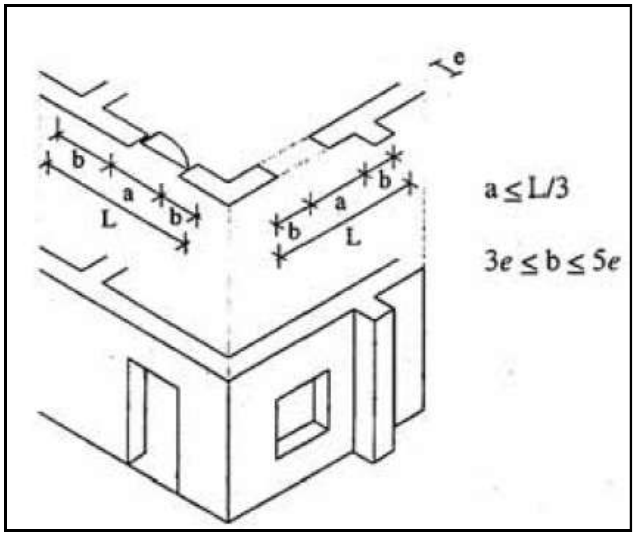

Figure 4.5. Code specifications for wall openings (Vargas, et al, 2006)

4.3. Earthen Construction Materials

McHenry (1984) suggests that the soil of earthen structures is like concrete and must contain four elements: course sand or aggregate, fine sand, silt and clay. Any one of these items may be absent and the soil will still make good bricks or walls. They are similar to the components of concrete: aggregate, sand and cement. In the earthen material the course sand or aggregate represents the aggregate, the fine sand is the sand, and the silt and clay acts as the cement. The materials must be closely monitored because too much sand or aggregate and the structure will be vulnerable to erosion for rain. Too much clay will be more resistant to erosion, but less strong. McHenry sampled materials from several well performing buildings represented in table 4.1.

TABLE 3.1

Soil Material Composition for Adobes, Mortar, and Mud Plaster—Average Percent of Total Sample

Location	Gravel	C Sand	F Sand	Silt	Clay	Porosity
Tumacacori, Arizona*						
Adobes						
P1 10 samples	14.4	20.2	24.8	27.8	13.9	32.3
P2 8 samples	10.7	23.7	30.1	25.8	9.7	33.1
P3 12 samples	10.5	22.2	28.9	27.0	11.2	34.6
P4 8 samples	12.1	24.4	29.8	24.9	9.0	31.0
P5 13 samples	8.0	18.6	30.1	26.7	18.0	34.2
P6 10 samples	8.2	19.7	29.4	31.1	11.5	
Galisteo, New Mexico						
Soil source	6.0	10.0	43.0	34.0	7.0	—
For bricks	2.5	2.5	25.0	49.0	21.0	
Jemez Springs, New Mexico						
Mud plaster	5.0	6.0	51.0	26.0	12.0	—
Mud plaster	12.5	18.6	23.2	36.1	9.6	—
Trampas, New Mexico						
Mud plaster	4.6	5.4	14.4	50.5	25.1	
Mud plaster	10.6	21.0	23.1	28.3	17.0	—
Quari, New Mexico						
Mud plaster	0.3	9.0	24.9	48.1	17.7	—
Gunnison, Colorado						
Interior mud plaster	0.	12.0	51.0	21.0	16.0	—
Sasabe, Mexico						
High clay added for mixing	1.9	23.1	28.9	16.3	29.8	—
standard soil/bricks	7.9	17.1	16.0	40.9	18.1	—
Average	7.2	15.8	29.6	32.1	15.4	33.0

*Tumacacori Mission built around 1820 A.D.

Note: Particle size AASHO Standard: Gravel, over 2.000 mm; C sand, 2.000–0.425 mm; F sand, 0.425–0.075 mm; silt, 0.075–0.005 mm; clay, less than 0.005 mm.

Data Source: USDI—National Park Service, Western Archaeology Center, Tucson, Arizona.

Table 4.2. Composition of earthen building materials (McHenry, 1974)

Table 4.2 gives some general proportions.

Sand or course aggregate	23%
Sand or fine sane	30%
Silt	32%
Clay	15%

Table 4.3. Suggested earthen building materials proportions, McHenry (1984)

Brick tests on adobe samples in Colorado from soils gave the results shown in table 4.3.

TABLE 4.4
Brick Test Results—Colorado Samples[a]

Soil sample	Description—appearance	Soil analysis[c] Gravel (%)	Sand (%)	Silt (%)	Clay (%)	Brick test results[b] Brick code	Note	Sample No.	Comp. Str. PSI	Mod. Rupt.	Drop[d] test
					Manassa, Colorado						
#2	M&J yard top soil, with roots, sticky, thin layer (6–8 in.), black organic	?	43.0	44.8 57.0	12.2		W/roots W/O roots		—	—	— Passed
#3	City of Manassa surplus soil clean, slightly sandy	?	65.6	22.2 44.4	12.2	E	Straw added W/O straw	E-1 —	374 —	24	Passed Passed
#4	M&J standard adobe mix, estimated to be 70% "sand" + 30% "clay" Bricks crack when drying too fast from wind	?	69.3	16.0 30.7	14.7	F		F-1 F-2	376 397	43 57	Passed ?
#7	M&J modified mix, estimated to be 80% "sand" + 20% "clay" Minimal cracking on drying	?	71.4	12.7 28.6	15.9	D		D-1 D-2	302 291	—	Failed (defective brick)
					Salida, Colorado						
#13	Bank run, large stones, few fines, doubtful appearance	?	81.4	11.4 18.6	7.2	B		B-1	333	70	Passed
#14	Crusher tailings, uniform size sandy, minimum clay, clean	?	83.9	10.2 16.1	5.9	A	12% soil #15 88% soil #14	A-1 A-2	172 178	49	Passed
#15	Old "clay" pit for brick manufacturing white, chunks, small stones	?	72.6	11.5 27.4	15.9						
#17	Mixture sample: Crusher tail. 80%, "Adobe Park Clay" 20%. Appears to be an ideal mix	?	77.6	14.0 22.4	8.4	C		C-1 C-2 C-3	192 207 241	89 70	Passed
					Castle Rock, Colorado						
#20	Pumice appearance, grainy, few fines, from south side of Middle Knoll	?	86.4	5.2 13.6 #26 58.7 avg	8.4	G	80%–#20 20%–#26	G-1 G-2 G-3	309 268 346	74 52	Passed
#21	Clay appearance, 6 in. below surface from south side of Middle Knoll	?	42.6	36.5 57.4	20.9			—	—		
#24	Dry sample, clayey looking top soil, from 75 ft. south of "pumice" area	?	86.4	5.2 13.6	8.4	H		H-1	289	74	Passed
#25	Heavy "clay"—east face at road cut, Middle Knoll sticky, slow dry, massive cracking	?	56.4	18.9 43.6	24.7		Addn. of straw reduced cracking to accept. level			—	
#26	Top soil, apparent "clay"—from N. side of Middle Knoll	?	41.3	31.5 58.7	27.2		See #20 above				
#32	"Clay and sand"—from Compton's	?	82.6	7.7 17.4	9.7	I		I-1 I-2	137 170	67	Passed

[a]Preliminary draft Solar Adobe Masonry Systems, DOE, Colorado, 1981.
[b]Natural Resources Laboratory, Inc., Golden, Colorado, 8/26/81, 8/18/81.
[c]Grain size USDA std: clay, less than 0.002 mm; silt, 0.002 to 0.005 mm; sand, over 0.005 mm. —, not tested.
[d]Drop test passed, no damage; chipped corner; failed, shattered, broke in two or more pieces.

Table 4.4. Brick test results, McHenry (1984)

Table 4.4 summarizes test results from samples for all ranges of adobe bricks made in New Mexico.

TABLE 4.2
Summary of Physical Property Tests*

Name	Location	Type of adobe	Size of adobe (in.)	Compressive strength (psi)	Modulus of rupture (psi)	7-day water absorption %	Moisture content %
Small-scale adobe producers							
R. Vigil	Moriarty	Traditional	10 × 4 × 14	704	27	—	—
M. Martinez	Arroyo Seco	Traditional	8 × 4 × 12	486	49		—
Isleta Pueblo	Isleta	Terron	8 × 6 × 14	302	53	—	
Frank Gutierrez	Corrales	Traditional	10 × 4 × 14	312	42		—
Danny Porter	Pecos	Traditional	10 × 4 × 14	285	70	—	
Mariano Romero	Las Vegas	Traditional	10 × 4 × 14	329	25	—	
Charles C de Baca	La Cienega	Traditional	10 × 4 × 14	358	35		
D. Sandoval/E. Trujillo	Peña Blanca	Traditional	10 × 4 × 14	262	26		—
Edward Sandoval	Nambe	Traditional	10 × 4 × 14	281	42	—	—
Roman Valdez/James Lujan	Nambé	Traditional	10 × 4 × 14	242	no sample tested		—
Emilio Abeyta	Ranchos de Taos	Traditional	8 × 4 × 11½	442	38		
Adrian Madrid	Santa Fe	Traditional	12 × 10½ × 3½	331	33	—	—
Robert Leyba	Pecos	Traditional	10 × 3½ × 14	362	36		
Al Montano	La Cienega	Traditional	10 × 3½ × 14	328	23		—
Albert E. Baca	Nambé	Traditional	10 × 3½ × 14	140*	32*		
Albert E. Baca	Nambé	Traditional	10 × 4 × 14	119*	19*	—	—
Joe Pacheco	Taos	Traditional	8 × 4 × 10	153	38	—	
Felix Valdez	Cañones	Traditional	10 × 3½ × 14	321	40		—
Andy Trujillo	Abiquiu	Traditional	10 × 4 × 14	196	54	—	—
Aragon/Garcia Adobes	Aragon	Semistabilized	10 × 4 × 14	389	36	2.0	1.3
David Griego	Ledoux	Pressed adobe	10 × 3½ × 14	1,071	40	—	
David Griego	Ledoux	Pressed adobe	10 × 3½ × 14	1,036	58	—	—
Lawrence Tenorio	Corrales	Traditional	10 × 4 × 14	321	31	—	—
Big "M" Sand & Cinder	Bernalillo	Traditional	10 × 4 × 14	403	67	—	—
D. T. Wiley	Aztec	Traditional	10 × 4 × 14	300	89	—	—
Antonio Serrano	Cañones	Traditional	10 × 3½ × 14	262	41	—	—
Humberto Camacho	Mountainair	Traditional	10 × 4 × 18	536	36		—
Ralph Mondragon	Ranchos de Taos	Traditional	8 × 4 × 12	393	21	—	—
Leonardo Duran	Las Palomas, Mexico	Traditional	8 × 3½ × 16	484	13	—	
W. S. Carson	Columbus	Semistabilized	3½ × 3½ × 11½	590	34	12.7	2.2
W. S. Carson	Columbus	Traditional	3½ × 3½ × 11½	312	46	—	—
W. S. Carson	Columbus	Traditional	3½ × 4 × 11½	769	69	—	
Medium-scale adobe producers							
Otero Brothers	Los Lunas	Semistabilized	10 × 4 × 14	346	37	2.9	1.1
Pete Garcia	Corrales	Traditional	10 × 4 × 14	243	30		—
Taos Pueblo Native Products	Taos	Traditional	7½ × 4 × 13½	281	30	—	—
Taos Pueblo Native Products	Taos	Traditional	4 × 12 × 8	548	85	—	
Taos Pueblo Native Products	Taos	Traditional	10 × 14 × 4	492	50		—
Medina's Adobe Factory	Alcalde	Traditional	10 × 3½ × 14	303	46	—	
Joe Trujillo	Ranchos de Taos	Traditional	7½ × 4 × 10	615	88		—
Bachita Adobe	Deming	Semistabilized	10 × 4 × 14	330	103	2.2	1.2
Rodriguez Brothers	Santa Fe	Traditional	10 × 3½ × 14	714	36		—
Adobeworks	Artesia	Stabilized	10 × 4 × 14	320	74	1.7	0.4
Oliver Trujillo	Nambé	Traditional	10 × 4 × 14	231	37		
Robert Ortega	Dixon	Traditional	10 × 4 × 14	202	33		—
Alfonso Carrillo	Las Palomas, Mexico	Traditional	8 × 3½ × 16	426	31		—
Alfonso Carrillo	Las Palomas, Mexico	Quemado	8 × 3½ × 16	644	190	15.5	0.2
Large-scale adobe producers							
New Mexico Earth	Alameda	Traditional	10 × 4 × 14	489	66		
New Mexico Earth	Alameda	Stabilized	10 × 4 × 14	499	89	1.3	0.3
Adobe Enterprises, Inc.	Albuquerque	Stabilized	10 × 3½ × 14	249	51	1.7	0.75
Eight Northern Indian Pueblos Council	San Juan Pueblo	Semistabilized	10 × 4 × 14	317	39	4.3	0.9
Eight Northern Indian Pueblos Council	San Juan Pueblo	Stabilized	10 × 4 × 14	382	71	3.0	1.0
The Adobe Patch	La Luz	Stabilized	10 × 4 × 14	378	137	2.2	0.6
Adobe Farms	Española	Stabilized	10 × 3½ × 14	322	82	2.1	1.1
Victor Montano	Santa Fe	Traditional	10 × 3½ × 14	438	40		—
Western Adobe	Albuquerque	Semistabilized	10 × 4 × 14	416	96	11.3	1.1
Eloy Montano	Santa Fe	Traditional	10 × 4 × 14	320	42	—	—
Manuel Ruiz	Corrales	Traditional	10 × 4 × 14	311	55	—	—
Rio Abajo Adobe Works	Belen	Stabilized	10 × 3½ × 14	486	101	1.8	0.78
Hans Sumpf Co.	Madera, California	Stabilized	7½ × 4 × 16	611	135	0.33	0.54

*Bricks damaged en route to testing facility.

Note: Tests were performed on a limited sampling of adobe bricks from each adobe yard, and the results may not be representative of total annual production. The New Mexico State Building Code recommends testing of samples selected at random from each 25,000 bricks produced. Symbol — not applicable. Specification requirements for Uniform Building Code and New Mexico State Building Code: compressive strength, average of 5 bricks—300 psi minimum, 1 out of 5 bricks—250 psi minimum; modulus of rupture, average of 5 bricks—50 psi minimum; 7-day water absorption, 2.5% maximum by weight; moisture content, 4.0% maximum by weight.

Data Source: Edward W. Smith, *Adobe Bricks in New Mexico*, Circular 188, New Mexico Bureau of Mines and Mineral Resources, Socorro, 1982.

Table 4.5. Property tests of adobe bricks (McHenry, 1984)

McHenry (1984) determined common adobe brick sizes (see table 4.6).

TABLE 4.1
Common Sizes and Weights of Adobe Bricks

Type of adobe	Dimensions (in.)	Weight (lb)
Egyptian brick	3 × 5 × 10	8
Veneer brick	4 × 4 × 16	26
Half adobe	4 × 4 × 8	23
Burnt adobe (Las Palomas, Mexico)	8 × 3½ × 16	30
New Mexico standard adobe	4 × 10 × 14	30
Adobe (old style)	4 × 5½ × 16	28
Adobe (old style)	4 × 12 × 18	50
Mexico (standard Las Palomas adobe)	3½ × 10 × 16	35
Taos standard adobe	4 × 8 × 12	26
Hydra Brikcrete pressed adobe	3½ × 10 × 14	30
Porta Press pressed adobe	3 × 10 × 14	35
Terrón (Isleta Pueblo)	7 × 7 × 14	35
Dome brick (mosque)	2 × 10 × 6	8
CINVA-Ram pressed adobe	3½ × 5½ × 11½	20

From Adobe Bricks in New Mexico, Edward W. Smith, New Mexico Bureau of Mines and Mineral Resources, 1982

Table 4.6. Common sizes and weights of adobe bricks, McHenry (1984)

4.4. Earthen Construction Material Properties

Knowing the mechanical properties of a material is an important step in analyzing a building. Several researchers have done laboratory tests of earthen building materials. Yamin,et.al. (2004), determined the following table of properties for rammed earth and adobe:

Parameter	Adobe (metric Units)	Adobe (English units)	Rammed Earth (English Units)	Rammed Earth (English Units)
Density	1.80 ton/m3	102 lb/ft3	1.92 ton/m3	109 lb/ft3
Elasticity modulus	1170 kgf/cm2	16,641 lb/in2	800 kgf/cm2	11,378 lb/in2
Rigidity modulus	302 kgf/cm2	4,295 lb/in2	315 kgf/cm2	4,480 lb/in2
Compressive strength	12.2 kgf/cm2	173.52 lb/in2	3.3 kgf/cm2	46.94 lb/in2
Shear strength	0.31 kgf/cm2	4.409 lb/in2	0.37 kgf/cm2	5.26 lb/in2
Flexural Strength	---- kgf/cm2	--- lb/in2	0.15kgf/cm2	2.13 lb/in2

Table 4.7.Rammed earth and adobe properties, Yamin et al (2004)

Vera and Miranda (2004) compared handmade adobe bricks and manufactured adobe bricks in Mexico and the properties are shown in figure 4.6.

ADOBE TYPE	ORIGIN PLACE	MORTAR TYPE	f'm (MPa)	E Prom. MPa	v* , MPa	G Mpa
MANUFACTURED	METEPEC	TYPE I	0.757	494.30		
MANUFACTURED	METEPEC	TYPE II	0.635	490.92	0.076	59.34
MANUFACTURED	METEPEC	TYPE III	0.352	428.21		
MANUFACTURED	METEPEC	TYPE II SAND-SOIL	0.454	491.21		
HANDMADE	VALLE DE BRAVO	TYPE I	0.427	308.51		
HANDMADE	VALLE DE BRAVO	TYPE II	0.390	197.99	0.050	17.46
HANDMADE	VALLE DE BRAVO	TYPE III	0.181	131.36		
HANDMADE	AMATEPEC	TYPE II	0.274	119.00	0.037	11.63
HANDMADE	ORO	TYPE II	0.440	411.47	0.055	20.14
HANDMADE	TEMASCALCINGO	TYPE II	0.369	76.00	0.037	5.97
HANDMADE	SN MIGUEL TOTO	TYPE II	0.448	2,481.51	0.042	13.01

Figure 4.6. Adobe properties in New Mexico, Vera and Miranda (2004)

To compare the values with some common material properties, the same information is shown in English units.

Adobe Type	Origin Place	Mortar Type	F'm (psi)	E Prom (psi)	Vn (psi)	G (psi)
Manufactured	Metepec	Type I	109.8	71,692		
Manufactured	Metepec	Type II	92.1	71,107	11.02	8,607
Manufactured	Metepec	Type III	51.1	62,107		
Manufactured	Metepec	Type II sand-soil	65.8	71,244		
Handmade	Valle de Bravo	Type I	61.9	44,746		
Handmade	Valle de Bravo	Type III	56.5	28,716	7.25	2,532
Handmade	Valle de Bravo	Type II	26.3	19,052		
Handmade	Amatepec	Type II	39.7	17,259	5.36	1,687
Handmade	Oro	Type II	63.8	59,678	7.98	2,921
Handmade	Tamascalcingo	Type II	53.5	11,023	5.37	866
Handmade	Sn Miguel Toto	Type II	65.0	359,913	6.09	1,887

Table 4.8. Adobe properties from Vera and Miranda (2004) in English units

Vargas et al (2006) lists formulas from the Peruvian Building Code for adobe structures (figure 4.7).

The adobe walls must be designed to elastically withstand the seismic forces and to transmit them to the foundation. The allowable stresses are the following:

- Compressive strength of adobe blocks, f_o = average strength of 6 cubes, or $f_o = 12$ kg/cm^2 (1,2 MPa).
- Compressive strength of adobe masonry, $f_m = 0.25\, f'_m$, where f'_m is the compressive strength of adobe masonry piles, or $f_m = 2$ kg/cm^2 (0,2 MPa).
- Crushing strength of adobe masonry = $1.25\, f_m$.
- Shear strength of adobe masonry, $V_m = 0{,}40\, f'_t$, where f'_t is the ultimate strength of small walls in tested under diagonal compression, or $V_m = 0.25$ kg/cm^2 (0,025 MPa).

All adobe walls must be adequately braced by transverse walls, buttresses or reinforced concrete columns. Horizontal braces can be provided by wooden or concrete crown beams.

Figure 4.7. Formulas from the Peruvian Building Code, Vargas et al (2006)

McHenry (1984) calculated loads for foundations as seen in table 4.8.

Foundation Loading for Adobe Walls (pounds per lineal foot)

Wall height (ft)	Wall thickness 4 in.	8 in.	10 in.	12 in.	14 in.	16 in.	18 in.	20 in.	22 in.	24 in.	psi at bottom of wall
20	720	1440	1800	2160	2520	2880	3240	3600	3960	4320	15.00
19	684	1368	1710	2052	2394	2736	3078	3420	3762	4104	14.25
18	648	1296	1620	1944	2268	2592	2916	3240	3564	3888	13.50
17	612	1224	1530	1836	2142	2448	2754	3060	3366	3672	12.75
16	576	1152	1440	1728	2016	2304	2592	2880	3168	3456	12.00
15	540	1080	1350	1620	1890	2160	2430	2700	2970	3240	11.25
14	504	1008	1260	1512	1764	2016	2268	2520	2772	3024	10.50
13	468	936	1170	1404	1638	1872	2106	2340	2574	2808	9.75
12	432	864	1080	1296	1512	1728	1944	2160	2376	2592	9.00
11	396	792	990	1188	1386	1548	1782	1980	2178	2376	8.25
10	360	720	900	1080	1260	1440	1620	1800	1980	2160	7.50
9	324	648	810	972	1134	1296	1458	1620	1782	1944	6.75
8	288	576	720	864	1008	1152	1296	1440	1584	1728	6.00
7	252	504	630	756	882	1008	1134	1260	1386	1512	5.25
6	216	432	540	648	756	864	972	1080	1188	1296	4.50
5	180	360	450	540	630	720	810	900	990	1080	3.75
4	144	288	360	432	504	576	648	720	792	864	3.00
3	108	216	270	324	378	432	486	540	594	648	2.25
2	72	144	180	216	252	288	324	360	396	432	1.50
1	36	72	90	108	126	144	162	180	198	216	0.75

Note: This table is based on a weight of 108 lb/ft^3. Actual weights may vary ±15%.

Table 4.9. Weight of adobe walls, McHenry (1984)

May (1984) determined the compression strength and tensile strength of adobe bricks in New Mexico. The average compressive strength of all samples was 383 psi and the average modulus of rupture was 45 psi. Rammed earth walls have an initial strength of **30 psi** and achieve a dry strength of **300 psi**. Rammed earth walls tend to be thicker than adobe to give more room for compaction. Because of the compaction, for the same soil profile, rammed earth walls are at least as strong as adobe bricks. As stated by May (1984) laboratory tests by Patty in 1939 and Clough in 1949 have confirmed this:

Rammed earth compression strengths – 462 psi to 850 psi

Adobe brick compression strengths – 260 psi to 439 psi

The added strength comes from higher density. Clough found 10% greater dry density and Patty found slightly less. May suggests a factor of safety for compressive strength of 5 to 6 and that tensile strength should not be considered without reinforcement of some kind.

4.5. Earthquake Performance of Earthen Buildings

Earthen structures are heavy, so even small accelerations lead to high seismic forces. Unfortunately, the distribution of earthen structures around the world closely resembles the distribution of seismic activity. This can be seen in the maps in figure 4.8 and figure 4.9.

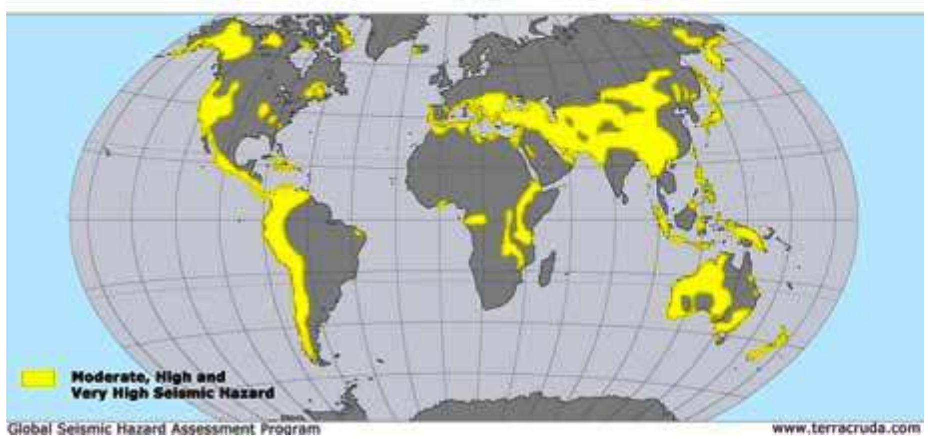

Figure 4.8. Distribution of earth architecture (Rodriguez and Blondet, 2004)

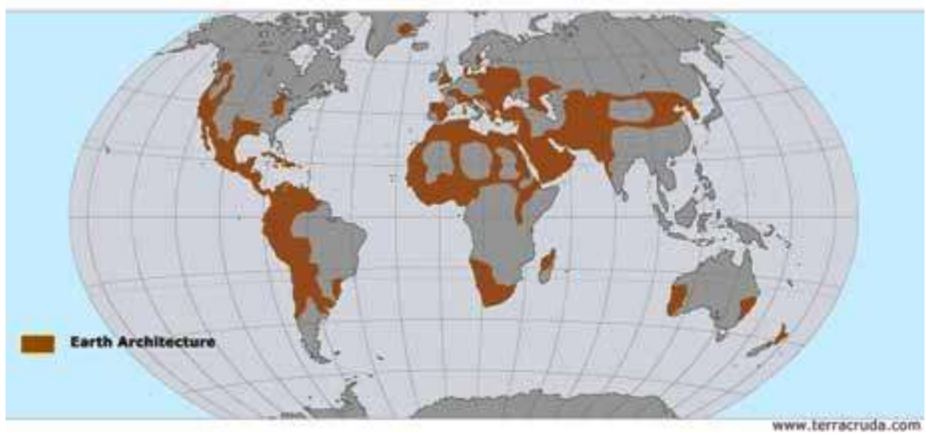

Figure 4.9. Distribution of seismic risk (Rodriguez and Blondet, 2004)

May (1984) shows the idealized action of earthquake loading on a building in the following diagram:

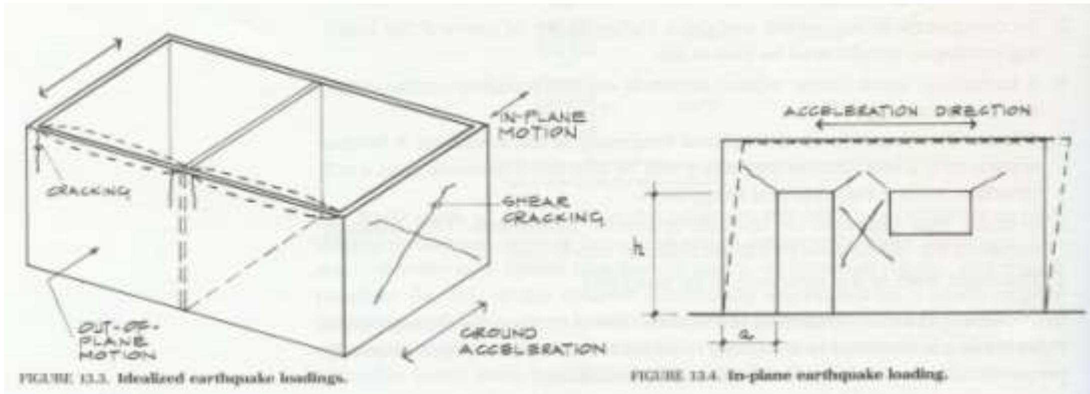

Figure 4.10. Earthquake loading on shear wall system (May, 1984)

The shear cracks are formed on a diagonal because a tension force is created on a diagonal. The force that creates the shear force deforms the wall and creates an elongation on the diagonal. Since most walls are made of materials that are stronger in compression than in tension, cracks are formed in the tension region.

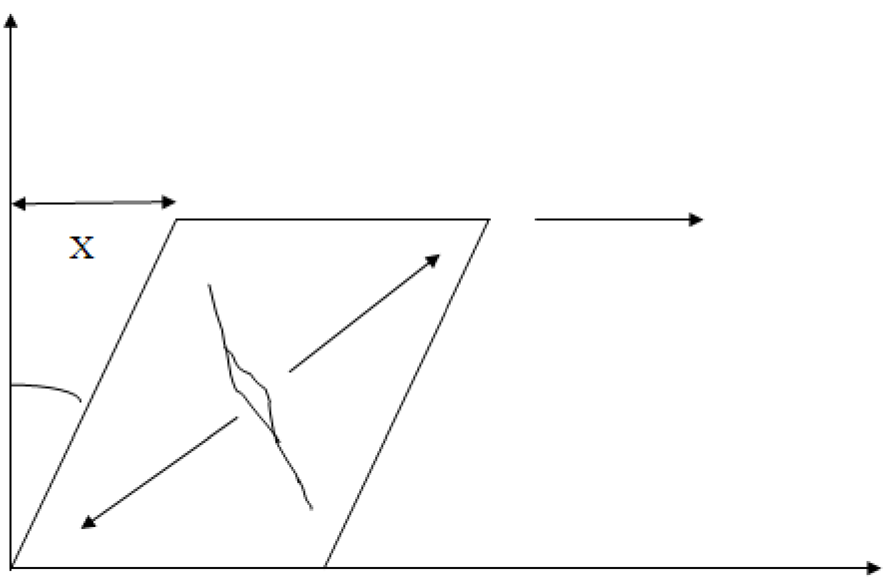

Figure 4.11. Diagram of the formation of shear cracks

May (1984) lists the critical parameters that must be kept in mind for out-of plane loading:

- The unsupported length of the wall should be kept as small as possible. Tensile stresses increase as the square of the unsupported length, so that doubling the length of an unsupported wall increases the stresses by a factor of four. Common practice is to limit the length of an unsupported wall. For example the New Mexico building codes allows a 10 in wall to span 24 ft without being laterally supported. Of course it is not the length of the wall that is important, but the length the wall is unsupported.
- The wall should be tied to the cross-walls with interlocking brick courses or reinforcement. If this tie is broken, damage is worse because of hammering between the disconnected and adjacent walls.
- A wall that is thicker near the bottom has more seismic resistance. This inhibits the collapse of the entire wall even if cracking has occurred near the top.
- A good structural tie between the roof and the wall braces the wall and helps transfer loads to the other walls. This well established and redundant load path prevents inward or outward collapse of the top of the wall.

The most important structural factor in building safe earthen buildings (as with all buildings) in seismic zones is the tie details between members. A building that is tied together well has better load path transfer and redundant structural systems. In earthen structures this can be seen in the connections between walls, particularly in corners. Different details for corner connections have evolved over the years and May gives the following examples:

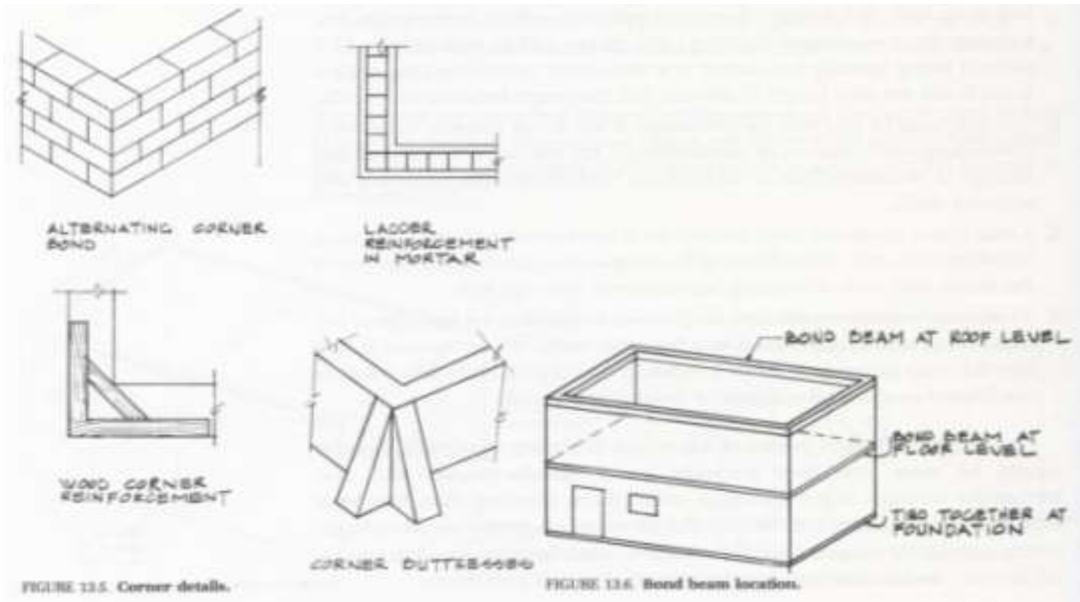

Figure 4.12. Earthen building reinforcement (May, 1984)

4.6. Strengthening Measures for Earthen Buildings

There are several alternatives for strengthening adobe buildings for better seismic performance. Some are required to be installed during construction and others can be installed years later as retrofits.

4.6.1. Ring Beams

Ring beams (or bond beams) can be installed around the building to confine or tie the building together much as a ring holds a wine barrel together. Usually these rings are made of timbers or reinforced concrete and are installed when the building is constructed. Ring beams have been recommended for years. However the Getty Seismic project (2000) found them most effective when combined with horizontal (pole type) reinforcement. Without vertical reinforcement they provided some additional strength but not as much as other methods. The same was true with strapping, which can be considered a ring beam applied later as a retrofit.

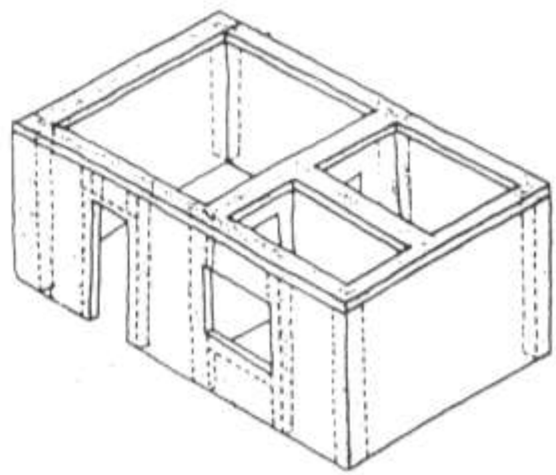

Figure 4.13. Example of a ring beam (sometimes called a bond beam)
http://www.world-housing.net/uploads/100168_010_17.jpg (March 26, 2009)

Cao and Watanabe (2004) tested adobe finite element models with wooden ring beams and found an increased strength. They also tested the model with the beam at the top of the wall and with the beam at the top of the windows and found no difference

4.6.2. Reinforced with Concrete Frames

Another method of retrofitting is to confine the adobe or taquezal with concrete frames or to remove the adobe entirely and replace with concrete frames in-filled with masonry (also called confined masonry). Confined masonry has shown to perform better than adobe.   Vera and Miranda (2004) tested adobe walls and confined adobe walls and found the confined walls had significantly improved ductility and energy absorption but had similar ultimate loads.

Figure 4.14. Retrofitting by removing taquezal walls and replacing with confined masonry

4.6.3. Reinforced with Wood Poles

An earthen structure with vertical (and sometimes additionally horizontal) wood elements increases the structural capacity of the building under seismic loads. Performance is better when these elements are installed in the building during construction of the building (Dowling, 2004; Yamin, 2004). The wood elements provide some elasticity much the way steel provides elasticity in reinforced concrete. However horizontal and vertical wood members applied to the building later as retrofitting did increase the performance of the building, but did not prevent collapse (Yamin, 2004).

Figure 4.15. Adobe test structure with bamboo external reinforcing (Samali et al 2006)

Figure 4.16. Adobe test structure with wood reinforcement (Yamin et al 2004)

4.6.4. Mesh

Covering adobe with plastic or wire mesh has become a popular method for retrofitting. When well applied and good contact is made with the wall, it increases the structural capacity of the wall, but otherwise it still confines the wall and keeps the rubble from falling on the occupants. (Blondet, 2006; Diaz 2007)

Figure 4.17. Adobe test structure with mesh reinforcement (Blondet 2006)

4.6.5. Pilasters

Installing Pilasters is another possibility. Since Pilasters are generally on the outside of a building it is possible to add them latter as a retro-fitting measure, however creating a solid tie to the existing building would be a challenge.

Figure 4.18. Photo of pilaster retrofit example

http://images.google.com/imgres?imgurl=http://www.panoramio.com/photos/original/1930378

Post-tensioning

At Middle East Technical University (METU) in Ankara, Turkey, an innovative approach to retrofitting earthen structures has been explored. Professor Turer (2003) and his colleages at METU are using old tires to strap down the building walls and increase the state of compression in the walls. The downside to this method is that it requires making large holes in the wall and then installing straps that must be covered. Also there is some maintenance involved in making sure the walls stay tensioned.

Figure 4.19. Building retro-fit using scrap tires (Turer, 2003)

4.6.6. Comparison of Retrofitting Techniques

It is generally agreed that during construction it is best to build adobe with vertical reinforcement and ring beams. Dowling (2004) compared all the strengthening measures and compared the skill and cost required and compiled the table 4.10.

	Improvement Systems						
	Ring Beam (reinforced soil-cement)	Vertical Reinforcement (internal bamboo)	Horizontal Reinforcement (internal barbed wire / chicken wire)	Vertical Reinforcement / Mesh (External) [*Estimated]	Horizontal Reinforcement / Mesh (External) [*Estimated]	Pilasters (intermediate)	Pilasters (corners)
Complexity (Skill/experience level required)	2-3	2-3	1	2*	2*	2	3
Cost (Resources required)	3	2	1	2*	2*	2-3	2-3

Complexity / Cost Key: 1 – Low, achievable by general population; 2 – Moderate, some building skill + experience / resources required; 3 – High, significant technical skill + experience / resources required.

Table 4.10. Complexity and costs of improvement systems for adobe construction, Dowling (2004)

Adobe retrofitting techniques were put to test during the 2001 Arequipa earthquake. Before this earthquake many adobe structures were retrofitted with steel wire mesh and mortar forming vertical and horizontal bands. This is the retrofitting technique shown in figure 4.11.

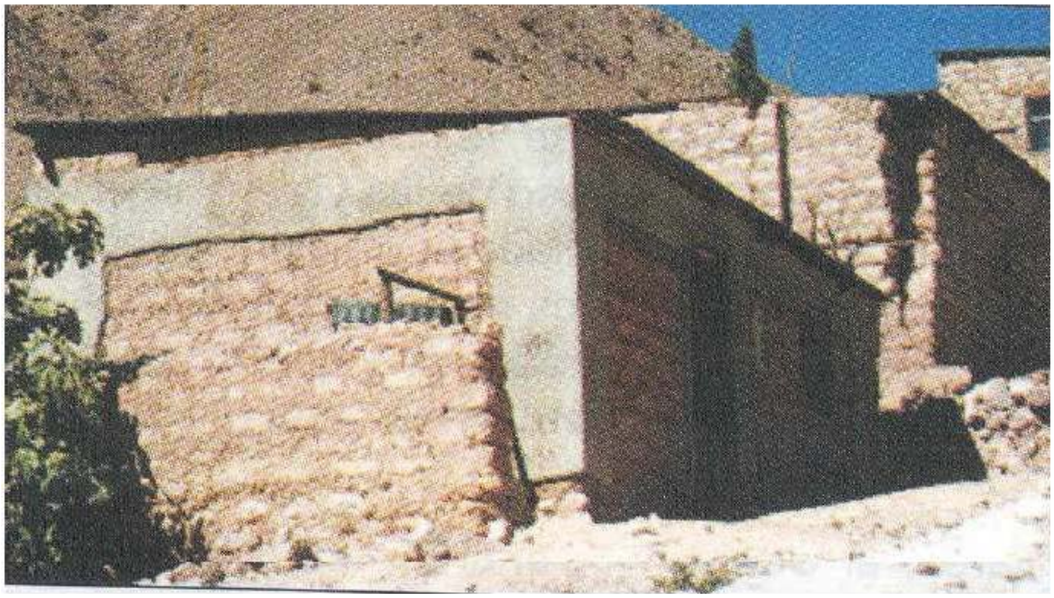
Figure 4.20. Rehabilitated adobe dwelling (San Bartolome, 2004)

The rehabilitated houses performed well and were not damaged. The nearby adobe structures that were not rehabilitated, were severely damaged or collapsed (San Bartolome, 2004).

5. Review of Confined Masonry Building Design and Analysis

Confined masonry construction is becoming more prevalent in many developing countries. The term, confined masonry, also called masonry-in filled frames, refers to concrete or steel frames filled in with non-structural masonry walls.

Figure 5.1. Confined masonry construction, San Juan del Sur, Nicaragua

This type of construction is well suited for fire resistance, has good thermal properties, and performs well under gravity loads. How this type of construction will perform during an earthquake is more difficult to predict.

5.1. Interaction

Engineers once believed that this non-structural masonry could be ignored during design because the in-fill would only increase the overall lateral capacity. This has since been disproved. The infill can drastically change the structural response of the building.

5.1.1. Influence of Masonry Infill on the Seismic Behavior of Frames

There was once misconception that non-structural masonry infill in a steel or concrete frame will only increase the lateral capacity of the structure, and therefore it can only be beneficial. Masonry infill can drastically reduce the structural response of the system. Kodur (1995) lists the comparisons of in filled frame behavior with reinforced concrete frame behavior in table 5.1.

Factor	RC frame	RC frame with brick infill
Load capacity	1	≈ 2
Initial stiffness	1	≈ 5
Stiffness at service load	1	≈ 2.7
Cumulative ductility	≈ 3	1
Energy dissipation capacity	1	≈ 1.5
Lateral strength	1	≈ 6
Natural period	1	< 6
Earthquake inertial forces	1	>1
Energy dissipation	See note *	See note **
Resistance to incremental collapse	1	>1
* Energy dissipation through large inelastic rotation at hinge regions ** Energy dissipation through hysteretic behavior (friction across panel cracks)		

Table 5.1. Comparison of RC frame with infilled RC frame (Kodur 1995)

The following are tw examples of common errors made with confined masonry from Paulay and Priestly (1992).

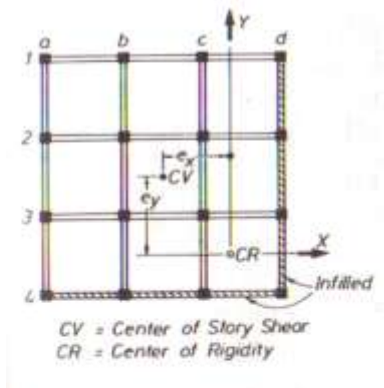

Figure 5.2. Floorplan of a multistory reinforced concrete frame building with infill of two boundary frames (Paulay 1992)

Example 1, (Paulay, 1992) - Consider the plan of a symmetric multistory concrete frame building with masonry-infill on two outside walls as shown below:

If the masonry infill is ignored in the design phase, then the building is designed as symmetric with all the frames carrying the same seismic load. In reality, the masonry infill is stiffer, the center of rigidity is no longer in the center of the building, and frame lines 4 and d take a much larger portion of the seismic load. Frames 4 and d are stiffer compared to the other frames. This will increase the stiffness of the building, which will decrease the natural period of the structure and seismic forces will in turn increase. The structure will also be subject to torsion created by the shift in the center of rigidity. This torsion is:

$M_{tx} = V_j e_y$ and (5.1)

$M_{ty} = V_j e_x$. (5.2)

where V_j is the total horizontal story shear and e_x and e_y are the eccentricities. When loaded, high shear forces will be generated in the infilled frames primarily as shear forces. These shear forces will cause failure in the masonry infill which may result in shedding of masonry inside the building or into the streets below, either of which are hazardous. This type of failure is shown in figure 5.3.

Figure 5.3. Failure of lower level of masonry-infilled reinforced concrete frame (Paulay 1992)

Example 2, (Paulay, 1992) – Consider masonry infill, which fills only a portion of the story height as shown below:

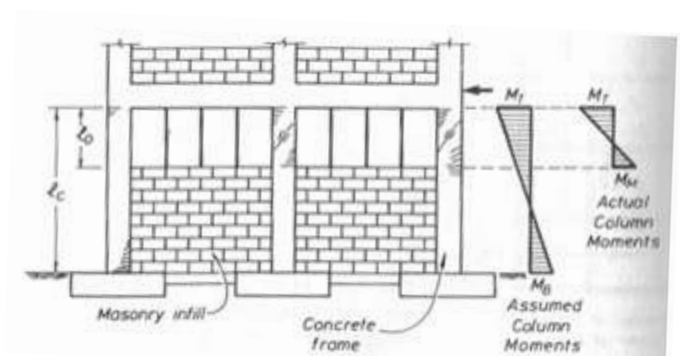

Figure 5.4. Partial masonry infill in concrete frames (Paulay 1992)

As in the previous example, the infill will stiffen the frame, reduce the natural period, and increase the seismic forces. If the frame is expected to behave in a ductile manner during a design-level earthquake, without taking into account the infill material, plastic hinges will be expected at the top and bottom of the columns, or even in the beams at the columns. These hinges might appear before the full design-level earthquake. However, the infill material will not allow these hinges to form. The infill will stiffen the beam and the column below the level of the infill. Instead, plastic hinges will form on the columns at the top of the infill material. This will cause a substantial increase in column shear. The design shear force would likely be:

$$V = \frac{M_T + M_B}{l_C} \tag{5.3}$$

M_T and M_B are the design moments at the top and bottom of the columns. These moments would be based on the design capacity.

Instead the design for will be:

$$V = \frac{M_T + M_M}{l_o} \tag{5.4}$$

If the structure is not designed for this higher shear force, shear failure can be expected. This higher shear force is accompanied by lower ductility. Figure 4 is an example of this type of failure.

Figure 5.5. Short column failure (Paulay 1992)

This type of design error is called short columns. It is very common in school buildings and has been seen in Nicaragua also.

5.2. Design Methods

There are two possible design approaches when constructing confined masonry. The panel and frame can be in full contact and designed to act together to resist seismic loads or they must be isolated from each other. The two can be isolated by providing a flexible strip between the two. A highly deformable material such as polystyrene should be used. The option of isolating the two is not very effective and should be avoided if possible. It is also difficult to provide support for out-of-plane bending.

5.2.1. Isolated Systems

Because isolated panels no longer have compression membrane action, they must be designed to fully resist out-of-plane forces. Shear connections will be required to connect the frame and panel through the flexible strip. These connections must be flexible in the plane of the infill panel, while stiff and strong in the out-of-plane direction to carry out-of-plane loads back to the frame.

Paulay recommends constructing the panel by laying the infill before the upper beam is poured and separating the top of the panel from the beam with a flexible material. The shear connection to the beam can be provided by extending the panel vertical reinforcement into the beam and taping layers of flexible material into the sides of the reinforcement in the in-plane direction up to the beam mid-height. After the beam concrete is placed, the flexible material will allow relative in-plane movement of the panel and frame, while restricting out-of-plane relative movements.

5.2.2. Combined Systems

At low lateral loads, the frame and in-fill panel will act in a full composite manner, as a structural wall with boundary elements. As the lateral loads and deflections increase, the response becomes more complicated. The frame attempts to deform in flexure while the panel attempts to deform in shear. This is shown in figure 5.6.

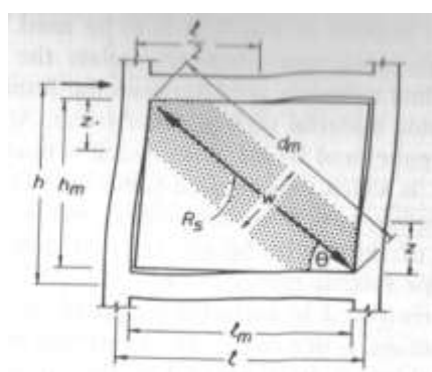

Figure 5.6. Confined masonry deformation under shear loading (Paulay, 1992)

The frame and panel begin to separate at the corners on the tension diagonal, and the development of a diagonal compression strut begins on the compression diagonal. Contact between the frame and panel occurs for a length z, as shown in figure 5. This separation can occur at 50 – 70% of the ideal lateral shear capacity of the infill. After separation the effective with of the diagonal strut, *w*, is less than the full panel.

The natural period should be calculated based on the structural stiffness after separation. The structure can be considered a braced frame, with the diagonal compression strut connected by pins to the frame corners. This is shown in figure 5.6. The effective width w of the diagonal strut depends on the relative stiffnesses of the frame and panel, the stress-strain curves of the materials, and the load level. Since a higher value of w will result in a stiffer structure, and therefore a high seismic response, it is conservative to consider a high value of:

$$W=0.25d_m \tag{5.5}$$

where d_m is the diagonal length.

5.2.3. Failure Modes

According to Paulay (1992) there are several different possible failure modes. Failure modes include: tension failure of the masonry tension column resulting from applied overturning moments, sliding shear failure of the masonry along horizontal mortar courses, diagonal tensile cracking of the panel, compression failure of the diagonal strut, and flexure or shear failure of the columns. In practice the failure may be a sequential combination of some of the mentioned failure modes. For example, flexural or shear failure of the columns will generally follow a sliding shear failure or diagonal compression failure of the masonry. The strength associated with each possible failure mode should be calculated and the lowest value used as the design strength. Paulay (1992) gives equations for the failure modes:

1. **Tension failure mode** - This can occur in infilled frames with a high aspect ratio. This critical failure mode is flexural and involves tensile yield of the steel in the masonry tension column. Under these conditions the wall is acting like a cantilevered wall. The system acts as a deep beam and the tension column as the flange of this deep beam. This is a relatively ductile failure mode. To prevent this failure mode, the design should be in accordance with masonry codes for wall systems.

2. **Sliding shear failure mode** – This mode of failure generally occurs at or close to mid-height. When this occurs, the equivalent structural system changes from the diagonally braced pin-jointed frame of figure 5.6 to the knee-braced frame shown in figure 5.7. The support provided by the masonry to the columns forces hinges to form at approximately mid-height and top or bottom of the columns and may result in column shear failure. Initially the shear will be carried by the infill panel, but as the sliding shear failure occurs, the increased displacements will cause moments and shears in the columns.

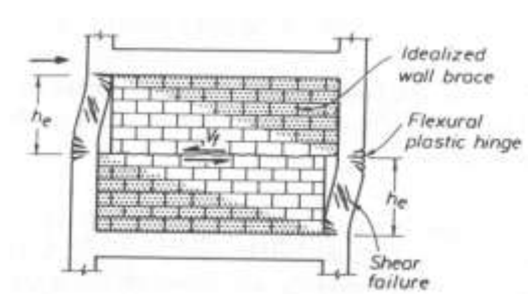

Figure 5.7. Sliding shear failure (Paulay 1992)

The shear force to initiate this failure is R_s is:

$$R_s = \frac{0.03 f'_m}{1 - 0.3(h/l)} d_m t \tag{5.6}$$

For several equal bays the base shear force to initiate sliding V_b is:

$$V_b = \frac{n 0.03 f'_m}{1 - 0.3(h/l)} l_m t \tag{5.7}$$

After sliding initiates, the columns and panels share the resistance of shear forces. The failure shear force for the panels becomes:

$$V_i = \sum_{i=1}^{n+1} \frac{2}{h_e} (M_{ct} + M_{cc})_i + V_b \tag{5.8}$$

The shear friction force in this equation V_b will degrade quickly with cyclic loading and should be conservatively ignored in calculating the ductile shear capacity of this failure mode. The effective column height between column hinges (see figure 5.7) is approximately half the story height h, both for exterior columns and for columns between two panels (where hinges tend to form at quarter points). This for a knee-braced frame n bays wide with n+1columns, where the ultimate story shear is:

$$V_i = \frac{4}{h} \sum_{i=1}^{n+1} M_{ci} \tag{5.9}$$

where M_{ci} is the strength of the ith column, including axial force effects. Column shear reinforcement should be based on a capacity design approach using over-strength column moments to avoid column shear failure.

Equation 4 should be used to determine the force required to initiate this failure mode. This value should be compared to the values given from flexural failure moment and diagonal crushing force. To ensure a ductile response, V_i should exceed R_s.

Compression Failure of Diagonal Strut mode – For most masonry infill panels, diagonal tensile splitting will precede diagonal crushing. However this failure mode should not be overlooked. The value of the diagonal compression failure force was found from testing and is proposed:

$$R_c = \frac{2}{3} Ztf'_m \sec\theta \qquad (5.10)$$

Where z is the vertical contact length between the panel and column, as shown in figure Y and is given by:

$$Z = \frac{\pi}{2}\left(\frac{4E_c I_g h_m}{E_m t \sin 2\theta}\right)^{1/4} \qquad (5.11)$$

Where E_c and I_g are the modulus of elasticity and the moment of inertia of the concrete columns, E_m and h_m are the modulus of elasticity and height of the infill, and C is the angle between the diagonal strut and the horizontal, as shown in figure Z. Flexural or shear failure of the concrete column can be designed using the concrete code.

5.3. Ductility

Ductility is the ability of a structure, its components, or its materials to offer resistance in the inelastic range (or beyond yield). It includes the ability to sustain large deformations and the ability to disipate energy by inelastic behavior. Lack of these qualities result in brittle failures and implies near complete loss of resistance without warning. Brittle failure can be said to be the overwhelming cause for the collapse of buildings in earthquakes, and the consequent loss of lives. For this reason it is the single most important property of structures in seismic areas.

5.4. Out-of-Plane Strength

If the infill panel is reinforced and adequately connected to the frame, the out-of-plane forces can be treated as a two-way slab with the appropriate boundary conditions (Paulay, 1992). The flexural strength can be assessed using standard masonry design for flexure techniques for walls.

Masonry panels unreinforced in their plane may still be able to resist out of plane forces without failure. It has been shown with shaker table tests that when the unreinforced panels are surrounded by very stiff frames, the panels can resist very large out-of-plane accelerations. This unexpected good performance is the result of resistance provided by compression membrane action. This is illustrated in figure 5.8.

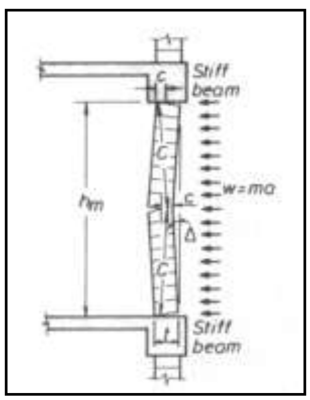

Figure 5.8. Compression membrane forces (Paulay 1992)

5.5. Current Confined Masonry Research

5.5.1. Scale Models

Seismic Evaluation of Frames with Infill Walls Using Pseudo-dynamic Experiments

Mosalam et al, 1997 provide an exhaustive study exploring the characteristics of steel frames in-filled with un-reinforced concrete block masonry. One-quarter models of the two-bay, two-story steel frame in-filled with un-reinforced masonry were tested under pseudo-dynamic loads. The steel frames were connected using ASD "Type 2" pin-connections. The model was subjected to three earthquake records: Kern County California (July 1952), El-Centro (May 1940), and North Nahanni River, Canada (1985). The Nahanni River earthquake was selected because the natural period of the infilled frame is close to the main peak period of the spectra.

The study showed that the masonry should not be neglected in seismic areas. The masonry increases the stiffness which in turn reduces the natural period of the system. The system also changes the magnitude and distribution of the straining actions in the bare frame. This can lead to un-conservative or poorly detailed structures.

Irregularities induced by nonstructural masonry panels in framed buildings

Negro and Colombo (1997) explored the effects of nonstructural masonry infills on the seismic behavior of reinforced concrete frames. Several full-scale 4-

story frames configurations were constructed based on the requirements of Eurocode 8 and subjected to pseudo-dynamic tests. Three frames were tested, a bare frame, a uniformly infilled frame, and a soft-story infilled frame.

The infill was shown to have both positive and negative effects on the frame. The uniformly infilled frame caused irregular behaviors, including torsional effects, soft stories, short-column effects, and irregularities in both plan and height. It also however, increased stiffness, strength and energy dissipation. However these improvements do not offset the negative effects and the masonry should be considered in the design.

Effect of masonry infills on seismic performance of a 3-story R/C frame with non-seismic detailing

Lee et al, (2002) evaluated the effect of masonry in-fills on R/C frames modeled with a 1:5 scale and constructed according to Korean standards without seismic detailing. The model was subjected to Korean design earthquakes varying from 0.12g to 0.4g and also a static pushover test to determine the ultimate capacity.

The results showed the masonry increased the stiffness and strength while also increasing the earthquake inertia forces. The study concluded that the masonry was mostly beneficial in that it increased the strength more than it increased the inertia force. It also limited the lateral displacements. However the failure mode is more complicated.

5.5.2. Whole Building Systems Tests

Response Assessment of Mexican Confined Masonry Structures Through Shaking Table Tests

In Mexico, Alcocer et al (2004), tested half-scale models of typical low-cost one and two story houses commonly built in Mexico. The models were subjected to a serious of typical ground motions recorded in Mexico. The purpose of the paper was to determine if buildings built to Mexico building standards are sufficient for earthquake loading. Below are drawings of the buildings tested.

During the test, the specimens were instrumented with acceleration, displacement, and strain transducers. During testing, story displacements, shaker table and story accelerations, wall deformations, and reinforcement strains were recorded.

The models were subjected to the ground motion of the Acapulco, Guerrero earthquake of April 25, 1989 (M=6.8, PGA=0.34g) and the Manzanillo, Colima earthquake of October 10, 1995 (M=8.0, PGA=0.40g). Both earthquakes were scaled to subject the models to larger events. The Acapulco record was scaled to earthquakes of magnitudes 7.6, 7.8, 8.0, and 8.3, while the Manzanillo record was scaled to magnitudes 8.1, 8.2, and 8.3. Both models were subjected to subsequently larger earthquakes until the final damage state was reached.

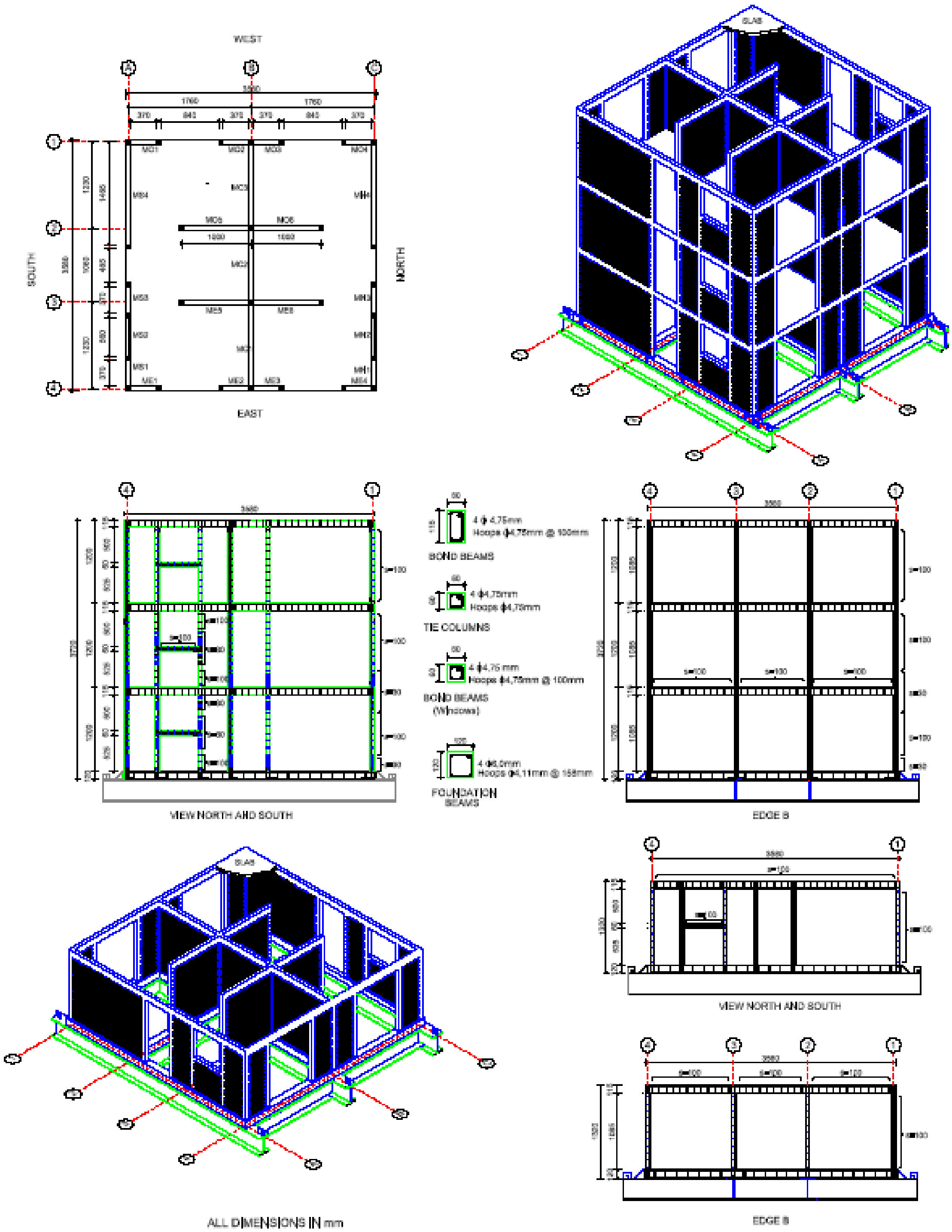

Figure 5.9. Test specimens (Alocer, 2004)

The final crack patterns are shown below. Analysis later showed that shear deformations controlled the response. In general, walls exhibited one or two large inclined cracks at 45 degrees. First cracking appeared at 0.36%. The cracks propagated to the columns and sheared these elements at 0.67% and maximum recorded drift was at 1.75%.

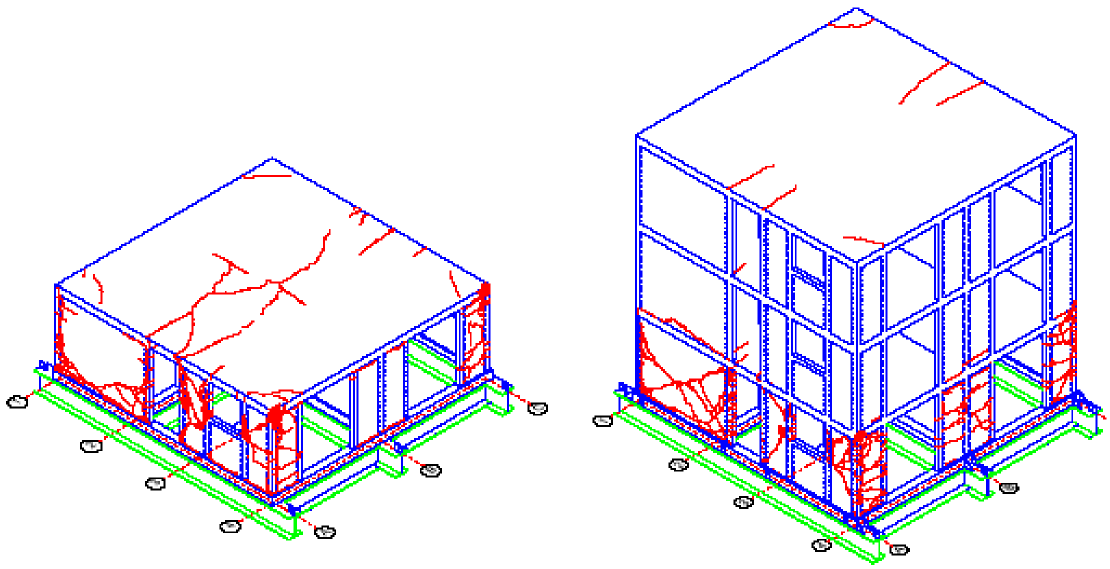

Figure 5.10. Final crack patterns (Alocer, 2004)

The tests concluded that confined masonry buildings built to the Mexican building code are quite safe and perform well during earthquakes. It was found that the buildings have an over strength value of 2 and therefore the Building Code of Mexico may be too conservative.

Seismic Behaviour of Confined Masonry Buildings and Verification of Seismic Resistance of Confined Masonry Buildings

Tomaževič, et al (1996) in two separate articles covering one of the largest test of confined masonry buildings, 1:5 models were built according to engineering practice and conformed to the Eurocode 8. The models were built and tested to verify calculations and verify the proposed numerical models, most notably the Eurocode force reduction factor, *q*. The two models were three story houses. A sketch of the structures is shown below:

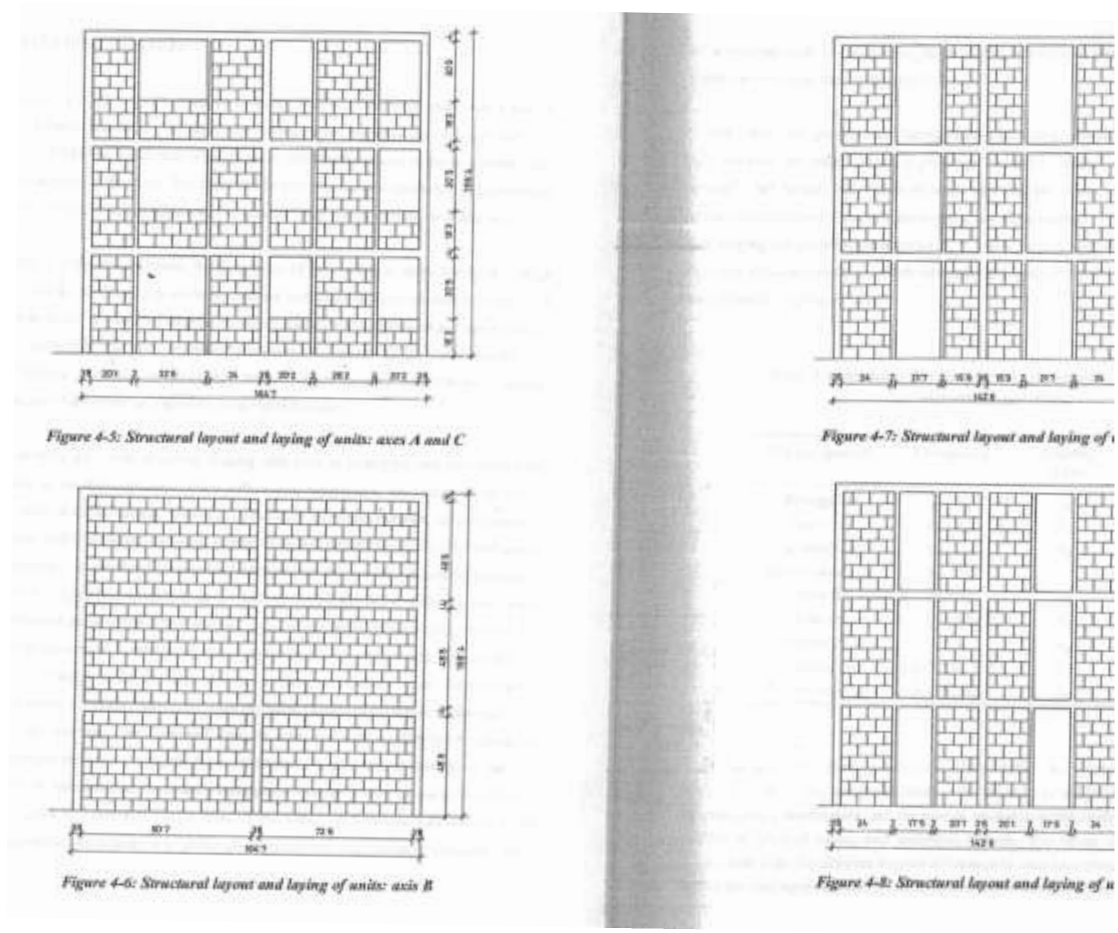

Figure 5.11. Structural layouts (Tomazevic 1996)

One model was tested in the longitudinal direction and the other was tested in the lateral direction. The models were subjected to repeat shaking with peak ground acceleration more than 1.3g. Both models performed well and the results are listed in the following table:

Description of limit state	Maximum ground acceleration (g)	Base shear coefficient	Dynamic amplification factor
Model M1 –longitudinal direction			
Elastic limit (initiation of cracking)	0.49	0.98	1.03
Maximum resistance (diagonal cracks in both directions)	0.73	1.49	2.99
Before collapse (disintegration of walls)	1.44	0.53	0.43
Model M2 – transverse direction			
Elastic limit (initiation of cracking)	0.36	0.53	2.53
Maximum resistance (diagonal cracks in both directions)	0.71	1.08	1.99
Before collapse (disintegration of walls)	1.19	0.56	0.64

Table 5.2. Seismic response of prototype structures (Tomazevic 1996)

Both models failed with diagonally propagating cracks on the perimeter walls and shear behavior defined the mechanism of failure.

It was concluded that the full size structures will resist even the strongest expected earthquake without significant damage. They did however find that resistance of the confined masonry panels also degrade soon after reaching the maximum loading.

Verification of Seismic Resistance of Confined Masonry Buildings

In another article Tomaževič (1997) compares the building model to Eurocode

8. The article compared the factor of reduction of elastic loads q, which is the ratio between the elastic seismic load capacity He and the ultimate seismic load capacity Hu (q = He/Hu). Eurocode 8 suggests q = 2.0 for confined masonry, while the models tested resulted in q = 2.91 and q = 2.47, suggesting the code maybe conservative. However, when you take into account that story drift must be limited to avoid excessive damage the value of q seems reasonable.

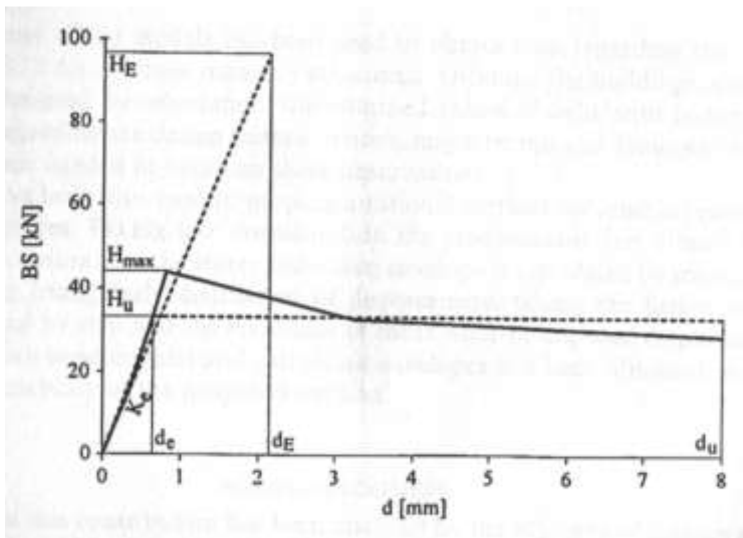

Figure 5.12. Evaluation of behavior factor q (Tomazevic 1997)

The study also evaluated the use of push-over analysis for this type of construction and found it to be accurate.

5.5.3. Detailing

Experimental Behavior of Masonry Structural Walls Used in Argentina

Zabala et al (2004) discusses the effect of detailing on the performance of confined masonry is just beginning to be explored. To determine the performance of confined masonry walls six models were constructed varying the column reinforcement and the horizontal reinforcement at the joints. In these six wall models compression failure of the masonry strut did not control and the wall strength was controlled by vertical reinforcement of the columns. "The amount of transverse reinforcement in the critical zones of the columns and beams normally used in practice is insufficient in order to sustain this shear force" (Zabala et al 2004). The results of the tested walls are shown in Table 5.3.

Wall	Vertical reinforcement	Horizontal reinforcement	Vertical load. [kN]	Theoretical flexural capacity (1) [kN]	Estimated shear capacity. (2) [kN]	Maximum measured strength [kN]
1	4 ϕ10 (3.12 cm^2)	-	100	142	109	118
2	4 ϕ 10 (3.12 cm^2)	-	100	142	109	93
3	4 ϕ 16 (8.05cm^2)	-	200	342	138	207
4	4 ϕ 16 (8.05cm^2)	-	200	342	138	235
5	4 ϕ 8 (2.01 cm^2)	2 ϕ 6 each 2 mortar joint. (3.1 cm^2/m)	100	105	109+ 72 (3)	157
6	4 ϕ 8 (2.01 cm^2)	2 ϕ 6 each 2 mortar joint (3.1 cm^2/m)	100	105	109+ 72 (3)	169

Notes:
(1) Considering the horizontal load applied at the horizontal actuator level, the applied vertical load and σs= 420 MN/ m^2 (yield stress of the steel)
(2) Vur= (0.3 σ +0.6 τmo)[1]. Where σ = compression stress, τmo = diagonal shear strength of small masonry probes. τmo= 0.3 MN/ m^2
(3) Additional strength due to horizontal masonry reinforcement.

Table 5.3. Results (Zabala et al 2004)

Experimental Study on Effects of Height of Lateral Forces, Column Reinforcement and Wall Reinforcements on Seismic Behavior of Confined

Masonry Walls

To explore the effects of height of lateral forces, column reinforcement, and vertical and horizontal wall reinforcement on the seismic resistance of confined masonry walls, Yoshimura et al (2004) tested twelve 1:2 scale models of confined masonry walls. The test showed how following factors affect ultimate lateral strength:

- Shear span ratio (height to length of masonry ratio) – the lateral strength increases as the shear span ratio decreases.
- Inflection height ratio (height of applied load to length of masonry ratio) – the lower the inflection ratio the higher the lateral strength increases
- Tensile reinforcement ratio – ultimate lateral strength increases with increased steel reinforcement in the confining R/C columns.
- Effect of vertical axial stress – increased in vertical axial stress tends to increase the ultimate lateral strength.

Experimental Study for Developing High Seismic Performance of Brick Masonry Walls

This study investigated the lateral strength of confined masonry walls with and without wall reinforcing bars and U-shaped connecting bars. The following conclusions were made:

- Confined masonry wall systems are superior to increase lateral load capacity to un-reinforced masonry wall systems

- Confined masonry wall systems with connecting bars at the vertical wall-to-column connections and horizontal wall reinforcing bars develop higher ultimate lateral strength
- The separation of the R/C confining columns to the walls can be avoided with U-shaped connecting bars
- An increase in axial stress tends to increase the lateral load carrying capacity

5.5.4. Effects of Opening Sizes, Column Spacing, Other Variability

Experimental Evaluation of Confined Masonry Walls with Several Confining-Columns

To determine the effect of the number of vertical confining elements, called confining-columns in this paper, Marinilli et al (2004) constructed four full-scale walls of the same nominal area. The walls contained two, three and four confining columns. The walls are shown below.

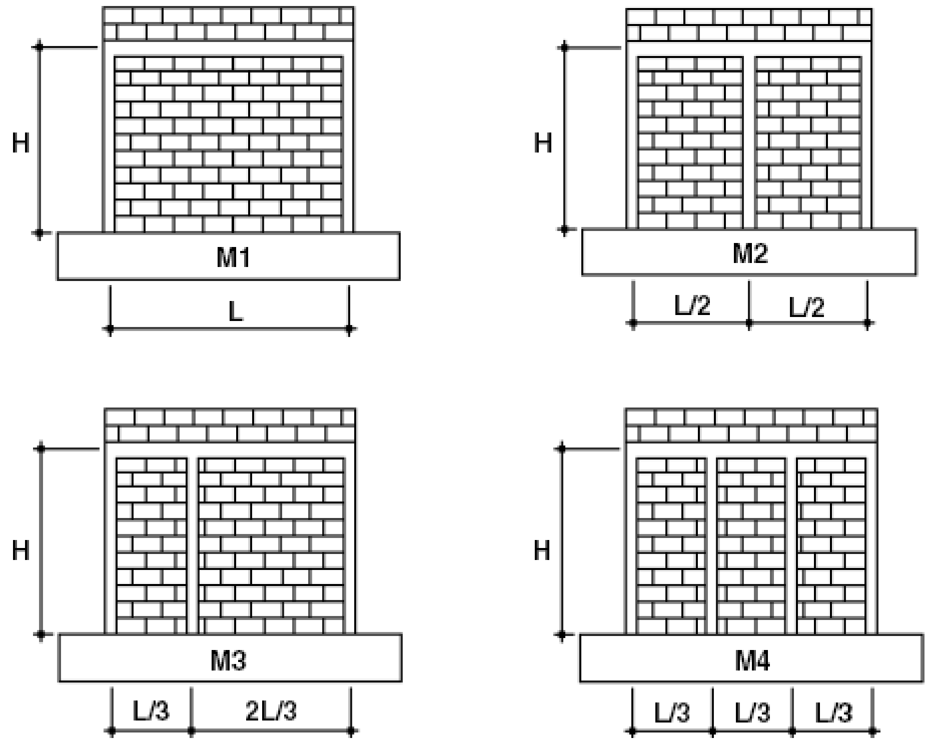

Figure 5.13. Test specimens (Marinilli 2004)

The results show that including more columns in the same wall length increases the initial stiffness, the system ductility, strength, and allows damage distribution in the masonry panels. Including more columns does not seem to improve energy dissipation (or equivalent damping ratio), and decreases the equivalent ductility of the wall.

Behavior of Confined Masonry Shear Walls with Large Openings

To explore the effect of openings in confined masonry shear walls, Yanez (2004) constructed sixteen full scale specimens. Half of the specimens were constructed of concrete masonry blocks and half with hollow clay bricks and the opening sizes were varied. The walls are shown in figure 5.14.

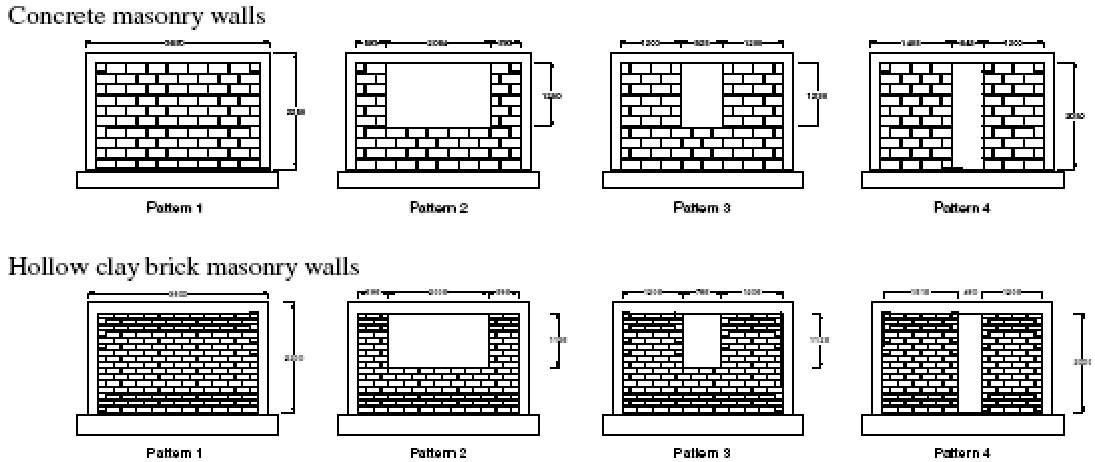

Figure 5.14. Wall dimensions (Yanez 2004)

The specimens all failed in shear. The stiffness of specimens with opening size ratios of 11% of the total wall area is close to that of the specimens without openings. It was determined that it is conservative to consider the shear capacity proportional to the net transverse area of walls with window openings.

Experimental Study on Earthquake-Resistant Design of Confined Masonry Structures

To investigate the effect of window and door openings on confined masonry structures built to Mexico City building codes, three wall segments were constructed and subjected to dynamic loads (Ishibashi, 1992)

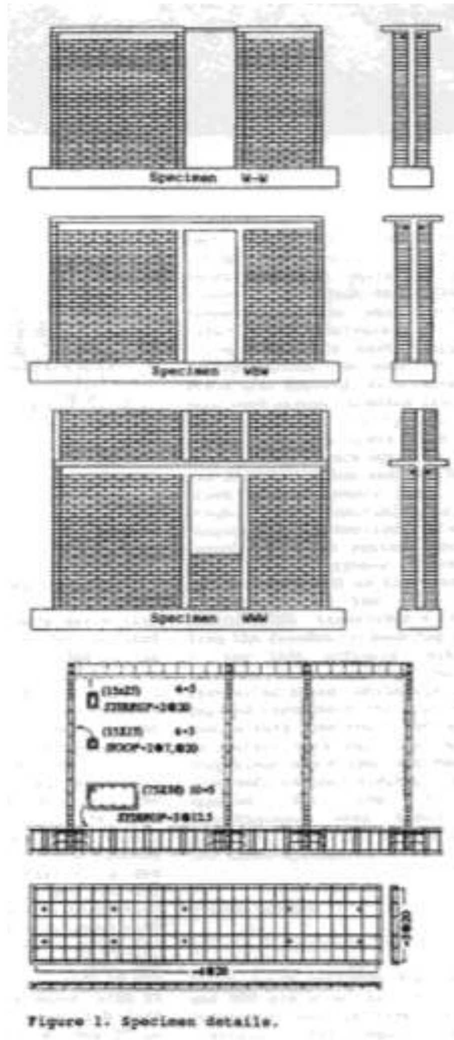

Figure 5.15. Specimen details (Ishibashi, 1992)

The specimens failed in shear developing typical X-shaped cracks. The conclusions were very similar to those found in other studies. They include:

- The strength of the masonry units is depends more on the strength of the bricks, than on the strength of the mortar.
- Vertical load increases shear capacity and stiffness. However, large vertical forces reduce the ductility of the structure.

- Tie-columns and tie-beams provide confinement to the masonry and increase the energy dissipation of the system.
- The shape of the opening affects the final crack pattern, however the mode of failure was controlled by shear and not dependent upon the shape of the opening.

5.5.5. Out-of-plane Strength

Strength Behavior and Repair of Masonry Infills

To investigate the out-of plane strength of confined masonry panels, Abrams and Angel (1994) constructed nine panels varying the materials (concrete blocks or clay bricks), the number of wythes (1 or 2), the h/t ratio for the infill and the mortar mix. The panels were all built with the two confining concrete frames, one stronger and one weaker. The weaker frame is constructed to be typical of older construction designed only for gravity loadings.

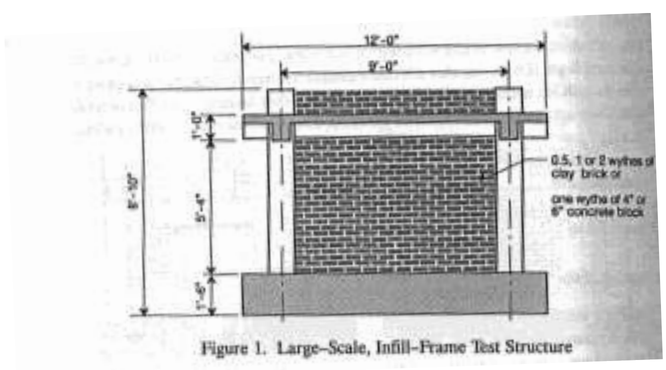

Figure 5.16. Test panels (Abrams and Angel, 1994)

The test panels were subjected to a series of static in-plane lateral forces reversals to crack-them, and then are loaded normal to their plane until ultimate strengths are detected. Damage patterns are repaired and retested with out-of-plane loads to examine possible strength requirements.

"Results of the experiments showed that in-plane cracking can reduce out-of-plane strength by approximately one-half of relatively slender panels. However, the strength of cracked infills can still be appreciable. Infill panels with h/t ratios as high as 34 were able to resist lateral pressures as large as 125 psf.

Transverse strength is sensitive to h/t ratio. In relatively stocky panels (h/t less than 20), arching was a dominant mechanism that resulted in sufficient strength to resist pressures exceeding 600 psf for cracked panels.

A simple repair technique using a ferrocement plaster coating proved to be effective for increasing strength of a cracked slender panel."

Dynamic Testing of Unreinforced Brick Masonry Infills

In a another study by the same Al-Chaar et al (1994), built half-scale test specimens consisting of single-story, single-bay reinforced concrete frames with singe-wythe clay brick infill panels.

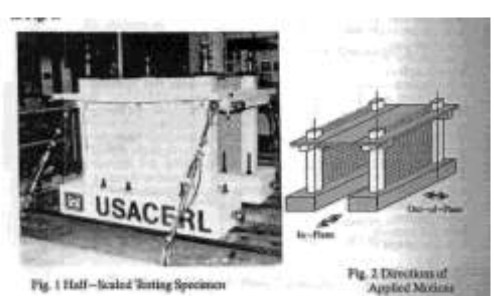

Figure 5.17. Test panels (Al-Chaar et a, 1994)

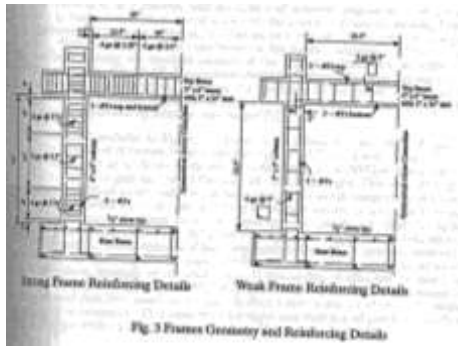

Figure 5.18. Test panel details (Al-Chaar et a, 1994)

The panels were subjected to simulated earthquake motions applied parallel with the infill plane to crack the infill panels. Then the panels will be rotated 90 degrees and subjected to out-of-plane accelerations. The following conclusions were made:

- In-plane cracking can reduce out-of-plane strength by a factor of or 2 or higher for slender panels
- Dynamic response was weakened by the crack pattern that caused by slipping between masonry units.
- Dynamic and static responses were found to be similar
- Repair methods consisting of applying wire mess with a ferrocement coating were effective but could be improved by improving bond by attaching the mesh with studs.

5.5.6. Computer Modeling

Finite Element Models of Confined Masonry Structures

Ishibashi and Katsumata carried out a series of tests of five full-sized confined masonry walls subjected to reversed cyclic horizontal loads. The results of the full-sized tests were then compared to the results of a finite element computer model of the same confined masonry walls. The dimensions and reinforcing of the full-sized test model are shown in figures 5.19, 5.20, and 5.21.

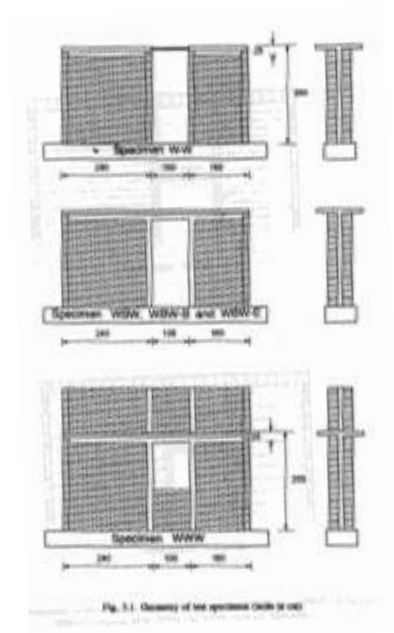

Figure 5.19. Models (Ishibashi and Katsumata, 1994)

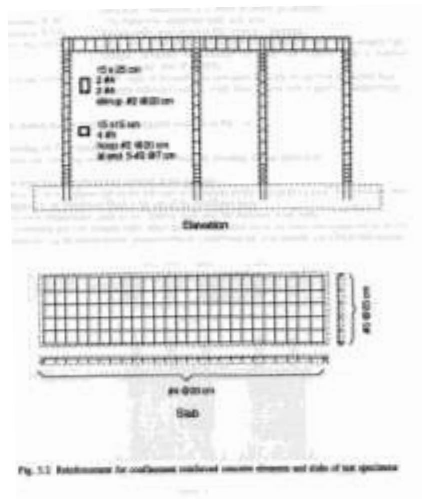

Figure 5.20. Model details of reinforcing for confinement elements and slabs (Ishibashi and Katsumata, 1994)

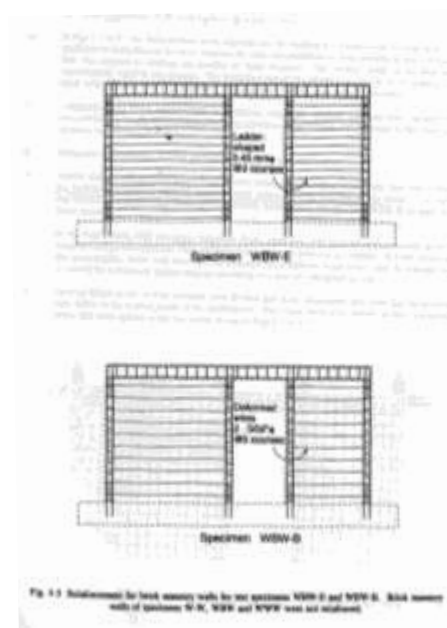

Figure 5.21. Model reinforcement for models WBW-E and WBW-B, (Ishibashi and Katsumata, 1994)

The five models varied by the specifications shown in table 5.4.

WBW	Two walls were connected by a beam and a slab. Brick walls were not reinforced. (referred to as the prototype specimen)
W-W	Two walls were connected with steel rods.
WWW	Parapet walls were added to WBW.
WBW-E	Brick walls were added to the prototype specimen were reinforced with ladder-shaped high strength horizontal reinforcement at every two courses with a nominal reinforcement ratio of 0.089%
WBW-B	Brick walls of the prototype specimen were reinforced with horizontal high strength deformed wires at every tree courses with a nominal reinforcing of 0.089%

Table 5.4. Model specifications, Ishibashi and Katsumata, 1994)

The following assumptions were made when creating the computer models:

1. Plane stress conditions were assumed.
2. Effect of foundations was assumed to be minimal. Specimens were fixed at the foundation.
3. Four-node quadrilateral plane stress elements were used for modeling the brick walls.
4. A tie-column and two buttress walls which were connected to the tie-beam were assumed to be one element having the superimposed characteristics of a reinforced concrete element and a brick wall element.
5. Steel rods of specimen WW were replaced with a truss element.
6. In the figures of the finite element models the meshing and loading are shown. Each element has the same properties as those obtained in masonry prism tests. The element height is equal to two courses. The

horizontal height is chosen to be equal to the height. This was assumed for all specimens.

7. Longitudinal and shear reinforcement in peripheral reinforced concrete elements were replaced with elements having tensile stiffness in one direction and those elements were superimposed on the plane stress elements for columns and beams.
8. Horizontal reinforcement was replaced by truss elements.
9. Tensile strength of horizontal joint mortar in brick walls was about three times larger than that of bricks. Horizontal joints were replaced with equivalent spring elements having two nodes. Each spring was located between the upper nodes of a lower brick finite element and the lower nodes of an upper brick finite element.
10. During the experiments, as the horizontal loads increased, separation and slipping was observed along the boundary surface between the brick walls and the peripheral reinforced concrete tie-columns. In order to simulate this, brick wall elements and elements for peripheral bond-beams and tie-columns were connected by a two-node linkage element consisting of a pair of orthogonal springs.
11. External forces in the vertical direction were divided into three components and were applied to the nearest three nodes to the loading points of the experiments. Horizontal loads were divided in two concentrated forces and were applied to two nodes. This is shown in figures 5.22 and 5.23.

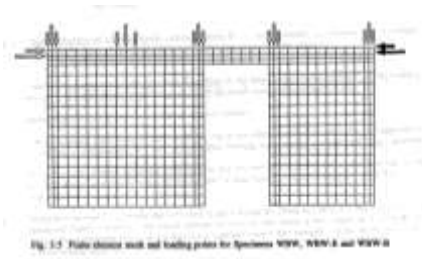

Figure 5.22. Model details (Ishibashi and Katsumata, 1994)

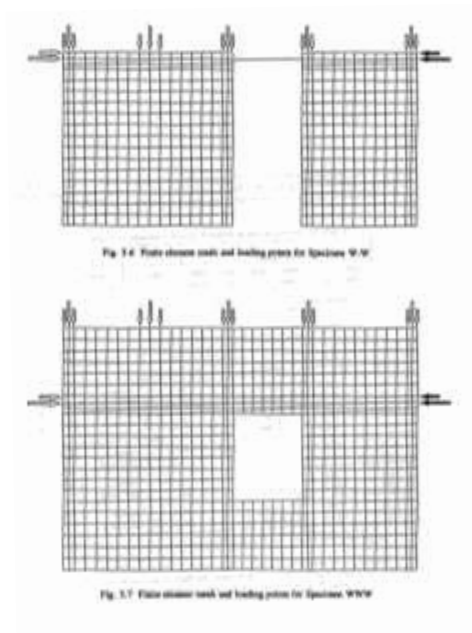

Figure 5.23. Model details (Ishibashi and Katsumata, 1994)

A graphical representation of these results can be seen in figure 5.24.

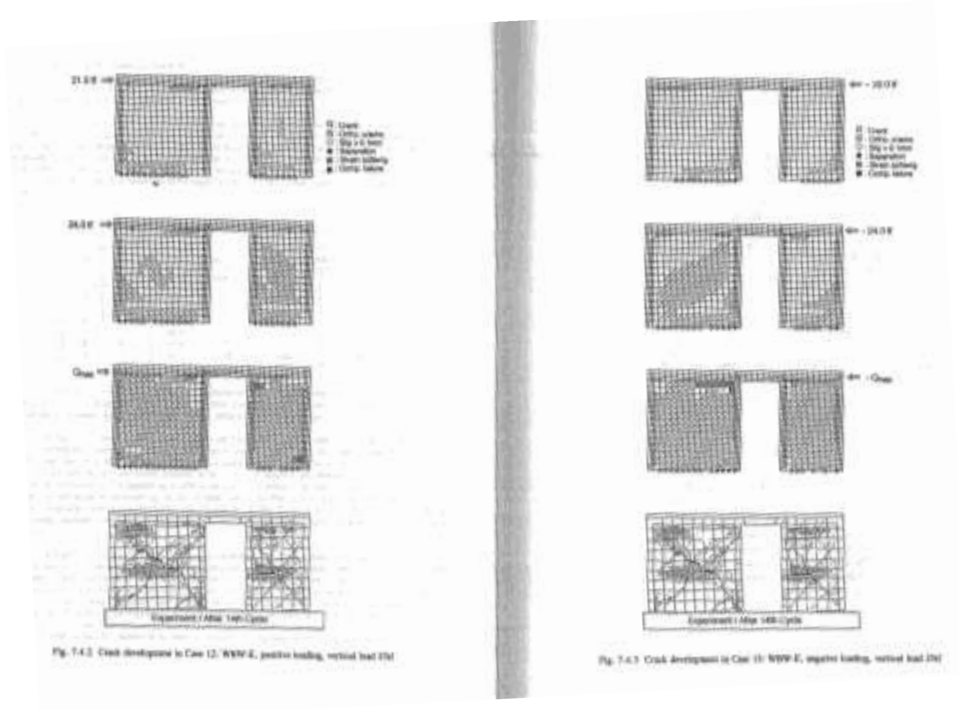

Figure 5.24. Finite element model and results (Ishibashi and Katsumata, 1994)

The horizontal load displacement relationships calculated were generally in good agreement with the tested values. In some cases the values did not correlate well and this was attributed to an inadequate modeling of the boundary conditions.

Finite Element Models Comparing Discrete and Smeared Cracking

In 1997 Mosalam et al did an extensive study to compare discrete finite element modeling techniques with smeared finite element techniques. The comparison of the two computer models can be seen in the following diagram.

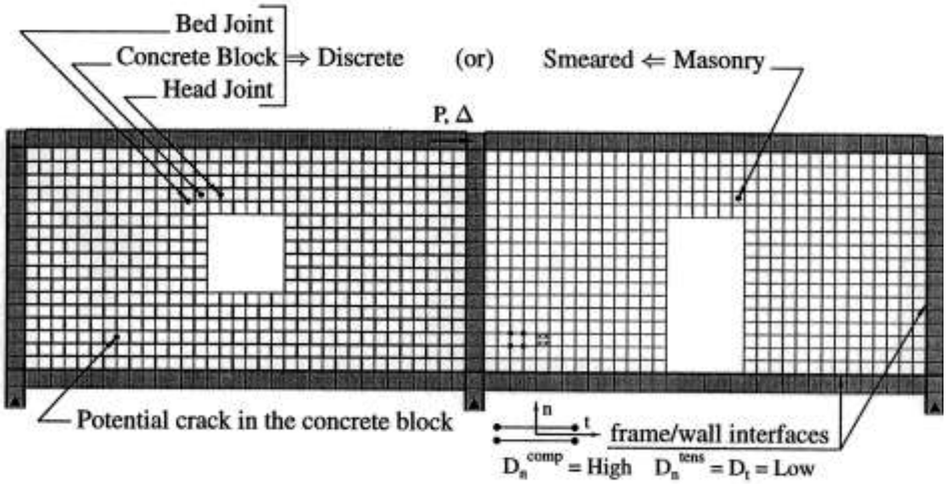

FIGURE 2-1 Finite element models for masonry infills.

Figure 5.25. Finite element models for masonry infills (Mosalam, 1997)

Discrete Approach

To model the joints between the bricks interface elements were used.

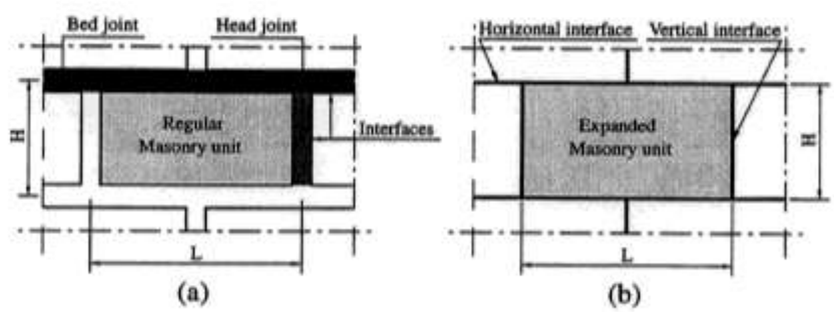

FIGURE 2-2 Modeling of masonry composite; (a) Detailed model; (b) Approximate model.

Figure 5.26. Joint models (Mosalam, 1997)

The interface elements were essentially nonlinear springs along the normal and tangential direction of the interface. These interface elements in the normal direction are governed by normal stress vs. relative displacement. This can be seen in the following diagram.

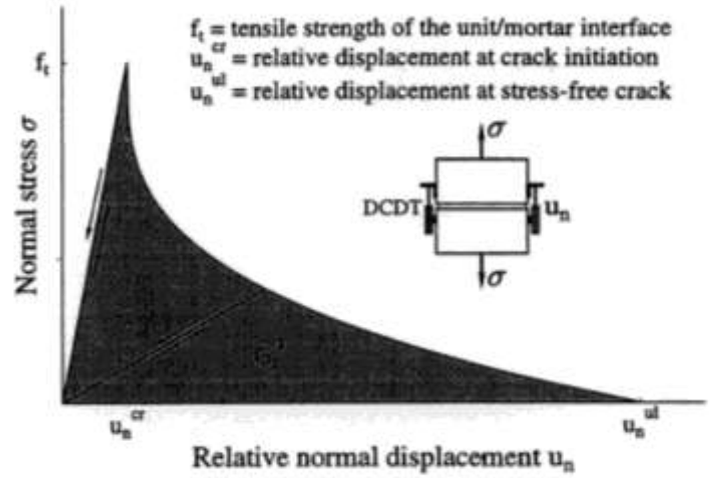

FIGURE 2-4 Normal stress versus relative displacement relation.

Figure 5.27.Normal stress vs. relative displacement (Mosalam, 1997)

From the figure 5.27 distinct stages can be identified: contact, development of separation, and complete separation. In the tangential direction, the stress vs. relative displacement relationship was assumed nonlinear elasto-plastic following the Mohr-Coulomb criterion supplemented with softening criteria for cohesion and for internal friction.

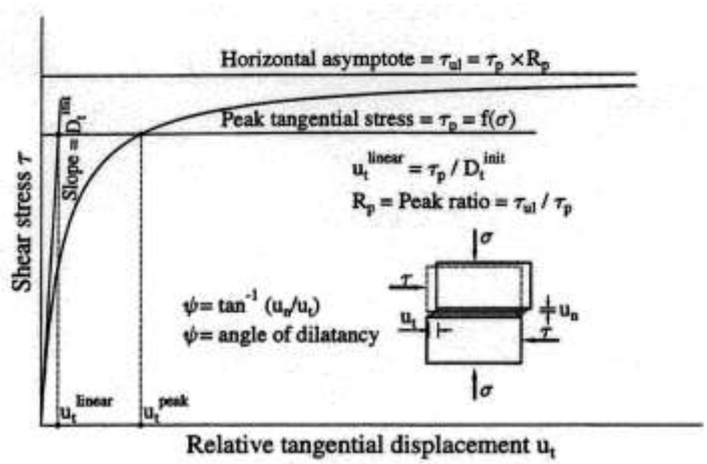

FIGURE 2-5 Pre-peak shear stress versus relative displacement relation.

Figure 5.28. Shear stress vs. relative displacement (Mosalam, 1997)

To test this approach, the following computer model was created and compared with a physical test model.

The comparison of the computer and physical models can be seen in the following diagram:

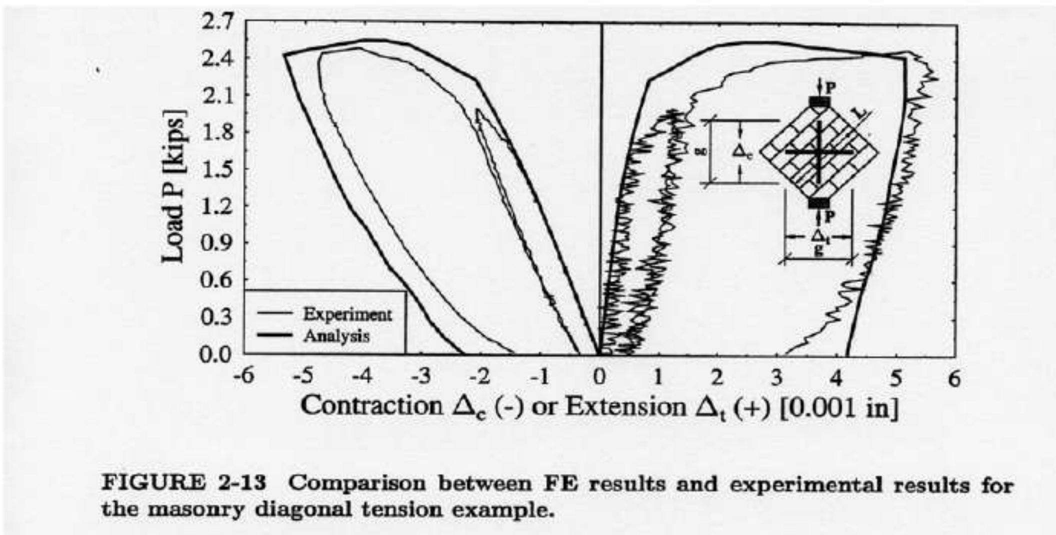

Figure 5.29. Comparison between finite element results and experimental results (Mosalam, 1997)

This same idealization was applied to the brick frame interface and a complete wall was modeled both physically and a computer model. The comparison of the results is shown in figure 5.30.

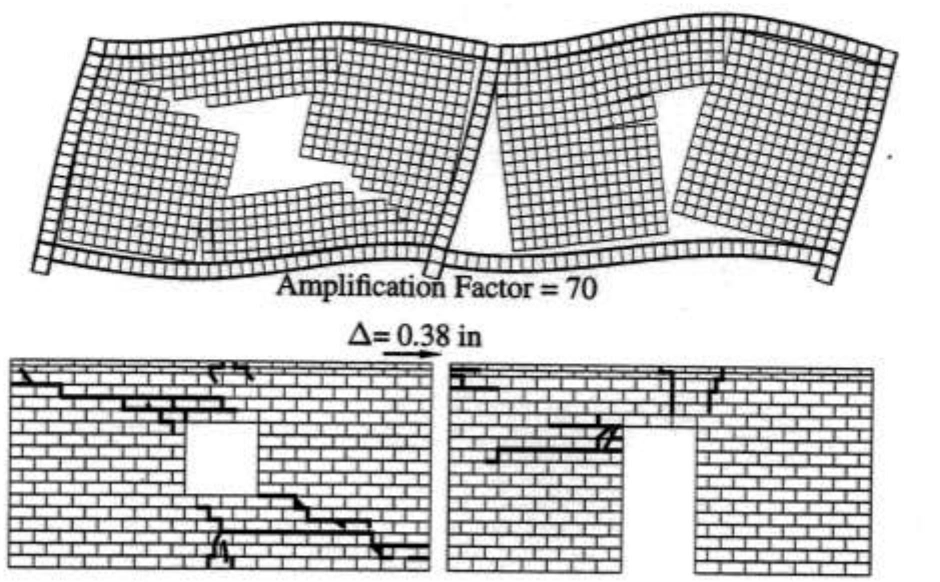

FIGURE 2-16 Comparison between the FE results (top) and the experimental (bottom) crack patterns for the two-bay single-story infilled frame.

Figure 5.30 Comparison between finite element results and experimental results (Mosalam, 1997)

Smeared Approach

The previously described discrete approach is accurate but may require enormous computing capabilities, in particular when modeling full structures. Two methods were used to account for the evolution of material damage produced by smeared cracking. The first method is based on continuous change of the topology of the finite element mesh. The second method utilizes the continuous change of the so-called crack band width.

Strut Models of Confined Masonry Structures

To investigate the effect of masonry infills on the performance of reinforced concrete frames, DeCanini et al (2004) evaluated the elastic and inelastic response of a multi-story shear-type frame model with and without infills. The infills were modeled with equivalent strut elements which can only carry compressive loads. Three different types of masonry were considered: weak, intermediate, and strong infills. The mathematical model was validated with test results. Several computer models were constructed varying the number of stories.

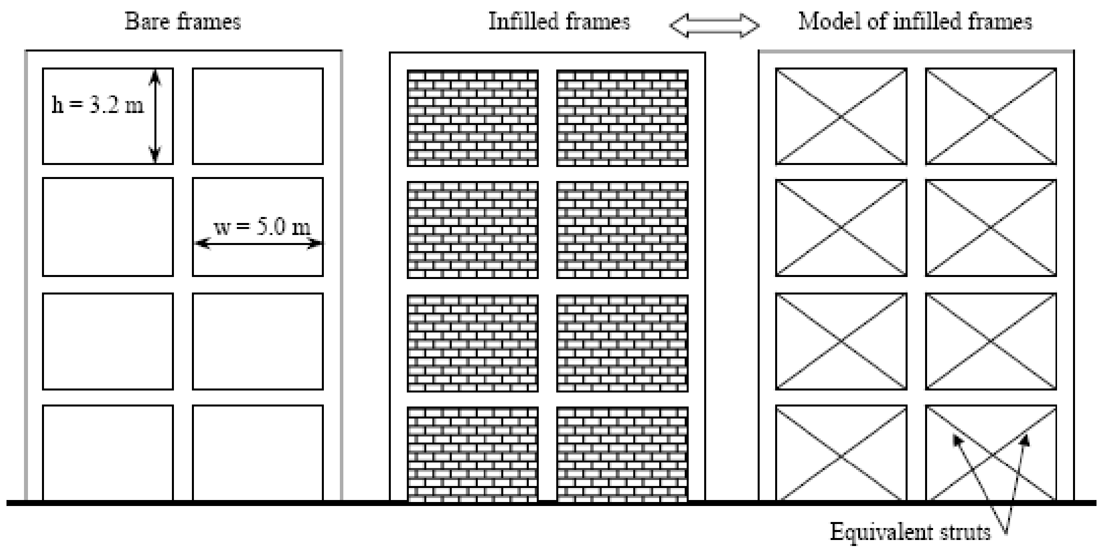

Figure 5.31. Structural layout of bare and infilled frames (DeCanini, 2004)

The individual masonry units are assumed to be ineffective in tension and are represented as compression only members. The following lateral force-displacement curve was used to model the struts. This curve has four branches including: linear elastic ascending branch corresponds to the un-cracked stage, the second is the post-cracked state up to the development of the maximum strength, the third stage corresponds to the descending post-peak strength deterioration of the until it reaches the residual strength of the fourth stage where it continues horizontally. The values of K_{mfc} and H_{mfc} can be calculated based on the material properties and the geometry.

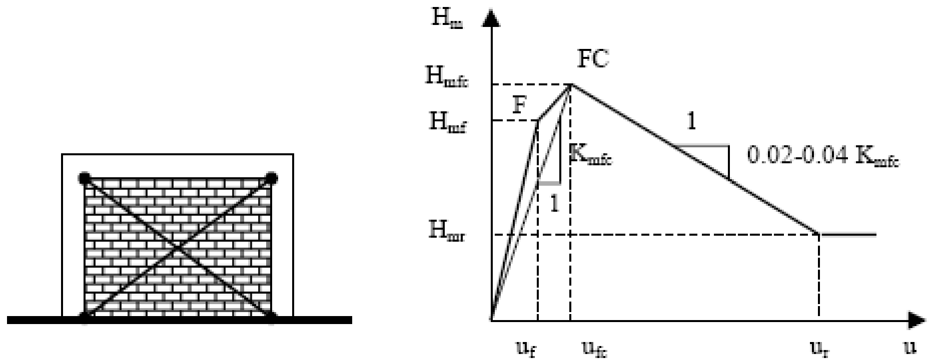

Figure 5.32. Force displacement envelope curve for the equivalent strut (DeCanini, 2004)

The result of the cyclic testing is shown in table 5.5.

N. of stories	T (s) infilled t1	T (s) infilled t2	T (s) infilled t3	T (s) bare frames
2	0.148	0.117	0.088	0.286
4	0.266	0.218	0.168	0.536
6	0.366	0.298	0.227	0.761
8	0.479	0.389	0.296	1.015
10	0.581	0.470	0.356	1.251
12	0.674	0.544	0.411	1.465
14	0.764	0.616	0.465	1.664
16	0.862	0.695	0.523	1.874
20	1.048	0.841	0.630	2.338
24	1.209	0.970	0.725	2.689

Table 5.5. Comparison between numerical and experimental results (DeCanini, 2004)

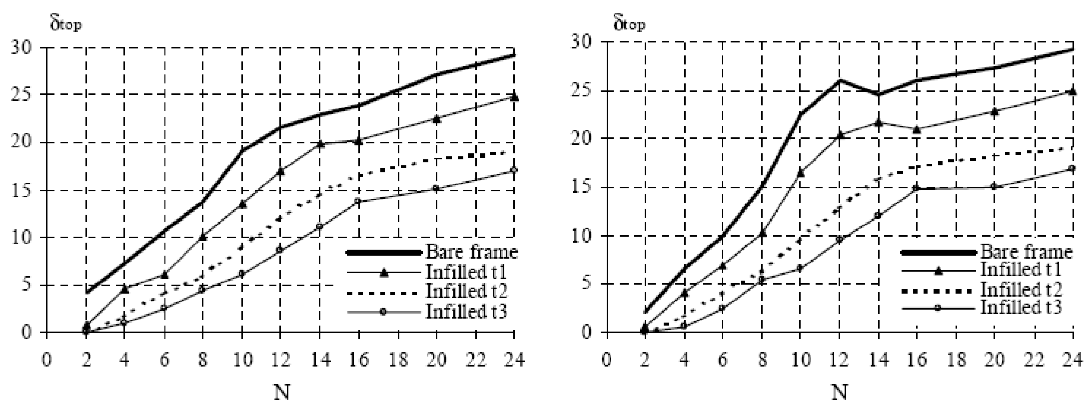

Figure 5.33. Top story displacement vs. number of stories (DeCanini, 2004)

6. Performance Based Design

Design procedures based on deflections or building performance rather than strength or stress parameters are generally referred to as performance based design. A static, non-linear analysis is often referred to as a pushover analysis and is one type of performance based analysis. In the event of an earthquake, it is permissible for a structure to deform beyond its yield point. Therefore, the properties of a structure beyond yield must be known and analyzed. A pushover analysis consists of applying a static lateral load (which simulates an earthquake load) to a structure and determining the deformation of that structure which will include deformations beyond the yield limit. The amount of deformation is then used to determine the damage state. These damage states have been defined by ATC 40 (Applied Technology Counsel – Seismic Evaluation and retro-fit of concrete Buildings) as:

Immediate Occupancy – Non-structural elements and systems are generally in place and only minor disruption and clean-up are required.

Life Safety – Considerable damage to non-structural elements and systems but should not include collapse or falling of heavy items.

Structural Stability – The building is on the verge of partial or total structural collapse.

Buildings are required to be designed to resist minimum loads laid out in the Building Code. In the past most building codes required that during a design event (for instance, the largest earthquake for which a building must be designed) the building must maintain enough structural integrity to protect human life. Economic loss was not considered. This could mean that the building would have to be demolished after the event. But what if a building owner wanted to ensure that his building was still useable after the event? There were no guidelines for ensuring that a building remained functional after the event. There are also different levels of functionality. For example, there could be only minor repairs required or no repairs required. Performance Based design considers economic loss in addition to protecting loss of life. It allows the design team, which includes the building owner, architect, and engineer, to understand and choose a desired level of performance for buildings and nonstructural components when they are subjected to a specified level of ground motion. Performance based design also works well with design models of structures, since it is easy to determine the performance at different magnitudes of loads. This would be very difficult with tradition stress calculations.

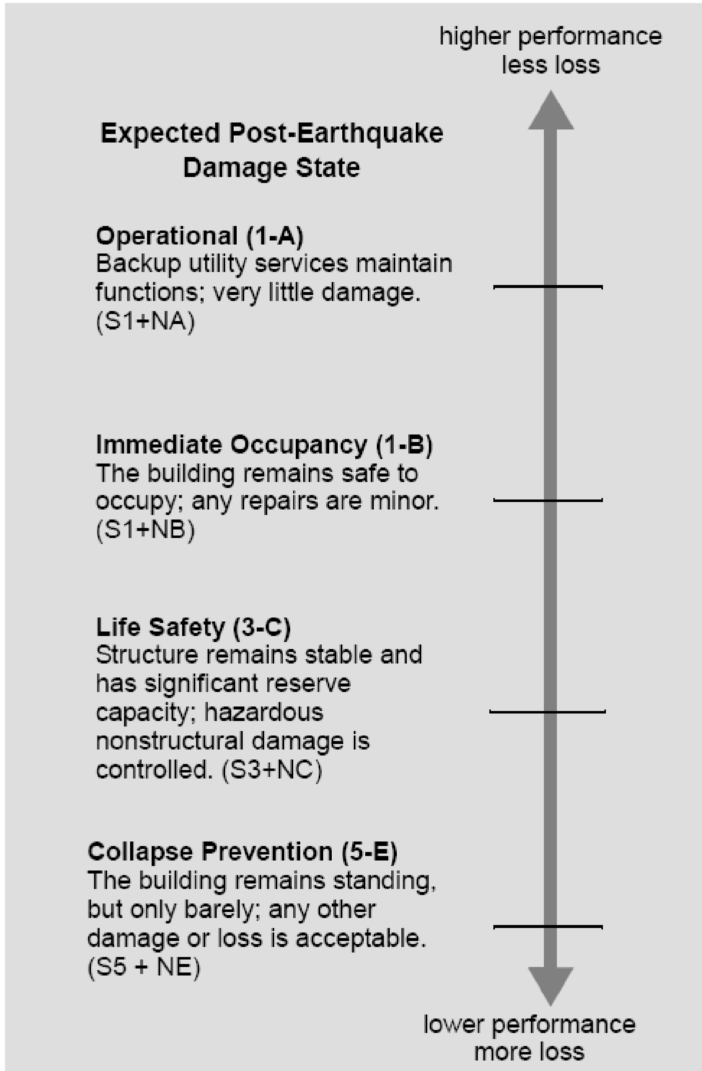

Figure 6.1. Target performance levels and ranges (FEMA 356, 2000)

6.1. FEMA 440

FEMA 440 (2005) lays out the procedures for nonlinear static seismic analysis. It is based on two previous documents ATC 40 (Applied Technology Counsel – Seismic Evaluation and retro-fit of concrete Buildings) and FEMA 356 (2000) (Prestandard and Commentary for the Seismic Rehabilitation of Buildings). These are two early documents that laid out the procedures for performing a nonlinear static analysis of buildings and created pushover curves. The two methods used two different methods and gave different results. FEMA 356 used the coefficient method which calculated the displacement demand by modifying the elastic predictions. ATC 40 uses the Capacity-Spectrum Method. This method uses a smoothed out response spectrum (which represents the design ground motion) to determine the modal displacement demand. It determines this demand by locating the intersection of the capacity curve, with the demand curve. FEMA 440 is the results of the investigation that compared these two methods and determined they are both valid methods with strengths and weaknesses. Perform 3-D, a non-linear finite element program developed by Computers and Structures Inc., has the ability to do pushover analysis based on:

Fema 440 Linearization Method.

FEMA 440 modifications of the coefficient Method (also known as the Displacement Modification Method).

FEMA 356 Coefficinet Method.

Capacity Spectrum Method, with options for the ATC 40 procedure or a modified procedure that may be more accurate.

FEMA 440 Introduction

Performance based design predicts expected damage to structural and nonstructural components and contents. Damage does not occur in the elastic range and therefore structural damage implies inelastic behavior. Inelastic seismic analysis aims to estimate the magnitude of inelastic deformations. The process of inelastic analysis is as follows:

Develop a model of the building structure

Subject structure to a representation of the anticipated seismic ground motion

Results are usually measured by global displacements (roof or other reference point), story drifts, story forces, etc.

The different inelastic analysis procedures vary by types of structural models used for analysis and different methods for characterizing the seismic ground shaking.

Models

The models used in inelastic seismic analysis are similar to those used in linear elastic analysis but also contain post elastic strength and deformation characteristics. As with any model there are assumptions and estimations at every level of building the model.

Pushover or Capacity Curves

Pushover or Capacity curves are generated by subjecting the model to one or more lateral loads and then increasing the magnitude to generate a nonlinear inelastic force-deformation for the structure. The loads applied are usually related to the accelerations associated with the first mode of vibration of the structure. From this curve an equivalent single degree of freedom system can be idealized. Below is a diagram from FEMA 440 that illustrates this process:

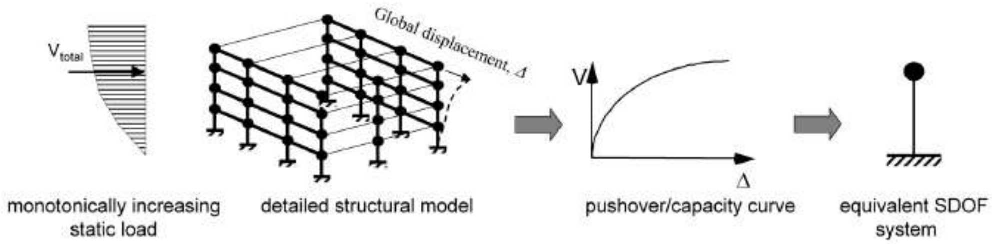

Figure 6.2. Schematic depicting the development of an equivalent SDOF system from a pushover/capacity curve (FEMA 440)

6.2. FEMA 356

FEMA 356 defines the structural performance levels of a building as follows:

Immediate Occupancy Structural Performance Level (S1)

The post-earthquake damage state that remains safe to occupy, essentially retains the pre-earthquake design strength and stiffness of the structure and in which only very limited structural damage has occurred. The basic vertical- and later-force-resisting systems of the building retain nearly all of the pre-earthquake strength and stiffness. The risk of life-threatening injury as a result of structural damage is very low, and although some minor structural repairs may be appropriate, these would generally not be required prior to reoccupancy (FEMA 356)

Damage Control Structural Performance Range (S-2)

The post earthquake damage state defined as the continuous range of damage between life safety Structural Performance Level (S-3) and the Immediate Occupancy Structural Performance Level (S-1)….This range may be desirable to minimize repair time and operation interruption, as a partial means of protecting valuable equipment and contents or to preserve important historic features when the cost of design for immediate occupancy is excessive. (FEMA 356)

Life Safety Structural Performance Level (S-3)

The post-earthquake damage state that includes damage to structural components but retains a margin against the onset of partial or total collapse. This damage state may contain significant damage to the structure, but some margin against either partial or total collapse. Some structural elements and components are severely damaged, but this has not resulted in large falling debris hazards, either within or outside the building. Injuries may occur during eh earthquake; however, the overall risk of life-threatening injury as a result of structural damage is expected to be low. It should be possible to repair the structure; however, for economic reasons this may not be practical. While the damaged structure is not an imminent collapse risk, it would be prudent to implement structural repairs or install temporary bracing prior to reoccupancy. (FEMA 356)

Limited Safety Structural Performance Range (S-4)

The continuous range of damage state between the Life Safety Structural Performance Level (S-3) and the Collapse Prevention Structural Performance Level (S-5)….This post–earthquake damage state includes damage to structural components such that the structure continues to support gravity loads but retains no margin against collapse. (FEMA 356)

Collapse Prevention Structural Performance Level (S-5)

The post-earthquake state that includes damage to structural components such that the structure continues to support gravity loads but retains no margin against collapse….The building is on the verge or partial or total collapse. Substantial damage to the structure has occurred, potentially including significant degradation in the stiffness and strength of the lateral-force resisting systems, large permanent lateral deformation of the structure, and – to a more limited extent – degradation in the vertical-load-carrying capacity. However, all significant components of the gravity load-resisting system must continue to carry their gravity load demands. Significant risk of injury due to falling hazards from structural debris may exist. The structure may not be technically practical to repair and is not safe for reoccupancy, as aftershock activity could induce collapse. (FEMA 356)

Structural Performance Not Considered (S-6):

The building's performance is not considered. (FEMA 356)

Fema 356 goes on to give the following table of damage Control and building performance levels:

	Target Building Performance Levels			
	Collapse Prevention Level (5-E)	Life Safety Level (3-C)	Immediate Occupancy Level (1-B)	Operational Level (1-A)
Overall Damage	Severe	Moderate	Light	Very Light
General	Little residual stiffness and strength, but load-bearing columns and walls function. Large permanent drifts. Some exits blocked. Infills and unbraced parapets failed or at incipient failure. Building is near collapse.	Some residual strength and stiffness left in all stories. Gravity-load-bearing elements function. No out-of-plane failure of walls or tipping of parapets. Some permanent drift. Damage to partitions. Building may be beyond economical repair.	No permanent drift. Structure substantially retains original strength and stiffness. Minor cracking of facades, partitions, and ceilings as well as structural elements. Elevators can be restarted. Fire protection operable.	No permanent drift. Structure substantially retains original strength and stiffness. Minor cracking of facades, partitions, and ceilings as well as structural elements. All systems important to normal operation are functional.
Nonstructural components	Extensive damage.	Falling hazards mitigated but many architectural, mechanical, and electrical systems are damaged.	Equipment and contents are generally secure, but may not operate due to mechanical failure or lack of utilities.	Negligible damage occurs. Power and other utilities are available, possibly from standby sources.
Comparison with performance intended for buildings designed under the *NEHRP Provisions*, for the Design Earthquake	Significantly more damage and greater risk.	Somewhat more damage and slightly higher risk.	Less damage and lower risk.	Much less damage and lower risk.

Table 6.1. Damage control and building performance levels (FEMA 356)

FEMA 356 also describes the performance levels based on damage and drift as shown in table 6.2.

Table C1-3 Structural Performance Levels and Damage[1, 2, 3]—Vertical Elements

		Structural Performance Levels		
Elements	Type	Collapse Prevention S-5	Life Safety S-3	Immediate Occupancy S-1
Concrete Frames	Primary	Extensive cracking and hinge formation in ductile elements. Limited cracking and/or splice failure in some nonductile columns. Severe damage in short columns.	Extensive damage to beams. Spalling of cover and shear cracking (<1/8" width) for ductile columns. Minor spalling in nonductile columns. Joint cracks <1/8" wide.	Minor hairline cracking. Limited yielding possible at a few locations. No crushing (strains below 0.003).
	Secondary	Extensive spalling in columns (limited shortening) and beams. Severe joint damage. Some reinforcing buckled.	Extensive cracking and hinge formation in ductile elements. Limited cracking and/or splice failure in some nonductile columns. Severe damage in short columns.	Minor spalling in a few places in ductile columns and beams. Flexural cracking in beams and columns. Shear cracking in joints <1/16" width.
	Drift	4% transient or permanent	2% transient; 1% permanent	1% transient; negligible permanent
Steel Moment Frames	Primary	Extensive distortion of beams and column panels. Many fractures at moment connections, but shear connections remain intact.	Hinges form. Local buckling of some beam elements. Severe joint distortion; isolated moment connection fractures, but shear connections remain intact. A few elements may experience partial fracture.	Minor local yielding at a few places. No fractures. Minor buckling or observable permanent distortion of members.
	Secondary	Same as primary.	Extensive distortion of beams and column panels. Many fractures at moment connections, but shear connections remain intact.	Same as primary.
	Drift	5% transient or permanent	2.5% transient; 1% permanent	0.7% transient; negligible permanent
Braced Steel Frames	Primary	Extensive yielding and buckling of braces. Many braces and their connections may fail.	Many braces yield or buckle but do not totally fail. Many connections may fail.	Minor yielding or buckling of braces.
	Secondary	Same as primary.	Same as primary.	Same as primary.
	Drift	2% transient or permanent	1.5% transient; 0.5% permanent	0.5% transient; negligible permanent

Table 6.2. Structural performance levels and damage for vertical elements, (FEMA 356)

Table C1-3 Structural Performance Levels and Damage[1, 2, 3]—Vertical Elements (continued)				
		Structural Performance Levels		
Elements	Type	Collapse Prevention S-5	Life Safety S-3	Immediate Occupancy S-1
Concrete Walls	Primary	Major flexural and shear cracks and voids. Sliding at joints. Extensive crushing and buckling of reinforcement. Failure around openings. Severe boundary element damage. Coupling beams shattered and virtually disintegrated.	Some boundary element stress, including limited buckling of reinforcement. Some sliding at joints. Damage around openings. Some crushing and flexural cracking. Coupling beams: extensive shear and flexural cracks; some crushing, but concrete generally remains in place.	Minor hairline cracking of walls, <1/16" wide. Coupling beams experience cracking <1/8" width.
	Secondary	Panels shattered and virtually disintegrated.	Major flexural and shear cracks. Sliding at joints. Extensive crushing. Failure around openings. Severe boundary element damage. Coupling beams shattered and virtually disintegrated.	Minor hairline cracking of walls. Some evidence of sliding at construction joints. Coupling beams experience cracks <1/8" width. Minor spalling.
	Drift	2% transient or permanent	1% transient; 0.5% permanent	0.5% transient; negligible permanent
Unreinforced Masonry Infill Walls	Primary	Extensive cracking and crushing; portions of face course shed.	Extensive cracking and some crushing but wall remains in place. No falling units. Extensive crushing and spalling of veneers at corners of openings.	Minor (<1/8" width) cracking of masonry infills and veneers. Minor spalling in veneers at a few corner openings.
	Secondary	Extensive crushing and shattering; some walls dislodge.	Same as primary.	Same as primary.
	Drift	0.6% transient or permanent	0.5% transient; 0.3% permanent	0.1% transient; negligible permanent
Unreinforced Masonry (Noninfill) Walls	Primary	Extensive cracking; face course and veneer may peel off. Noticeable in-plane and out-of-plane offsets.	Extensive cracking. Noticeable in-plane offsets of masonry and minor out-of-plane offsets.	Minor (<1/8" width) cracking of veneers. Minor spalling in veneers at a few corner openings. No observable out-of-plane offsets.
	Secondary	Nonbearing panels dislodge.	Same as primary.	Same as primary.
	Drift	1% transient or permanent	0.6% transient; 0.6% permanent	0.3% transient; 0.3% permanent

Table 6.3. Structural performance levels and damage for vertical elements continued (FEMA 356)

Table C1-3 Structural Performance Levels and Damage[1, 2, 3]—Vertical Elements (continued)

Elements	Type	Structural Performance Levels: Collapse Prevention S-5	Life Safety S-3	Immediate Occupancy S-1
Reinforced Masonry Walls	Primary	Crushing; extensive cracking. Damage around openings and at corners. Some fallen units.	Extensive cracking (<1/4") distributed throughout wall. Some isolated crushing.	Minor (<1/8" width) cracking. No out-of-plane offsets.
	Secondary	Panels shattered and virtually disintegrated.	Crushing; extensive cracking; damage around openings and at corners; some fallen units.	Same as primary.
	Drift	1.5% transient or permanent	0.6% transient; 0.6% permanent	0.2% transient; 0.2% permanent
Wood Stud Walls	Primary	Connections loose. Nails partially withdrawn. Some splitting of members and panels. Veneers dislodged.	Moderate loosening of connections and minor splitting of members.	Distributed minor hairline cracking of gypsum and plaster veneers.
	Secondary	Sheathing sheared off. Let-in braces fractured and buckled. Framing split and fractured.	Connections loose. Nails partially withdrawn. Some splitting of members and panels.	Same as primary.
	Drift	3% transient or permanent	2% transient; 1% permanent	1% transient; 0.25% permanent
Precast Concrete Connections	Primary	Some connection failures but no elements dislodged.	Local crushing and spalling at connections, but no gross failure of connections.	Minor working at connections; cracks <1/16" width at connections.
	Secondary	Same as primary.	Some connection failures but no elements dislodged.	Minor crushing and spalling at connections.
Foundations	General	Major settlement and tilting.	Total settlements <6" and differential settlements <1/2" in 30 ft.	Minor settlement and negligible tilting.

1. Damage states indicated in this table are provided to allow an understanding of the severity of damage that may be sustained by various structural elements when present in structures meeting the definitions of the Structural Performance Levels. These damage states are not intended for use in post-earthquake evaluation of damage or for judging the safety of, or required level of repair to, a structure following an earthquake.
2. Drift values, differential settlements, crack widths, and similar quantities indicated in these tables are not intended to be used as acceptance criteria for evaluating the acceptability of a rehabilitation design in accordance with the analysis procedures provided in this standard; rather, they are indicative of the range of drift that typical structures containing the indicated structural elements may undergo when responding within the various Structural Performance Levels. Drift control of a rehabilitated structure may often be governed by the requirements to protect nonstructural components. Acceptable levels of foundation settlement or movement are highly dependent on the construction of the superstructure. The values indicated are intended to be qualitative descriptions of the approximate behavior of structures meeting the indicated levels.
3. For limiting damage to frame elements of infilled frames, refer to the rows for concrete or steel frames.

Table 6.4. Structural performance levels and damage for vertical elements continued (FEMA 356)

Table C1-4 Structural Performance Levels and Damage[1, 2]—Horizontal Elements

Element	Structural Performance Levels: Collapse Prevention S-5	Life Safety S-3	Immediate Occupancy S-1
Metal Deck Diaphragms	Large distortion with buckling of some units and tearing of many welds and seam attachments.	Some localized failure of welded connections of deck to framing and between panels. Minor local buckling of deck.	Connections between deck units and framing intact. Minor distortions.
Wood Diaphragms	Large permanent distortion with partial withdrawal of nails and extensive splitting of elements.	Some splitting at connections. Loosening of sheathing. Observable withdrawal of fasteners. Splitting of framing and sheathing.	No observable loosening or withdrawal of fasteners. No splitting of sheathing or framing.
Concrete Diaphragms	Extensive crushing and observable offset across many cracks.	Extensive cracking (<1/4" width). Local crushing and spalling.	Distributed hairline cracking. Some minor cracks of larger size (<1/8" width).
Precast Diaphragms	Connections between units fail. Units shift relative to each other. Crushing and spalling at joints.	Extensive cracking (<1/4" width). Local crushing and spalling.	Some minor cracking along joints.

1. Damage states indicated in this table are provided to allow an understanding of the severity of damage that may be sustained by various structural elements when present in structures meeting the definitions of the Structural Performance Levels. These damage states are not intended for use in post-earthquake evaluation of damage or for judging the safety of, or required level of repair to, a structure following an earthquake.

2. Drift values, differential settlements, crack widths, and similar quantities indicated in these tables are not intended to be used as acceptance criteria for evaluating the acceptability of a rehabilitation design in accordance with the analysis procedures provided in this standard; rather, they are indicative of the range of drift that typical structures containing the indicated structural elements may undergo when responding within the various Structural Performance Levels. Drift control of a rehabilitated structure may often be governed by the requirements to protect nonstructural components. Acceptable levels of foundation settlement or movement are highly dependent on the construction of the superstructure. The values indicated are intended to be qualitative descriptions of the approximate behavior of structures meeting the indicated levels.

Table 6.5. Structural performance levels and damage for horizontal elements (FEMA 356)

6.2.1. Using Ground Motions to Determine Static Load

To determine the seismic load to apply for a static non-linear analysis FEMA 356 uses a spectral response acceleration diagram. Because force is equal to mass times acceleration, a building's stiffness or period determines how much load it will need to resist in and earthquake. This chart determines the load based on period. Each diagram represents one seismic hazard and therefore one diagram should be made for each different location hazard. The FEMA 356 diagram is shown in figure 6.3.

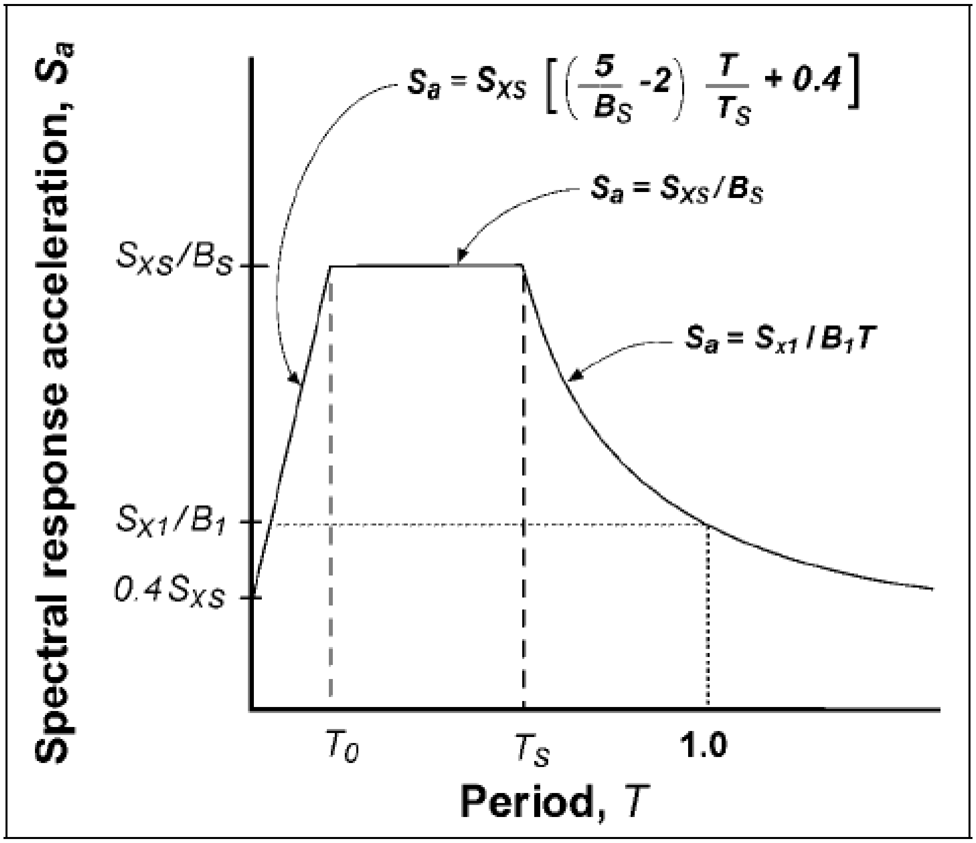

Figure 6.3. General horizontal response spectrum (FEMA 356)

For Nicaragua, response spectrums were determined (see figure 6.4). From the response spectra, the response acceleration (Sa) can be determine.

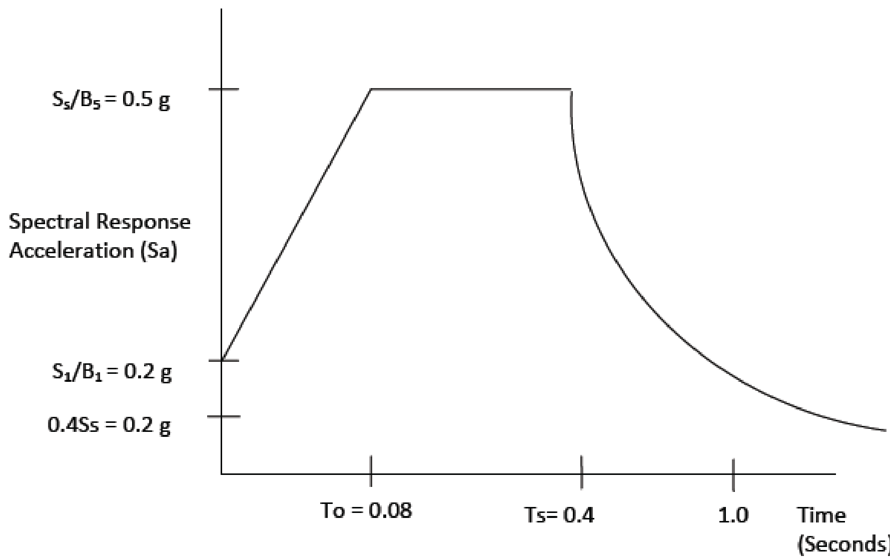

Figure 6.4. Response spectra for Nicaragua

FEMA 356 recommends the following formula for the equivalent static force:

$V = C_1C_2C_3C_mS_aW$ (6.1)

V - Pseudo lateral load

C_1 – Modification factor to relate expected maximum inelastic displacements to displacement calculated for linear elastic response

C_1 = 1.5 for T<0.10 second

C_1 = 1.0 for T> Ts second

C_2 – Modification factor to represent the effects of pinched hysteresis shape, stiffness degradation, and strength deterioration on maximum displacement response (for linear procedures C_2 shall be taken as 1.0)

C_3 –Modification factor to represent increased displacement due to dynamic P-Δ effects

Cm –Effective mass factor to account for higher mode mass participation effects (This value is 1 for buildings with 1 or 2 stories)

Sa – Spectral response acceleration, g

W –weight of the building

The building is subjected to monotonically increasing lateral loads until a target displacement is exceeded. Figure 6.5 shows the idealized force-displacement curves from this analysis.

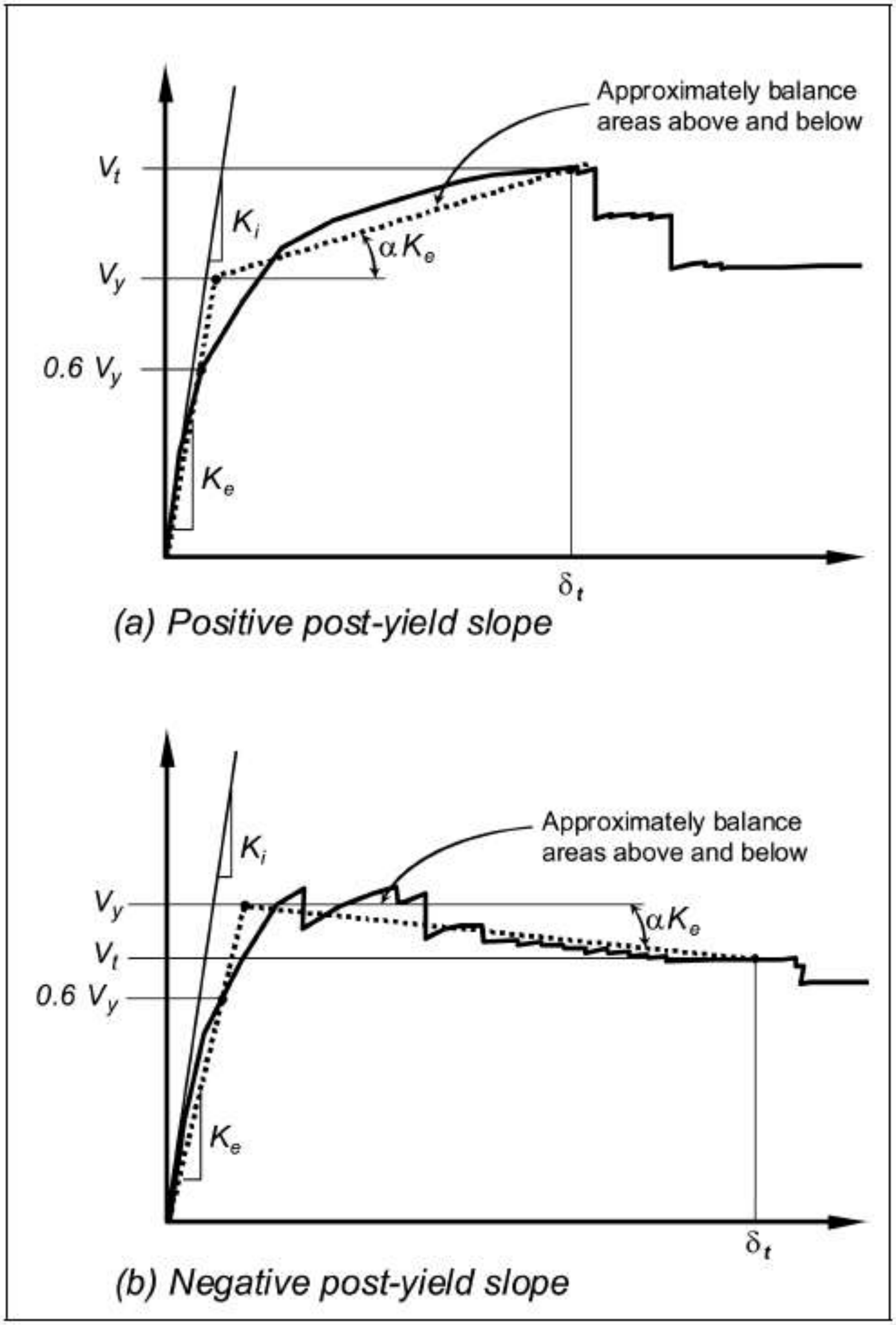

Figure 6.5. Idealized force displacement curve (FEMA 356)

6.2.2. Target Displacement

The target displacement, δ_t, is calculated for all buildings with a rigid diaphragm at each floor level. For buildings with non-rigid diaphragms the diaphragm flexibility is included in the model. The target displacement is amplified by the ratio of the maximum displacement at any point on the roof to the displacement at the center of mass of the roof ($\delta_{max}/ \delta_{cm}$). The formula for the target displacement is as follows:

$$\delta_t = C_o C_1 C_2 C_3 S_a \frac{T_e^{\,2}}{4\Pi^2} g \tag{6.2}$$

where:

Co - Modification factor to relate spectral displacement of an equivalent SDOF system to the roof displacement of the building MDOF system (for any load pattern this value is 1.0 for 1 story buildings and 1.2 for 2 story buildings)

C1 - Modification factor to relate expected maximum inelastic displacement to displacements calculated for linear elastic response:

= 1.0 fpr Te>Ts

= [1.0+(r-1)Ts/Te] R for Te<Ts but not less than 1

Te - Effective fundamental period of the building in the direction under consideration, sec

Ts - Characteristic period of the response spectrum as previously calculated

R - Ratio of elastic strength demad to calculated yield strength coefficient calculated by:

$$R = \frac{S_a}{V_y / W} \bullet C_m$$

(6.3)

V_y = yield strength

W - effective weight of the building

Cm - Effective mass factor to account for higher mode

mass participation effects obtained from Table 3-1.

Sa - response spectrum acceleration, g

C2 - Modification factor to represent the effect of pinched hysteretic shape, stiffness degradation and strength deterioration. See table 3-3 (generally 1.0)

C3 - Modification factor to represent P-Δ effects, with positive post yield strengths the value is 1.0

Sa - Response spectrum acceleration, g

g - acceleration of gravity

7. Experiences in Nicaragua

During many trips over the last few years, some for work and some for pleasure, two towns have been surveyed: Rivas and San Juan Del Sur.

7.1. Survey of Buildings

When the study first began, the scope of the project included surveying at least one medium sized town in Nicaragua and compiling a complete Seismic Vulnerability study according to FEMA guidelines. After beginning the project, it became apparent how enormous a task this it is. Fortunately, NORSAR (Norwegian Seismic Array) a much larger organization has taken on the task of surveying several Nicaragua cities and completing a vulnerability study on the cities. However the towns of Rivas and San Juan Del Sur were surveyed. This consisted of taking a picture of every structure inside the city.

7.2. INETER

Nicaragua does have an office devoted to natural disaster studies. This office employs several hard working engineers working with few resources. The office did not have any information required for this study: maps of soil types, soil properties, structures survey, material properties, etc.

7.3. Office of Historic Building Preservation

On one trip to Nicaragua, Alvaro Amador at INETER suggested visiting the Office of Historic Building Preservation in the town of Leon. There was a meeting with Director Ana Carolina Olivas who discussed historic preservation issues and particularly adobe issues. Ms Olivas received a phone call that an adobe structure had collapsed. Upon arriving at the job-site it was obvious the wall had collapsed.

Figure 7.1. Adjacent adobe wall that has not collapsed

The contractor began to explain what happened. They were trying to preserve the adobe walls and build a new structure inside the walls. They consulted an engineer who instructed them to leave 30 cm of foundation next to the adobe walls while excavating the basement. This was not sufficient and the wall collapsed by sliding out from the bottom.

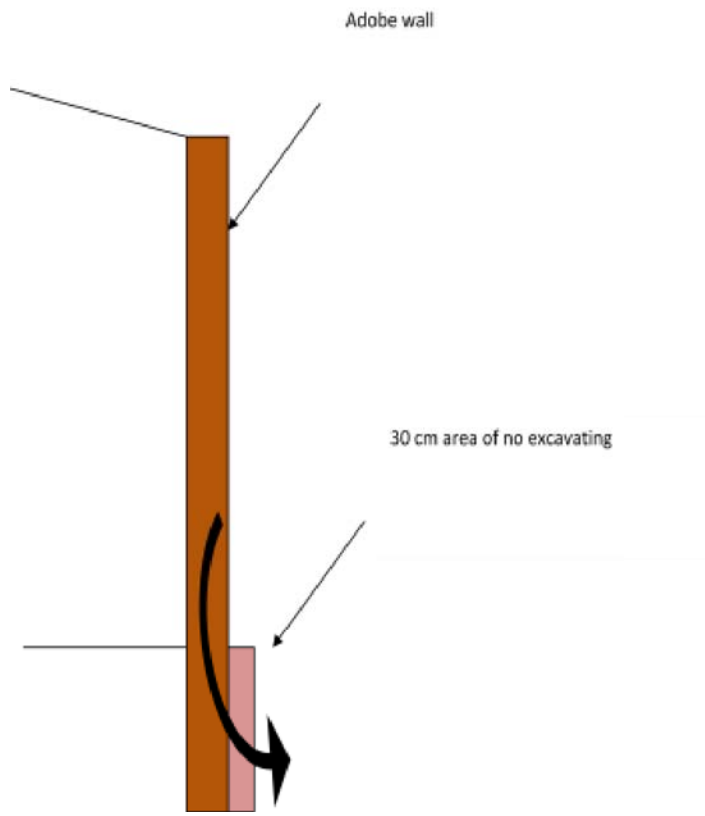

Figure 7.2. Illustration of adobe wall collapse

Upon returning to the office, Mrs. Olivas discussed the standards for repair of adobe buildings. The office recommends that residents not “mix materials” therefore you should always repair earthen materials with earth. This means not adding steel or concrete to repair adobe walls. Mrs Olivas then asked if this is okay. This showed that standards for repairing adobe are not well defined and even the experts are not certain of repair methods.

Figure 7.3. Construction manager in front of the collapsed adobe wall

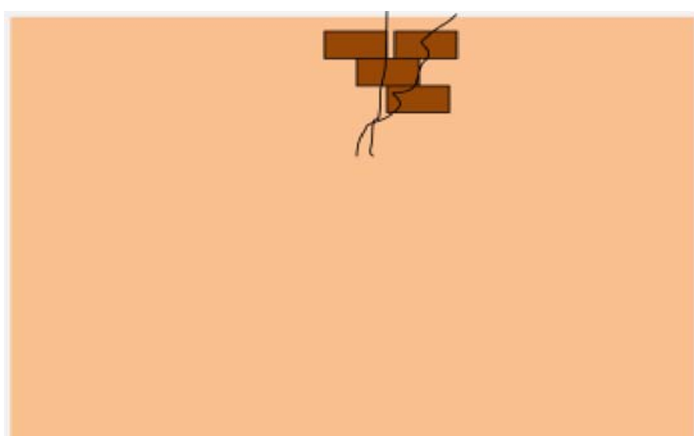

Figure 7.4. Repair for adobe as illustrated by the Office of Historic Preservation

7.4. Convention Held by NORSAR

When NORSAR took on the project of surveying and determining the vulnerability or residential structures in Central America in 2006, they organized a convention for all the interested parties. There were professors and government representatives from all over Central America. The experts specialized in transportation, structural engineering, geology, seismology, city planning, and etc. I was fortunate to receive an invitation, give a presentation, and meet all of the participants.

7.5. Residential Building Types in Nicaragua

There are many types of residential building types in Nicaragua. Some are vernacular and made with local materials, while others are made of engineered products seen elsewhere around the world. Norsar has compiled a list of the 11 common building types in Central America and most of them can be found in Nicaragua. The document Norsar used to survey the cities of Nicaragua is shown in table 7.5.

Table 7.1. Catalog of buildings for Norsar survey (Norsar, 2007)

Label	Description	Examples	
MF	'Mini-Falta' (engl.: miniskirt) half stone (blocks; bottom part), half wood (upper part)	 Masaya (NIC)	 Guatemala City (GUA)

Label	Description	Examples	
AD	‘Adobe’ bricks of clay/mud, splices/joints out of clay/mud or lime	 Masaya (NIC)	 Guatemala City (GUA)
TP	‘Tapial’ (rammed earth) wooden formwork/form boards (only during construction) filled with earth (adobe material)		
TZ	‘Taquezal’ wooden slats or shelves filled with earthen material and stones	 Masaya (NIC)	 Masaya (NIC)
BQ	‘Bahareque’ bamboo (canes) filled with earthen material (and stones)	 San Ramon (NIC)	 Rivas (NIC)
CC	‘Calycanto’ (fieldstone masonry) fieldstones, lime (chalk), and clay 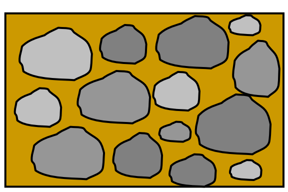	 Masaya (NIC)	 Masaya (NIC)
CL	claybricks		

Label	**Description**	**Examples**	
	a) unreinforced or reinforced with internal steel rods	 Guatemala City (GUA)	
	b) confined with RC	 San Salvador (ELS)	 San Salvador (ELS)
CB	concrete blocks		
	a) unreinforced or reinforced with internal steel rods	 San Salvador (ELS)	 San Salvador (ELS)
	b) confined with RC	 San Salvador (ELS)	 Guatemala City (GUA)
PC	'Piedra de Cantera' masonry out of cut (quarry) stones (unreinforced, confined with timber)	 Leon (NIC)	 Leon (NIC)

Label	**Description**	**Examples**	
BP	'Blocke Panel' confined (precast) concrete panels vertical: welded steel connections horizontal: wood connection to roofing	 Masaya (NIC)	 Masaya (NIC)
		 Leon (NIC)	 Leon (NIC)
LT	'Laminada Troquelada' steel frames and decorated steel sheets	 Guatemala City (GUA)	 Guatemala City (GUA)

8. Analysis of Some Common Buildings

8.1. Concrete Structures with Concrete Shear Walls

The use of concrete in Nicaragua becomes more common every day. The design of concrete buildings is a well studied area of structural engineering and the following material is not meant to re-state volumes of others work. The area of reinforced concrete design that is not well documented may be that of designing concrete buildings in less than perfect circumstances. For instance, which is most cost effective, adding extra steel or using better concrete? What inexpensive measures can be utilized? If additional funds are available, where should they be spent?

To investigate these questions, a typical Nicaraguan concrete building was chosen from the town of Rivas. This structure seems typical, the size is average, the openings are representative, and it is a simple design made from reinforced concrete.

Figure 8.1. Typical concrete building chosen for analysis

Several variations of this building were analyzed. The first variation was the building without windows, doors, or a canopy to serve as a control structure that could be analyzed as a baseline. The variations were analyzed to determine not only how these variations effect the structural adequacy of the building, but also to extend the analysis to buildings of other geometries so as to determine how the geometry changes the structural adequacy.

The variations also included:

- The building as it is seen, as an actual building in Nicaragua.
- The building without a canopy (only windows and doors). This variation was analyzed to get a better understanding of how openings affect the overall performance of the building.
- The building but longer in one direction (rectangular). This variation was analyzed to determine how the shape of a structure affects the performance and also to apply conclusions to rectangular buildings.
- The building but taller. This variation was analyzed to determine how the height of a structure affects the performance and also to generalize conclusions to taller buildings.
- The building with increased steel.
- The building with increased concrete strength.

The last two variations were analyzed to determine which might be more beneficial and therefore which would be worth spending additional resources.

8.1.1. Assumptions and Verification

Buildings without frames rely on the shear capacity of the walls for lateral stability. Concrete walls are generally very stiff in shear and therefore any bending or other deformations can be ignored in a simplified model. To verify the building, a simplified version of the building was created with one element per side. The linear shear deformation of a wall is shown in the following sketch:

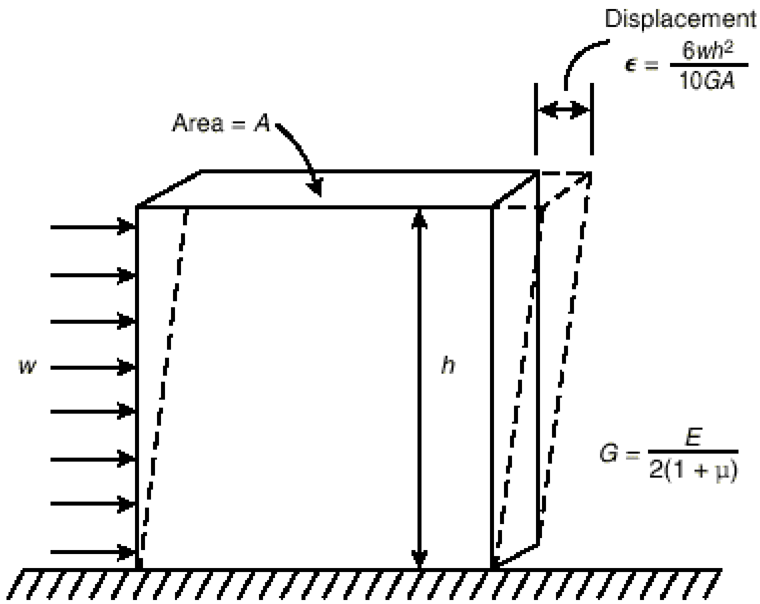

Figure 8.2. Strain resulting from shear forces on a body.
(Cement Association of Canada, 2009)

Alternatively, the displacement due to a point load is estimated as:

$$displacement = \frac{5Ph}{6GA} \tag{8.1}$$

In this formula P is the point load, h is the height, G is the shear modulus, and A is the cross sectional area. For the verification building h= 120", G=1500, A=240" tall x 6" thick x 2 sides in shear = 2,880. Substituting these parameters into the equation gives:

$$displacement = P(.00002)$$

At P=600 kips, the displacement is 0.012. The displacement divided by the height of the structure gives the drift =0.012”/120” = 0.0001.

At P = 449 kips, the drift is 0.000075.

This result is compared to the drift in the linear portion of the Perform 3D pushover curve which gives a drift of 0.0001067, at P=449 kips.

Extrapolated to P=600 kips the drift would be 0.0001425, as shown in figure 8.3.

These results are close enough to give confidence that the program is analyzing the structure as intended. The relevant results are given in table 8.1.

Load	Drift by hand calculations	Perform 3D drift
449 kips	0.00007483	0.0001067
600 kips	0.0001	0.0001425

Table 8.1. Deformation results for Perform 3D and hand calculations

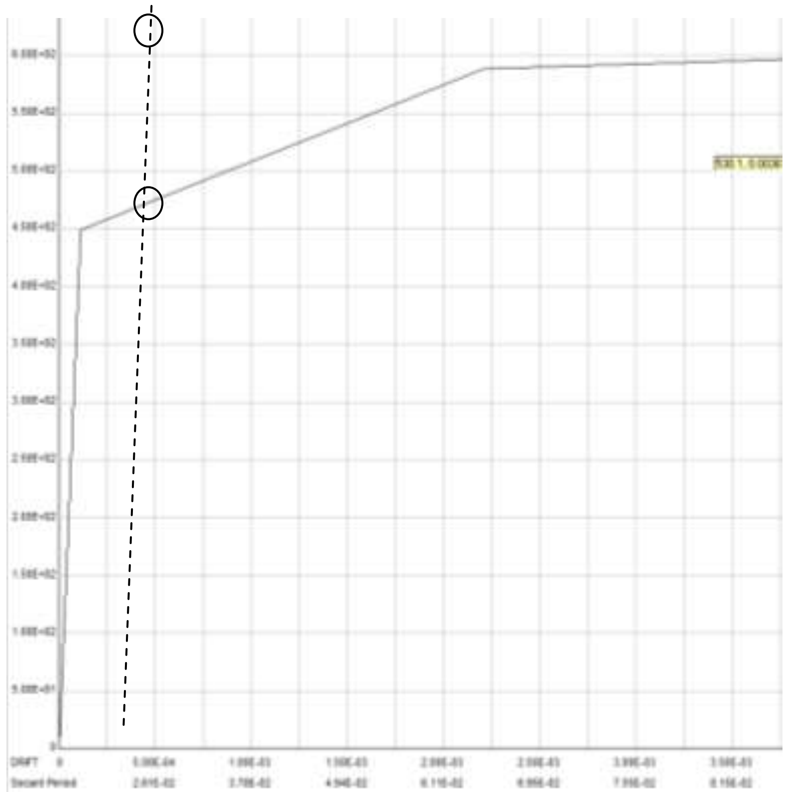

Figure 8.3. Perform 3D deformations for baseline model

8.1.2. Geometry

The building was scaled from the photograph to the extent possible, but the geometry that was unknown was assumed. For instance the front of the building was scaled from the picture. The common height of a door was used and then that length determined the scale used to measure the rest of the front of the building. All geometry behind the front face of the building was assumed based on experience entering this type of building. The geometry that was analyzed is shown in figure 8.4 and figure 8.5.

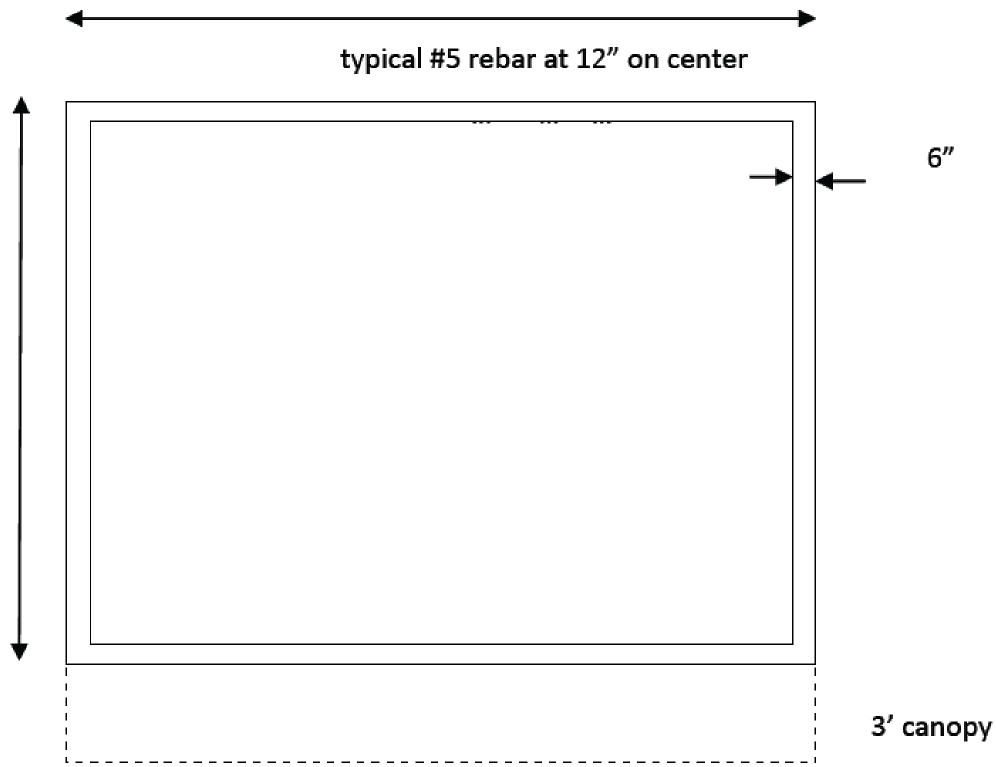

Figure 8.4. Plan view of concrete building

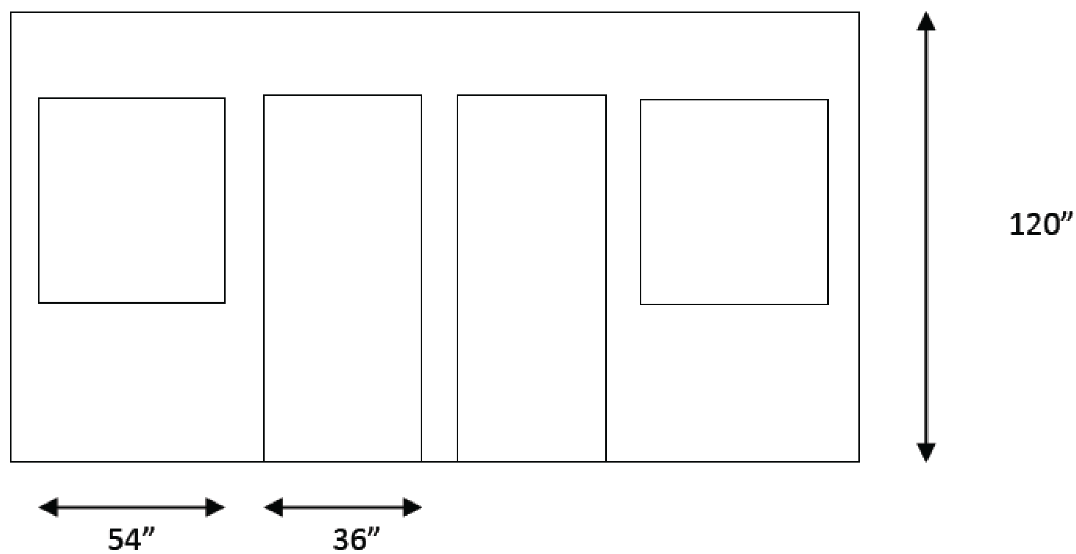

Figure 8.5. Front view of concrete building

8.1.3. Material Properties

Because materials in Nicaragua have been observed to be generally less consistent in material quality than they are in the US, the properties used for the model were reduced from US standards. The material properties were assumed to be:

property	value used for steel	value used for concrete	Value used for shear wall
Dx (define Dx)	0.4	0.004	
Fu (ultimate strength)	50 ksi	2.5 ksi	0.2 ksi
E (modulus of elasticity)	29,000 ksi	2,850 ksi	
G (shear modulus)		1,187 ksi	2,000 ksi

Table 8.2. Material properties used in concrete model

Steel is generally produced consistently around the world, so steel properties were not reduced. However, concrete is mixed locally and its properties can vary greatly, so concrete properties were reduced accordingly.

The moduls of elasticity (E) for concrete was calculated from E= 57,000√(f’c), and the shear modulus (G) was estimated as G = 1,187 ksi. G was calculated from $G = \frac{E}{2(1+\mu)}$ where μ=0.2 Poisson's ratio for concrete is generally taken as 0.1 to 0.2, while steel is 0.27 to 0.3. 0.2 was used for the combined system to account for the steel in the concrete.

The ultimate strength of the inelastic shear material (F_u) was calculated to be 5% of compressive strength which gives F_u = 0.125 but this value was increased to 0.2 to account for steel reinforcing in concrete. Also the shear modulus (G=2,000 ksi) was assumed higher than for plain concrete to account for the steel.

The total building weight was estimated to be 90,000 lbs without a canopy and 94,500 lbs with the canopy. The calculations for the building weight are shown in table 8.3. Based on concrete density of 150 pcf, 6" concrete walls and roof, the concrete would weigh 75 psf.

Member	Calculation	Weight
walls	(75 psf)(20'x10')(4)	60,000 lbs
roof	(75psf)(20'x20')(1)	30,000 lbs
canopy	(75 psf) (3'x20')	4,500 lbs

Table 8.3. Calculations used to determine the weight of the concrete building

8.1.4. Perform 3D Model

The models were created by setting up a system of nodes and then creating elements between the nodes. To create the nodes, all the dimensions were laid out on a grid system and the points that create the geometry were specified. Elements were then defined as regions between the nodes as seen in figure 8.6. Once the elements were created, they were assigned the material properties listed in table 8.3. The seven models were created in much the same fashion. The models with openings were created with additional nodes and smaller elements to simulate the openings. The resulting frames are shown in figures 8.6 to 8.10

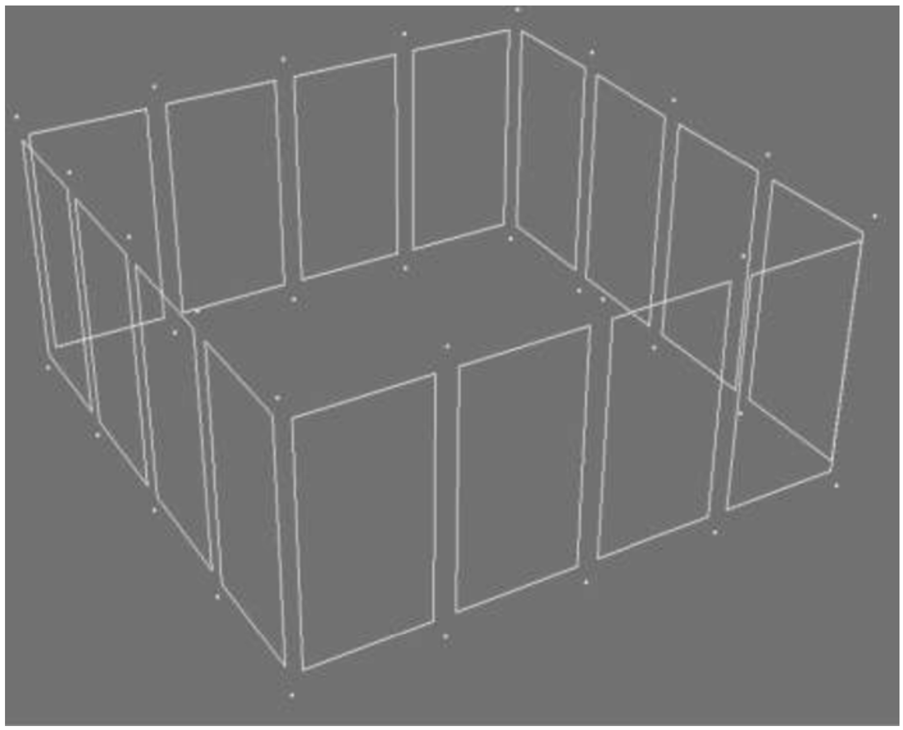

Figure 8.6. Concrete model #1- building without windows, doors, or canopy

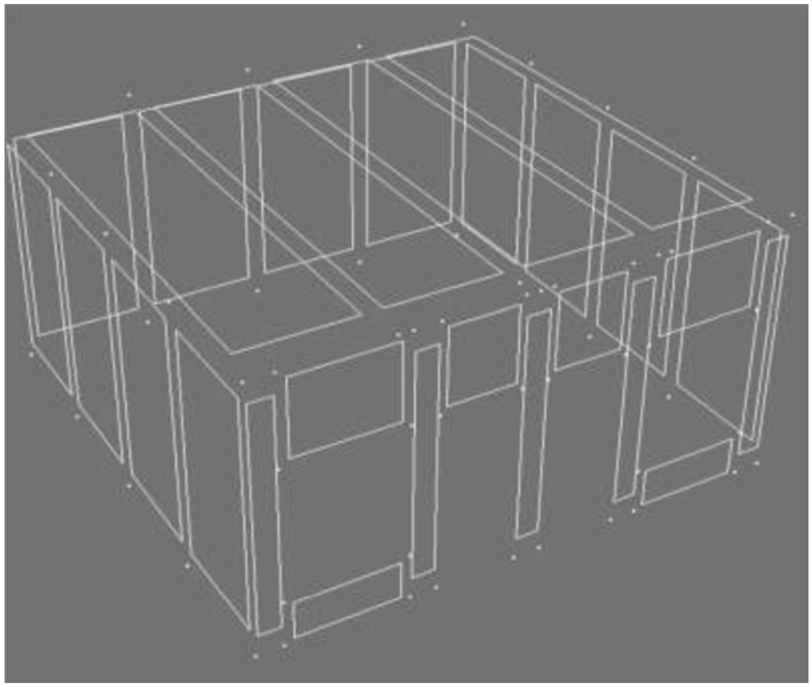

Figure 8.7. Model #2 - concrete building with windows

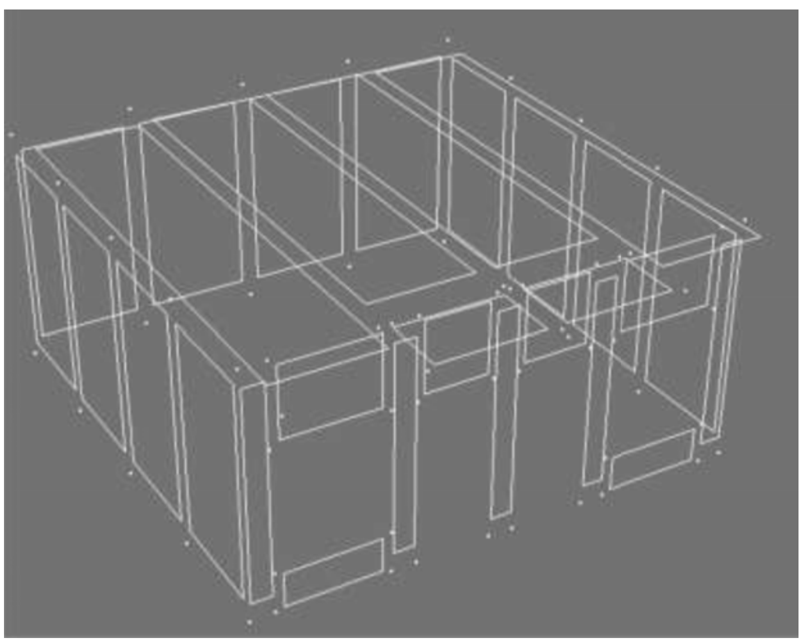

Figure 8.8. Model #3 – concrete building with canopy and openings

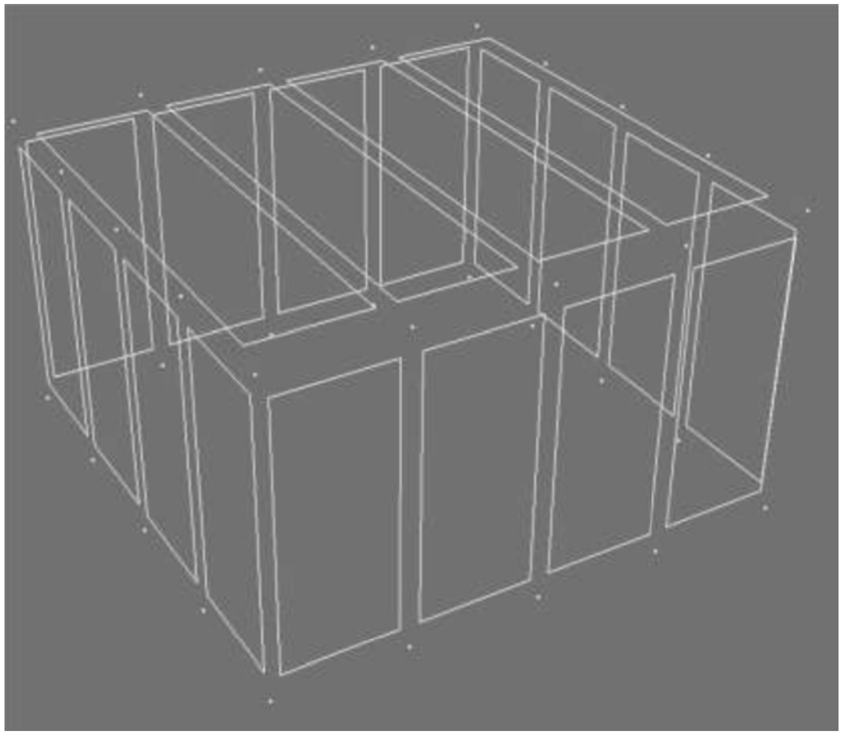

Figure 8.9. Model #4- taller concrete building

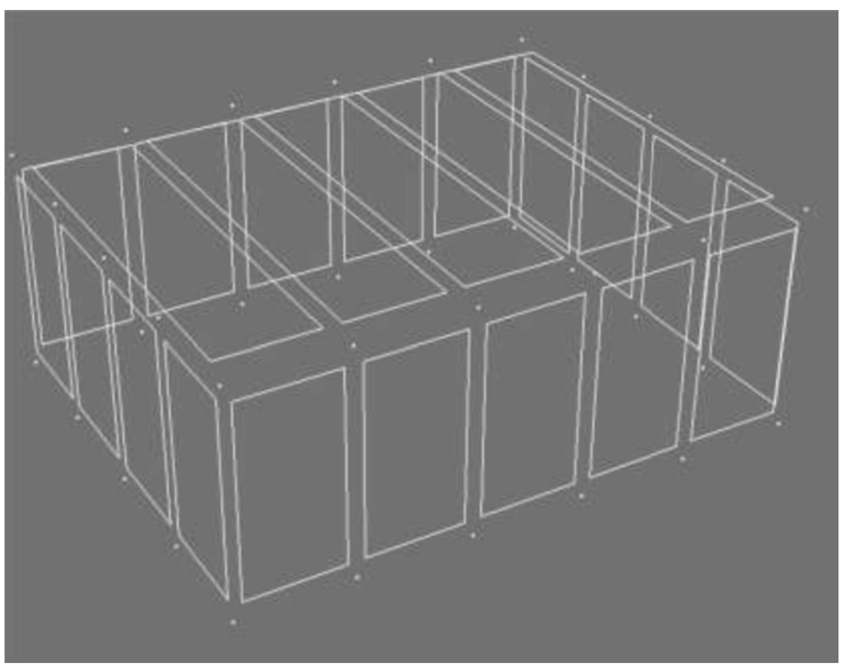

Figure 8.10. Model #5 – longer concrete building

The pictures for models #6 and #7 of buildings with additional steel and additional concrete look much the same as model #1.

The weight of the building was applied evenly to the top nodes. The forces appear upward because that is the only direction the arrows will display in Perform 3D. The direction is determined by the negative sign.

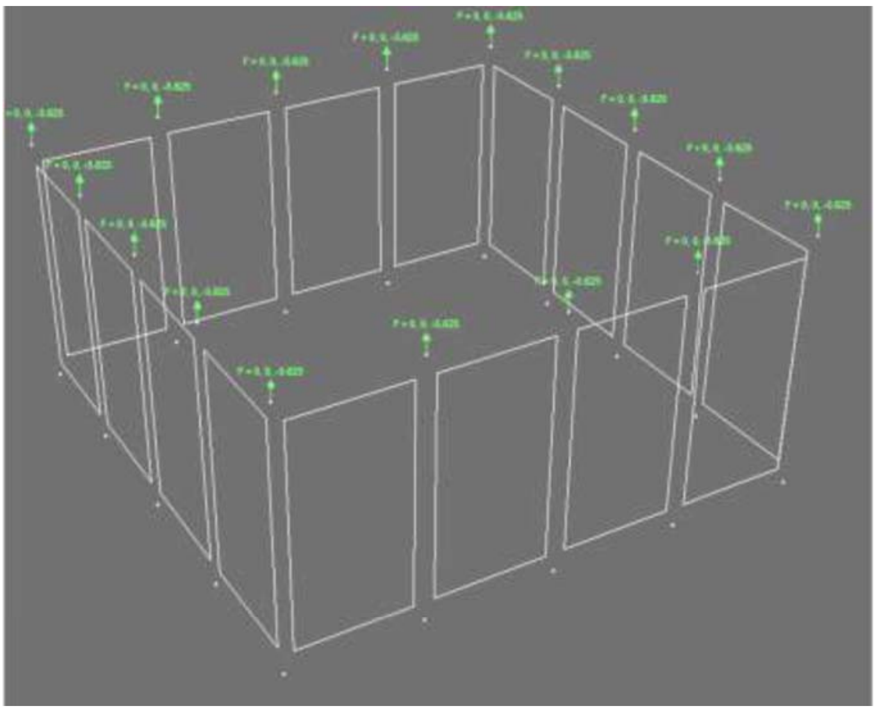

Figure 8.11. Dead load on concrete building

The models with the canopy had an additional 4,500 lbs distribute to the structural model. When this load was applied over the windows the structure failed under dead load. Failure in this sense means the deflections were large and went into the non-linear zone and therefore the program stops applying load. This model did not have any additional reinforcement beams over the windows and this might have been too harsh an assumption to consider the load above the windows. This assumes the load path applied the roof load above the windows without any additional header beams above the window, which is probably unrealistic to assume, so the load was moved to nodes away from the windows to the nodes creating the jambs of the windows.

For the pushover analysis lateral load was applied at two corner nodes. This is a standard procedure for static this form of analysis. Simulations of each of the buildings were made with the lateral load distributed to all the nodes of two sides of the building and the results were similar. So for sake of simplicity, the loads were applied at the two corners, as shown.

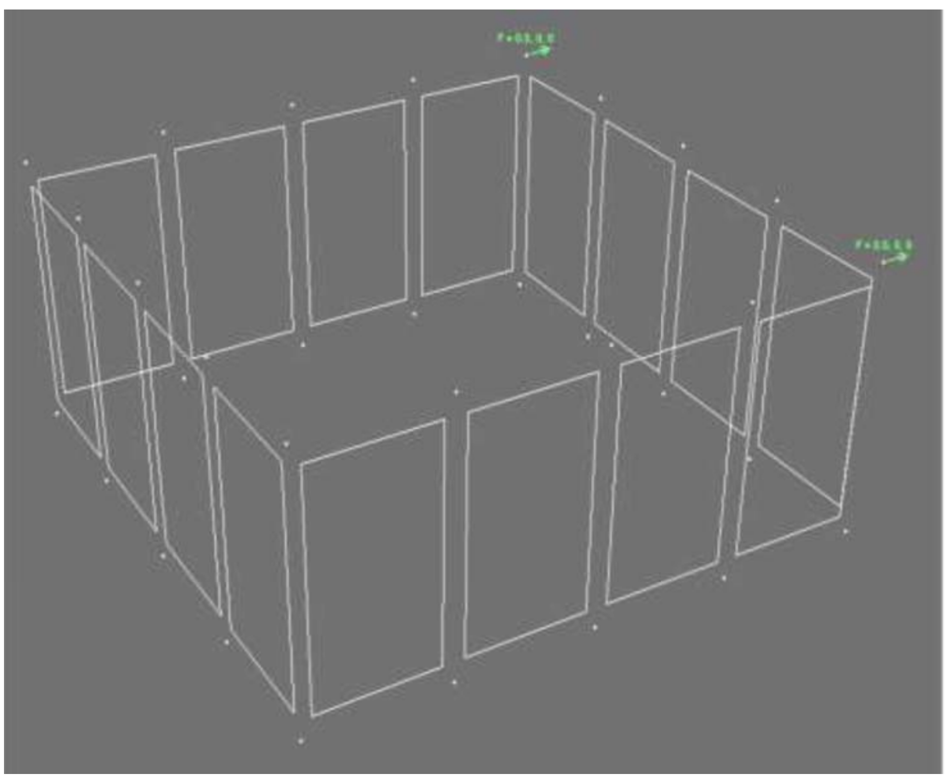

Figure 8.12. Pushover loads applied

The building was fixed at its base at all node locations. During an early analysis the building was fixed only at the corners and this allowed in-plane bending in the walls and gave results that did not agree with hand calculations, so the model was fixed at intermediate node locations as shown, to better simulate the actual connection to the foundation.

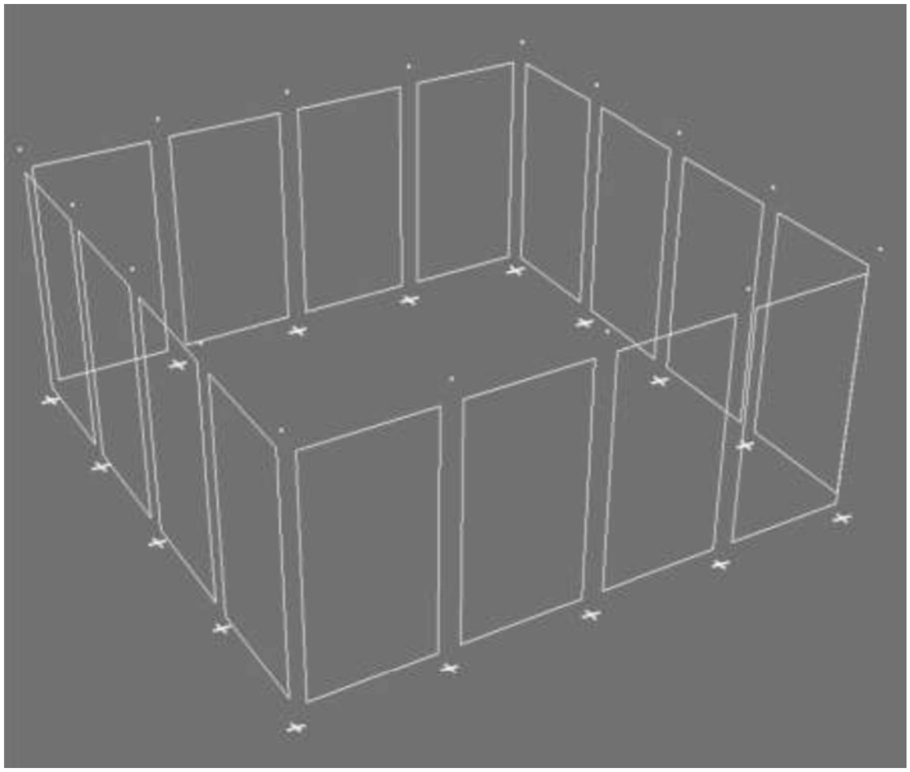

Figure 8.13. Foundation attachment as modeled

The 4 corners of the roof plane were tied together to create a diaphragm. Not all roof nodes were tied together to create a diaphragm because buildings in Nicaragua are not always well tied to their roof diaphragms and this connection creates a model that is closer to the actual condition of these structures.

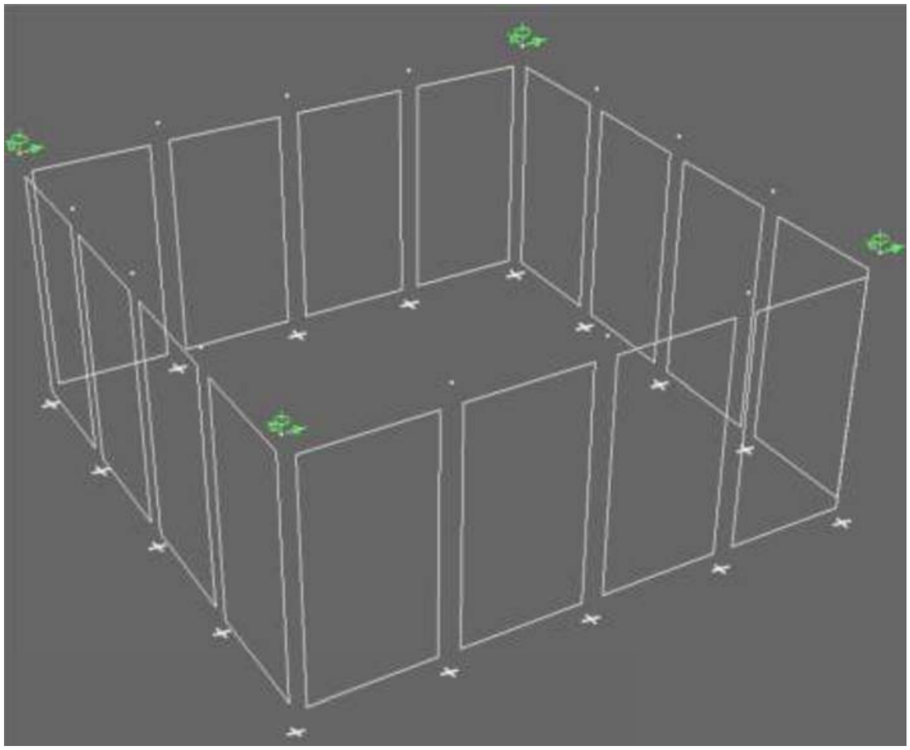

Figure 8.14. Model with roof diaphragm connections as modeled

8.1.5. Pushover Analysis (Static Non-linear Analysis)

During the pushover analysis the following mode shapes were determined:

Model #1	Period	Description of mode shape
1st period of vibration	0.1378	vertical deformation
2nd period of vibration	0.1378	lateral deformation
3rd period of vibration	0.1373	torsional deformation
4th period of vibration	0.1373	shrink and swell
Model #4 (with canopies and openings)		
1st period of vibration	0.7552	vertical deformation
2nd period of vibration	0.7552	lateral deformation
3rd period of vibration	0.5713	torsional deformation
4th period of vibration	0.1367	shrink and swell

Table 8.4. Natural period of vibration for models 1 and 4

Notice the first and second periods are identical, from this it seems the building is likely to be excited laterally and vertically at the same frequency. Also notice the period increases greatly for the structure when the canopy and openings are added, as the structure becomes much more flexible.

The deflected shape can be seen in the following image:

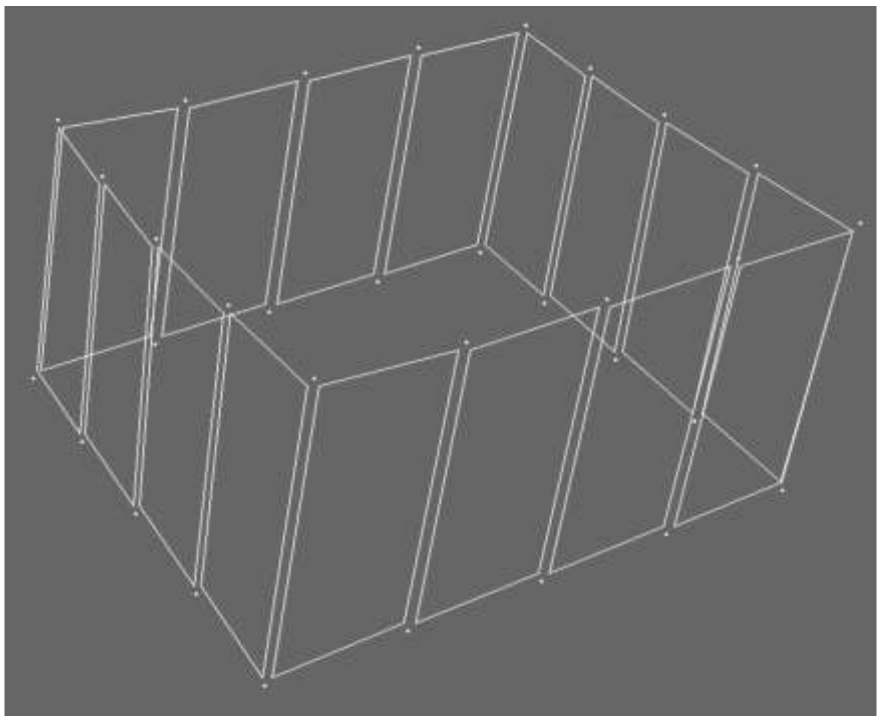

Figure 8.15. Model #1 - 1st period of vibration

The static non-linear analysis or pushover curve for model #1 is shown:

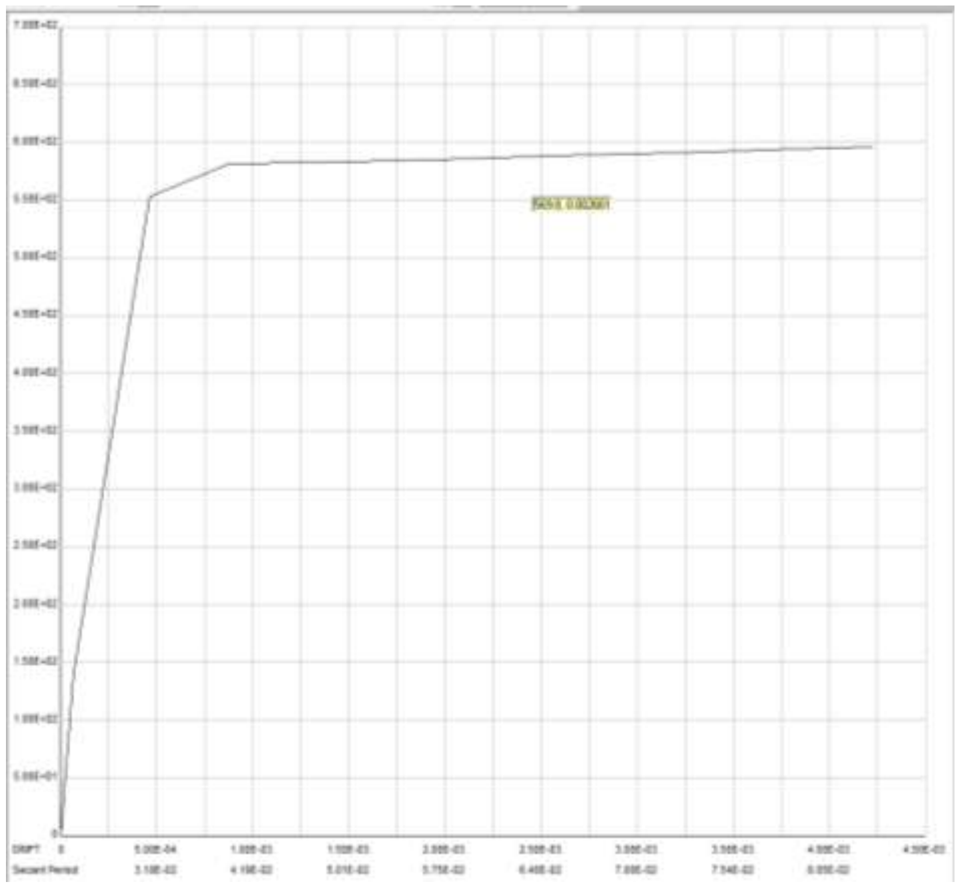

Figure 8.16. Pushover curve for concrete building Model #1

The object of the pushover analysis is to determine performance points, which are usually defined in terms of drift limits, and these performance points are then correlated to static loads. This method gives several (usually 3) static loads for which a building can be expected to respond at different levels of performance. These levels of performance describe the post-earthquake damage state that remains. Immediate occupancy suggests the building will have only minor architectural damage and will be fully functional after an earthquake. Life safety implies the building will require architectural repairs but will remain safe. And collapse prevention implies the building is on the verge of collapse and is not safe.

FEMA356 suggests the following performance drift limits for reinforced concrete buildings:

- Immediate occupancy - negligible
- Life safety - 0.005
- Collapse prevention – 0.02.

These limits do no relate well to the model. The model fails before it reaches the collapse prevention limit, suggesting the limits are too large for this structure. Professor Polat Gülkan (Gülkan, 2006) in his class on Performance Based Engineering suggested a more general approach to determining the performance points.

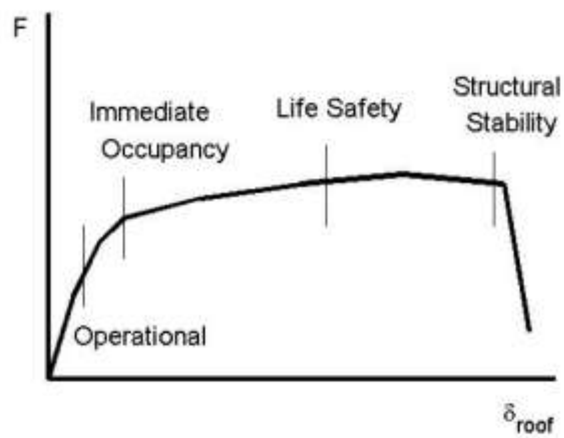

Figure 8.17. Performance points suggested by Dr. Pulat Gülkan (Gülkan, 2006)

Taking the more generalized approach, as suggested by Dr. Pulat Gülkan, the pushover curve for model #1 was chosen as the standard curve to set the values of immediate occupancy, life safety, and structural stability. On this curve the roof displacement at the general first yield point was determined and set as the point of Immediate Occupancy (IO). Also the roof displacement at general collapse (or loss of stiffness) was chosen as the structural stability point (SS). Then the point half way between IO and SS was set as life safety (LS). These points were then set as the performance points for all the variations of the concrete building. The limits are given by:

- Immediate Occupancy – 0.0005 (occurs at 550 kips)
- Life safety – .0023 (occurs at 580 kips)
- Collapse prevention (occurs at 590 kips).

The pushover curves for each model, with the performance points overlaid, are shown below:

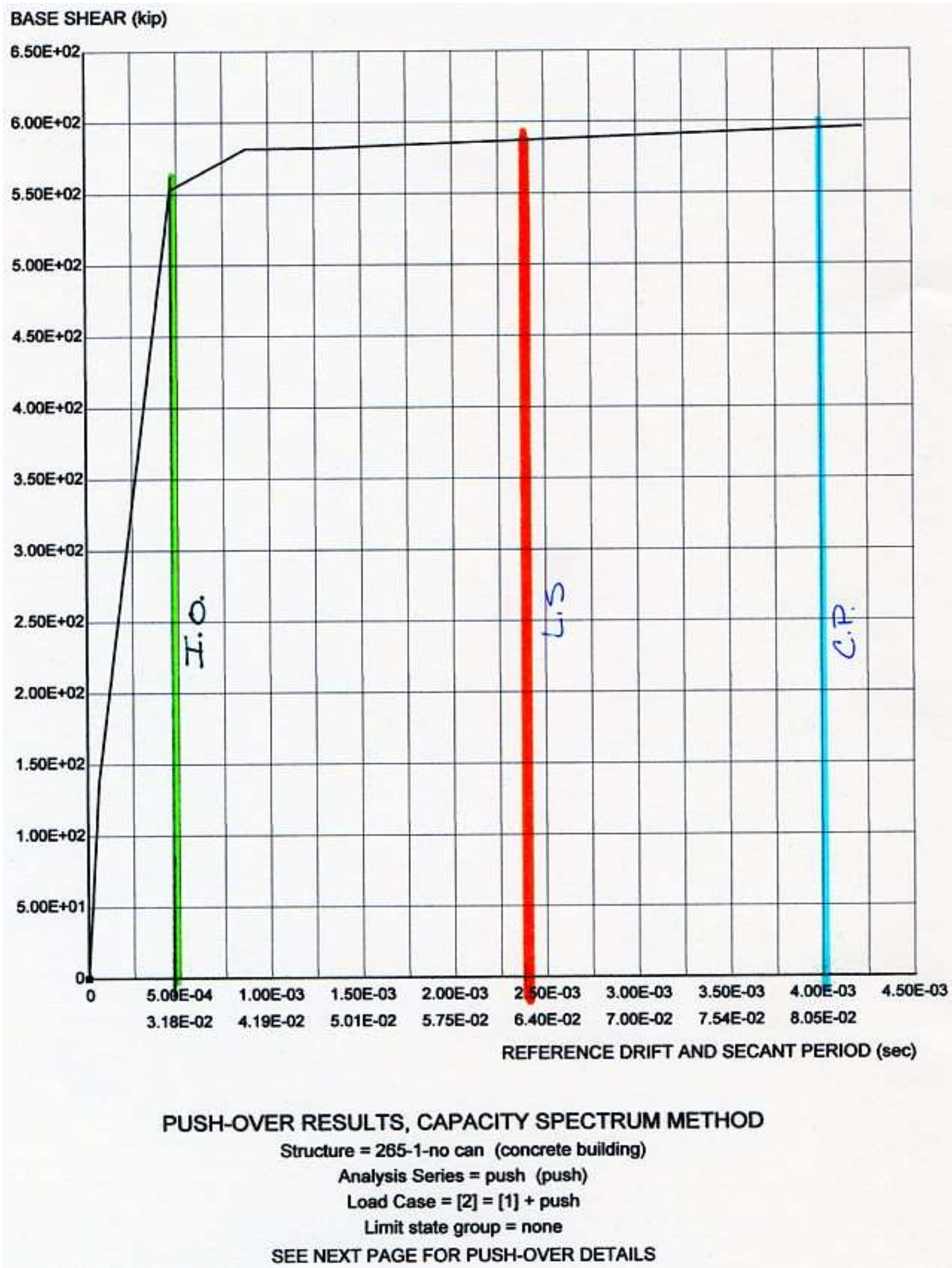

Figure 8.18. Model #1 pushover results

The models can then be compared by holding the same performance points for each of the models.

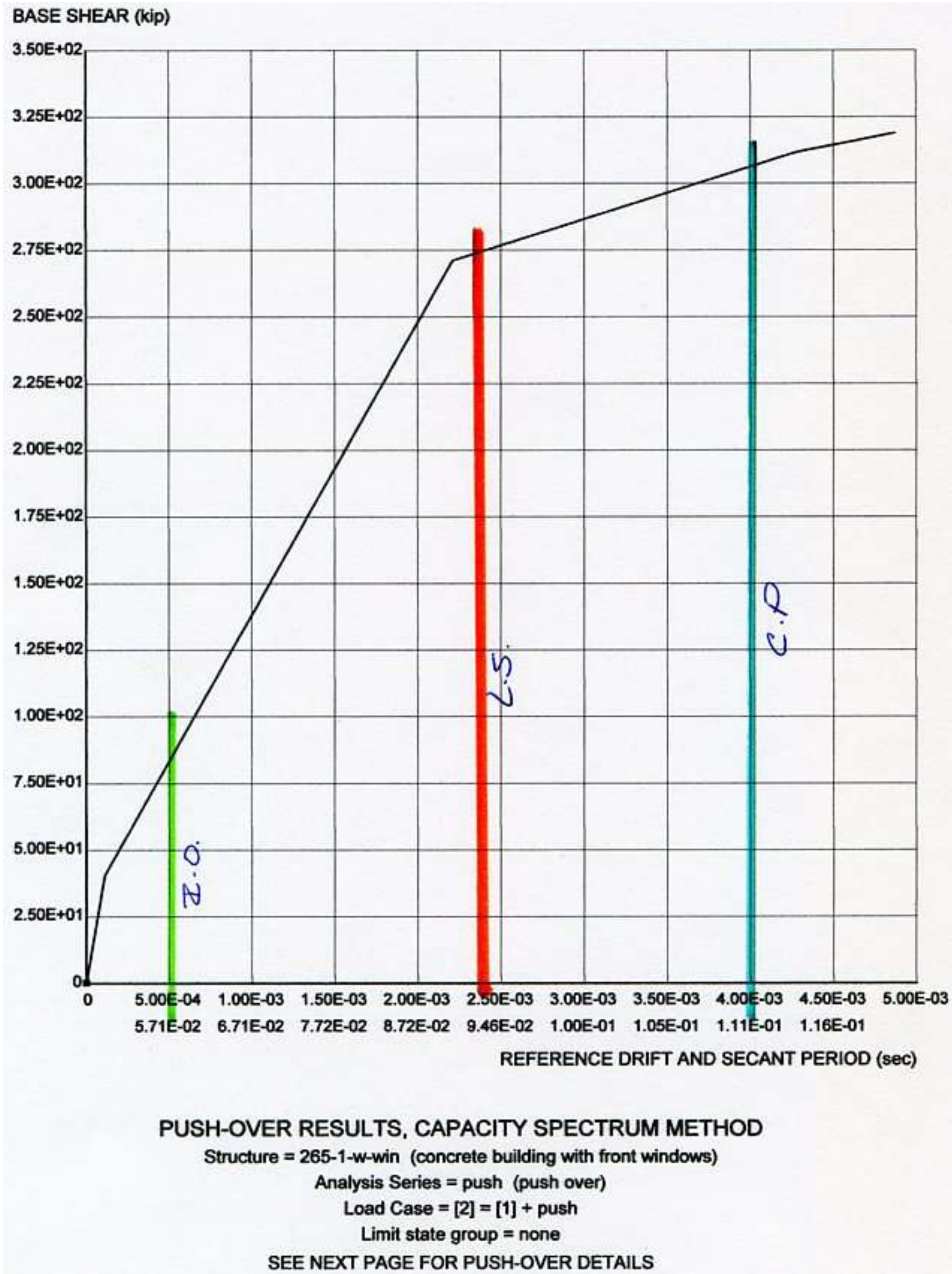

Figure 8.19. Model #2 pushover results

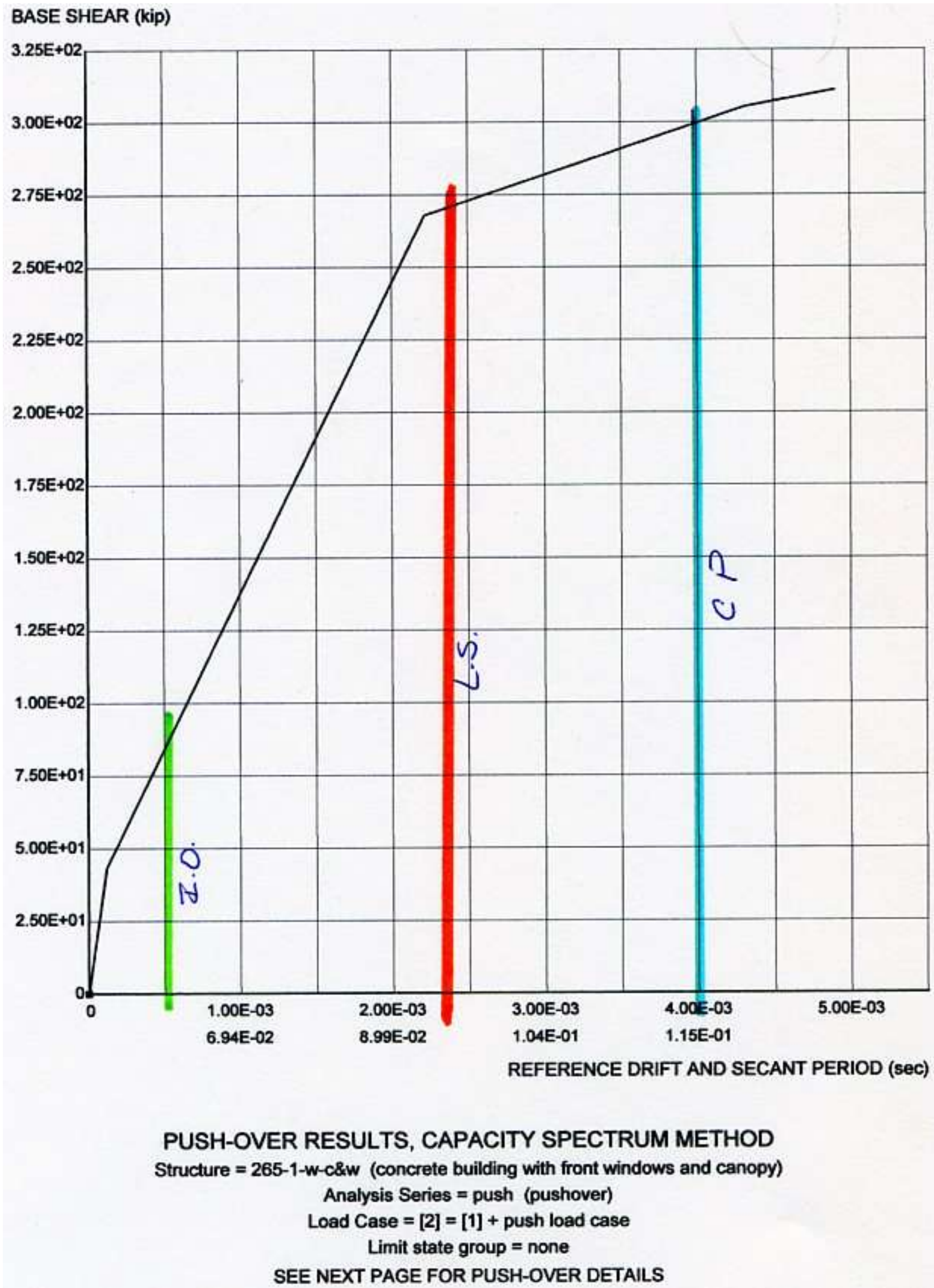

Figure 8.20. Model #3 pushover results

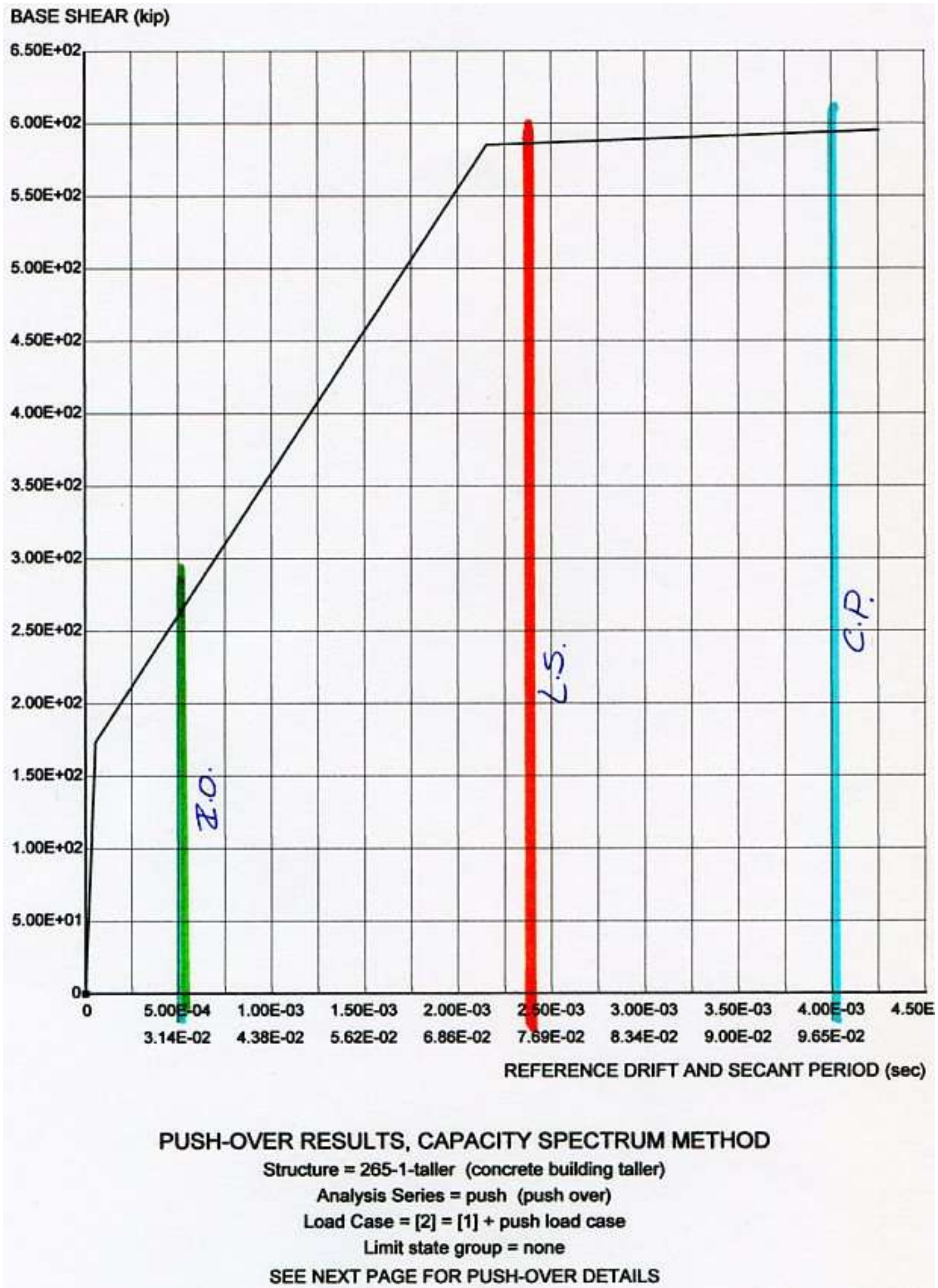

Figure 8.21. Model #4 pushover results

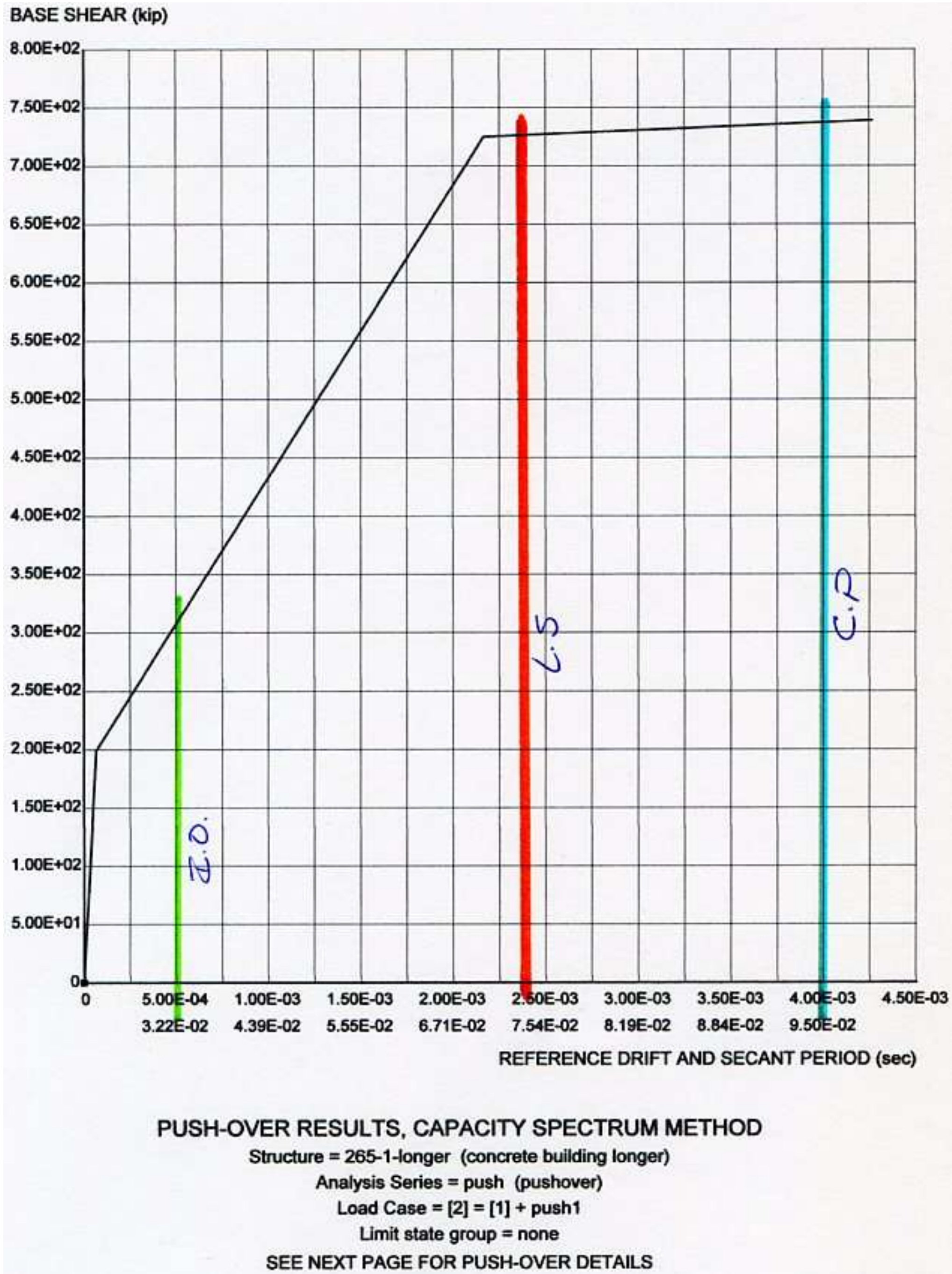

Figure 8.22. Model #5 pushover results

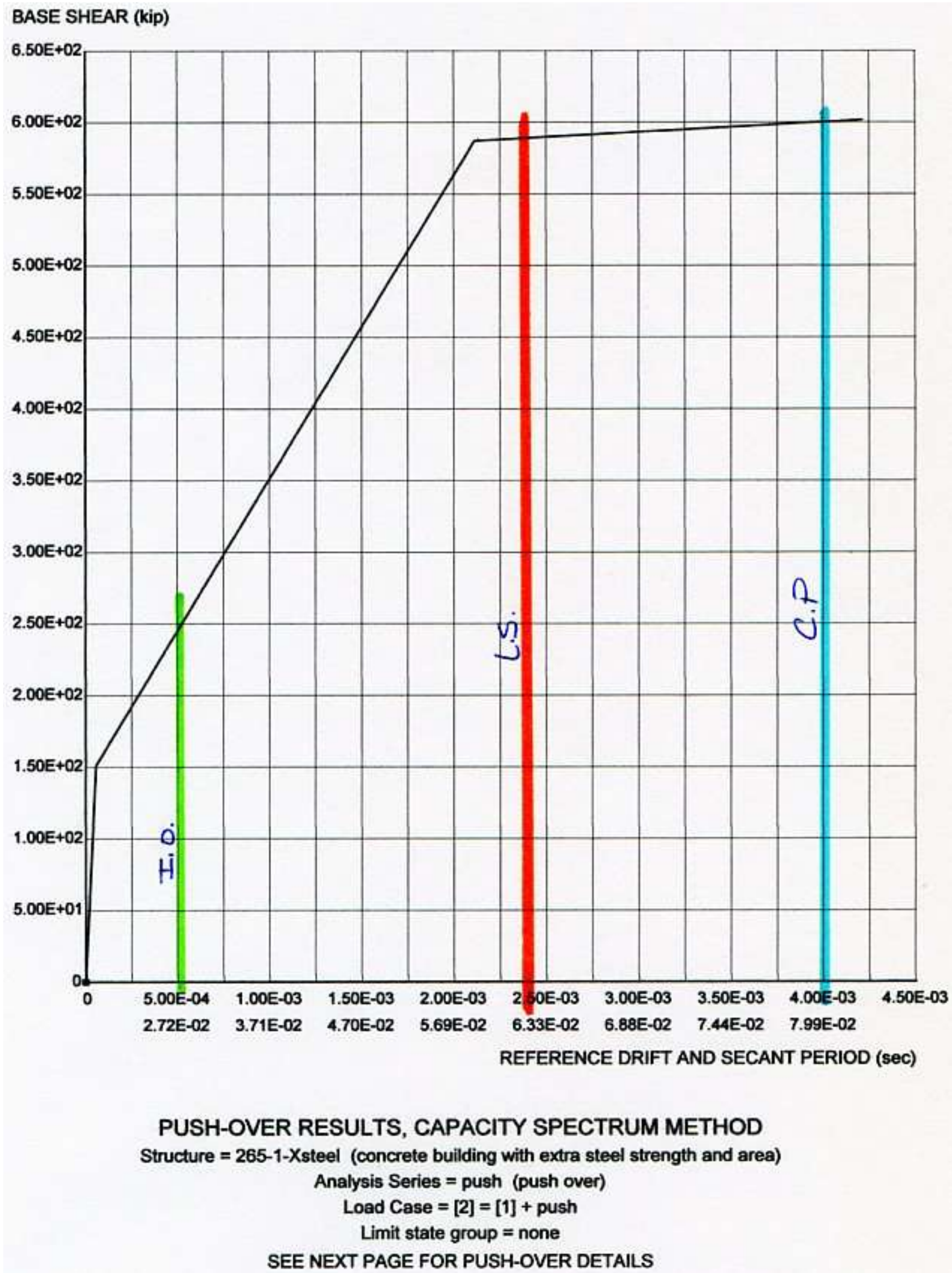

Figure 8.23. Model #6 pushover results

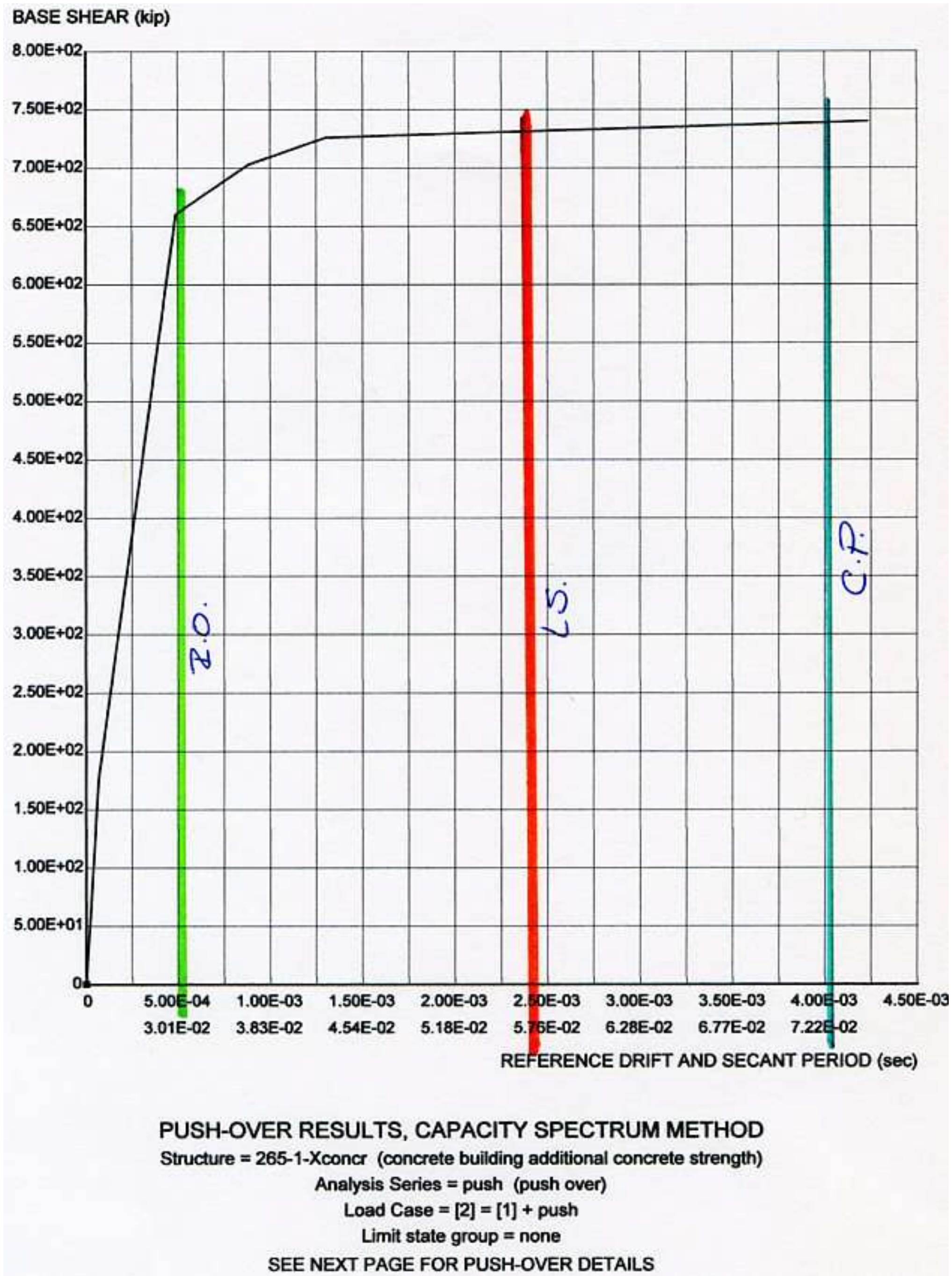

Figure 8.24. Model #7 pushover results

The results are summarized in the following table:

Model	Load at Immediate Occupancy	Load at Life Safety	Load at Collapse Prevention
#1	550 kips	580 kips	590 kips
#2 (w/ windows)	80 kips	270 kips	310 kips
#3 (w/ canopy and windows)	85 kips	240 kips	300 kips
#4 (taller)	260 kips	575 kips	590 kips
#5 (longer)	310 kips	725 kips	740 kips
#6 (additional steel)	250 kips	570 kips	600 kips
#7 (additional concrete)	660 kips	730 kips	740 kips

Table 8.5. Load at performance points for each model

There are several things worth noticing in this table. First, the doors and windows dramatically reduce the load at immediate occupancy. If buildings could be built without windows and doors, structural capacity would almost double, but of course this is not a viable option. Second, the taller building had a lower capacity at IO but almost the same capacity at CP. This leads the conjecture that within some average the height of a floor is ultimately not very important in determining the structural capacity. The taller wall deflected more quickly, which is what one would expect, but ultimately the shear walls performed similarly and the load at collapse prevention is identical. The longer building had an increased capacity at ultimate capacity. This leads to the conclusion that a longer shear wall is a better shear wall, which agrees with physical intuition.

8.1.6. Dynamic Analysis

The Managua earthquake of 1972 seemed the best earthquake record to use for a dynamic analysis for this region. Since the earthquake did occur, its characteristics must be appropriate for the area. Unfortunately, a digital record could not be located. A photocopy was made of the record from the Esso Refinery that was published in the Engineering Report on the Managua Earthquake of 23 December 1972 by the National Academy of Sciences. The photocopy was enlarged numerous times until it was 48" wide, and then it was digitized.

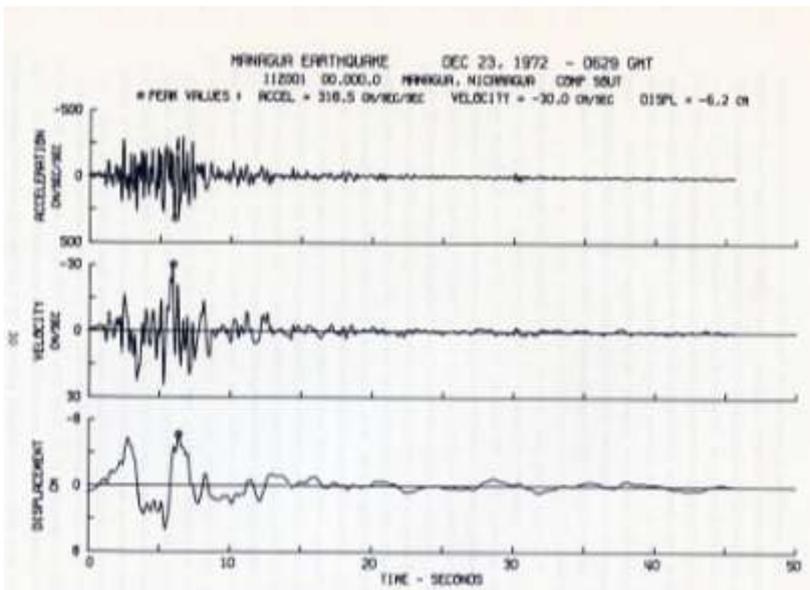

FIGURE 11-4a South Horizontal Component of Corrected Ground Motion Record ESSO Location.

Figure 8.25. Ground motion record from the Esso Refinery during the Managua earthquake of 1972 (Sozen and Matthiesen, 1975)

Each second on the record was divided into 64 parts and the value at that time interval was noted. The graph of the digitized record is shown in figure 8.26.

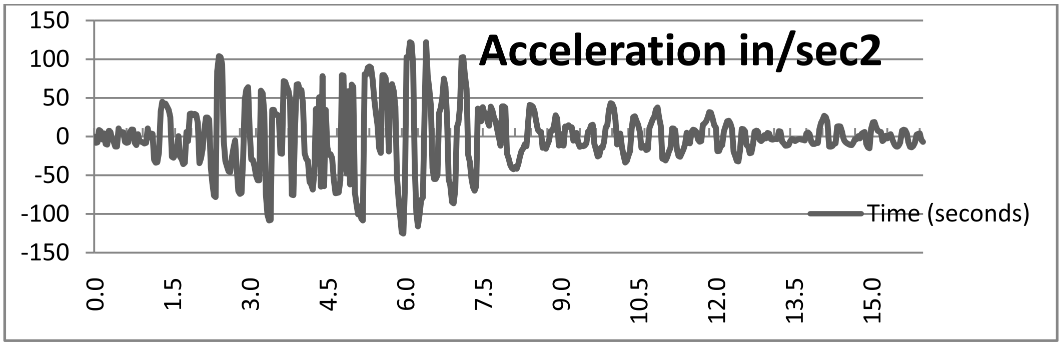

Figure 8.26. digitized Managua earthquake of December 1972

The graph looks reasonably similar to the original earthquake recording. The time vs. acceleration for the north-south and east-west component of the earthquake are shown in the appendix.

The buildings were subject to the Managua earthquake and the corresponding time-histories are shown in figure 8.27.

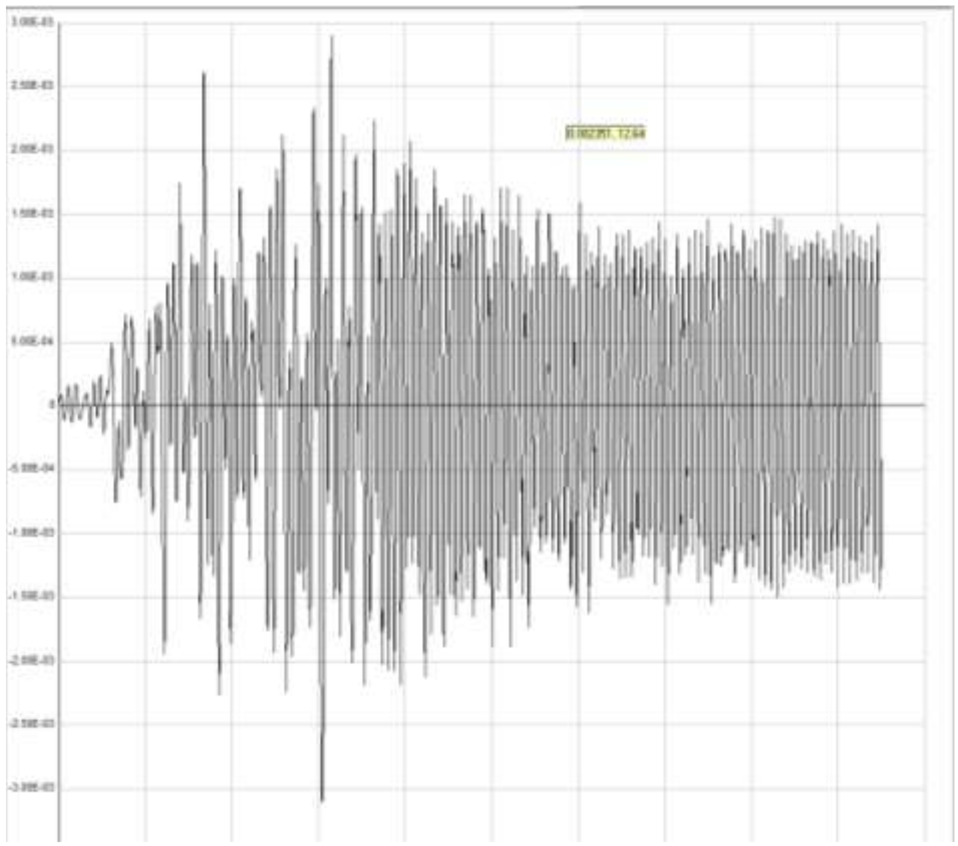

Figure 8.27. Time history for Model #1

The maximum displacement in inches for model #1 is 0.0031 inches. To determine the maximum relative drift the displacement is divided by the height, so that the drift-ratio = 0.0031/120 = 0.0000258. This is less than the immediate occupancy drift limit of 0.00005.

This result relates well with the results of the Managua earthquake because concrete buildings did not suffer significant damage during the earthquake and this is the strongest of the models. However, it is not reasonable to assume a building would have no doors or windows, so the more fragile structures must be considered. The time history for the building with doors, windows, and a canopy is shown in figure 8.28.

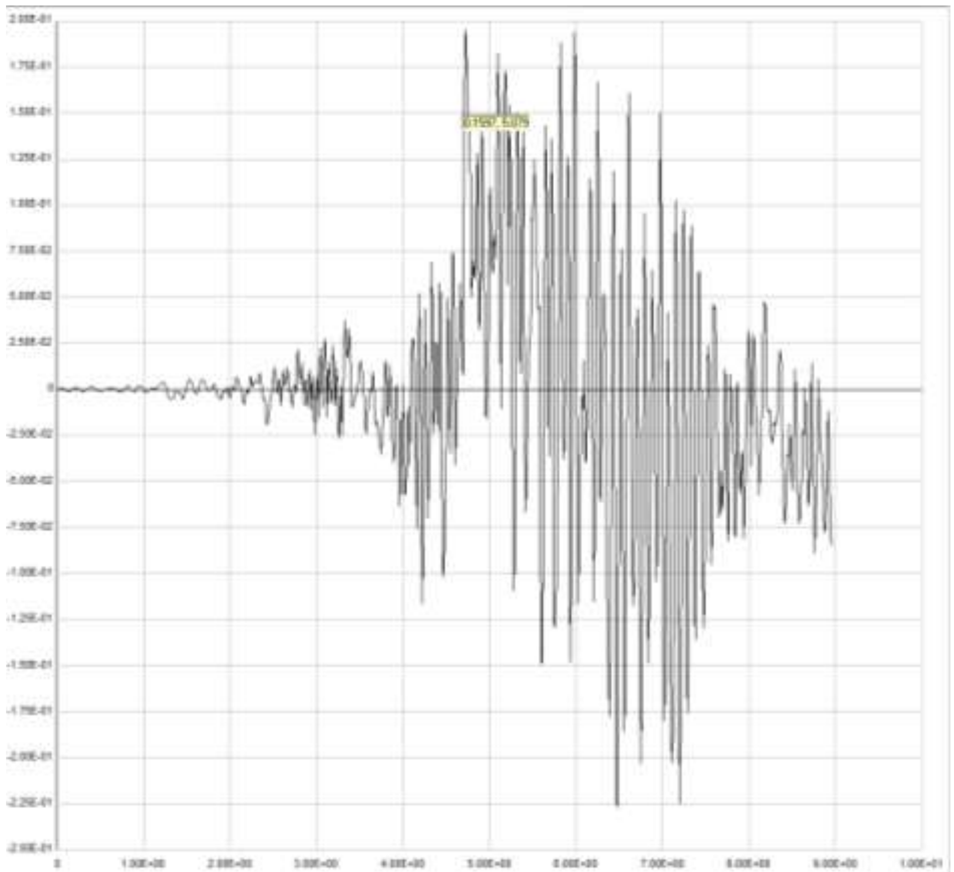

Figure 8.28. Time history for Model #3 (with doors, windows and a canopy)

The maximum relative displacement is 0.225 inches or a drift ratio of 0.225/120 = 0.001875. This falls between immediate occupancy and life safety. In other words, this building would sustain damage but potentially not enough to endanger lives. This seems reasonable based on the strength of the earthquake.

8.1.7. Possible Improvements

Comparing the results of the pushover analysis from the different buildings yields a few conclusions which are summarized in table 8.6.

Model	Load at Immediate Occupancy	Load at Life Safety	Load at Collapse Prevention
#1	550 kips	580 kips	590 kips
#2 (w/ windows)	80 kips	270 kips	310 kips
#3 (w/ canopy and windows)	85 kips	240 kips	300 kips
#4 (taller)	260 kips	575 kips	590 kips
#5 (longer)	310 kips	725 kips	740 kips
#6 (additional steel)	250 kips	570 kips	600 kips
#7 (additional concrete)	660 kips	730 kips	740 kips

Table 8.6. Pushover analysis results

8.1.7.1. Windows Doors and Canopies

The windows, doors and canopies substantially reduced the capacity of the building (less than 1/5). The reduction is due to the loss of material stiffness in the shear walls. They are however necessary, but it would be best if they are not all located on one wall. This reduces greatly the shear capacity in this wall and creates a weak link created by a reduction in shear strength in that wall. It would increase structural capacity if the openings could be distributed better throughout the building. It would also improve structural performance if the roof load was supported by the sidewalls instead of the weak front walls. However it is most convenient to span the slab in the direction of the front wall since the steel in the roof could continue past the front wall to create a canopy. It would take more effort to ensure the load path was directed to the sidewalls instead.

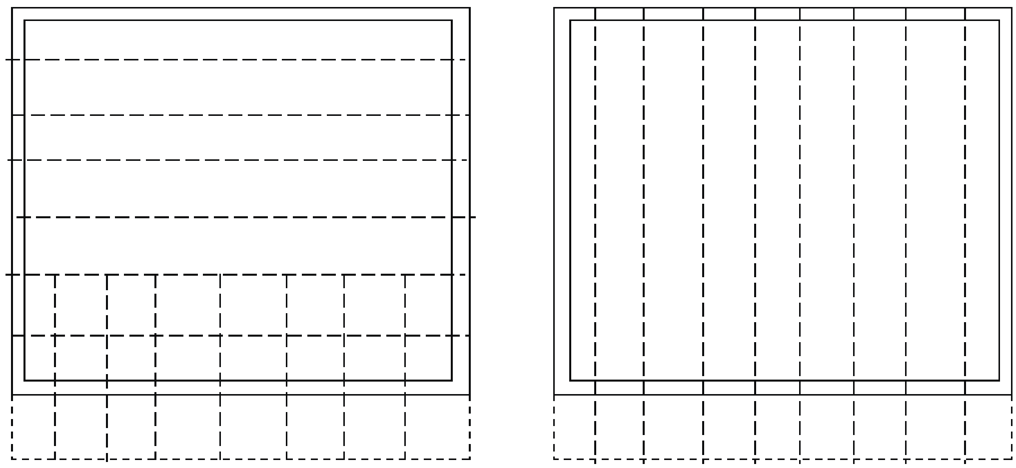

Figure 8.29. Possible reinforcement options

8.1.7.2. Taller

The taller building (12' tall rather than 10' tall) had reduced capacity at the onset of immediate occupancy but was virtually the same strength at life safety and collapse prevention. This seems reasonable when you consider a taller wall would deflect more. Therefore it is easy to conclude that the height of the structure is not a great concern as long as the height is reasonable (with respect to the thickness of the wall). However, the increased deflection and reduced load at immediate occupancy show that a building with taller walls will sustain more architectural damage and require more repairs after an earthquake.

8.1.7.3. Longer

The longer building (40' long rather than 20' long) has some reduced capacity early in the pushover curve but had increased capacity at life safety and collapse prevention. This seems reasonable because this is a shear wall system and the strength of shear walls has increased with the greater length. However the shear wall's length has doubled and the capacity has not doubled, so it is not a proportional increase in capacity, but the general conclusion is that more shear walls is better than less shear capacity.

8.1.7.4. More Steel or More Concrete

With the option of spending some additional money and not knowing if it should be spent on more steel or better concrete, the choice is clear – purchase better concrete. This seems reasonable for a building relying on shear walls. Unfortunately, it is probably the more difficult of the two options. Purchasing more steel is relatively easy but mixing better concrete takes training and controlled conditions.

8.1.8. Summary

To build a concrete building in Nicaragua that will perform better during an earthquake, this study makes the following recommendations:

- Use high quality concrete. Higher strength concrete increases the performance of the building both at immediate occupancy level and collapse prevention level of performance. This requires having strict mixing and pouring standards and also using high quality sand and aggregate and avoiding the use of local pierda pomez aggregate.
- Use enough steel to meet minimum requirements and provide flexibility to the structures. Additional longitudinal or lateral reinforcement does not increase the capacity of the structure but in fact reduces the capacity.
- Height should be restricted to reduce deflections and cracking.

- Columns should have sufficient ties. Insufficient ties have been observed on jobsites on many occasions. It seems that ties are not considered structural elements, by local construction personnel, but their purpose instead is to merely hold the longitudinal reinforcement in place.
- Special attention should be paid to inter-element ties. Structural elements should be well tied to one another. For example walls and should be well tied to the foundation and roof.
- Building openings (windows and doors) should not be concentrated in one area, where they may create a weak wall or soft story. It is best if windows and doors are not excessive in size and are well distributed around the building.

8.2. Concrete Frames with Brick Infill (Confined Masonry)

Figure 8.30. Confined masonry building in Rivas, Nicaragua

In recent years, concrete frames with brick infills have become a popular method of construction in Nicaragua. These types of buildings have proven to hold up better than earthen buildings in earthquakes and are relatively easy to construct

(PAulay, 1984). However, building with these modern materials without engineering advice can lead to dangerous building designs. The establishment of basic guidelines regarding concrete reinforcement, maximum spans, maximum heights and detailing would help minimize such dangers.

8.2.1. Assumptions

From Paulay and Priestley's book (1992) confined masonry has four failure modes:

1. Tension in the column resulting from overturning moments
2. Sliding shear failure
3. Compression failure of the diagonal strut
4. Flexural or shear failure of the column.

Of these four failure modes, two are a result of the columns that surround the masonry (tension in the column, and flexural or shear failure of the column) and two are a failure of the masonry. Using Perform 3D, the frame that surrounds the masonry will be analyzed. Additionally the masonry infill will be analyzed as a strut. The strut capacity will be determined as the lower capacity of the two failure modes (sliding shear failure or compression failure of the diagonal strut).

Sliding shear failure:

Paulay and Priestley's formula for sliding shear failure simplifies to:

$$Rs = \frac{0.03\, f'm}{1 - 0.3(\frac{h}{l})} d_m t \tag{8.2}$$

where dm is the diagonal length, t is the thickness, h is the height, and l is the length. If the panel is assumed to be 40" high and 60' wide that gives:

h= 40

l=60

dm=(40^2+60^2)^1/2 = 72.11

w=effective width of the diagonal strut =0.25(dm) = 18"

t= 4"

This gives Rs = 10.82f'm.

The formula for compression failure of the diagonal strut is:

$$Rc = \frac{2}{3} Z\, f'm \sec\theta \tag{8.3}$$

where Z and Θ are expressed by:

$$Z = \sqrt[4]{\frac{\pi}{2}\left(\frac{4\, E_c I_g h_m}{E_m t \sin 2\theta}\right)} \tag{8.4}$$

$\Theta = \tan^{-1}(40/60) = 33.69^0$

and t, E_m, H_m, Ig, Ec, are expressed by:

t=4"

E_m=600 f'_m if we assume f'_m=250 psi then E_m=150,000 psi

Hm=40"

$$I_g = \frac{bh^3}{12} = \frac{6^4}{12} = 108\ in^4 \tag{8.5}$$

(for the 6” concrete column)

Ec=2,850,000 psi (for the concrete column)

This results in:

Z = 19.33

Rc =19.33 f’m.

If we compare Rs and Rc, Rc has a lower value and will control:

Rc=10.82(250 psi) = 2,705 lbs.

To determine the ultimate stress Fu=2,705 lbs/(18”x4”)=37.6 psi.

8.2.2. Geometry

The geometry of the building was scaled from the photograph and was assumed to be as shown in figure 8.30.

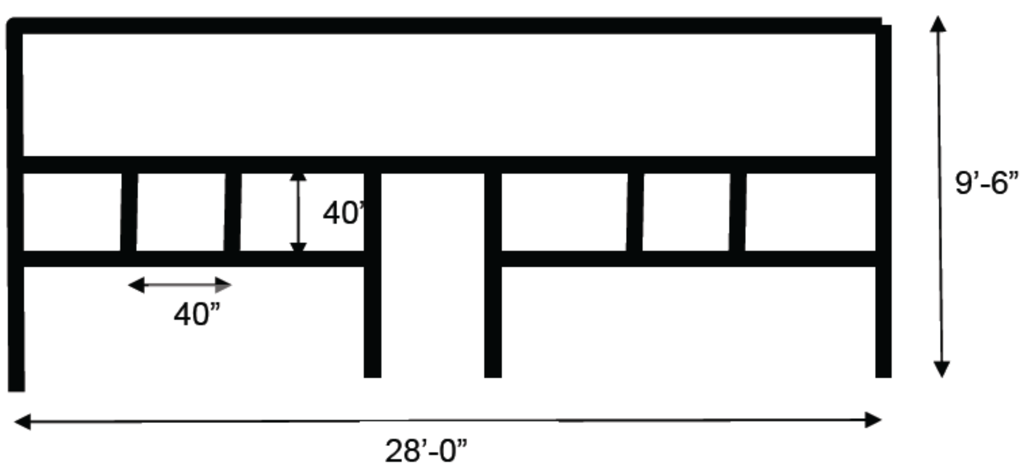

Figure 8.31. Front view of confined masonry model

The concrete frame (shown in bold lines) was assumed to be made of 6” x 6” concrete beams and columns, each with (4) #5 bars as shown in figure 8.31.

Model #1 was modeled as shown in figure 8.30. Model #2 was modeled with beams at the top and bottom as shown in figure 8.32. Model #3 was modeled without beams at the top and bottom as shown in figure 8.33. Model #4 was created with more distance between the beams and Model #5 had less distance between the columns.

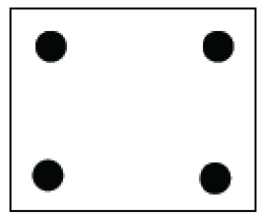

Figure 8.32. Cross-section of reinforced concrete column

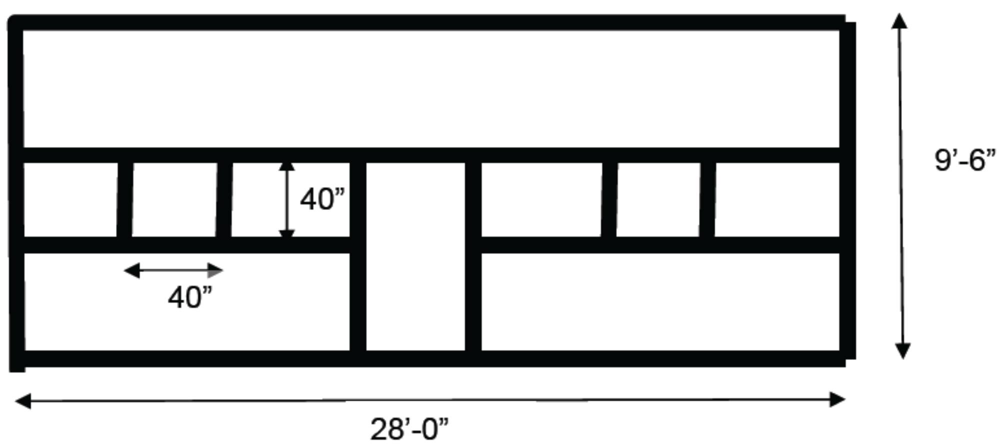

Figure 8.33. Model #2 (with beams at the top and bottom)

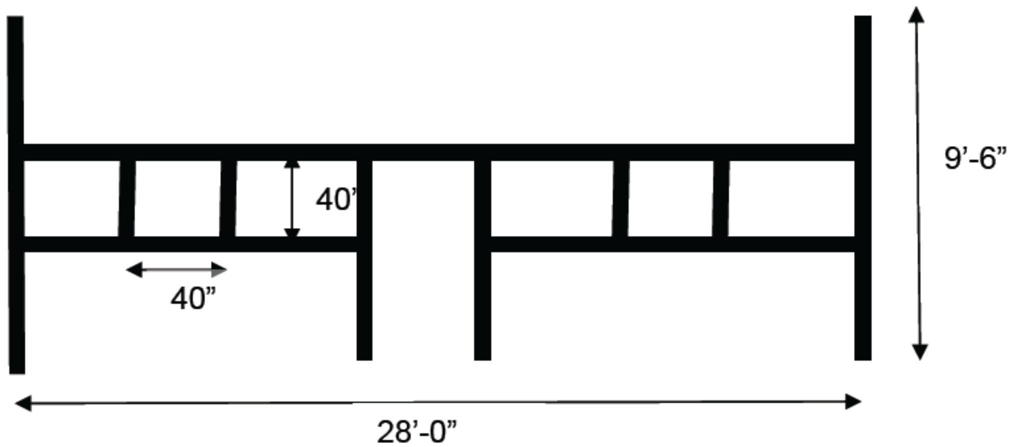

Figure 8.34. Model #3 (without beams at top and bottom)

8.2.3. Material Properties

The properties used for the model were reduced from US standards because materials in Nicaragua have been observed to be generally less consistent in material quality than in the US. This was done by reducing the concrete strength and the strength of the masonry infill. The material properties were assumed to be:

property	steel	concrete	shear walls	Infill walls
Dx	0.04	0.004		
Fu	50 ksi	2.5 ksi	0.2	37.6 psi
E	29,000 ksi	2,850ksi		
G		1,187 ksi	2,000 ksi	

Table 8.7. Confined masonry model properties

For the shear walls, E was calculated from E= 57,000√(f'c), where f'c was assumed to be 2.5 ksi. G was calculated from $G = \frac{E}{2(1+\mu)}$ where μ=0.2. This gives a G = 1,187 ksi. This value was then increased to 2,000 ksi to account for the increased capacity from the steel in the shear wall.

8.2.4. Building Weight

The total building weight was estimated to be 51,471 lbs. The total weight was calculated as follows:

Assumed wall weight = 63 psf

Building overall dimensions: 28’ x 15’ x 9.5’

The wall weights are then [(28’x9.5x2) + (15’x9.5’x2)] = 51,471 lbs.

The weight of the roof was ignored because of its relatively low weight compared to the weight of the walls.

8.2.5. Models

The building as-built computer model is shown in figure 8.34. Model #1 has a continuous beam at the top but not the bottom. The top beam cannot be seen in the figure, but is assumed to exist because it would give a flat edge to support the roof members.

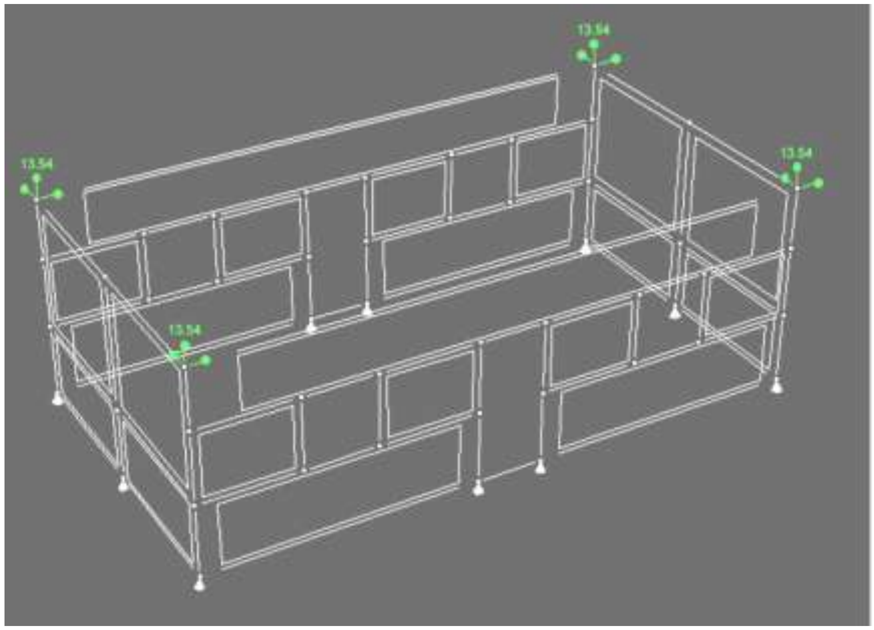

Figure 8.35. Model #1

Notice in figure 8.34 the supports are located only at column locations and the weight is applied at the four corners. Similarly, the diaphragm at the top is only connected at the column locations.

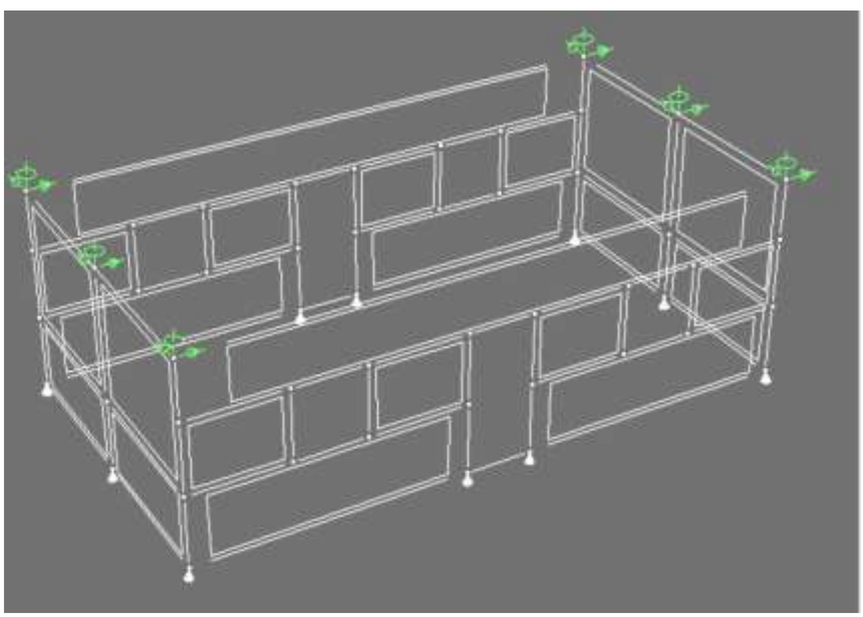

Figure 8.36. Model #1 with diaphragm connections

In figure 8.35 the pushover load was applied at the corners.

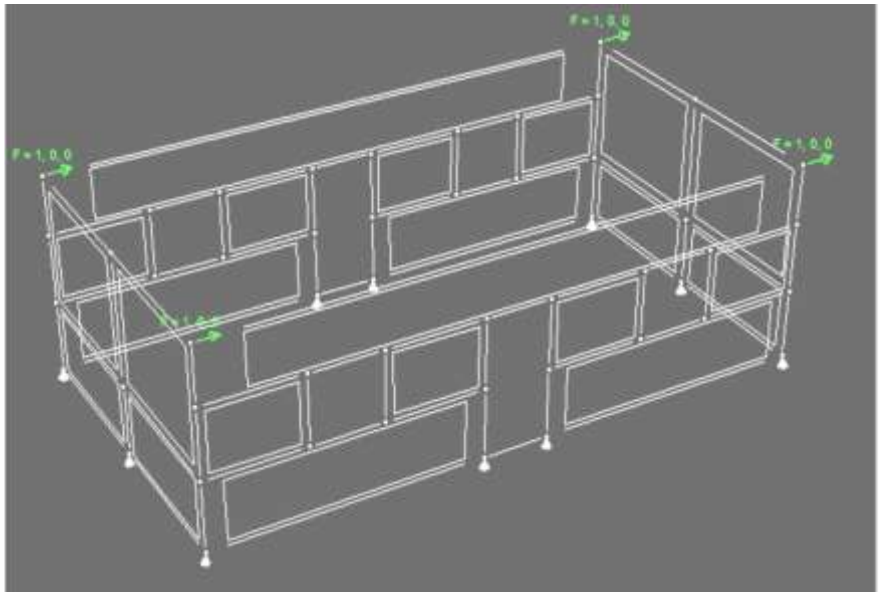

Figure 8.37. Model #1 with pushover load applied

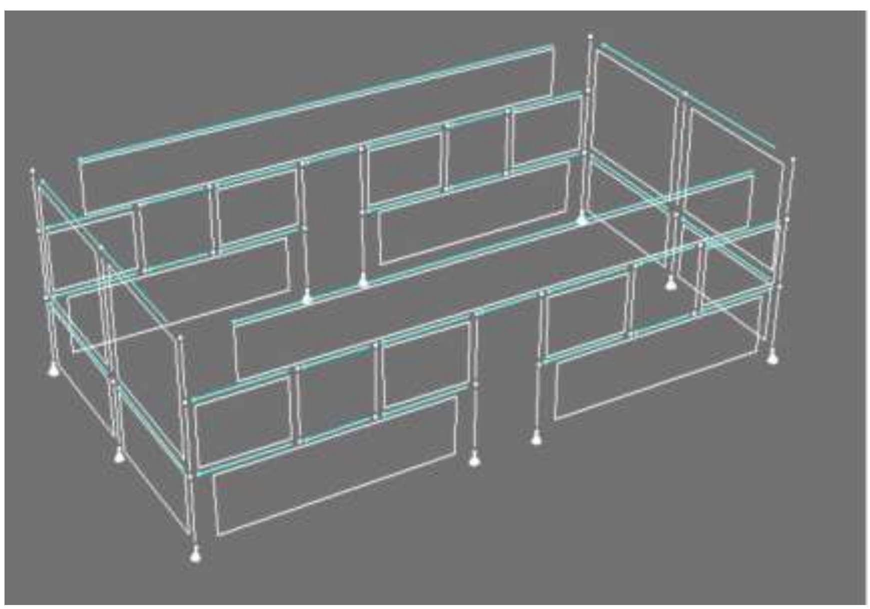

Figure 8.38. Model #1 with a beam at the top

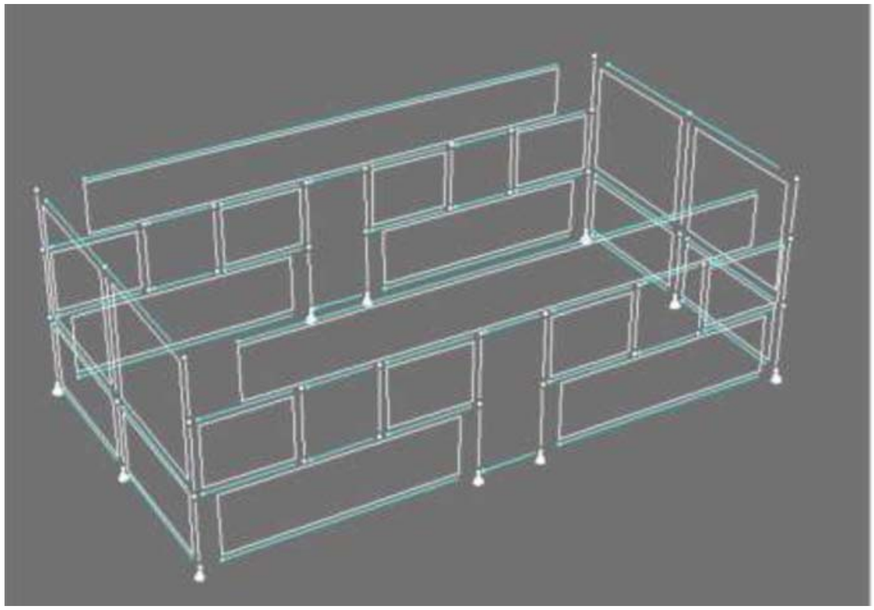

Figure 8.39. Model #2 with beams at the top and bottom

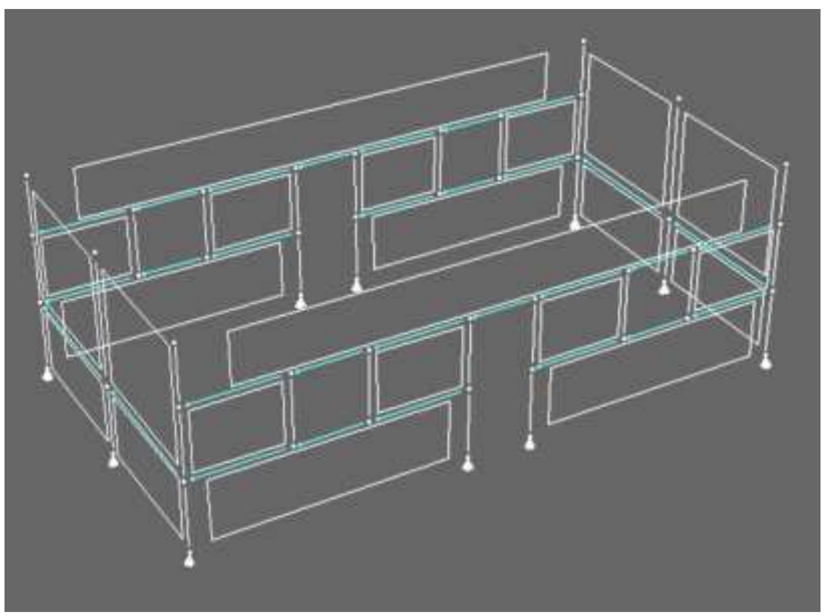

Figure 8.40. Model #3 without beams at top and bottom

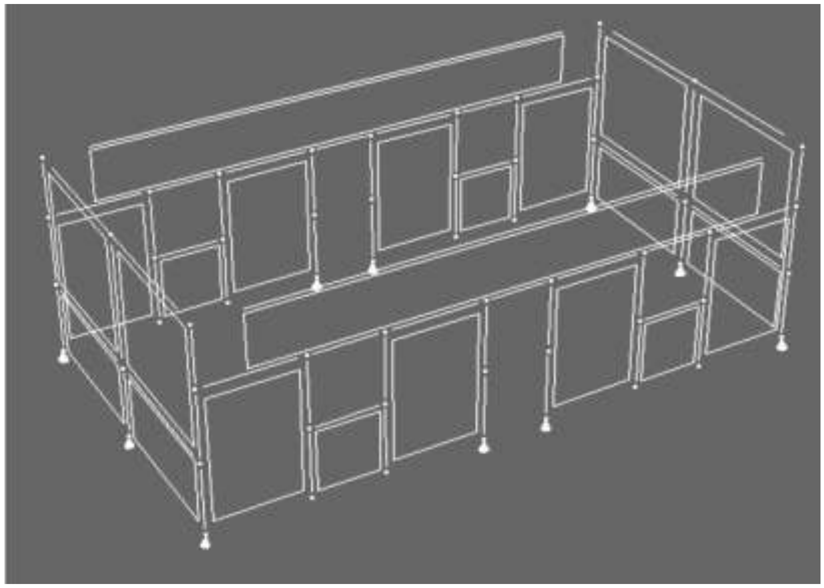

Figure 8.41. Model #4 with greater distance between beams

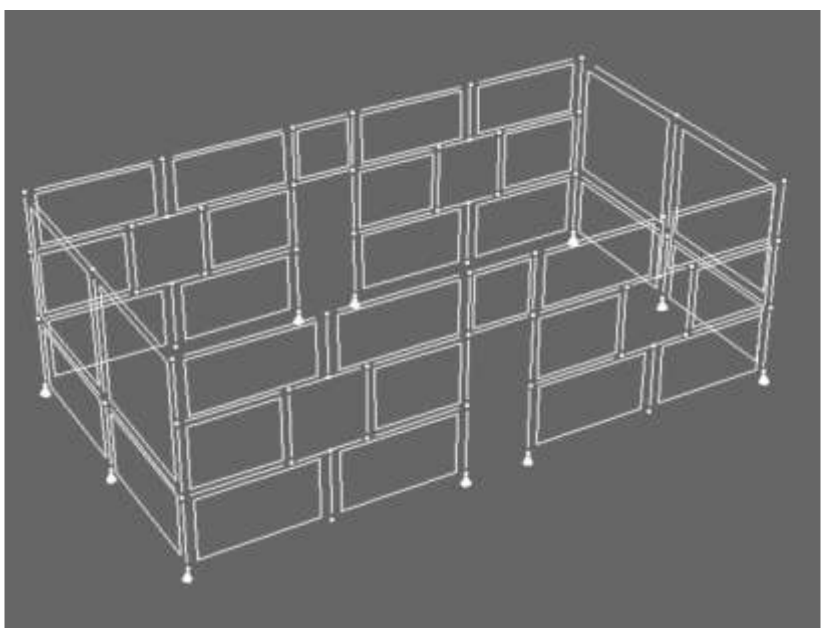

Figure 8.42. Model #5 with less distance between columns

8.2.6. Pushover Analysis

The pushover analysis terminated when the model either reached the maximum deflection or a member failed. The points for immediate occupancy, life safety, and collapse prevention were taken from FEMA 356 as:

- drift ratio at immediate occupancy .002
- drift ratio at life safety .002
- drift ratio at collapse prevention .003

The pushover charts are shown in the following graphs:

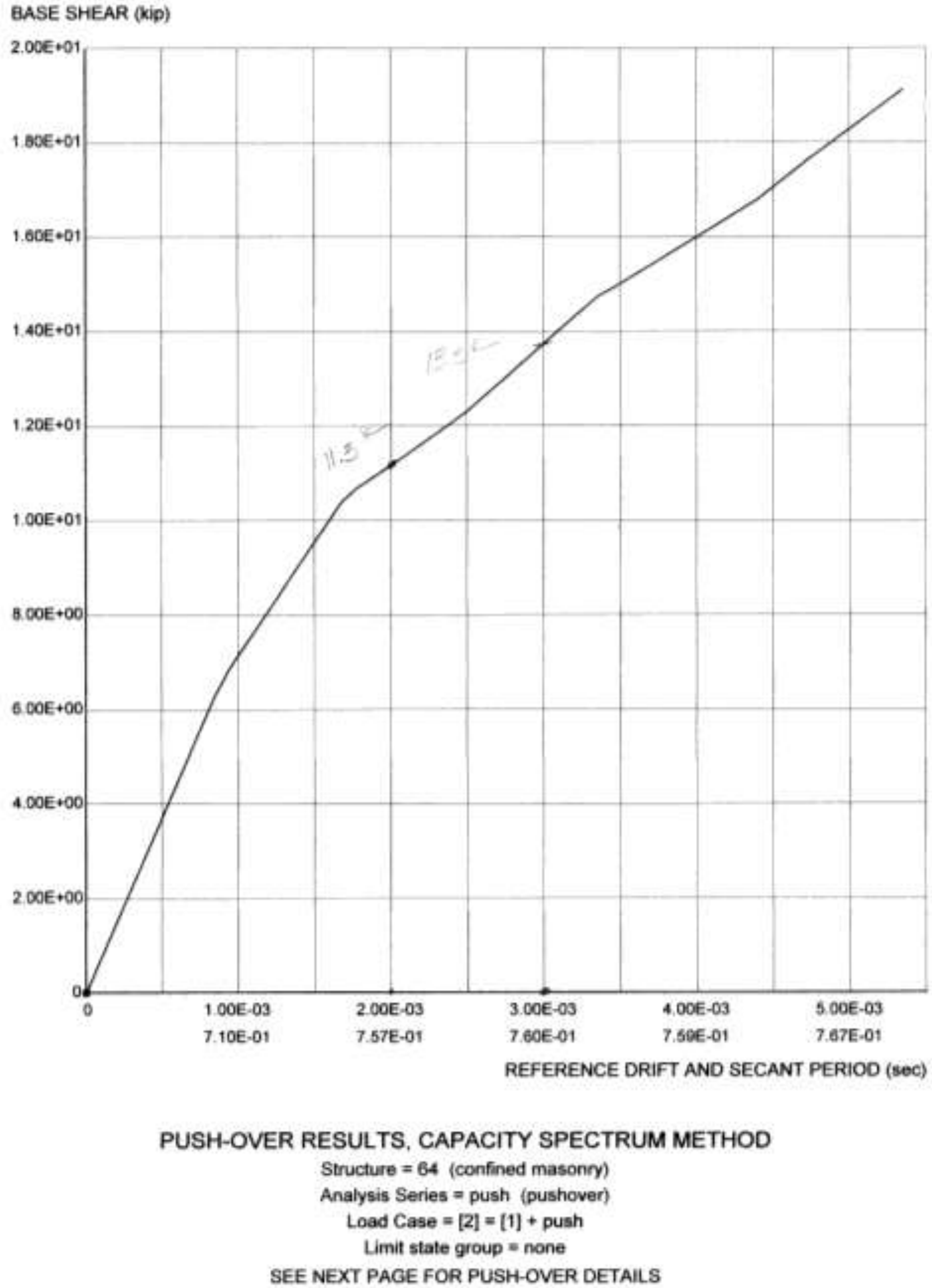

Figure 8.43. Pushover analysis for model #1

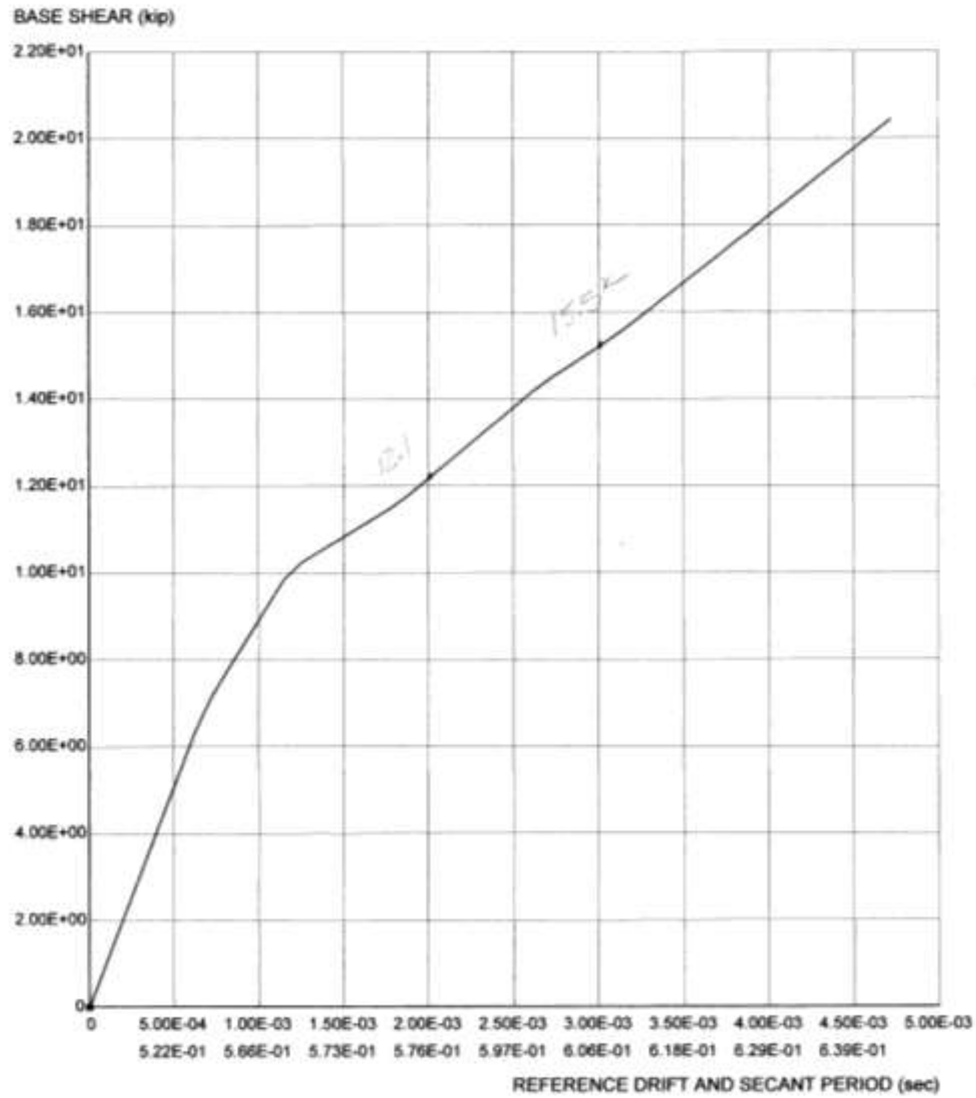

PUSH-OVER RESULTS, CAPACITY SPECTRUM METHOD
Structure = 64-A (confined masonry with beams at top and bottom)
Analysis Series = push (pushover)
Load Case = [2] = [1] + push
Limit state group = none
SEE NEXT PAGE FOR PUSH-OVER DETAILS

Figure 8.44. Pushover analysis for model #2

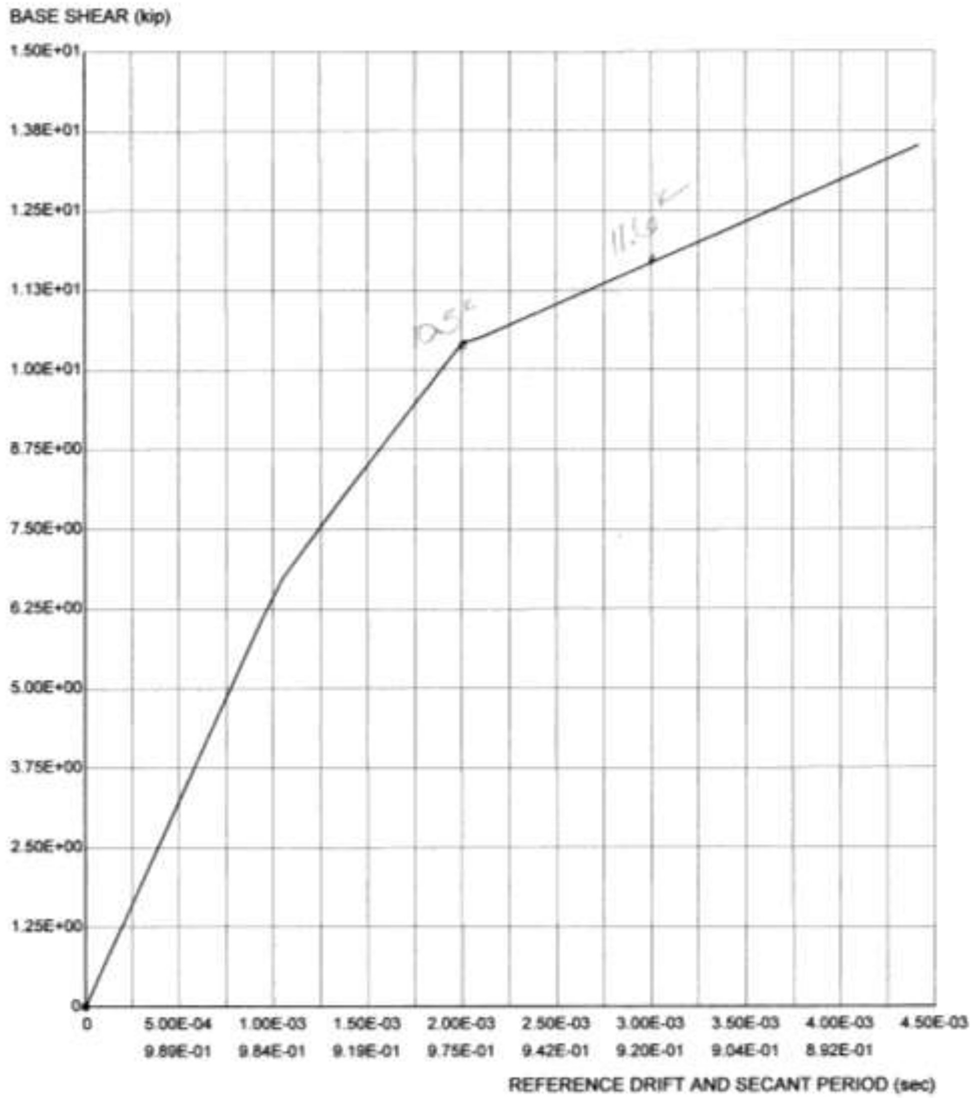

PUSH-OVER RESULTS, CAPACITY SPECTRUM METHOD

Structure = 64-B (confined masonry without beams at top and bottom)

Analysis Series = push (pushover)

Load Case = [2] = [1] + push

Limit state group = none

SEE NEXT PAGE FOR PUSH-OVER DETAILS

Figure 8.45. Pushover analysis for model #3

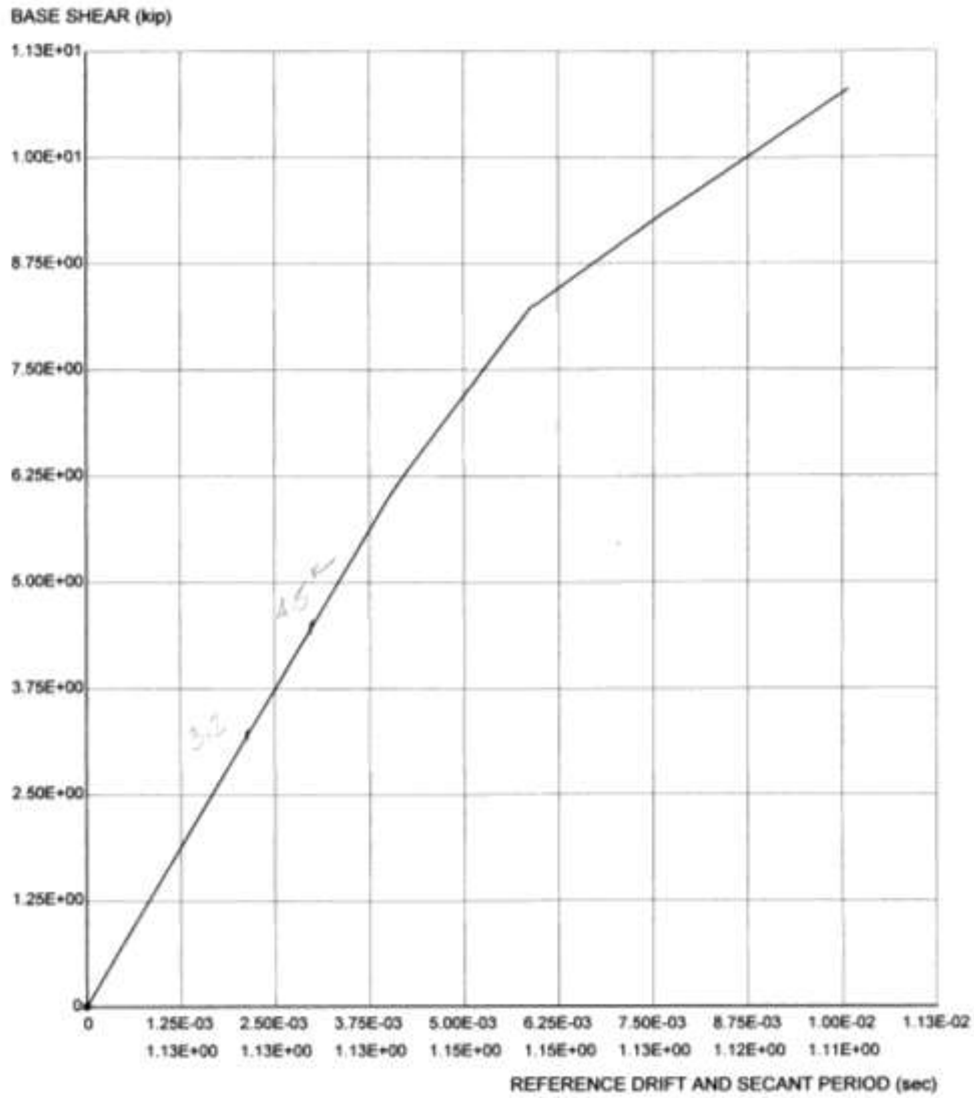

PUSH-OVER RESULTS, CAPACITY SPECTRUM METHOD

Structure = 64-C (confined masonry greater distance between beams)

Analysis Series = push (pushover)

Load Case = [2] = [1] + push

Limit state group = none

SEE NEXT PAGE FOR PUSH-OVER DETAILS

Figure 8.46. Pushover analysis for model #4

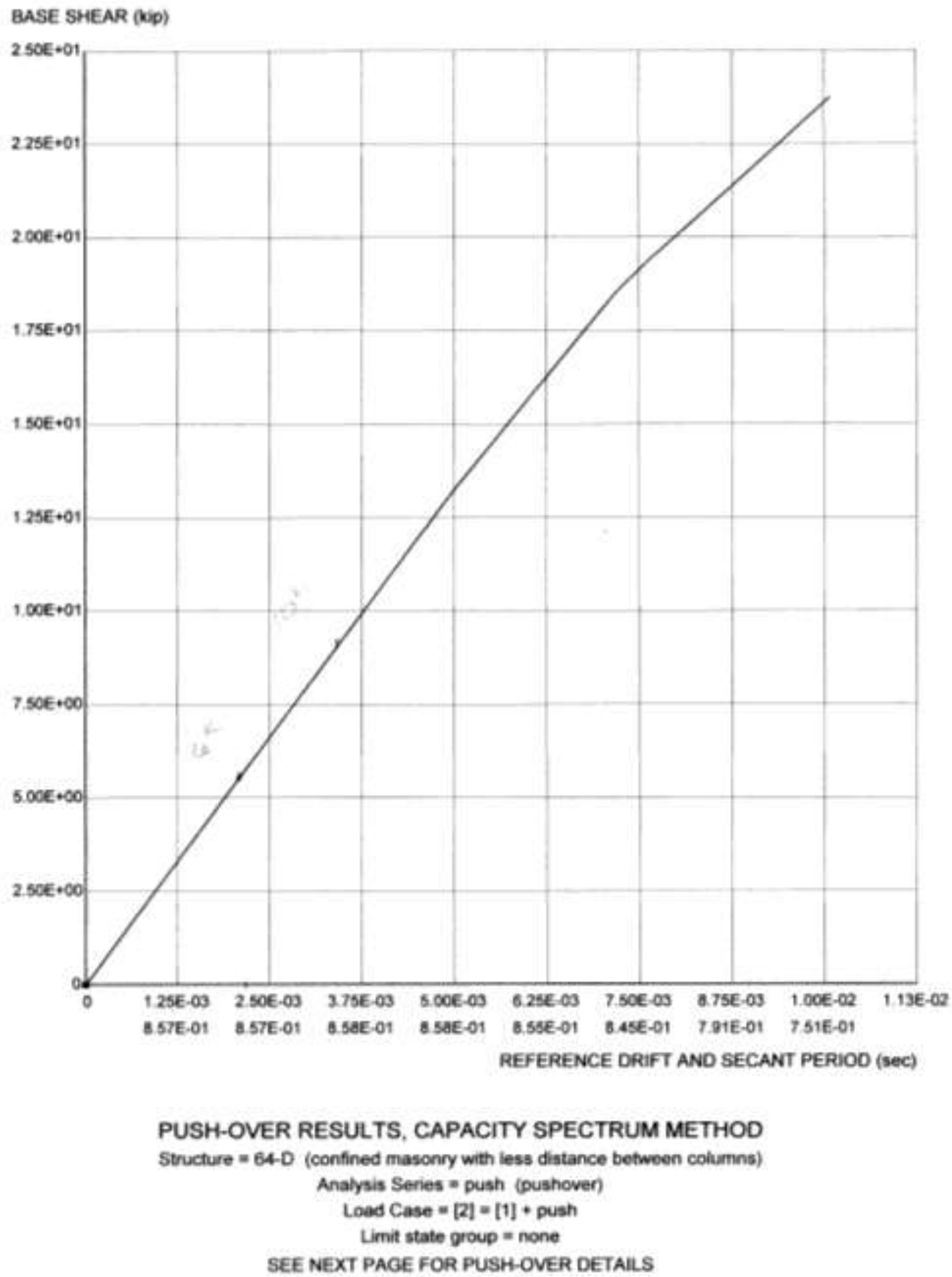

Figure 8.47. Pushover analysis for model #5

Table 8.8 shows the results:

Model	Load at Immediate Occupancy	Load at Life Safety	Load at Collapse Prevention
#1 Building as built	11.3 kips	11.3 kips	13.5 kips
#2 (with beams at top and bottom)	12.1 kips	12.1 kips	15.5 kips
#3 (without beams at top and bottom)	10.5 kips	10.5 kips	11.6 kips
#4 (w/ greater distance between beams	3.2 kips	3.2 kips	4.5 kips
#5 (w/ less distance between columns	6 kips	6 kips	10 kips

Table 8.8. Comparison of model performances

8.2.7. Possible Improvements

It has been noted with shear wall systems the importance of having a structural ring around the top and bottom to tie the system together (Getty, 2000; Cao and Watanabe, 2004; May, 1984). This ring acts in the same way a steel ring holds a wooden barrel together. As expected, adding beams at the top and the bottom increased the load capacity. Adding a beam at the top and adding a beam at the bottom are both equally important and both make an equal contribution to the building load capacity. However, doing so did not increase the capacity as much as expected. With no beams the load at collapse prevention was found to be 11.6 kips, with one beam the capacity was 13.5 kips and with beams at the top and bottom the load was found to be 15.5 kips.

Increasing the distance between the beams dramatically decreased the capacity resulting in a decrease of nearly two-thirds. This was an unexpected result and further investigations into this case will be carried out in subsequent research efforts.

Additionally, it was expected that the capacity of the building would increase with more columns and yet the capacity went down. This decrease was possibly the result of the increase in rigidity caused by adding more columns. However, the columns did increase the ductility of the building.

8.2.8. Summary

The following changes are recommended to improve the seismic performance of confined masonry buildings:

- A structural ring around the top and bottom are most important to increasing the structural capacity in the event of an earthquake. This ring should consist of a continuous reinforced beam with adequate longitudinal reinforcement, sufficient ties, and sufficient development lengths.
- In addition to structural rings, additional beams should be located no more than 5' on center. Where possible these beams should be continuous. In every case, the beams should have adequate longitudinal reinforcement, sufficient ties, and sufficient development lengths.
- Infill bricks should be reinforced. If not possible they should be tied to the frames surrounding them.
- Tall walls should be avoided as they create large deflections.

8.3. Taquezal

Taquezal models are difficult to verify the results because they have never been tested in a laboratory and their properties are not well known. What is known about taquezal buildings is their performance during the 1972 earthquake in Managua.

Their performance during this earthquake is the only known property of this building type and is therefore what was used to verify the models in the following sections.

8.3.1. Assumptions

To create a model of a taquezal building the details of some common buildings in Rivas, Nicaragua were used. The nature of the construction of taquezal buildings was observed by documenting various damaged or unmaintained buildings.

Figure 8.48. Taquezal building, Rivas, Nicaragua

Generally taquezal construction fills an entire city block. The building is shaped like a square donut with a courtyard in the center and the building (the size of a block) is subdivided into smaller units.

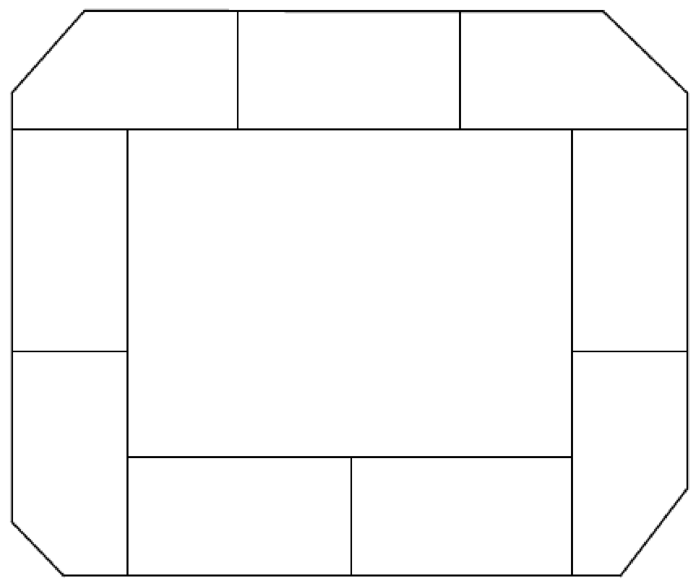

Figure 8.49. Typical taquezal city block plan

8.3.2. Geometry

For the purpose of this study one corner of a block was analyzed.

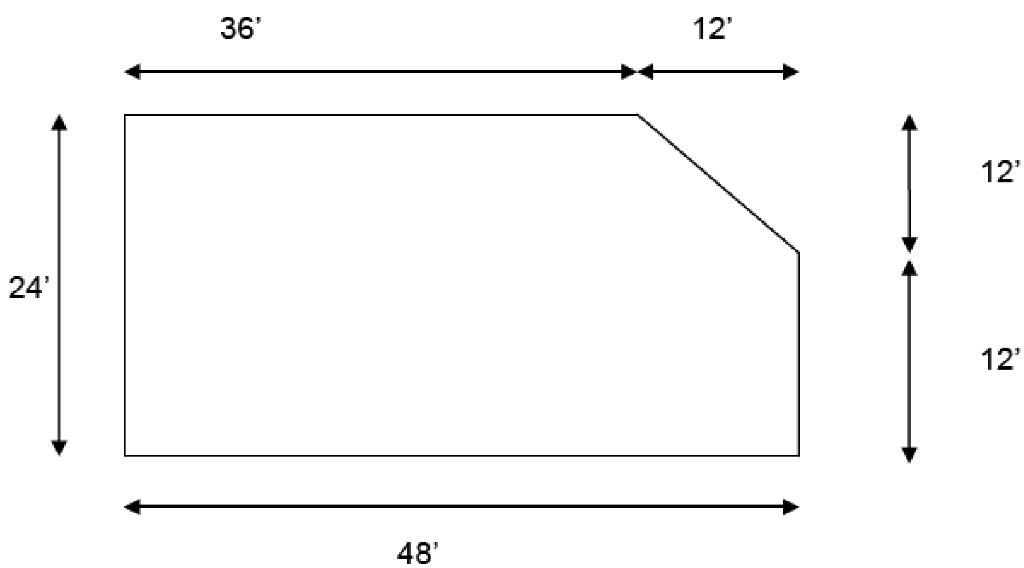

Figure 8.50. Taquezal corner layout

The framing of the building was estimated from photographs of taquezal buildings like the one shown in figure 8.51.

Figure 8.51. Typical taquezal framing used for model

The following estimates were made:

- Large framing columns are 6"x 6" posts and located 12' on center

- Smaller columns are 2”x 2” posts and located 12” on center
- Wall depth is 10” total
- Horizontal framing members provide a grid for the soil to attach and are therefore non-structural and not included in the model

8.3.3. Material Properties

Table 8.9 depicts the properties applied to the models:

property	wood	earth	shear walls
Dx	0.004	0.004	0.004
Fu (compression)	1 ksi	0.189 ksi	0.00945
Fu (tension)		0.0189 ksi	
E	1,800 ksi	783 ksi	
G		692 ksi	1,500 ksi

Table 8.9. Taquezal model material properties

E was calculated from $E = 57{,}000\sqrt{(f'c)}$. For the Inelastic shear wall material, the ultimate strength (F_u) was determined to be 0.00945 ksi. Fu was calculated as 5% of compressive strength. Shear modulus (G) was assumed to be 1,500 ksi (to account for wood and earth).

The building was estimated to weigh a total of 205,500 lbs. This was calculated by assuming the weight of the walls to be 100 psf. The weight of the 15’ tall walls was then calculated to be: 100 psf x 15’ = 1,500 plf. The example building has 137 linear feet of walls resulting in a total weight = 1,500 plf x 137’ = 205,500 lbs.

8.3.4. Models

The taquezal model was constructed in much the same way the previous models were created.

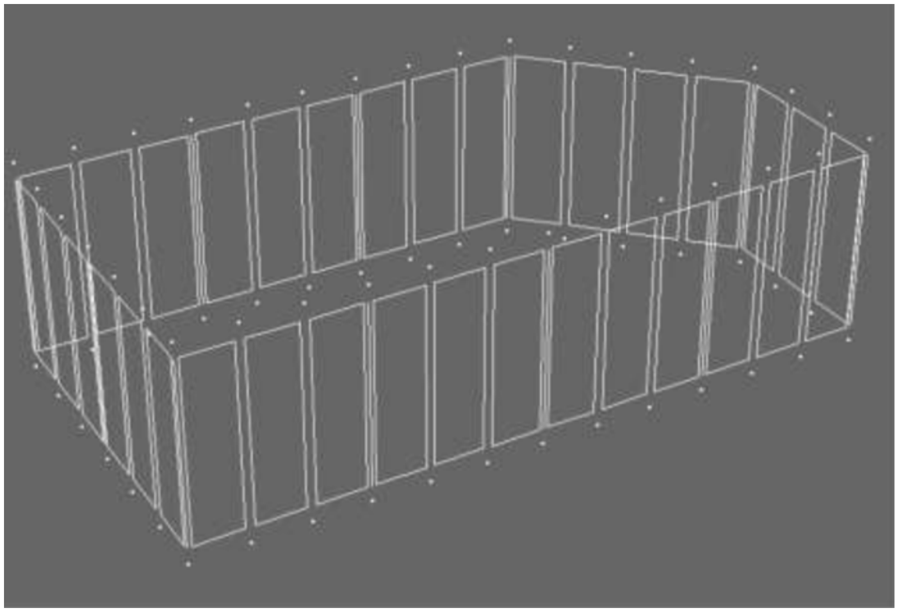
Figure 8.52. Taquezal model elements

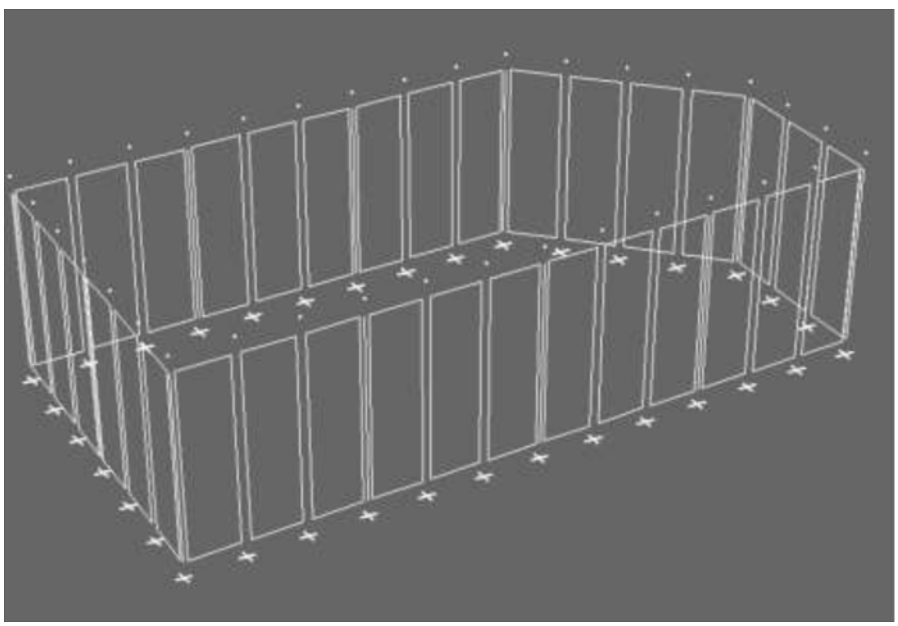
Figure 8.53. Taquezal model foundation attachment

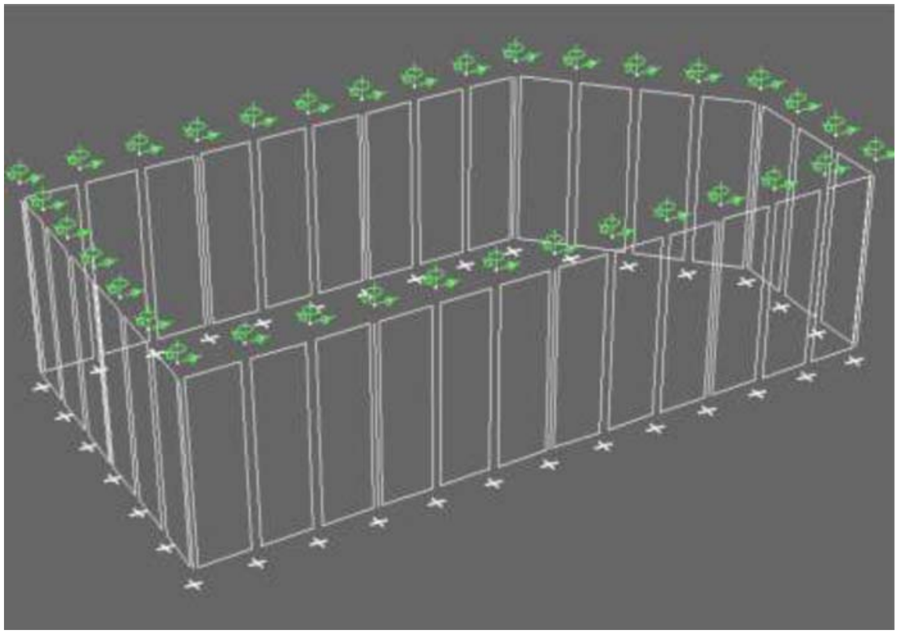

Figure 8.54. Model with restraints at roof

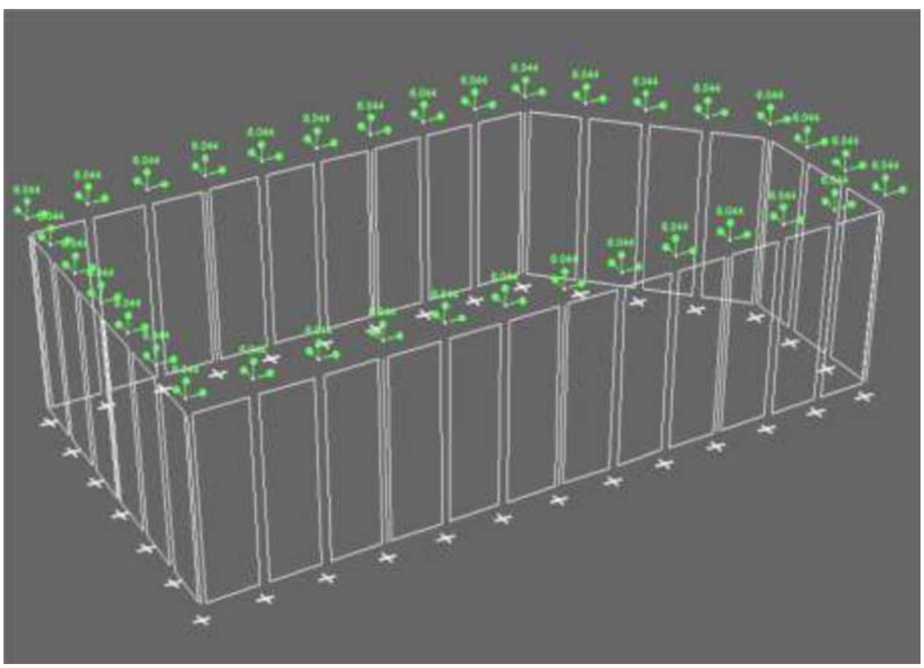

Figure 8.55. Model with self weight evenly applied

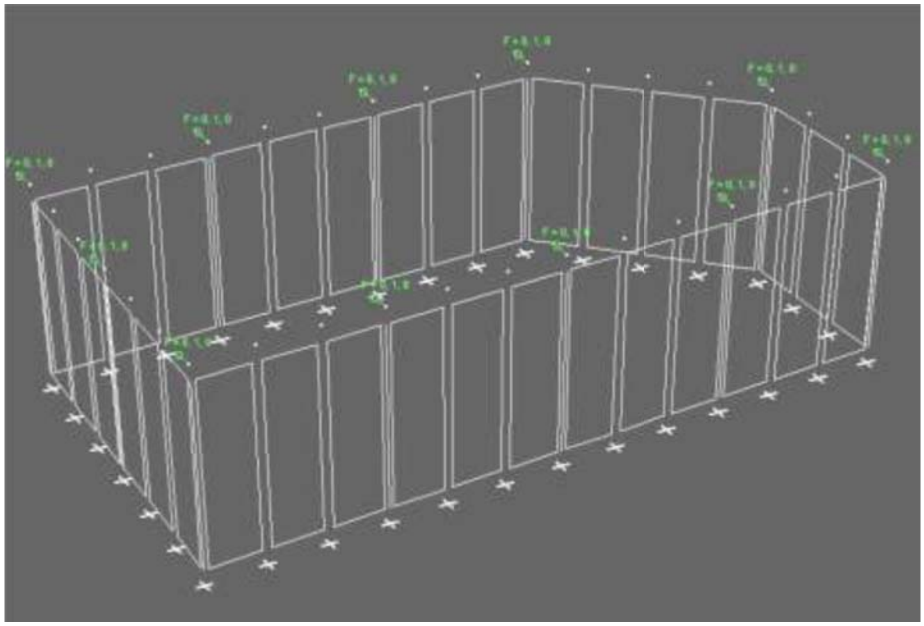

Figure 8.56. Model with roof acting as localized diaphragm

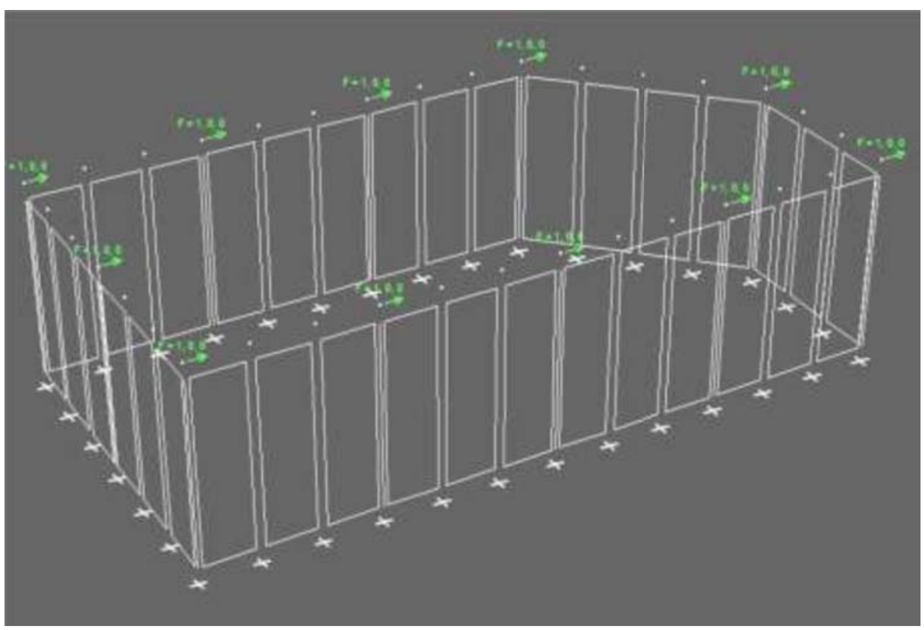

Figure 8.57. Model with self weight applied at local diaphragm locations

8.3.5. Pushover Analysis

The first five modes are described in table 8.10:

Model #1		Description of mode shape
1^{st} period of vibration	0.02593	lateral deformation
2nd period of vibration	0.01693	longitudinal deformation
3rd period of vibration	0.01528	torional deformation
4th period of vibration	0.01103	accordion up and down
5^{th} period of vibration	0.0105	torsional and accordian

Table 8.10. First five modes of vibration for the taquezal model

8.3.5.1. Pushover in the Lateral Direction

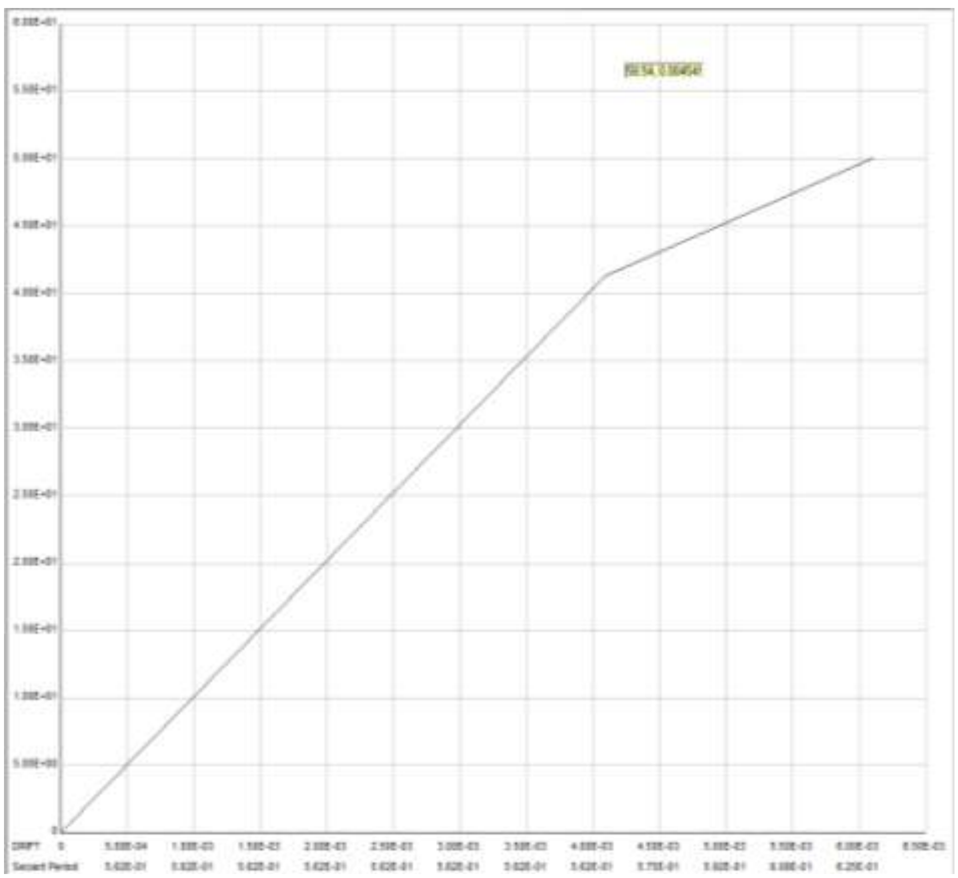

Figure 8.58. Taquezal pushover analysis (lateral direction)

8.3.5.2. Pushover in the Longitudinal Direction

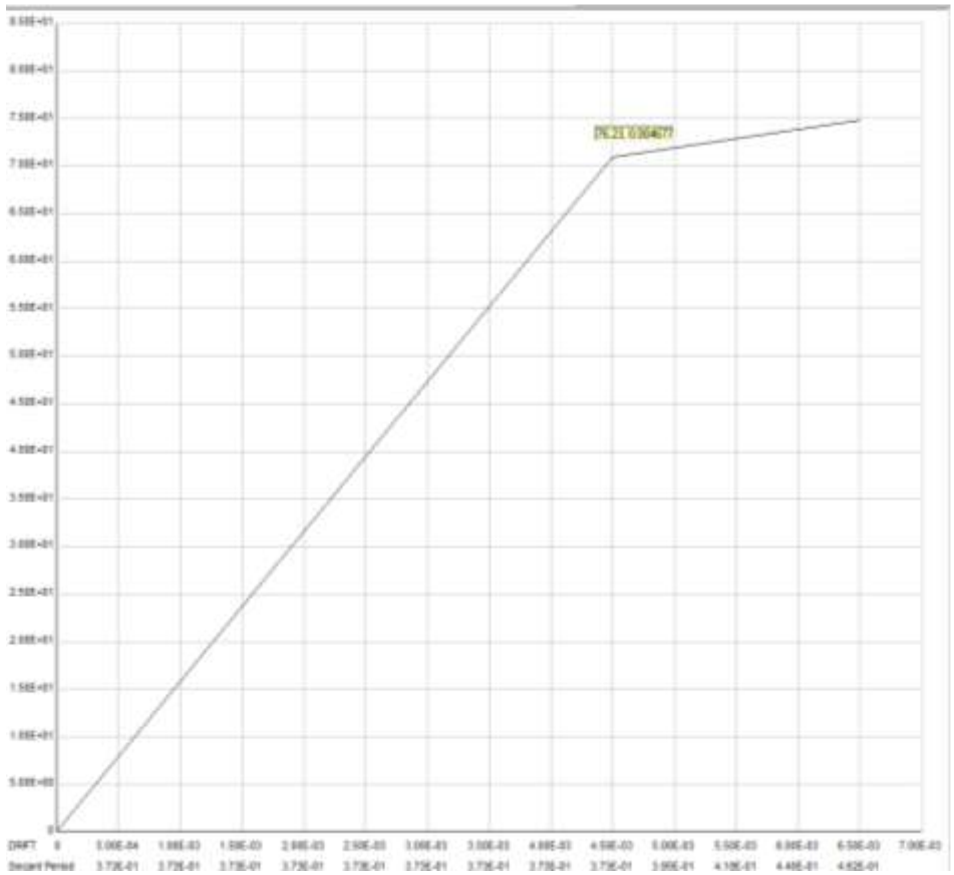

Figure 8.59. Taquezal pushover analysis (longitudinal direction)

The points for immediate occupancy, life safety, and collapse prevention were taken from FEMA 356 as:

- drift ratio at immediate occupancy - negligible
- drift ratio at life safety .0022
- drift ratio at collapse prevention .004

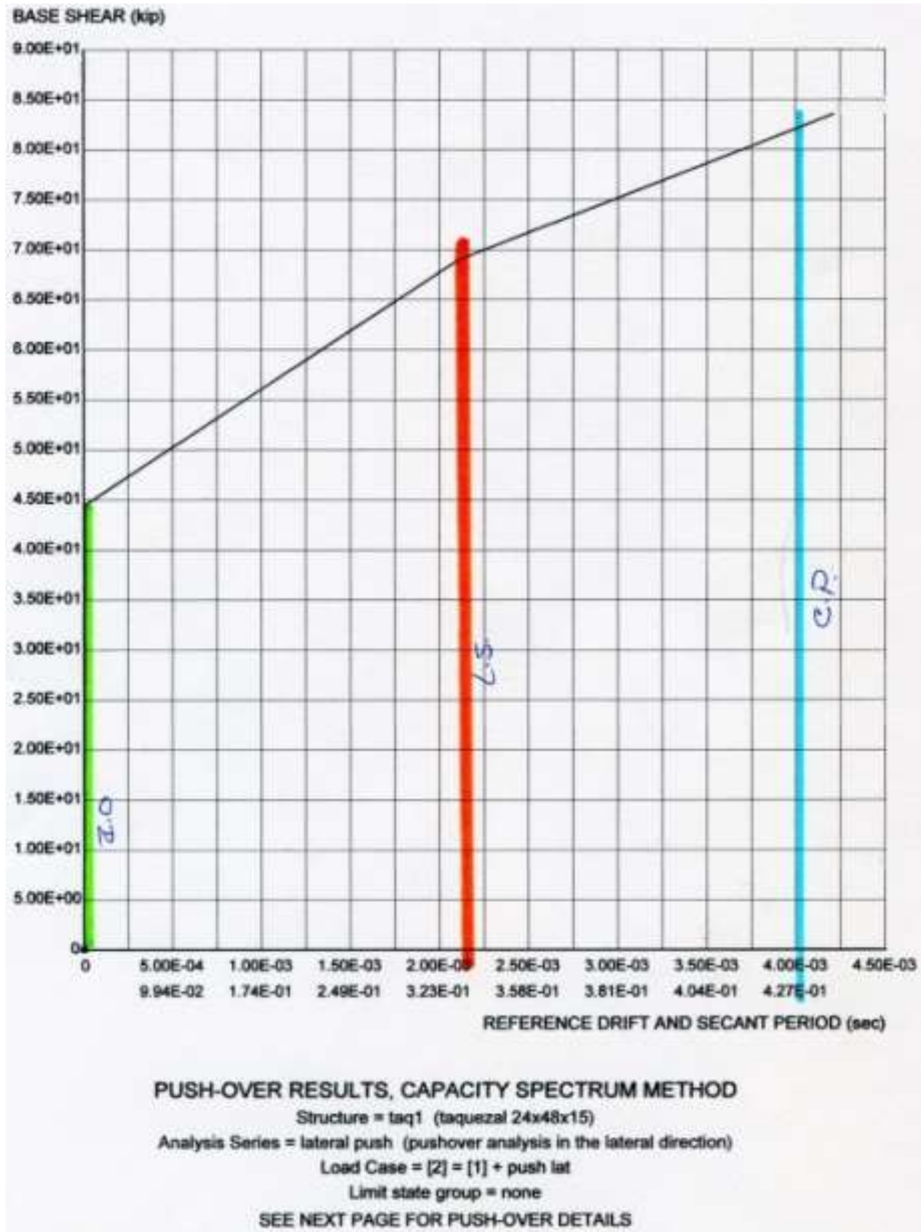

Figure 8.60. Taquezal lateral pushover results with performance points

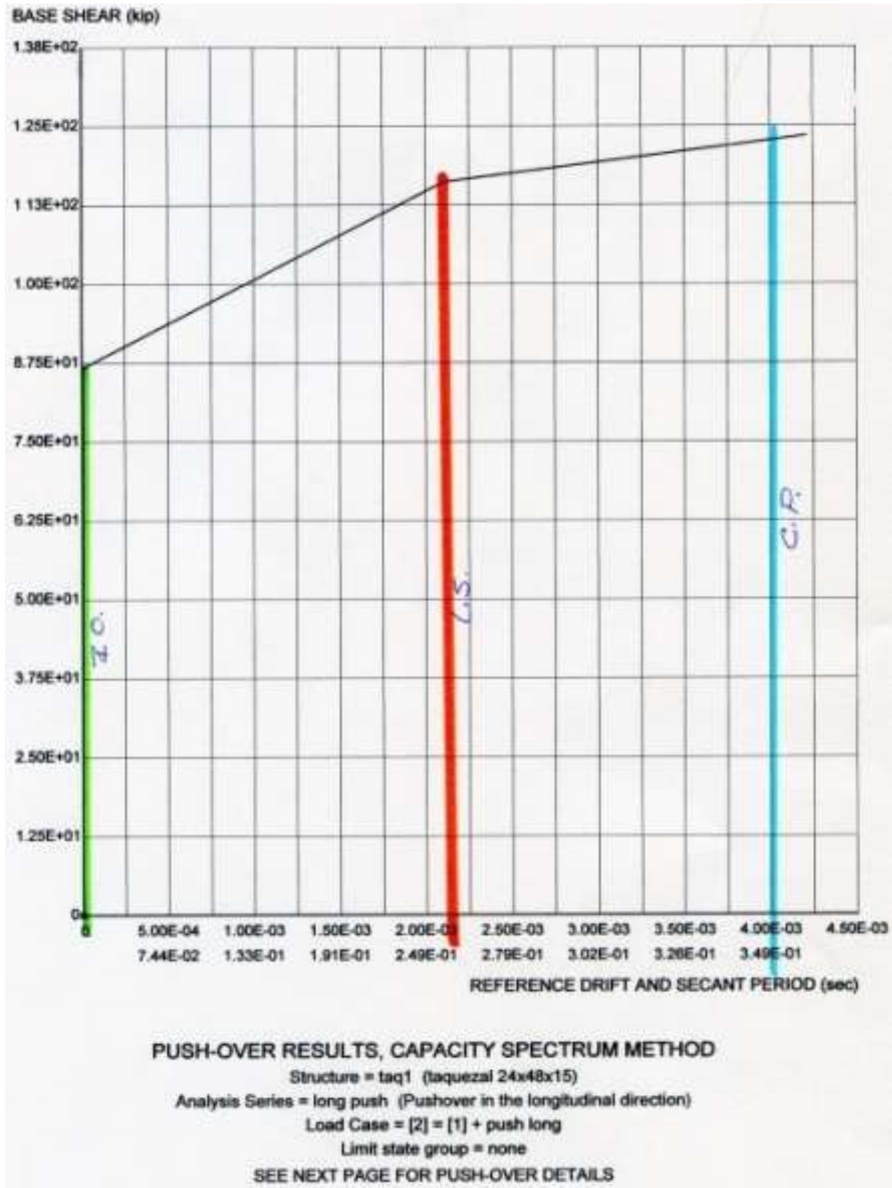

Figure 8.61. Taquezal longitudinal pushover results with performance points

To simulate decay of the wood, several supports were removed and the model was re-analyzed. Two support conditions were considered. The first time one support was removed as below:

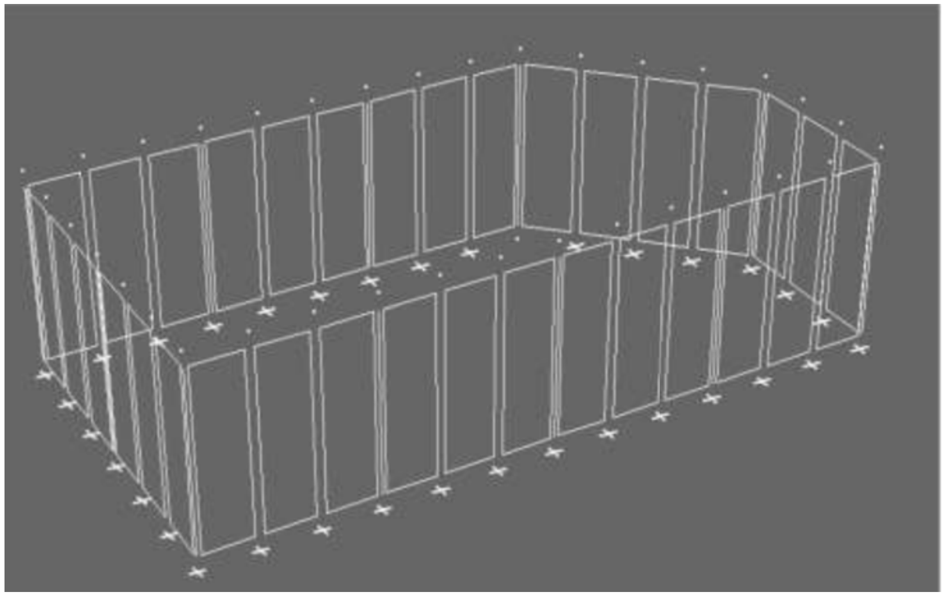
Figure 8.62. Taquezal model with one missing support

In the next model several supports were removed to model more extensive rotten wood.

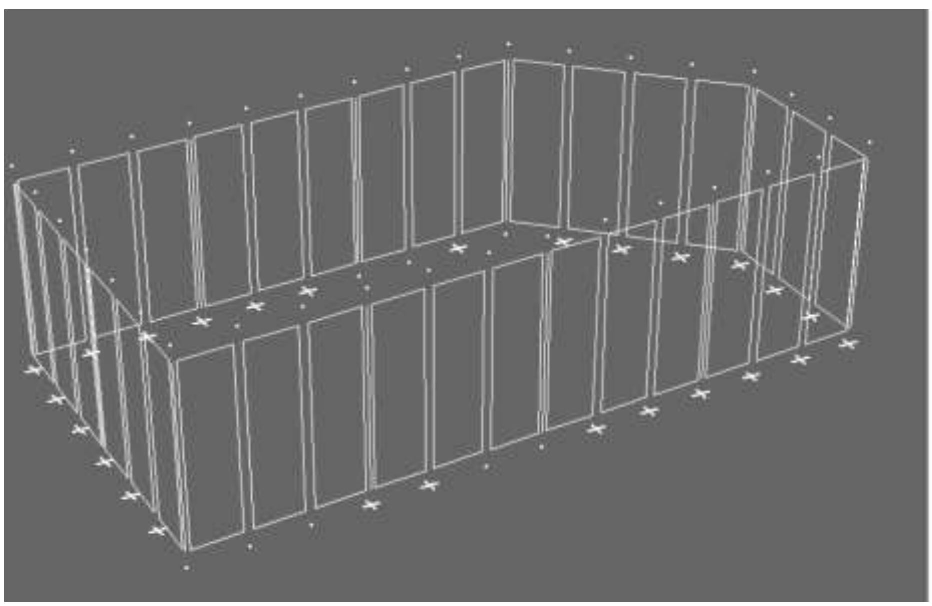
Figure 8.63. Taquezal model with eight missing supports

And finally a model with the foundation support and roof diaphragm support removed at eight locations was considered.

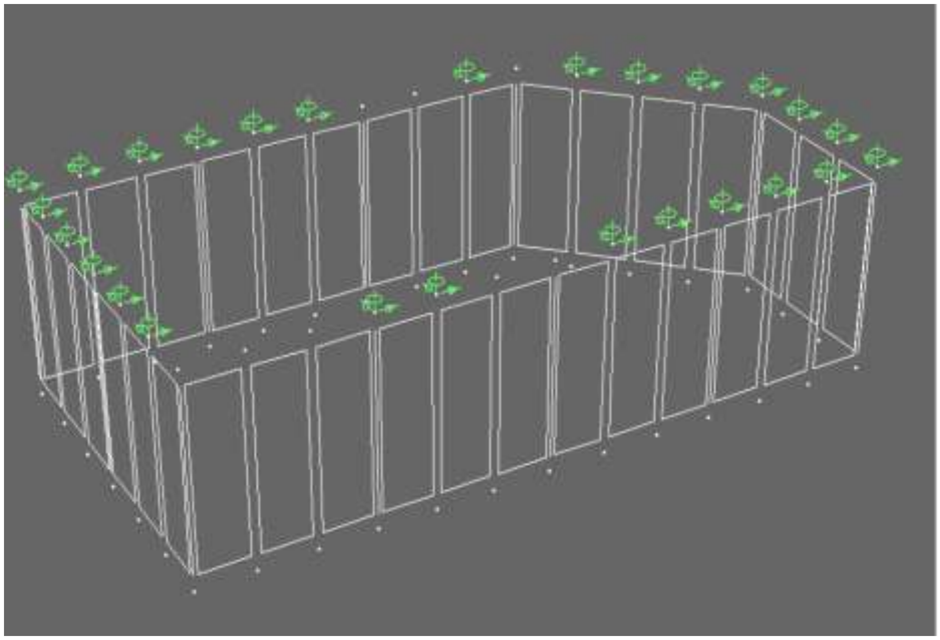

Figure 8.64. Taquezal model with missing supports at foundation and roof

The pushover curves for the taquezal buildings with some wood rot are shown in figures 8.65 and 8.66.

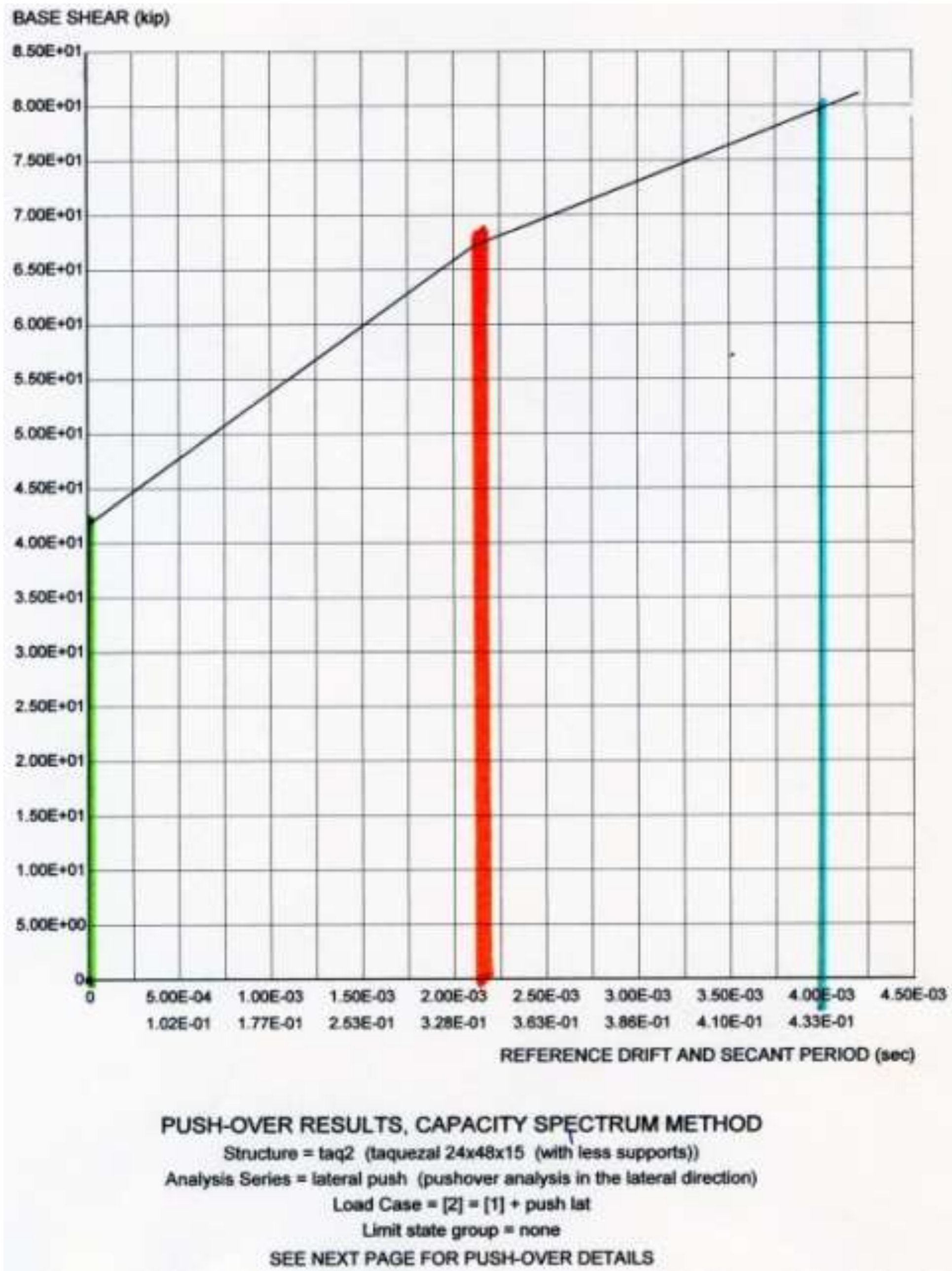

Figure 8.65. Taquezal building with weak supports – lateral pushover analysis

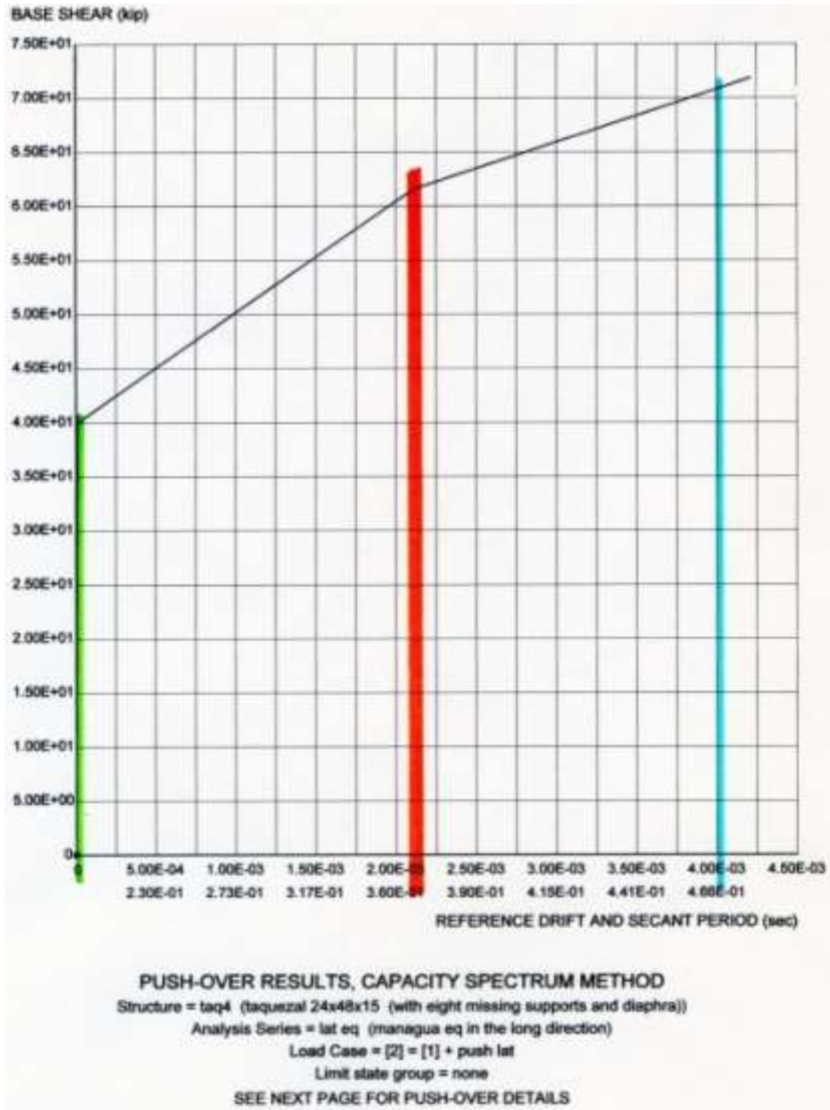

Figure 8.66. Taquezal building with weak supports – longitudinal pushover analysis

The comparison of the lateral pushovers loads are shown in table 8.11.

Model	Load at Immediate Occupancy	Load at Life Safety	Load at Collapse Prevention
Standard	44 kips	68 kips	83 kips
One missing support	42 kips	67 kips	79 kips
Eight missing supports	41 kips	66 kips	78 kips
Eight missing supports and diaphragm connections	40 kips	62 kips	71 kips

Table 8.11 Taquezal model pushover analysis results comparison

Comparisons of the modes of vibration are shown in table 8.12.

model	1st mode	2nd mode	3rd mode	4th mode	5th mode
standard	0.02593	0.01693	0.01528	0.01103	0.0105
Eight missing supports and diaphragm connections	0.2481	0.1753	0.1708	0.1708	0.1539

Table 8.12 Taquezal modes of vibration

Removing the support and diaphragm connection points modeled a deteriorated foundation connection thus increasing the deflections dramatically. This increased flexibility is also shown in the modes of vibration, which increased by a factor of 10 when the 8 supports and diaphragm locations were removed.

8.3.6. Dynamic Analysis

The taquezal building was analyzed dynamically using the Managua earthquake of 1972. The results for the lateral and longitudinal direction are shown in figures 8.67 and 8.68.

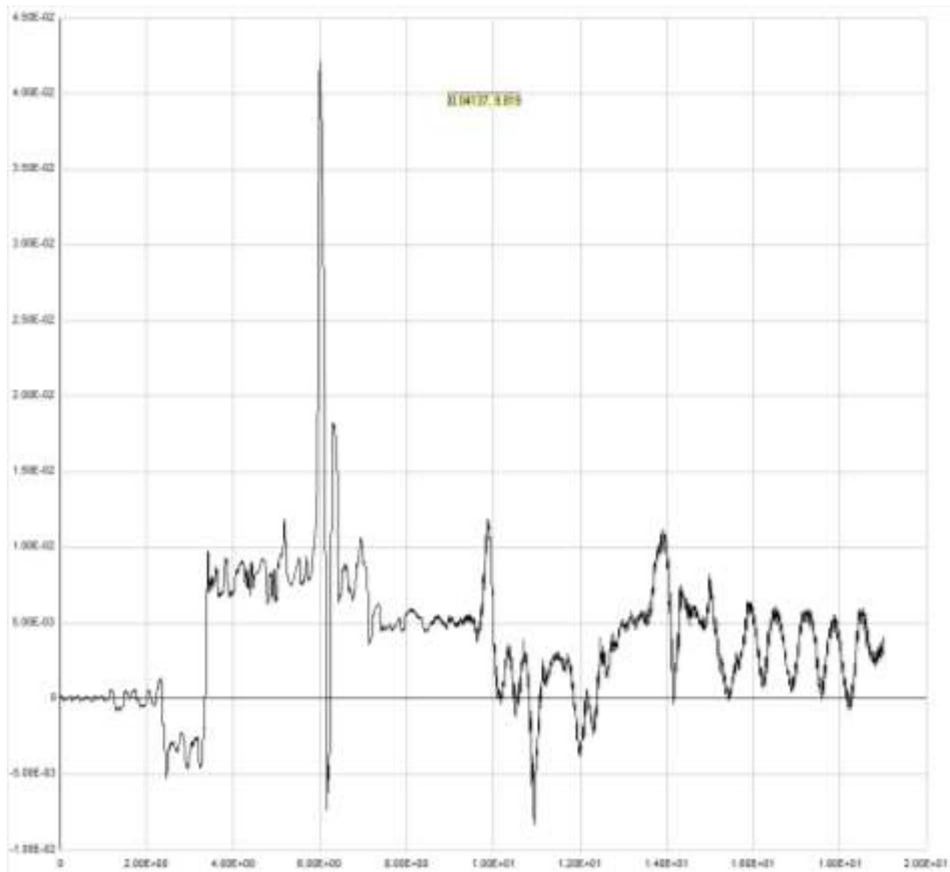

Figure 8.67. Taququezal lateral earthquake simulation

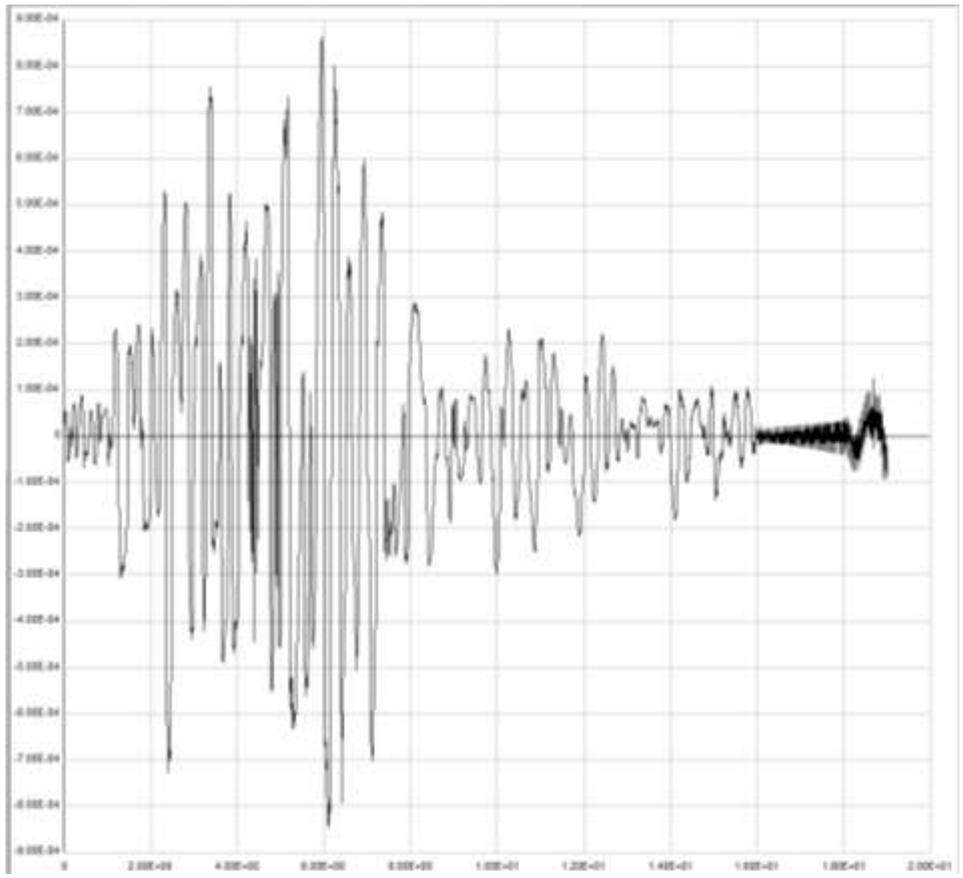

Figure 8.68. Taquezal longitudinal earthquake simulation

The maximum deflection recorded in the lateral direction is 0.42 inches. This equates to a drift ratio (deflection/height) = (.042"/(15'x12)) = 0.0023. This drift ratio is close to the value set for life safety, 0.0022, which confirms the results from the earthquake. The buildings that were well maintained performed fairly well, but buildings that had damaged or rotted columns suffered greater damage.

8.3.7. Possible Improvements

To build a taquezal building in Nicaragua that will perform better during an earthquake, the following recommendations are made:

- Proper maintenance is important to maintaining structural integrity of the taquezal shear walls. The areas that need to be inspected regularly are the connections of the vertical support wood at the base and the roof. The wood can be damaged by water or termites. The overhangs are important to reduce the water the splashes on the building and the roof must be kept water tight to reduce the possibility of leaks. To reduce the chance of termites, some buildings are built on a concrete curb. Anything to keep the wood structure from being in contact with the ground should help but ultimately termite treatment may be necessary.
- Cross bracing would provide an additional lateral force resisting system and create redundancy if the building was not properly maintained. Cross bracing could consist of wooden members on the diagonal, strapping, or frames.
- The roof material should be kept as light as possible to reduce the risk of injury. Clay tiles should be avoided unless great care is taken to ensure the roof is well constructed.

8.4. Rammed Earth (Tapial)

The rammed earth model geometry was chosen to match a rammed earth building that was tested at Fears Structural Engineering Laboratory at the University of Oklahoma.

8.4.1. Geometry

The geometry of the buildings is duplicated from a physical model built to scale at Fears Structural Engineering Laboratory. The building is 12’ x 12’ x 9’ tall with one 6’8” tall by 3’ wide door centered in one wall.

8.4.2. Material Properties

The material properties were assumed to be:

property	Value used for earthen material	Value used for shear wall
Dx	0.004	
Fu (ultimate strength)	0.8 ksi	0.04 ksi
E (modulus of elasticity)	1612 ksi	
G (shear modulus)		361 ksi

Table 8.13. Tapial model material properties

E for concrete was calculated from E= 57,000√(f’c).

G was calculated from $G = \frac{E}{2(1+\mu)}$ where μ=0.2 Poisson’s ratio for concrete is generally taken as 0.1 to 0.2, while steel is 0.27 to 0.3. 0.2 was used for the combined system to account for the steel in the concrete.

Fu for the inelastic shear material was calculated to be 5% of compressive strength which gives 0.8 ksi x.05 = 0.04. Also the shear modulus (G=361 ksi) was calculated from G=57,000√(f’c) = (57,000√(40))/1000 = 361 ksi

The total building weight was estimated to be 62,505 lbs. This is based on a wall thickness of 18” and a density of 100 pcf which yields a weight per square foot of 150 psf. The weight of the walls minus the door opening is 150 psf (12’x9’x4) -150 psf (3’x6.7’) = 61,785 lbs. The weight of the roof was assumed to be 5 psf and this gives and additional weight of 5 psf (12’x12’) = 720 lbs. for a total of 62,505 lbs.

8.4.3. Models

The tapial model was created with elements in a similar manner to the model made of concrete elements. The elements are shown in figure 8.69. The vertical elements were all fixed to the foundation and the load was applied evenly at the roof.

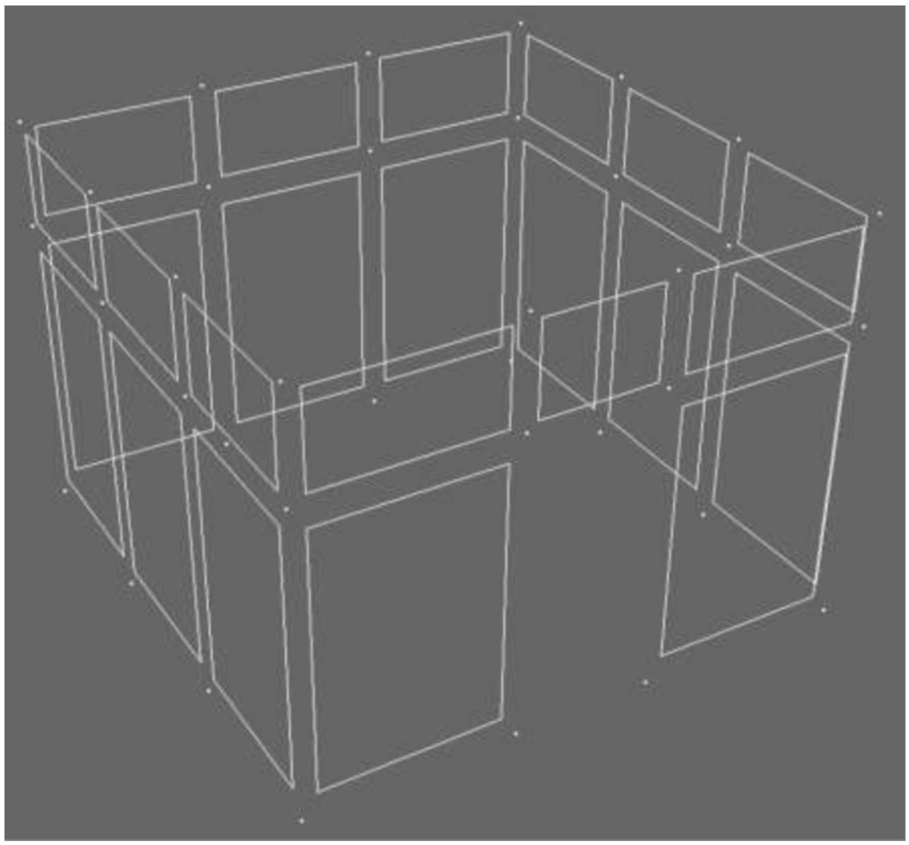

Figure 8.69. Tapial model

8.4.4. Pushover Analysis

The pushover analysis for the tapial model is seen in figure 8.70:

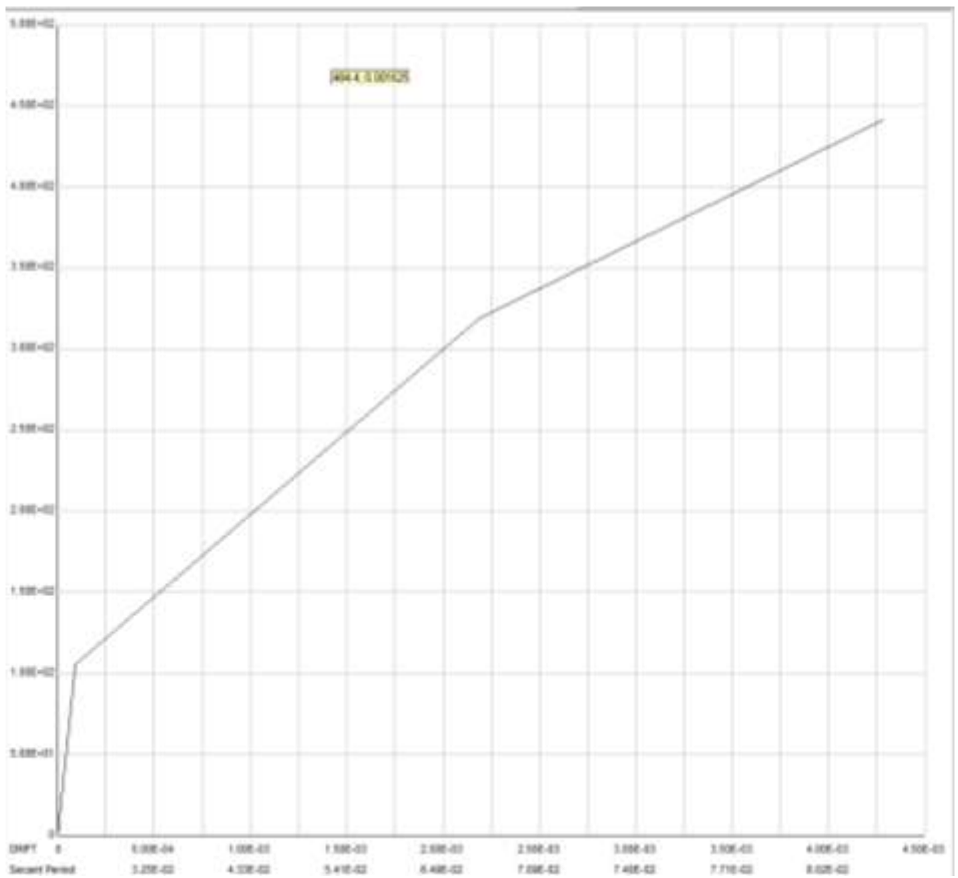

Figure 8.70. Tapial building pushover analysis

8.4.5. Dynamic Analysis

The dynamic analysis for the tapial model is seen in figures 8.71 and 8.72 both with and without damping.

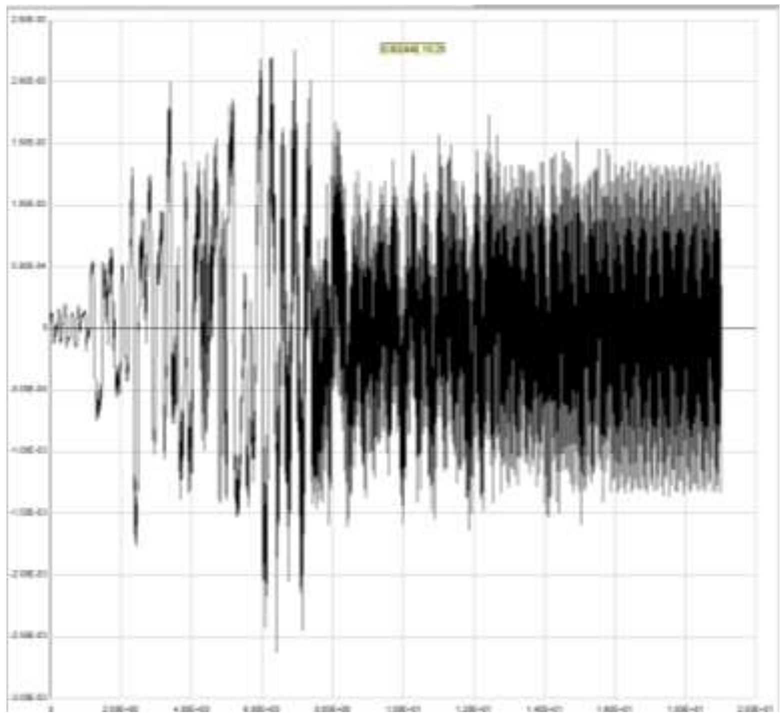

Figure 8.71. Tapial model dynamic analysis without damping

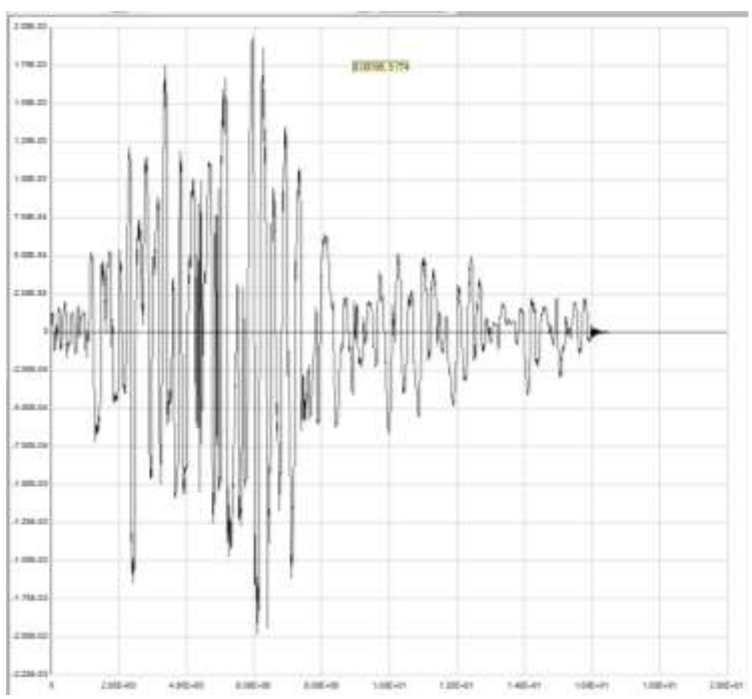

Figure 8.72. Dynamic analysis of tapial model with damping

The first tapial model at Fears Structural Engineering lab was created and tested dynamically at several different frequencies until the structure failed. It was not subjected to a specific earthquake. The second model will be constructed and tested using the Managua earthquake of 1973 which will facilitate more accurate verification of these results.

8.4.6. Summary

The analysis of rammed earth buildings in this study was created to give future research a model to compare future models and reactions. It was not created to analyze possible solutions however some structural advice can be summarized:

- The quality of the rammed earth is important. Any inconsistencies may result in a fracture plane during an earthquake. Care should be given to the mix proportions, and construction to ensure consistency.
- Creating a ring beam along the top and bottom of the structure is thought to increase structural capacity.
- Openings should be kept to a minimum in shear walls.

9. Conclusions

There have been several devastating earthquakes in Nicaragua's history and there will almost certainly be more. The focus of this research is to evaluate the structural systems of existing buildings, and then to make recommendations for low-cost enhancements that will improve the structural integrity of buildings in developing nations. It targets inexpensive measures that will save lives, such as improvements that can be made to both new and existing structures to increase structural stability during devastating seismic events. The types of buildings generally found in Nicaragua can be found in table 9.1.

Label	Description	Examples	
MF	'Mini-Falta' (engl.: miniskirt) half stone (blocks; bottom part), half wood (upper part)	 Masaya (NIC)	 Guatemala City (GUA)
AD	'Adobe' bricks of clay/mud, splices/joints out of clay/mud or lime	 Masaya (NIC)	 Guatemala City (GUA)
TP	'Tapial' (rammed earth) wooden formwork/form boards (only during construction) filled with earth (adobe material)		

Label	Description	Examples	
TZ	‘Taquezal’ wooden slats or shelves filled with earthen material and stones	 Masaya (NIC)	 Masaya (NIC)
BQ	‘Bahareque’ bamboo (canes) filled with earthen material (and stones)	 San Ramon (NIC)	 Rivas (NIC)
CC	‘Calycanto’ (fieldstone masonry) fieldstones, lime (chalk), and clay 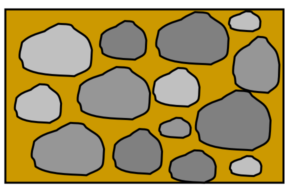	 Masaya (NIC)	 Masaya (NIC)
CL	claybricks		
	a) unreinforced or reinforced with internal steel rods	 Guatemala City (GUA)	
	b) confined with RC	 San Salvador (ELS)	 San Salvador (ELS)
CB	concrete blocks		

Label	Description	Examples	
	a) unreinforced or reinforced with internal steel rods	 San Salvador (ELS)	 San Salvador (ELS)
	b) confined with RC	 San Salvador (ELS)	 Guatemala City (GUA)
PC	'Piedra de Cantera' masonry out of cut (quarry) stones (unreinforced, confined with timber)	 Leon (NIC)	 Leon (NIC)
BP	'Blocke Panel' confined (precast) concrete panels vertical: welded steel connections horizontal: wood connection to roofing	 Masaya (NIC)	 Masaya (NIC)
		 Leon (NIC)	 Leon (NIC)

Label	Description	Examples	
LT	'Laminada Troquelada' steel frames and decorated steel sheets	 Guatemala City (GUA)	 Guatemala City (GUA)

Table 9.1. Common construction types found in Nicaragua (NORSAR, 2006)

Four of the building types were selected and analyzed. They include: reinforced concrete, confined masonry, taquezal, and rammed earth (tapial).

Figure 9.1. Concrete building

Figure 9.2. Rammed earth building (Diaz, 2007)

Figure 9.3. Taquezal building

Figure 9.4. Confined masonry building

Recommended building design practices for Nicaragua can be summarized by the following:

9.1. Concrete Buildings

- Use high quality concrete. Higher strength concrete increases the performance of the building both at immediate occupancy level and collapse prevention level of performance. Quality concrete requires strict mixing and pouring standards and also the usage of high quality sand and aggregate and avoids the use of local piedra pomez.
- Use enough steel to meet design minimum requirements and provide flexibility to the structure. Additional longitudinal or lateral reinforcement does not increase the capacity of the structure but in fact reduces the capacity.
- Height should be restricted to reduce deflection and cracking.

- Columns should have sufficient ties. Insufficient ties have been observed on jobsites on many occasions. It seems that ties are not considered structural elements but their purpose instead is to hold the longitudinal reinforcement in place.
- Special attention should be paid to the connections between structural elements. For example, walls should be well tied to both the foundation and the roof.
- Building openings (windows and doors) should not be concentrated in one area where they may create a weak wall or soft story. The opening area to wall area ratio should be kept to a minimum.

9.2. Confined Masonry Buildings

- A structural ring around the top and bottom are important for increasing the structural capacity in the event of an earthquake. Each ring should consist of a continuous reinforced beam with adequate longitudinal reinforcement, sufficient ties, and sufficient development lengths.
- In addition to structural rings around the top and bottom, additional beams should be located no more than 5’ on center. Where possible, these beams should be continuous, and should have adequate longitudinal reinforcement, sufficient ties, and sufficient development lengths.
- Infill bricks should be reinforced. If not possible infill bricks should be tied to the frames surrounding them.
- Height should be restricted to reduce deflection and cracking.

9.3. Taquezal Buildings

- Proper maintenance is important to the structural integrity of the taquezal shear walls. The areas that need to be inspected regularly are the connections of the vertical support wood to the base and the roof. The wood can be damaged by water or insects. The overhangs are important to reduce water splashing on the building and the roof must be kept watertight to reduce the possibility of leaks. To reduce the risk of insect damage, some buildings are built on a concrete curb. Anything to keep the wood structure from being in contact with the ground would be beneficial however insect treatment may be necessary.
- Cross bracing would provide an additional lateral force resisting system and create redundancy in the event of deferred maintenance. Cross bracing could consist of wooden members on the diagonal, strapping, or frames.
- The roof material should be kept as light as possible to reduce the risk of injury. Clay tiles should be avoided unless great care is taken to ensure the roof is well constructed.

9.4. Rammed Earth (Tapial) Buildings

- The quality of the rammed earth is important. Any inconsistencies may result in a fracture plane during an earthquake. Care should be given to the mix proportions, and construction to ensure consistency.
- Creating a ring beam along the top and bottom of the structure is thought to increase structural capacity.
- Openings should be kept to a minimum in shear walls.

9.5. Building Comparison

The four model buildings were then compared to each other in table 9.2.

Construction	Load at I.O.	Drift at I.O.
Reinforced concrete	200 kips*	$5.0 \times E^{-2}$
Confined masonry	12 kips	2.0×10^{-3}
Taquezal	44 kips	Negl.
Rammed earth	100 kips	Negl.

* Approximated assuming less windows

Table 9.2. Comparison of different building types

From comparing the construction type performance, some conclusions can be drawn. Reinforced concrete is the strongest of the four construction types. This is true as long as minimum design standards are maintained. Of the four types, confined masonry has the lowest load at immediate occupancy. Taquezal performs better than confined masonry however, taquezal requires more maintenance.

10. Further Research

The construction of earthquake resistant structures in developing countries is an area of research that deserves more attention. This study has barely scratched the surface of what is needed. Even the structures reviewed in this document could be analyzed in greater detail. Additional areas of research are:

Concrete buildings – Concrete buildings could be studied with more detail, including varied reinforcement and varied openings.

Confined masonry buildings – The frames could be studied in more detail including the reinforcing and tie requirements.

Taquezal buildings – The geometry could be varied and the roof diaphragm could be studied in greater detail.

Rammed earth buildings – Ring beams could be analyzed.

In addition to the suggestions for the previous building types, there are other building types, like piedra de cantera, that remain largely unstudied.

References

Abrams, Daniel P., Richard Angel. 1993. Strength, Behavior and Repair of Masonry Infills. *Structural Engineering in Natural Hazards Mitigation*: 1439 – 1444.

Aktan, Haluk M., and Robert D. Hanson. 1973. Dynamic Behavior of the Hotel Managua Intercontinental in the Managua Earthquake of December 23, 1972. *Earthquake Engineering Research Institute Conference Proceedings: Managua, Nicaragua Earthquake of December 23, 1972*, Volume 2: 586-603

Al-Chaar, Ghassan, Richard Angel and Daniel Abrams. 1994. Dynamic Testing of Unreinforced Brick Masonry Infills. *Structures Congress:* 791 – 796. Atlanta, GA.

Alcocer, Sergio M., Juan Guillermo Arias and Alejandro Vázquez. 2004. Response Assessment of Mexican Confined Masonry Structures Through Shaking Table Tests. *13th World Conference on Earthquake Engineering Conference Proceedings*: Paper No. 2130. Vancouver, Canada. August 1-6, 2004.

Amrhein, J.E., G.A. Hegemier and G. Krishnamoorthy. 1973. Performance of Native Construction, Masonry Structures and Special Structures in the Managua, Nicaragua Earthquake. *Earthquake Engineering Research Institute Conference Proceedings: Managua, Nicaragua Earthquake of December 23, 1972*, Volume 1: 342-403.

Anstead, Leroy. 1973. A Study of Seismic Damage Patterns by Photointerpretation. *Earthquake Earthquake Engineering Research Institute Conference Proceedings: Managua, Nicaragua Earthquake of December 23, 1972*, Volume 1: 265-270.

Berg, Glen V. and Henry J. Degenkolb. 1973. Engineering Lessons from the Managua Earthquake. *Earthquake Engineering Research Institute Conference Proceedings: Managua, Nicaragua Earthquake of December 23, 1972*, Volume 2: 746-767.

Blondet, Marcial, et al. 2006. Seismic Reinforcement of Adobe Houses Using External Polymer Mesh. Earthquake Engineering Research Institute. *8th U.S. National Conference on Earthquake Engineering Conference Proceedings*: Paper No. 979. San Francisco, CA. April 2006.

California State Office of Emergency Services (OES), 1973. The Managua, Nicaragua Earthquake of December 23, 1972 An Emergency Response Evaluation. *Earthquake Engineering Research Institute Conference Proceedings: Managua, Nicaragua Earthquake of December 23, 1972*, Volume 2: 955-975.

Caldera, Humberto Porta. 1973. Geodetic and Gravity Survey of Managua and its Surroundings. *Earthquake Engineering Research Institute Conference Proceedings: Managua, Nicaragua Earthquake of December 23, 1972*, Volume 1: 143-172.

Cao, Zengyan and Hiroyuki Watanabe. 2004. Earthquake Response Prediction and Retrofit Techniques of Adobe Structures. *13th World Conference on Earthquake Engineering Conference Proceedings*: Paper No. 412. Vancouver, B.C., Canada. August 2004.

Chamorro C., Filadelfo. 1973. Local Structural Engineering Practice Before and After the 1972 Managua Earthquake. *Earthquake Engineering Research Institute Conference Proceedings: Managua, Nicaragua Earthquake of December 23, 1972*, Volume 1: 309-312.

Das, Diptesh nd C.V.R. Murty. 2004. Brick masonry infills in seismic design of RC framed buildings: Part 1 and Part 2. *Indian Concrete Journal*, Volume 78, Issue 7 and 8, July and August 2004.

DeCanini, Luis, et al. 2004. Seismic Performance of Masonry Infilled R/C Frames, *13th World Conference on Earthquake Engineering Conference Proceedings*: Paper No. 165. Vancouver, B.C., Canada. August 2004.

Dewey, J.W., S.T. Algermissen, C. Langer, W. Dillinger and M. Hopper. 1973. The Managua Earthquake of 23 December 1972: Location, Focal Mechanism, Aftershocks and Relationship to Recent Seismicity of Nicaragua. *Earthquake Engineering Research Institute Conference Proceedings: Managua, Nicaragua Earthquake of December 23, 1972*, Volume 1: 66-88.

Diaz, Carmen Marlene. 2007. *Shake Table Testing of Scaled Rammed Earth Models*. Master's Thesis. University of Oklahoma: College of Civil Engineering and Environment Science. Norman, OK.

Dowling, Dominic. 2004. Improved Adobe Mudbrick in Application: Child-Care Centre Construction in El Salvador. *13th World Conference on Earthquake Engineering Conference Proceedings*: Paper No. 705. Vancouver, B.C., Canada. August 2004.

Dyke, C. Martin. 1973. Impact of Managua on Earthquake Engineering. *Earthquake Engineering Research Institute Conference Proceedings: Managua, Nicaragua Earthquake of December 23, 1972*, Volume 1: 1-7.

EERI Investigative Team I. 1973. Survey of Damages and Earthquake Performance of Managua Buildings. *Earthquake Engineering Research Institute Conference*

Proceedings: Managua, Nicaragua Earthquake of December 23, 1972, Volume 1: 420-480.

Faccioli, Ezio, Enrique Santoyo V. and Jose L. Leon T. 1973. Microzonation Criteria and Seismic Response Studies for the City of Managua. *Earthquake Engineering Research Institute Conference Proceedings: Managua, Nicaragua Earthquake of December 23, 1972*, Volume 1: 271-291.

Federal Emergency Management Agency. 2000. *FEMA 356: Prestandard and Commentary for the Seismic Rehabilitation of Buildings,* by American Society of Civil Engineers.

Gulkan, Polat. 2006. Performance Based Engineering, Fall 2006. Lecture, Middle East Technical University, Ankara, Turkey.

Hanson, Robert D., and Subhash C. Geol. 1973. Behavior of the Enaluf Office Building in the Managua Earthquake of December 23, 1972. *Earthquake Engineering Research Institute Conference Proceedings: Managua, Nicaragua Earthquake of December 23, 1972*, Volume 2: 604-620.

Hasen, Francisco, and victor M. Chavez. 1973. Isoseismal Maps of the Managua December 23, 1972 Earthquake. *Earthquake Engineering Research Institute Conference Proceedings: Managua, Nicaragua Earthquake of December 23, 1972*, Volume 1: 104-114.

Hays, Walter W. and Ken W. King. 1973. Use of Managua Earthquake Aftershock Data to Estimate Main Shock Response Spectra. *Earthquake Engineering Research Institute Conference Proceedings: Managua, Nicaragua Earthquake of December 23, 1972*, Volume 1: 292-299.

Ishibashi, K., et al. 1992. Experimental Study on Earthquake-Resistant Design of Confined Masonry Structure: Earthquake Engineering, *Tenth World Conference on Earthquake Engineering July 1992 Conference Proceedings*: 3469-3474. Madrid. Spain. ISBN 90 5410 060 5.

Ishibashi, Kazuhiko, and Hideo Kastumata. 1994. *A Study of Non-Linear Finite Element Analysis of Confined Masonry Walls*. Centro Nacional de Prevencion de Desastres.

Johnson, J.A., T. Yee, and C.M. Duke. 1973. Preliminary Ground Motion Calculation and Site Effects at Banco Central. *Earthquake Engineering Research Institute Conference Proceedings: Managua, Nicaragua Earthquake of December 23, 1972*, Volume 1: 300-308

Knudson, Charles F., and Francisco Hanson A. 1973. Accelerograph and Seismoscope Records from Managua, Nicaragua Earthquakes. *Earthquake Engineering Research Institute Conference Proceedings: Managua, Nicaragua Earthquake of December 23, 1972*, Volume 1: 180-205.

Kodur, V.K.R., M.A. Erkl and J.H.P. Quenneville. 1995. Seismic design and analysis of masonry-in filled frames. *Canadian Journal of Civil Engineering*: 576-587.

Larsson, Torleif, and Christina Mattson. 1987. *Seismic hazard analysis in Nicaragua*, Master's Thesis, Department of Soil and Rock Mechanics, Royal Institute of Technology (KTH), Stockholm, Sweden.

Lee, Han-Seon, and Sung-Woo Woo. 2002. Effect of masonry infills on seismic performance of a 3-story R/C frame with non-seismic detailing. *Earthquake Engineering and Structural Dynamics*, Volume 31:353-378.

Leeds, David J. 1973. Destructive Earthquakes of Nicaragua. *Earthquake Engineering Research Institute Conference Proceedings: Managua, Nicaragua Earthquake of December 23, 1972*, Volume 1: 26-51.

Marinilli, Angelo, and Enrique Castilla. 2004. Experimental Evaluation of Confined Masonry Walls with Several Confining-Columns. *13th World Conference on Earthquake Engineering Conference Proceedings*: Paper No. 2129. Vancouver, Canada. August 1-6, 2004.

Matumoto, Tosimatu and Gary Latham. 1973. Aftershock and Intensity of the Managua December 23, 1972 Earthquake. *Earthquake Engineering Research Institute Conference Proceedings: Managua, Nicaragua Earthquake of December 23, 1972*, Volume 1: 97-103.

May. 1984. *Adobe and Rammed Earth Buildings: Design and Construction.* Chapter 13. University of Arizona Press. AZ.

McHenry P. G. 1984. *Adobe and Rammed Earth Buildings: Design and Construction.* University of Arizona Press. AZ.

McLean, Ralph S. 1973. Three Reinforced Concrete Frame Buildings, Managua Earthquake, December 1972. *Earthquake Engineering Research Institute Conference Proceedings: Managua, Nicaragua Earthquake of December 23, 1972*, Volume 1: 481-528.

Meehan, John F. 1973. Response of Several School Building to the Managua, Nicaragua December 23, 1972 Earthquake. *Earthquake Engineering Research*

Institute Conference Proceedings: Managua, Nicaragua Earthquake of December 23, 1972, Volume 1: 404-419.

Meehan, John F. et al. 1973. Managua , Nicaragua Earthquake of December 23,1972, *Earthquake Engineering Research Institute Reconnaissance Report*, May 1973.

Mosalam, Khalid M., Richard N. White and Peter Gergely. 1997. *Seismic Evaluation of Frames with Infill Walls Using Pseudo-dynamic Experiments.* National Center for Earthquake Engineering Research, Technical Report 97-0020. ISSN 1088-3900.

Mosalam, Khalid M., Richard N. White and Peter Gergely. 1997. Computational Strategies for Frames with Infill Walls: Discrete and Smeared Crack Analyses and Seismic Fragility. *Technical Report NCEER-97-0021.* ISSN 1088-3800. December 1997.

Negro, P., and A. Colombo. 1997. Irregularities induced by nonstructural masonry panels in framed buildings. *Engineering Structures,* Vol 19, No 7: 576-585.

Nicoletti, Joseph P. and Felix Kulka. 1973. Response of the Enaluf building to the Managua Earthquake. *Earthquake Engineering Research Institute Conference Proceedings: Managua, Nicaragua Earthquake of December 23, 1972*, Volume 2: 621-673.

Norwegian Seismic Array (NORSAR). 2006. *Earthquake Risk Reduction in Guatemala, El Salvador and Nicaragua with Regional Cooperation to Honduras, Costa Rica and Panama*. Project proposal. Guatemala City, Guatemala. July 2006.

Paulay, T. and M.J.N. Priestly. 1992. *Seismic Design of Reinforced Concrete and Masonry Building*. John Wiley & Sons Inc. ISBN 0-471-54915-0.

Pereira, Enrique H. Ing. and Ing. Patrick J. Creegan. 1973. Statistical Damage Reports – Managua Related to Seismic Events of 12/23/72. *Earthquake Engineering Research Institute Conference Proceedings: Managua, Nicaragua Earthquake of December 23, 1972*, Volume 2: 733-745.

Perez, Virgilio. 1973. Time Dependant Spectral Analysis of Four Managua Earthquake Records. *Earthquake Engineering Research Institute Conference Proceedings: Managua, Nicaragua Earthquake of December 23, 1972*, Volume 1: 206-231.

Plakfer, George and R.D. Brown Jr. 1973. Surface Geological Effects of the Managua Earthquake of December 23, 1972. *Earthquake Engineering Research Institute*

Conference Proceedings: Managua, Nicaragua Earthquake of December 23, 1972, Volume 1: 115-142.

Reinoso, Eduardo, Franklin Moore and Guillermo Chavez Moore. 2004. *Study of the Seismic Vulnerability of Managua.* Nicaraguan Institute of Territorial Studies. April 2, 2004.

Rodriguez, Mario and Marcial Blondet. 2004. Evaluation of housing losses in recent earthquakes in Latin America, *13th World Conference on Earthquake Engineering Conference Proceedings*: Paper No. 2203. Vancouver, B.C., Canada. August 2004.

Rojan, Christoper. 1973. Analysis of Banco de America and Banco Central Post-earthquake Ambient Vibration Observation. *Earthquake Engineering Research Institute Conference Proceedings: Managua, Nicaragua Earthquake of December 23, 1972*, Volume 2: 674-692.

Saint-Amand, Pierre. 1973. The Seismicity and Geological Structure of the Managua, Nicaragua Area. *Earthquake Engineering Research Institute Conference Proceedings: Managua, Nicaragua Earthquake of December 23, 1972*, Volume 1: 8-25.

Samali, B., et al. 2006. Shake Table Testing and Dynamic Response of U-Shaped Adobe Mudbrick Wall Units. Earthquake Engineering Research Institute. *8th U.S. National Conference on Earthquake Engineering Conference Proceedings*: Paper No. 1903. San Francisco, CA. April 2006.

San Bartolome, A., et al. 2004. Effective System for Seismic Reinforcement of Adobe Houses. *13th World Conference on Earthquake Engineering Conference Proceedings*: Paper No. 3321. Vancouver, B.C., Canada. August 2004.

Santana, Guillermo. 1983. *Seismic Code Evaluation: Nicaragua.* http://www.consilient-health.com/download.php?id=11486&link=aHR0cDovL3d3dy5hY3MtYWVjLm9yZy9Eb2N1bWVudHMvRGlzYXN0ZXJzL1Byb2plY3RzL0FDU19ORF8wMDEvTklDQVJzY2UucGRm.

Santos, Carlos. 1973. Hydro-Geological Factors in the Occurrence of the Earthquakes of Managua. *Earthquake Engineering Research Institute Conference Proceedings: Managua, Nicaragua Earthquake of December 23, 1972*, Volume 1: 52-65.

Selna, L.G., and M.D. Cho. 1973. Banco de America, Managua a High-Rise Shear Wall Building Withstanding a Strong Earthquake. *Earthquake Engineering Research*

Institute Conference Proceedings: Managua, Nicaragua Earthquake of December 23, 1972, Volume 2: 551-570.

Shah, Haresh C., Christian P.Morgat, Anne Kiremidjian, and Theodore C. Zsutty. 1975. *A Study of Seismic Risk for Managua,* Report 11. Stanford University: John A. Blume Earthquake Engineering Center.

Shah, Haresh c., Joseph Nicoletti and Felix Kulka. 1973. Post Earthquake Dynamic Measurements of Four Structures in Managua. *Earthquake Engineering Research Institute Conference Proceedings: Managua, Nicaragua Earthquake of December 23, 1972*, Volume 2: 693-708.

Solís ,Armando Ugarte et al. 2004. *Estudio De La Vulnerabilidad Y Riesgo Sísmico De La Ciudad De León*, Echo – Movimondo. Managua, Nicaragua. May 2004.

Sozen, M.A., and Akenori Shibata. 1973. An Evaluation of the Performance of the Banco de America Building Managua, Nicaragua. *Earthquake Engineering Research Institute Conference Proceedings: Managua, Nicaragua Earthquake of December 23, 1972*, Volume 2: 429-550.

Sozen, Mete A., R.B. Matthiesen. 1975. *Engineering Report on the Managua Earthquake of 23 December 1972.* National Academy of Sciences. Washington, D.C.

Strauch, Wilfried, et al. 2000. *Microzonificatión Sísmica de Managua.* Instituto Nicaragüense de Estudios Territoriales. Managua, Nicaragua June 2000.

Teran, Jose Francisco. 1973. Historical Context of Building Forms in Managua. *Earthquake Engineering Research Institute Conference Proceedings: Managua, Nicaragua Earthquake of December 23, 1972*, Volume 1: 313-341.

Tolles, E. Leroy, Edna E. Kimbro, Frederick A. Webster and William S. Ginell. 2000. *Seismic Stabilization of Historic Adobe Structures: Final Report of the Getty Seismic Adobe Project*. The Getty Conservation Institue. Los Angeles, CA.

Tomaževič, M., I. Klemenc, L. Petkovic, and M. Lutman. 1996. *Seismic Behavior of Confined Masonry Buildings, Part One: Shaking-Table Tests of Model Buildings M1 and M2 – Test Results.* A Report to the Ministry of Science Technology of Republic of Slovenia: Grant No. J2-5208-1502.

Tomaževič, Miha, Iztok Klemenc. 1997. Verification of Seismic Resistance of Confined Masonry Buildings. *Earthquake Engineering and Structural Dynamics*, Volume 26: 1073-1088.

Turer, Ahmet. 2003. *Seismic Performance Improvement of Masonry Houses*. World Bank Development Marketplace. Middle East Technical University. Ankara, Turkey.

US Department of Homeland Security, Federal Emergency Management Agency. 2005. *FEMA 440: Improvement of Nonlinear Static Seismic Analysis Procedures*, by Applied Technology Council.

Valera, Julio E. 1973. Soil Conditions and Local Soil Effects during the Managua Earthquake of December 23, 1972. *Earthquake Engineering Research Institute Conference Proceedings: Managua, Nicaragua Earthquake of December 23, 1972*, Volume 1: 232-264.

Vargas, J., Marcial Blodnet and N. Tarque. 2004. Building Codes for Earthen Buildings in Seismic Areas: The Peruvian Experience. *8th U.S. National Conference on Earthquake Engineering Conference Proceedings*: Paper No. 1554. San Francisco, CA. April 2006.

Vera, Raul and Sandra Miranda. 2004. Experimental Study of Retrofitting Techniques for Adobe Walls. 1*13th World Conference on Earthquake Engineering Conference Proceedings*: Paper No. 2861. Vancouver, B.C., Canada. August 2004.

Wallace, Robert E. 1973. Plan for Zoning Managua, Nicaragua to Reduce Hazards of Surface Faulting. *Earthquake Engineering Research Institute Conference Proceedings: Managua, Nicaragua Earthquake of December 23, 1972*, Volume 1: 173-179.

Ward, Peter L. 1973. David Harlow and James Gibbs, Location of the Main Fault that slipped During the Managua Earthquake as Determined from Locations of Some Aftershocks. *Earthquake Engineering Research Institute Conference Proceedings: Managua, Nicaragua Earthquake of December 23, 1972*, Volume 1: 89-96.

Wright, Richard N., Samuel Kramer. 1973. *Building Performance in the 1972 Managua Earthquake.* Technical Note 807: National Bureau of Standards. November 1973.

Wyllie, Loring a. Jr. 1973. Performance of the Banco Central Building. *Earthquake Engineering Research Institute Conference Proceedings: Managua, Nicaragua Earthquake of December 23, 1972*, Volume 2: 571-585.

Yamin, L., et al. 2004. Seismic Behavior and Rehabilitation Alternatives for Adobe and Rammed Earth Buildings. *13th World Conference on Earthquake Engineering Conference Proceedings*: Paper No. 2942. Vancouver, B.C., Canada. August 2004.

Yanev, Peter I. 1973. Industrial Damage. *Earthquake Engineering Research Institute Conference Proceedings: Managua, Nicaragua Earthquake of December 23, 1972*, Volume 2: 709-732

Yanez, Fernando, Maximiliano Astroza, Augusto Holmberg, and Oscar Ogaz. 2004. *Behavior* of Confined Masonry Shear Walls with Large Openings. *13th World Conference on Earthquake Engineering Conference Proceedings*: Paper No. 3438. Vancouver, Canada. August 1-6, 2004.

Yoshimura, Koji, et al. 2004. Experimental Study for Developing Higher Seismic Performance of Brick Masonry Walls. *13th World Conference on Earthquake Engineering Conference Proceedings*: Paper No. 1597. Vancouver, Canada. August 1-6, 2004.

Yoshimura, Koji, et al. 2004. Experimental Study on Effects of Height of Lateral Forces, Column Reinforcement and Wall Reinforcements on Seismic Behavior of Confined Masonry Walls. *13th World Conference on Earthquake Engineering Conference Proceedings*: Paper No. 1597. Vancouver, Canada. August 1-6, 2004.

Zabala, Francisco, Jose Luis Bustos, Alberto Masanet, and Jorge Santalucia. 2004. Experimental Behavior of Masonry Structural Walls Used in Argentina. *13th World Conference on Earthquake Engineering Conference Proceedings*: Paper No. 1093. Vancouver, Canada. August 1-6, 2004

Appendix

Discrete Record of the Managua Earthquake of December 23, 1972

Time (sec)	Acceleration (in/sec^2) North - South	Acceleration (in/sec^2) East - West
0	0	0
0.03125	-8.165171224	-16.38526461
0.0625	-7.581944708	-15.79302613
0.09375	8.456784482	4.935320664
0.125	6.998718192	20.23481472
0.15625	-3.790972354	24.67660332
0.1875	4.082585612	-25.66366745
0.21875	-9.623237514	-31.09252018
0.25	-10.49807729	-29.11839192
0.28125	7.29033145	9.870641329
0.3125	5.83226516	14.80596199
0.34375	-2.91613258	15.29949406
0.375	-6.415491676	-21.22187886
0.40625	-12.83098335	-12.83183373
0.4375	-12.83098335	-11.35123753
0.46875	10.49807729	16.78009026
0.5	4.665812128	0
0.53125	5.83226516	-18.26068646
0.5625	5.249038644	-17.27362232
0.59375	-6.998718192	-11.84476959
0.625	-8.165171224	-7.402980996
0.65625	-7.581944708	-3.948256531
0.6875	5.249038644	22.20894299
0.71875	9.040010998	-9.870641329
0.75	8.74839774	-7.64974703
0.78125	-8.165171224	10.85770546

Time (sec)	Acceleration (in/sec^2) North - South	Acceleration (in/sec^2) East - West
0.8125	-11.0813038	-9.377109262
0.84375	2.91613258	-5.428852731
0.875	-5.83226516	-22.20894299
0.90625	-6.707104934	-21.71541092
0.9375	-7.581944708	-12.83183373
0.96875	-9.040010998	17.27362232
1	-8.165171224	-2.467660332
1.03125	10.49807729	-8.883577196
1.0625	-1.166453032	-20.72834679
1.09375	3.790972354	-18.26068646
1.125	3.499359096	15.79302613
1.15625	-30.32777883	-21.71541092
1.1875	-33.82713793	-22.20894299
1.21875	-33.24391141	-19.74128266
1.25	-20.99615458	-8.390045129
1.28125	32.07745838	-6.662682897
1.3125	44.90844173	6.415916864
1.34375	41.99230915	-35.53430878
1.375	42.57553567	-29.61192399
1.40625	38.49295006	-6.415916864
1.4375	34.41036444	4.935320664
1.46875	25.07874019	11.84476959
1.5	-26.24519322	23.68953919
1.53125	-27.41164625	45.89848218
1.5625	-23.32906064	9.377109262
1.59375	-15.74711593	3.454724465
1.625	0.583226516	-9.377109262
1.65625	-26.24519322	-10.36417339
1.6875	-29.1613258	-24.67660332
1.71875	-35.57681748	-50.34027078
1.75	-33.82713793	-65.14623277
1.78125	5.83226516	-68.10742517

Time (sec)	Acceleration (in/sec^2) North - South	Acceleration (in/sec^2) East - West
1.8125	-5.83226516	-54.28852731
1.84375	29.1613258	12.33830166
1.875	29.74455232	-33.80694655
1.90625	27.70325951	-44.91141804
1.9375	29.1613258	-45.15818408
1.96875	27.99487277	-38.49550118
2	17.49679548	40.46962945
2.03125	-34.41036444	43.43082185
2.0625	-27.99487277	7.402980996
2.09375	-16.03872919	13.32536579
2.125	9.331624256	-47.37907838
2.15625	24.49551367	-46.88554631
2.1875	24.49551367	19.24775059
2.21875	21.87099435	-7.402980996
2.25	-39.07617657	56.26265557
2.28125	-60.65555766	58.23678384
2.3125	-76.4026736	-42.44375771
2.34375	-78.15235314	-53.79499524
2.375	84.56784482	-53.30146317
2.40625	103.8143198	-39.97609738
2.4375	102.6478668	-1.480596199
2.46875	93.31624256	-0.7402981
2.5	-5.83226516	-31.58605225
2.53125	-31.49423186	-20.72834679
2.5625	-38.49295006	45.65171614
2.59375	-44.90844173	54.28852731
2.625	-46.07489476	56.75618764
2.65625	-27.99487277	-45.40495011
2.6875	-14.5806629	-69.0944893
2.71875	-4.957425386	-68.60095723
2.75	-40.82585612	6.415916864
2.78125	-70.57040844	13.07859976

Time (sec)	Acceleration (in/sec^2) North - South	Acceleration (in/sec^2) East - West
2.8125	-74.06976753	-32.57311638
2.84375	-72.9033145	-23.44277316
2.875	-29.1613258	-2.467660332
2.90625	47.2413478	-0.987064133
2.9375	60.65555766	-44.41788598
2.96875	63.8633035	-38.98903325
3	6.998718192	-28.62485985
3.03125	-29.74455232	59.71738004
3.0625	-30.32777883	63.1721045
3.09375	-38.49295006	61.6915083
3.125	-50.74070689	51.82086697
3.15625	-56.57297205	-85.38104749
3.1875	-56.57297205	-98.70641329
3.21875	59.19749137	-98.21288122
3.25	55.98974554	-18.26068646
3.28125	31.49423186	45.15818408
3.3125	-74.65299405	45.40495011
3.34375	-100.8981873	16.28655819
3.375	-108.480132	16.78009026
3.40625	-107.8969055	105.6158622
3.4375	34.41036444	108.0835225
3.46875	34.41036444	0
3.5	27.99487277	-29.11839192
3.53125	28.28648603	-26.15719952
3.5625	26.24519322	36.52137292
3.59375	-21.57938109	-28.62485985
3.625	-22.16260761	-46.88554631
3.65625	71.73686147	-50.34027078
3.6875	70.57040844	6.662682897
3.71875	64.15491676	16.28655819
3.75	59.48910463	16.28655819
3.78125	47.82457431	-30.59898812

Time (sec)	Acceleration (in/sec^2) North - South	Acceleration (in/sec^2) East - West
3.8125	-75.23622056	-55.76912351
3.84375	-75.81944708	-74.52334203
3.875	9.914850772	-74.02980996
3.90625	67.07104934	-57.74325177
3.9375	67.65427586	-56.75618764
3.96875	59.48910463	-43.43082185
4	60.07233115	65.63976483
4.03125	42.28392241	97.22581709
4.0625	-21.57938109	68.3541912
4.09375	-29.1613258	41.20992755
4.125	-31.49423186	37.75520308
4.15625	-58.61426486	35.53430878
4.1875	-61.8220107	68.10742517
4.21875	-68.52911563	33.56018052
4.25	-46.65812128	-91.79696436
4.28125	35.57681748	-80.44572683
4.3125	-34.99359096	24.42983729
4.34375	50.74070689	27.63779572
4.375	-64.73814328	-10.36417339
4.40625	78.15235314	-68.10742517
4.4375	-64.15491676	-61.6915083
4.46875	34.41036444	1.974128266
4.5	-13.99743638	-1.974128266
4.53125	-23.6206739	-69.58802137
4.5625	-22.74583412	-67.12036103
4.59375	-27.70325951	51.32733491
4.625	-54.8232925	49.35320664
4.65625	-73.19492776	-8.390045129
4.6875	-72.9033145	50.83380284
4.71875	-72.32008798	-14.80596199
4.75	-57.15619857	-9.377109262
4.78125	79.31880618	-15.79302613

Time (sec)	Acceleration (in/sec^2) North - South	Acceleration (in/sec^2) East - West
4.8125	78.73557966	-16.78009026
4.84375	-31.49423186	6.90944893
4.875	-47.82457431	10.61093943
4.90625	58.55594221	-22.20894299
4.9375	-61.8220107	-35.53430878
4.96875	67.07104934	-35.53430878
5	64.15491676	35.53430878
5.03125	-72.32008798	45.89848218
5.0625	-86.90075088	50.34027078
5.09375	-100.606574	30.59898812
5.125	-90.40010998	24.67660332
5.15625	-105.8556127	24.18307125
5.1875	-108.480132	36.27460688
5.21875	80.48525921	29.61192399
5.25	79.90203269	-70.08155343
5.28125	88.94204369	-77.9780665
5.3125	90.40010998	-71.56214963
5.34375	88.94204369	-58.23678384
5.375	73.48654102	3.948256531
5.40625	48.99102734	-32.57311638
5.4375	30.91100535	-32.57311638
5.46875	15.74711593	-21.22187886
5.5	-15.16388942	0
5.53125	-21.28776783	7.896513063
5.5625	79.31880618	-45.15818408
5.59375	79.31880618	-70.08155343
5.625	75.81944708	-69.0944893
5.65625	53.07361296	41.45669358
5.6875	-19.24647503	76.99100236
5.71875	58.3226516	98.70641329
5.75	67.65427586	99.69347742
5.78125	58.61426486	-9.870641329

Time (sec)	Acceleration (in/sec^2) North - South	Acceleration (in/sec^2) East - West
5.8125	38.49295006	-42.93728978
5.84375	-51.90715992	-41.95022565
5.875	-80.48525921	20.48158076
5.90625	-102.9394801	-4.935320664
5.9375	-124.2272479	-3.948256531
5.96875	-125.3937009	4.935320664
6	-63.28007699	42.93728978
6.03125	102.6478668	41.95022565
6.0625	102.0646403	28.13132779
6.09375	121.8943418	82.41985509
6.125	120.7278888	90.80990022
6.15625	92.73301604	90.80990022
6.1875	-37.32649702	-132.2665938
6.21875	-98.27366795	-138.1889786
6.25	-116.0620767	-130.7859976
6.28125	-100.8981873	-53.79499524
6.3125	-82.23493876	-42.69052375
6.34375	-78.73557966	-17.27362232
6.375	24.49551367	17.27362232
6.40625	121.8943418	53.30146317
6.4375	78.73557966	56.75618764
6.46875	61.23878418	-36.02784085
6.5	39.65940309	-37.01490498
6.53125	-40.82585612	-27.14426365
6.5625	-54.8232925	-18.26068646
6.59375	-54.8232925	22.70247506
6.625	-50.15748038	-10.85770546
6.65625	30.32777883	-5.922384797
6.6875	36.74327051	33.06664845
6.71875	49.57425386	43.43082185
6.75	74.65299405	-23.19600712
6.78125	64.15491676	-71.56214963

Time (sec)	Acceleration (in/sec^2) North - South	Acceleration (in/sec^2) East - West
6.8125	23.32906064	-79.95219476
6.84375	-55.40651902	-79.95219476
6.875	-62.98846373	-56.75618764
6.90625	-84.56784482	-39.48256531
6.9375	-86.31752437	47.37907838
6.96875	-69.4039554	-65.14623277
7	11.66453032	-63.1721045
7.03125	18.37163525	-53.30146317
7.0625	38.49295006	11.35123753
7.09375	102.0646403	21.22187886
7.125	102.6478668	23.68953919
7.15625	79.90203269	-37.50843705
7.1875	61.23878418	-33.31341448
7.21875	-23.91228716	-29.61192399
7.25	-32.6606849	-27.14426365
7.28125	-53.65683947	-6.16915083
7.3125	-65.32136979	14.80596199
7.34375	-69.98718192	18.26068646
7.375	-64.15491676	-3.948256531
7.40625	36.16004399	-1.480596199
7.4375	34.99359096	9.870641329
7.46875	19.82970154	-36.52137292
7.5	37.90972354	-43.92435391
7.53125	29.74455232	-73.5362779
7.5625	29.74455232	-70.08155343
7.59375	19.24647503	-51.82086697
7.625	13.99743638	-35.53430878
7.65625	38.49295006	-4.441788598
7.6875	33.82713793	35.53430878
7.71875	24.49551367	35.53430878
7.75	19.24647503	27.63779572
7.78125	8.165171224	37.01490498

Time (sec)	Acceleration (in/sec^2) North - South	Acceleration (in/sec^2) East - West
7.8125	-1.166453032	3.948256531
7.84375	-11.95614358	3.948256531
7.875	39.07617657	12.33830166
7.90625	39.07617657	-4.935320664
7.9375	37.32649702	-4.441788598
7.96875	-21.87099435	-1.480596199
8	-28.57809928	54.28852731
8.03125	-36.74327051	0
8.0625	-40.82585612	-26.65073159
8.09375	-42.28392241	-27.63779572
8.125	-39.07617657	-23.68953919
8.15625	-41.70069589	-22.20894299
8.1875	-35.57681748	-16.28655819
8.21875	-26.24519322	-7.896513063
8.25	-18.66324851	17.76715439
8.28125	-15.16388942	23.19600712
8.3125	-9.914850772	29.61192399
8.34375	-12.53937009	38.98903325
8.375	17.49679548	38.98903325
8.40625	40.82585612	-41.45669358
8.4375	40.2426296	-40.46962945
8.46875	38.49295006	-32.57311638
8.5	32.6606849	9.377109262
8.53125	20.41292806	6.90944893
8.5625	8.74839774	-16.28655819
8.59375	6.123878418	-13.32536579
8.625	5.83226516	11.35123753
8.65625	-14.5806629	25.66366745
8.6875	-11.66453032	10.85770546
8.71875	-15.74711593	10.61093943
8.75	-10.49807729	31.58605225
8.78125	-5.249038644	5.922384797

Time (sec)	Acceleration (in/sec^2) North - South	Acceleration (in/sec^2) East - West
8.8125	6.998718192	15.29949406
8.84375	7.29033145	66.873595
8.875	13.99743638	-48.61290854
8.90625	27.41164625	-50.34027078
8.9375	23.32906064	-44.41788598
8.96875	-11.66453032	-34.54724465
9	3.499359096	-19.74128266
9.03125	-11.0813038	-15.29949406
9.0625	-11.66453032	-5.922384797
9.09375	12.83098335	-25.17013539
9.125	12.24775684	-44.41788598
9.15625	14.5806629	-49.84673871
9.1875	11.66453032	-54.28852731
9.21875	11.95614358	-54.78205937
9.25	-5.249038644	-50.34027078
9.28125	4.082585612	-36.02784085
9.3125	4.665812128	-27.63779572
9.34375	-8.165171224	-14.80596199
9.375	-13.41420987	22.20894299
9.40625	-11.66453032	25.66366745
9.4375	-12.53937009	10.36417339
9.46875	-11.66453032	2.961192399
9.5	-8.74839774	2.961192399
9.53125	6.123878418	25.66366745
9.5625	8.165171224	29.61192399
9.59375	14.28904964	8.390045129
9.625	15.16388942	0.493532066
9.65625	-9.331624256	5.922384797
9.6875	-17.49679548	5.428852731
9.71875	-25.6619667	15.29949406
9.75	-24.49551367	14.80596199
9.78125	-14.28904964	0.7402981

Time (sec)	Acceleration (in/sec^2) North - South	Acceleration (in/sec^2) East - West
9.8125	-14.5806629	-3.454724465
9.84375	-6.707104934	-3.454724465
9.875	11.66453032	6.415916864
9.90625	14.5806629	7.896513063
9.9375	33.82713793	11.35123753
9.96875	43.15876218	23.68953919
10	41.99230915	35.04077672
10.03125	36.74327051	49.35320664
10.0625	20.99615458	48.36614251
10.09375	-10.20646403	32.07958432
10.125	-4.082585612	33.56018052
10.15625	3.790972354	5.428852731
10.1875	-12.83098335	-30.10545605
10.21875	-23.91228716	-51.82086697
10.25	-33.53552467	-57.24971971
10.28125	-31.49423186	-54.28852731
10.3125	-24.78712693	-27.14426365
10.34375	-18.95486177	-5.428852731
10.375	9.914850772	-10.85770546
10.40625	25.07874019	-19.74128266
10.4375	26.24519322	-20.97511282
10.46875	20.41292806	-21.22187886
10.5	15.45550267	-23.68953919
10.53125	6.415491676	-18.01392042
10.5625	-14.5806629	10.36417339
10.59375	-12.83098335	17.27362232
10.625	-12.24775684	8.390045129
10.65625	-17.49679548	4.935320664
10.6875	-16.33034245	0
10.71875	10.78969055	-3.454724465
10.75	16.33034245	-7.402980996
10.78125	21.87099435	-17.76715439

Time (sec)	Acceleration (in/sec^2) North - South	Acceleration (in/sec^2) East - West
10.8125	26.24519322	-28.13132779
10.84375	34.99359096	-26.65073159
10.875	37.61811028	-14.80596199
10.90625	23.91228716	-15.79302613
10.9375	13.70582313	-4.935320664
10.96875	-28.57809928	-10.85770546
11	-29.1613258	-17.27362232
11.03125	-30.91100535	-24.18307125
11.0625	-26.53680648	-18.75421852
11.09375	-19.24647503	-13.32536579
11.125	-14.5806629	19.74128266
11.15625	10.49807729	27.14426365
11.1875	10.20646403	33.06664845
11.21875	6.998718192	34.54724465
11.25	-16.91356896	18.75421852
11.28125	-25.07874019	16.28655819
11.3125	-26.24519322	8.883577196
11.34375	-21.57938109	3.454724465
11.375	-16.33034245	-5.922384797
11.40625	-9.914850772	-14.80596199
11.4375	4.957425386	-20.23481472
11.46875	-8.165171224	-19.74128266
11.5	-8.74839774	-12.33830166
11.53125	5.83226516	-3.948256531
11.5625	8.74839774	20.72834679
11.59375	8.165171224	26.15719952
11.625	5.83226516	10.85770546
11.65625	-4.082585612	3.454724465
11.6875	-6.707104934	-6.16915083
11.71875	-5.83226516	-4.195022565
11.75	15.16388942	10.85770546
11.78125	16.91356896	11.84476959

Time (sec)	Acceleration (in/sec^2) North - South	Acceleration (in/sec^2) East - West
11.8125	19.24647503	-3.948256531
11.84375	24.49551367	-9.870641329
11.875	31.49423186	-8.883577196
11.90625	30.91100535	0.493532066
11.9375	23.32906064	-13.81889786
11.96875	14.5806629	-20.72834679
12	11.66453032	-24.67660332
12.03125	-18.95486177	-22.20894299
12.0625	-18.66324851	-16.78009026
12.09375	-12.83098335	-18.26068646
12.125	-11.0813038	-14.80596199
12.15625	6.415491676	-9.870641329
12.1875	12.83098335	-2.961192399
12.21875	19.82970154	7.402980996
12.25	20.41292806	-2.467660332
12.28125	16.91356896	16.78009026
12.3125	9.914850772	22.20894299
12.34375	-19.53808829	21.22187886
12.375	-25.07874019	-0.493532066
12.40625	-31.49423186	0
12.4375	-32.07745838	12.33830166
12.46875	-18.080022	15.29949406
12.5	9.914850772	18.26068646
12.53125	9.506592211	9.870641329
12.5625	6.998718192	3.454724465
12.59375	-11.0813038	-5.922384797
12.625	-12.53937009	-8.390045129
12.65625	-21.57938109	-8.390045129
12.6875	-20.99615458	-12.33830166
12.71875	-10.20646403	-16.28655819
12.75	6.415491676	-22.20894299
12.78125	7.581944708	-21.22187886

Time (sec)	Acceleration (in/sec^2) North - South	Acceleration (in/sec^2) East - West
12.8125	6.415491676	-10.85770546
12.84375	-4.082585612	11.35123753
12.875	-5.83226516	18.26068646
12.90625	-3.790972354	19.74128266
12.9375	1.749679548	-8.390045129
12.96875	-2.332906064	-24.18307125
13	4.665812128	-35.53430878
13.03125	3.790972354	-36.02784085
13.0625	-3.499359096	-25.91043349
13.09375	-4.082585612	-10.36417339
13.125	-3.499359096	25.17013539
13.15625	-2.91613258	24.67660332
13.1875	-3.499359096	5.428852731
13.21875	6.998718192	2.467660332
13.25	6.415491676	-14.55919596
13.28125	-6.415491676	-12.33830166
13.3125	-8.74839774	-5.428852731
13.34375	-11.95614358	12.33830166
13.375	-11.66453032	16.28655819
13.40625	-10.78969055	16.28655819
13.4375	-5.83226516	7.402980996
13.46875	-3.207745838	-2.467660332
13.5	-3.790972354	-9.377109262
13.53125	-5.83226516	-22.94924109
13.5625	-4.665812128	-18.26068646
13.59375	-3.499359096	-12.83183373
13.625	-3.207745838	-0.493532066
13.65625	-4.082585612	-12.09153563
13.6875	-4.37419887	-17.27362232
13.71875	-4.957425386	-19.24775059
13.75	4.082585612	-19.74128266
13.78125	5.249038644	-22.20894299

Time (sec)	Acceleration (in/sec^2) North - South	Acceleration (in/sec^2) East - West
13.8125	2.91613258	-20.72834679
13.84375	-6.707104934	-18.26068646
13.875	-9.623237514	-12.33830166
13.90625	-9.623237514	-1.974128266
13.9375	-8.165171224	15.79302613
13.96875	-8.456784482	-15.29949406
14	9.331624256	3.948256531
14.03125	17.49679548	0
14.0625	21.57938109	-4.441788598
14.09375	26.82841974	-2.961192399
14.125	25.07874019	2.467660332
14.15625	18.66324851	-3.948256531
14.1875	-12.83098335	-7.402980996
14.21875	-13.12259661	-7.402980996
14.25	-12.24775684	-2.467660332
14.28125	-9.623237514	-21.22187886
14.3125	-8.74839774	20.72834679
14.34375	12.83098335	-4.441788598
14.375	13.41420987	-5.428852731
14.40625	12.83098335	-8.390045129
14.4375	6.415491676	-14.80596199
14.46875	-3.499359096	-19.24775059
14.5	-6.998718192	-20.23481472
14.53125	-8.74839774	-15.79302613
14.5625	-9.914850772	-3.948256531
14.59375	-10.78969055	16.78009026
14.625	-11.0813038	17.27362232
14.65625	-7.873557966	-17.27362232
14.6875	-3.499359096	-18.50745249
14.71875	-3.499359096	-18.26068646
14.75	0.583226516	-10.36417339
14.78125	-2.332906064	-5.428852731

Time (sec)	Acceleration (in/sec^2) North - South	Acceleration (in/sec^2) East - West
14.8125	3.499359096	8.390045129
14.84375	4.957425386	-3.948256531
14.875	5.83226516	-8.390045129
14.90625	-9.623237514	-9.377109262
14.9375	-13.99743638	-8.390045129
14.96875	-15.16388942	-5.922384797
15	9.914850772	5.922384797
15.03125	18.37163525	1.974128266
15.0625	18.66324851	11.84476959
15.09375	12.24775684	-13.32536579
15.125	7.581944708	14.31242993
15.15625	6.415491676	-9.870641329
15.1875	5.83226516	-11.84476959
15.21875	-5.83226516	-9.377109262
15.25	-4.082585612	-5.428852731
15.28125	0.874839774	-6.90944893
15.3125	-2.332906064	-8.143279096
15.34375	1.166453032	-8.390045129
15.375	2.91613258	-7.402980996
15.40625	-3.207745838	-3.948256531
15.4375	-8.165171224	10.85770546
15.46875	-12.24775684	13.81889786
15.5	-12.83098335	13.32536579
15.53125	-11.95614358	-1.974128266
15.5625	-7.29033145	-6.90944893
15.59375	7.581944708	-6.90944893
15.625	8.74839774	-6.415916864
15.65625	8.165171224	-6.415916864
15.6875	4.082585612	-5.428852731
15.71875	-7.581944708	-5.428852731
15.75	-13.41420987	-6.90944893
15.78125	-13.99743638	-9.870641329

Time (sec)	Acceleration (in/sec^2) North - South	Acceleration (in/sec^2) East - West
15.8125	-12.24775684	-9.870641329
15.84375	-8.165171224	-6.415916864
15.875	2.332906064	-4.441788598
15.90625	3.499359096	-7.402980996
15.9375	4.082585612	-7.896513063
15.96875	-4.37419887	-6.90944893
16	-6.998718192	-2.961192399